MOLECULAR AND CELL BIOLOGICAL CHARACTERISATION OF NEURONAL NICOTINIC ACETYLCHOLINE RECEPTORS

Elizabeth Rae Baker

November 2003

A thesis presented for the degree of Doctor of Philosophy to the University of London

Department of Pharmacology

University College, London, WC1E 6BT

ProQuest LLC
789 East Eisenhower Parkway
P.O. Box 1346
Ann Arbor, MI 48106-1346

ABSTRACT

Molecular and cell biological characterisation of neuronal nicotinic acetylcholine receptors (nAChRs) provides an insight into their functional roles and potential as therapeutic targets for neurological disorders. Nicotinic receptors are oligomeric ligand-gated ion channels, comprising five subunits. Twelve vertebrate neuronal nAChR subunits (α2-α10 and β2-β4) have been cloned to date, with considerable diversity observed in nAChR subunit composition. Heterologous expression of cloned subunits is a powerful method for investigating ion channel receptor pharmacology and subunit composition, but achieving efficient expression of some nAChRs in cultured cell lines has proved difficult. In this study, chimeras containing the N-terminal domain of the nAChR subunits, fused to the C-terminal region of the 5-hydroxtryptamine type 3 receptor subunit, $5HT_{3A}$, were constructed to overcome some of the challenges of recombinant nAChR expression. When combinations of wild-type and chimeric subunits were expressed in human embryonic kidney tsA201 cells, inclusion of nAChR/$5HT_{3A}$ chimeras enhanced the expression of nAChRs containing each of the α2, α3, α4, α6, α7, α9, α10, β2 or β4 nAChR subunits, determined by detection of radioligand binding sites. This was particularly significant for α6- or α9/α10-containing nAChRs, as radioligand binding to wild-type nAChRs containing these subunits was not detected in tsA201 cells. A detailed pharmacological characterisation of receptors containing α9/$5HT_{3A}$ + α10/$5HT_{3A}$ chimeras in tsA201 cells via competition binding suggested that the chimeras provide suitable models for characterisation of wild-type nAChRs. Radioligand binding to intact cells and enzyme-linked assays to detect epitope-tagged subunits expressed in transfected cells, suggested that α9/$5HT_{3A}$-containing receptors were expressed at the cell surface in high levels. Comparison of radioligand binding to nAChR subtypes containing combinations of wild-type and chimeric α2-α6 and β2-β4 subunits implicated the N- and C-terminal domains of both the α and β type nAChR subunits in subunit oligomerisation events and provided an insight into nAChR assembly.

ACKNOWLEDGEMENTS

There are so many people to thank, without whom this project would not have been possible. This work was supported by grants from The Wellcome Trust.

My sincere thanks to Dr. Neil Millar, for the opportunity to work in his wonderful laboratory and to the rest of the Millar group, for making it a pleasure to come to work. Dr. Stuart Lansdell and Patricia Harkness, I simply cannot thank enough for their continued support, input, invaluable advice and friendship.

My thanks to Drs. Jim Boulter, Belén Elgoyhen and David Julius for generously providing the subunit cDNAs, and Dr. Ruth McKernan for donating the pAb5HT$_3$ antibody. Many thanks to Dr. Ruud Zwart and Dr. Emanuele Sher from Eli Lilly and Company Limited (Lilly Research Centre, Windlesham, Surrey, UK) for electrophysiology carried out with the α9/5HT$_{3A}$ and α10/5HT$_{3A}$ chimeras.

Last, but not least, to my family - Thank you, for everything.

CONTENTS

LIST OF FIGURES

LIST OF TABLES

ABBREVIATIONS

[^{125}I]	iodinated
[^{3}H]	tritiated
5HT	5-hydroxytryptamine
$5HT_{3A}$	'A' subunit of the 5-hydroxytryptamine type 3 receptor
$\alpha 2\chi$	chimeric subunit constructed using the amino-terminal domain of the $\alpha 2$ nicotinic subunit fused to the carboxy-terminal domain of the 5-hydroxytryptamine receptor 3A subunit
α-BTX	alpha bungarotoxin
A_{750}	absorbance at 750 nm
ACh	acetylcholine
ACh-BP	acetylcholine binding protein
ATP	adenosine triphosphate
BSA	bovine serum albumin
CIAP	calf intestinal alkaline phosphatase
CMV	cytomegalovirus
ddNTP	dideoxynucleotide triphosphate
DMEM	Dulbecco's modified Eagle's medium
DMPP	1,1-dimethyl-4-phenlypiperazinium
DMSO	dimethylsulphoxide
DNA	deoxyribonucleic acid
dNTP	deoxynucleotide triphosphate
DTT	dithiothreitol
EC_{50}	median effective concentration
EDTA	ethylenediaminetetraacetic acid
GABA	γ-aminobutyric acid
GH_4C_1	rat pituitary cell line
HA	nine amino acid influenza haemagglutinin peptide marker

HBSS	Hanks buffered saline solution
HEK293	human embryonic kidney fibroblast cell line
HEPES	*N*-2-hydroxyethylpiparazine-*N*-2-ethanesulphonic acid
HRP	horseradish peroxidase
IgG	immunoglobulin G
IPTG	isopropyl-1-thio-β-D-galactopyranoside
K_d	equilibrium binding constant
kDa	kilodalton
LB broth	Luria-Bertani medium
LTP	long term potentiation
M1	first putative transmembrane region
mAb	monoclonal antibody
MCC	methylcarbamylcholine
MLA	methyllycaconitine
MOPS	3-*N*-morpholino propanesulphonic acid
MQ	milli-Q
NAc	nucleus accumbens
nAChR	nicotinic acetylcholine receptor
n-BTX	neuronal bungarotoxin
n_H	Hill Coefficient
pAb5HT$_3$	polyclonal antibody raised to the intracellular loop region of the 5-hydroxytryptamine type 3 receptor 'A' subunit
PAGE	polyacrylamide gel electrophoresis
PBS	phosphate buffered saline
PC12	rat phaeochromocytoma cell line
PCR	polymerase chain reaction
PEI	polyethylenimine
PFA	paraformaldehyde
PMSF	phenylmethylsulfonyl fluoride

RIC-3	resistant to inhibitors of cholinesterase
SDM	site directed mutagenesis
SDS	sodium dodecyl sulphate
SH-SY5Y	human neuroblastoma cell line
SV40	Simian virus
TMB	3,3',5,5'-tetramethylbenzidine (liquid substrate system)
tsA201	temperature sensitive cell line derivative of the human embryonic kidney 293 cell line
TTX	tetrodotoxin
U	units
UB/OC-1	conditionally immortal auditory hair cell line derived from the H-2Kb-*ts*A58 transgenic "Immortomouse" (University of Bristol/Organ of Corti)
UB/OC-2	conditionally immortal auditory hair cell line derived from the "Immortomouse" (University of Bristol/Organ of Corti)
VTA	ventral tegmental area
X-Gal	5-bromo-4-chloro-3-indoyl-β-D-galactopyranoside

INTRODUCTION

CHAPTER 1

INTRODUCTION

Two types of ACh-sensitive receptor have been classified according to their activation by the plant alkaloids, muscarine and nicotine. These receptors are also distinguished by their sensitivity to different antagonists, where, for example, muscarinic acetylcholine receptors are sensitive to atropine and nicotinic acetylcholine receptors are sensitive to *d*-tubocurarine. In vertebrates, the nicotinic acetylcholine receptors (nAChRs) can be further divided into two broad classes defined by their location. "Muscle-type" nAChRs are expressed at the neuromuscular junction, while "neuronal" nAChRs are expressed widely in the central and peripheral nervous systems (Lukas *et al.*, 1999). These two subclasses of nicotinic receptor also differ with respect to their subunit composition and pharmacological profiles.

The nAChRs belong to a superfamily of neurotransmitter-gated ion channels that also includes the γ-aminobutyric acid type A ($GABA_A$) receptor, the glycine receptor and the 5-hydroxytryptamine type 3 ($5HT_3$) receptor (Stroud *et al.*, 1990). These oligomeric proteins, comprising five membrane-spanning subunits, are involved in fast communication events between nerve cells and sensory or effector cells. A chemical signal released by the nerve cell and detected by the ion channel receptor is converted into an electrical signal via the opening of the ion channel to allow a brief influx of ions into the cell (see also Section 1.6). The members of the superfamily can be classified according to the nature of the ions that pass through the channel, where nAChRs and $5HT_3$ receptors conduct cations and elicit an excitatory response, while glycine and $GABA_A$ receptors conduct anions and are, therefore, classified as inhibitory, as receptor activation leads to membrane hyperpolarisation.

1.1 The nicotinic acetylcholine receptor (nAChR)

1.1.1 The nAChR from the *Torpedo* electric organ

The electric organs of the marine rays, *Torpedo californica* and *Torpedo marmorata* and the electric eel, *Electrophorus electricus*, are comprised of stacks of electrocytes; cells that differentiate from embryonic tissue common to that of skeletal muscle. The nAChR isolated from these modified muscle cells resembles the nAChR isolated from the vertebrate neuromuscular junction (Section 1.1.2). The entire ventral surface of the electrocyte forms an excitable membrane, providing an extremely high density of nAChRs (100 pmol/mg protein) at levels approximately 1000-fold higher than those of skeletal muscle. The snake α-toxin, α-bungarotoxin (α-BTX), isolated from the venom of the Malayan banded krait, *Bungarus multicinctus* (Lee and Chang, 1966) binds almost irreversibly to *Torpedo* electric organ nAChRs to inactivate receptor function and allowed the purification of the nAChR from this rich source of receptors (Changeux *et al.*, 1970; Miledi *et al.*, 1971).

The *Torpedo* electric organ nAChR is composed of four different subunits designated α, β, γ and δ, arranged as a pentamer in the stoichiometry $\alpha_2\beta\gamma\delta$ (Hucho *et al.*, 1976; Reynolds and Karlin, 1978; Brisson and Unwin, 1985; Unwin, 1993). This pentameric glycoprotein has a molecular mass of approximately 290 kilodaltons (kDa), with each subunit contributing 40 - 64 kDa. The native *Torpedo* electric organ nAChR exists as a single pentamer and in a "dimeric" form, where two nAChR pentamers are cross-linked by a disulphide bond, determined by sucrose gradient centrifugation with sediment coefficients of 9S and 13S, respectively (Hamilton *et al.*, 1979; DiPaola *et al.*, 1989). The five membrane spanning subunits of each pentamer are arranged to form a ring around a narrow central pore, which comprises the ion channel and is impermeable to ions when the nAChR is in the resting state (Cooper *et al.*, 1991; Unwin, 1993). Upon ligand binding and nAChR activation, a conformational change occurs to open the

channel pore, allowing the selective passage of ions through the plasma membrane (e.g. Miyazawa *et al.*, 1999; Miyazawa *et al.*, 2003).

Cloning of the genes encoding the *Torpedo* electric organ α, β, δ and γ subunits (Noda *et al.*, 1982; Claudio *et al.*, 1983; Noda *et al.*, 1983c) allowed reconstitution of functional recombinant nAChRs in the oocytes of the South African clawed frog, *Xenopus laevis* (Sumikawa *et al.*, 1981; Barnard *et al.*, 1982) in an approach that has been widely used in the characterisation of nicotinic receptors.

1.1.2 The nAChR of the vertebrate neuromuscular junction

The nucleotide sequences of the *Torpedo* electric organ subunits were used to construct cDNA probes, then used to screen mammalian libraries and identify genes encoding nAChR subunits expressed at the vertebrate neuromuscular junction (Noda *et al.*, 1983b; LaPolla *et al.*, 1984; Nef *et al.*, 1984; Tanabe *et al.*, 1984). This approach identified mammalian α1, β1, γ and δ subunits and a novel subunit, designated ε, resembling the γ subunit (Takai *et al.*, 1985). The muscle nAChR can exist in two forms, where the $\alpha 1_2\beta 1\gamma\delta$ form occurs in foetal muscle and a switch during postnatal development produces the $\alpha 1_2\beta 1\varepsilon\delta$ form in adult muscle (Mishina *et al.*, 1986). Small changes in the biophysical properties of the two nAChR subtypes are observed, where channel conductance is low in foetal muscle ($\alpha 1_2\beta 1\gamma\delta$) and high in adult muscle ($\alpha 1_2\beta 1\varepsilon\delta$) (Mishina *et al.*, 1986).

The nAChRs at the vertebrate neuromuscular junction are situated postsynaptically within the membrane of the muscle endplate. In this location, nAChRs are involved in chemical signalling between motor neurones and the muscle effector cells.

1.1.3 Neuronal nAChRs

In addition to nAChRs of the neuromuscular junction, cholinergic innervation is observed in the brain and the peripheral ganglia (Green *et al.*, 1973; Hunt and Schmidt, 1978). High affinity α-BTX binding sites were identified in the brain and ganglia, but ganglia containing [^{125}I]-α-BTX binding sites also elicit nicotine-induced responses that are not inhibited by the application of α-BTX, suggesting the presence of two different receptors, one that binds α-BTX and one stimulated by nicotine (Patrick and Stallcup, 1977; Carbonetto *et al.*, 1978).

Since the cloning of the first neuronal nAChR subunit from a rat adrenal medulla phaeochromocytoma (PC12) cDNA library (Boulter *et al.*, 1986), twelve vertebrate neuronal-type subunits, designated α2 - α10 and β2 - β4 have been identified and cloned (Sargent, 1993; McGehee and Role, 1995; Elgoyhen *et al.*, 2001) (Table 1.1). The α8 subunit has only been identified in chick (Schoepfer *et al.*, 1990; Sargent, 1993). The α-subunits are classified by the presence of a pair of adjacent cysteine residues that are present in the muscle and *Torpedo* electric organ α subunits (α-Cys192 and α-Cys193 of the electric organ nAChR) and are thought to comprise at least part of the ligand binding site (Kao *et al.*, 1984; Kao and Karlin, 1986; Galzi *et al.*, 1991b) (Section 1.2.3). The non-α subunits (β2, β3 and β4) do not contain this cysteine pair (Lukas *et al.*, 1999).

Neuronal nAChRs show considerable diversity in subunit composition, with evidence for nAChRs containing one, two, or more different subunit subtypes in the pentameric structure (Millar, 2003). Expression of combinations of the different neuronal subunits in heterologous expression systems is one approach used to ascertain the possible subunit composition of native nAChRs.

Rat Subunit	Probe	Number of amino acids	Mr	Reference
α2	chicken α2	484	55.5	Wada *et al.*, 1988
α3	mouse α1	474	54.8	Boulter *et al.*, 1986
α4	rat α3 mouse α1	600	67.1	Boulter *et al.*, 1987 Goldman *et al.*, 1987
α5	rat β3	424	48.8	Boulter *et al.*, 1990
α6	PCR	463	53.3	Lamar *et al.*, 1990
α7	PCR (based on chicken α7 and α8 primers)	480	54.2	Séguéla *et al.*, 1993
α9	rat α7	457	52.0	Elgoyhen *et al.*, 1994
α10	rat α9	423	47.1	Elgoyhen *et al.*, 2001
β2	rat α3	475	54.3	Deneris *et al.*, 1988
β3	rat α3	434	50.2	Deneris *et al.*, 1989
β4	rat β2	475	53.3	Duvoisin *et al.*, 1989; Boulter *et al.*,1990

TABLE 1.1. Summary of the cloned rat nAChR subunits. Adapted from Sargent, 1993. The α8 subunit has only been identified in chicken (Schoepfer *et al.*, 1990).

In the majority of cases, a combination of both α and β subunits appears necessary for assembly of functional nAChRs. When expressed in *Xenopus* oocytes, the α2, α3 and α4 subunits each assemble into functional ion channels upon co-expression with β2 or β4 subunits (Boulter *et al.*, 1987; Ballivet *et al.*, 1988; Deneris *et al.*, 1988; Wada *et al.*, 1988; Sargent, 1993). The α5 subunit does not form functional nAChRs when expressed in pairwise combination with any β subunit (Boulter *et al.*, 1990; Couturier *et al.*, 1990b), but may participate in the formation of nAChRs containing more than two different types of subunit, such as α3β4α5 and α4β2α5 (Millar, 2003). Similarly, while the β3 subunit does not participate in the formation of functional channels when expressed in pairwise combinations of subunits, β3 may participate in nAChR complexes containing more than one type of β subunit, such as α4β2β3β4 nAChRs (Forsayeth and Kobrin, 1997; Boorman *et al.*, 2000; Kuryatov *et al.*, 2000). Heterologous expression of the chick α6 subunit in mammalian cells suggests the formation of functional α6β2 and α6β4 nAChRs (Fucile *et al.*, 1998), while expression of human subunits in *Xenopus* oocytes suggests α6 assembles more efficiently into complexes that contain more than one type of α or β subunit, such as α3β4α6 and α6β2α5 nAChRs (Fucile *et al.*, 1998; Kuryatov *et al.*, 2000). Each heteromeric nAChR subtype appears to be stimulated by the application of nicotine, though none of the aforementioned combinations shows sensitivity to α-BTX (McGehee and Role, 1995; Itier and Bertrand, 2001).

The α7, α8 and α9 subunits are capable of forming homomeric complexes that are sensitive to α-BTX when expressed alone in *Xenopus* oocytes (Couturier *et al.*, 1990a; Séguéla *et al.*, 1993; Elgoyhen *et al.*, 1994; Gerzanich *et al.*, 1994; Gotti *et al.*, 1994). Early studies suggested that the pharmacological properties of the α7 homomer were not affected by the co-injection of any of the α3, α5, β2, β3 or β4 subunits (Couturier *et al.*, 1990b; Séguéla *et al.*, 1993), but more recent data has suggested that *in vivo*, α7 may co-assemble with subunits such as β2, β3 or α5 (Yu and Role, 1998a; Yu and Role, 1998b; Palma *et al.*, 1999b; Khiroug *et al.*, 2002). In the chick nervous system, the α7 and α8 subunits are able to co-assemble to form heteromeric nAChRs in addition to homomeric

nAChRs (Keyser *et al.*, 1993; Gotti *et al.*, 1994; Gotti *et al.*, 1997). The α10 subunit does not form functional ion channels when expressed alone or in combination with any neuronal β subunit in *Xenopus* oocytes, but does appear to co-assemble with the α9 subunit (Elgoyhen *et al.*, 2001; Sgard *et al.*, 2002).

1.2 Structure of nAChRs

1.2.1 Primary structure of subunits

All nAChR subunit sequences contain a signal peptide at the extreme amino-terminal (N-terminal) that is cleaved during translocation to form the mature protein. The large hydrophilic extracellular N-terminal domain of each subunit contains potential sites for asparagine (N)-linked glycosylation (Nomoto *et al.*, 1986). Four hydrophobic stretches of amino acids comprise the putative transmembrane domains and are termed M1 - M4 (Noda *et al.*, 1983b; Sargent, 1993). Each subunit also contains a highly variable hydrophilic domain between M3 and M4 that is exposed to the cytoplasm and contains sites for phosphorylation (Huganir and Greengard, 1990). A short hydrophobic extracellular carboxy terminal region completes each subunit (Figure 1.1).

1.2.2 Subunit stoichiometry and arrangement

The native nAChR of the *Torpedo* electric organ exists predominantly in a "dimeric" form, in which two $\alpha_2\beta\gamma\delta$ nAChRs are cross-linked between δ subunits of adjacent nAChRs by a disulphide bond (Hamilton *et al.*, 1979; DiPaola *et al.*, 1989). The suggested arrangement of subunits in a pentameric ring around the ion pore of the monomer is shown in Figure 1.2 and places the γ subunit in a position between the two α subunits (Karlin *et al.*, 1983; Brejc *et al.*, 2001; Unwin *et al.*, 2002).

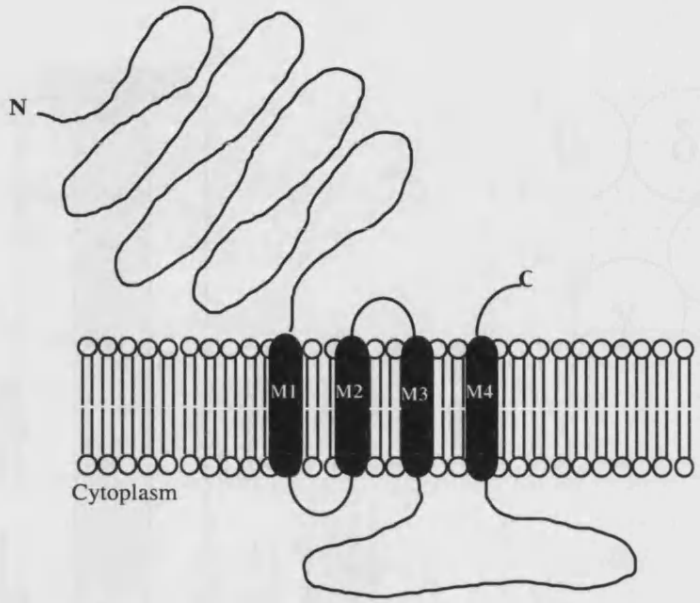

FIGURE 1.1. The predicted topology of the nAChR subunit family. The large hydrophilic extracellular N-terminal domain of each subunit contains potential sites for N-linked glycosylation and, in the case of the α-subunits, is thought to contain the ligand binding site. Four hydrophobic stretches of amino acids comprise the putative transmembrane domains and are termed M1 - M4. Each subunit possesses a highly variable hydrophilic domain exposed to the cytoplasm that contains sites for phosphorylation and a short hydrophobic extracellular carboxy terminal region.

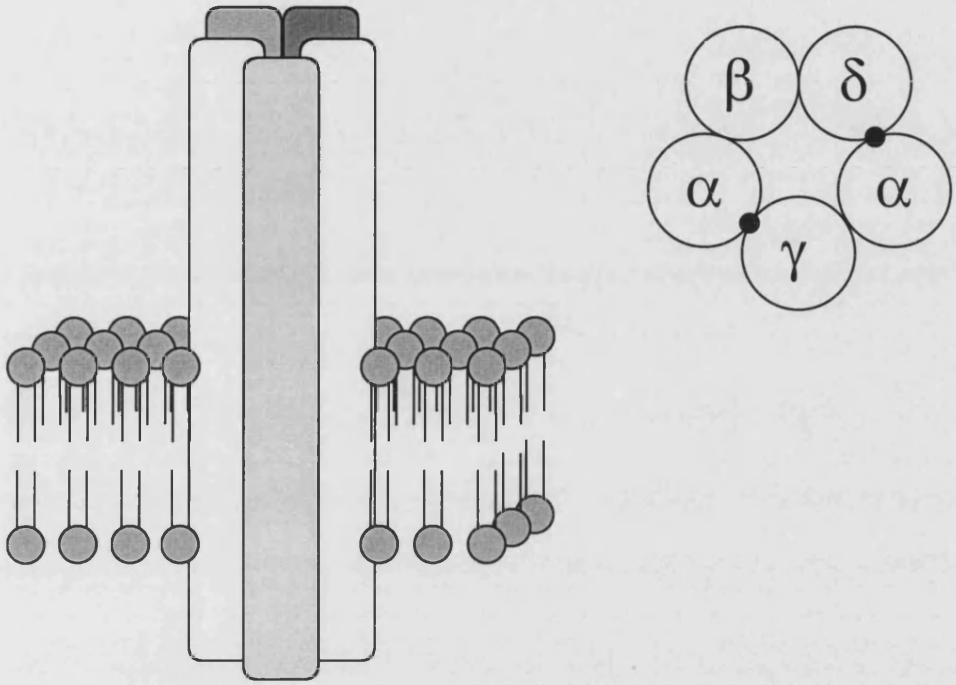

FIGURE 1.2. The structure and predicted stoichiometry of the nAChR of *Torpedo* electric organ and foetal muscle. The four α, β, γ and δ subunits oligomerise to form a pentameric transmembrane glycoprotein with stoichiometry $\alpha_2\beta\gamma\delta$. In adult muscle, the γ subunit is replaced by an ε subunit. The five subunits form a ring around a narrow central pore. The nAChR complex possess two agonist binding sites, represented by black circles, at the α-γ and α-δ subunit interfaces. The predicted order of the subunits around the ion channel pore positions the γ subunit between the two α subunits.

The sediment coefficients and molecular weights of neuronal nAChRs are comparable to those of the muscle-type nAChR, suggesting that neuronal nAChRs also exist as pentamers (Anand *et al.*, 1993b; Sargent, 1993). Immunoprecipitation of [^{35}S]-methionine labelled α4β2 nAChRs expressed in *Xenopus* oocytes, revealed an approximate α4:β2 subunit ratio of 1:1.5, suggesting the stoichiometry of neuronal nAChRs to be $\alpha_2\beta_3$ (Anand *et al.*, 1991). The putative arrangement of the subunits around the ion channel is αβαββ, consistent with the separation of the α subunits by a non-α subunit observed in the muscle-type nAChR, but is complicated by the existence of nAChRs containing more than one type of α or β subunit (e.g. Wang *et al.*, 1996; Gerzanich *et al.*, 1998; Kuryatov *et al.*, 2000). The existence of nAChRs with alternative stoichiometries has also been demonstrated, following expression of varying ratios of α4 and β2 subunits in *Xenopus* oocytes (Zwart and Vijverberg, 1998; Nelson *et al.*, 2003).

1.2.3 The ligand binding site

Affinity labelling of the *Torpedo* electric organ and muscle nAChR complexes localised the ACh-binding sites at the interface between the α subunit and the adjacent non-α subunit (Galzi *et al.*, 1991b; Changeux *et al.*, 1998; Taylor *et al.*, 2000). The muscle-type nAChR, with composition $\alpha_2\beta\gamma\delta$, contains two non-identical ligand binding sites at the interfaces between the α subunit and either the γ or δ subunit (Pederson and Cohen, 1990). Expression of pairwise combinations of muscle subunits in fibroblast cells revealed the assembly of αγ and αδ complexes able to bind the nicotinic antagonist, *d*-tubocurarine with differing affinities (Blount and Merlie, 1989). Residues from both the α and non-α subunit thus appear to contribute to the formation of the ligand binding site (Reynolds and Karlin, 1978; Neubig and Cohen, 1979; Pederson and Cohen, 1990). Expression of the α subunit alone or in combination with the β subunit does not produce high affinity binding sites for either ACh or *d*-tubocurarine (Kurosaki *et al.*, 1987; Blount and Merlie, 1988; Pederson and Cohen, 1990).

With a stoichiometry of $\alpha_2\beta_3$, heteromeric neuronal nAChRs would also contain two ligand binding sites at the interfaces between the α and non-α subunits. In the homomeric α7, α8 and α9 nAChR complexes, assembly of five α subunits provides five α-α subunit interfaces and five putative ligand binding sites (Wang *et al.*, 1996). Assembly of five ligand binding sites in the formation of homomeric α7 nAChRs was suggested by kinetic studies using the potent α7 nAChR antagonist, methyllycaconitine (MLA), an insecticide from the seeds of *Delphinium brownii* (Palma *et al.*, 1996). Inhibition of the α7 nAChR by MLA and the recovery from this block are best described by a five-site model, while the block of α4β2 nAChRs is best suited to a two-site model (Palma *et al.*, 1996).

Six loops, designated A - F, have been identified within the nAChR complex that are important for the formation of the ACh-binding site (Kao and Karlin, 1986; Galzi *et al.*, 1990; Czajkowski *et al.*, 1993; Fu and Sine, 1994; Corringer *et al.*, 1995; Martin *et al.*, 1996; Prince and Sine, 1996). The α subunit possesses the primary components of the ligand binding site and contains loops A, B and C, while the D, E and F loops are present at the subunit adjacent to the α subunit forming the ligand binding interface (Figure 1.3). Tyrosine residues and two cysteine residues are thought to be important in ligand binding. The electron-rich side chains of the tyrosine residues may interact with the diffuse positive charge of the quarternary ammonium group found in ACh (Dougherty and Stauffer, 1990; Galzi *et al.*, 1990).

Affinity labelling experiments have identified several residues within the A - F loops. For example, 4-(*N*-maleimido)benzyltri[^{3}H]-methylammonium iodide ([^{3}H]-MBTA), which competes with ligand for the binding site, was used to label Cys192 and Cys193 of the *Torpedo* electric organ nAChR α subunit (Kao *et al.*, 1984). Labelling with *p*-(*N,N*-dimethyl)aminobenzenediazonium fluoroborate (DDF) identified α-Trp86 and α-Tyr93 (in the A loop), α-Trp149 (in the B loop) and α-Tyr190 and α-Tyr198 (in the C loop) (Galzi *et al.*, 1991b; Galzi and Changeux, 1995). In the D loop, γ-Trp55 and δ-

Trp57 were labelled with nicotine and *d*-tubocurarine (Chiara *et al.*, 1998), while δ-Asp180 (in the F loop) was implicated in radioligand binding through mutation of this residue to asparagine, which caused a reduced affinity for ACh (Martin *et al.*, 1996).

The residues identified in loops A - C are conserved in all of the identified α subunits except α5, which does not contain tyrosine residues at positions analogous to α-Tyr93 or α-Tyr190 of *Torpedo* electric organ nAChR subunits (Boulter *et al.*, 1990; Couturier *et al.*, 1990b). The atypical α5 subunit may serve a more structural role associated with non-α subunits, assuming the position of the muscle-type β1 subunit in nAChR complexes that contain more than one α subunit (Ramirez-Latorre *et al.*, 1996; Wang *et al.*, 1996; Kuryatov *et al.*, 2000). The residues labelled in the D loop are conserved in the neuronal β2, β4, α7 and α8 subunits, such that the α7 subunit carries both the principal and complementary components of the ligand binding site (Corringer *et al.*, 2000). Mutation of the conserved Trp54, Tyr92, Trp149 and Tyr188 residues in the α7 subunit results in a reduction of the apparent affinity of the nAChR for agonists and competitive antagonists, demonstrating the involvement of these residues in ligand binding (Galzi *et al.*, 1991a; Corringer *et al.*, 2000).

Agonist affinities of nAChRs are dependent upon the subunit composition of the receptor, consistent with the involvement of residues from both the α subunit and its adjacent subunit in the formation of the ligand binding site (Parker *et al.*, 1998). Identification of conserved residues suggests amino acids essential in the formation of a ligand binding site, while the residues that differ between subunits must be responsible for the differences in pharmacology of each nAChR subtype. For example, mutation of residues within the D loop of the β2 subunit to the corresponding residues of the β4 subunit sequence, resulted in lower affinities for ACh and nicotine when the mutated β2 subunit was co-expressed with α2 in *Xenopus* oocytes (Parker *et al.*, 2001), compared to wild-type α4β2 nAChRs.

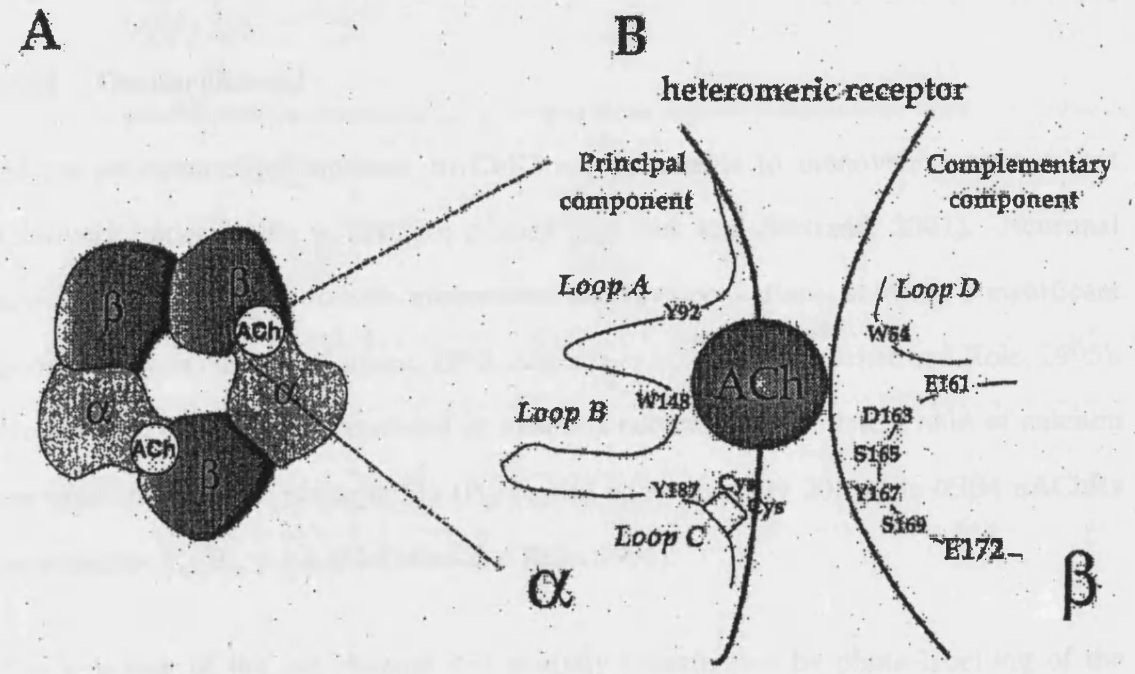

FIGURE 1.3. Model of the nAChR ligand binding domain. (*A*) Heteropentameric complex of neuronal nAChR α and β subunits. The ACh-binding site is located at the interface between the α subunit and the adjacent β subunit. (*B*) Representation of the principal component (α subunit), with its three loops, A, B and C and two of the loops (D and E) from the complementary component (β subunit) of the ligand binding site. Each loop is modelled with the principal amino acids identified within the chick α7 subunit. Adapted from Itier and Bertrand, 2001.

Whilst competitive nicotinic antagonists, such as α-BTX and MLA, probably interact at the agonist binding site, they are also thought to interact with additional residues outside of the A - F loops (Galzi *et al.*, 1991b; Sine, 1993). Neurotoxins, such as α-BTX, are highly flexible molecules with little secondary structure, so a large proportion of the toxin may be involved in binding to the nAChR, with parts of the toxin reaching down from the crest of the nAChR molecule to the agonist binding site (Stroud *et al.*, 1990).

1.2.4 The ion channel

At the neuromuscular junction, nAChRs are permeable to monovalent cations, but relatively impermeable to divalent cations (see Itier and Bertrand, 2001). Neuronal nAChRs are permeable to both monovalent and divalent cations, showing a significant permeability to calcium (Sargent, 1993; Séguéla *et al.*, 1993; McGehee and Role, 1995). Homomeric α7 nAChRs expressed in *Xenopus* oocytes demonstrate a ratio of calcium permeability: sodium permeability (P_{Ca}/P_{Na}) of approximately 20, while α3β4 nAChRs demonstrate $P_{Ca}/P_{Na} = 1.1$ (McGehee and Role, 1995).

The structure of the ion channel was initially investigated by photo-labelling of the muscle-type nAChR using non-competitive, open channel blockers, such as chlorpromazine, and suggested that the second putative transmembrane domain (M2) formed the lining of the ion channel (Giraudat *et al.*, 1986; Hucho *et al.*, 1986; Revah *et al.*, 1990; Stroud *et al.*, 1990). Evidence that M2 exists as an α-helix has been provided by electron microscopy of crystalline postsynaptic membranes of electric organ (Unwin, 1993; Miyazawa *et al.*, 2003) (Section 1.2.5). In an α-helical conformation, M2 is amphipathic, with an abundance of serine and threonine residues pointing towards the ion channel lumen. Chlorpromazine labels residues corresponding to α-Thr244, α-Ser248, α-Leu251, α-Val255 and α-Glu262 of M2 (Giraudat *et al.*, 1986; Hucho *et al.*, 1986; Revah *et al.*, 1990). Conservation of these residues across the different subunits within the pentameric nAChR, produces rings of residues with similar charge, side chain size or hydrophobicity within the lumen of the ion channel (Figure 1.4).

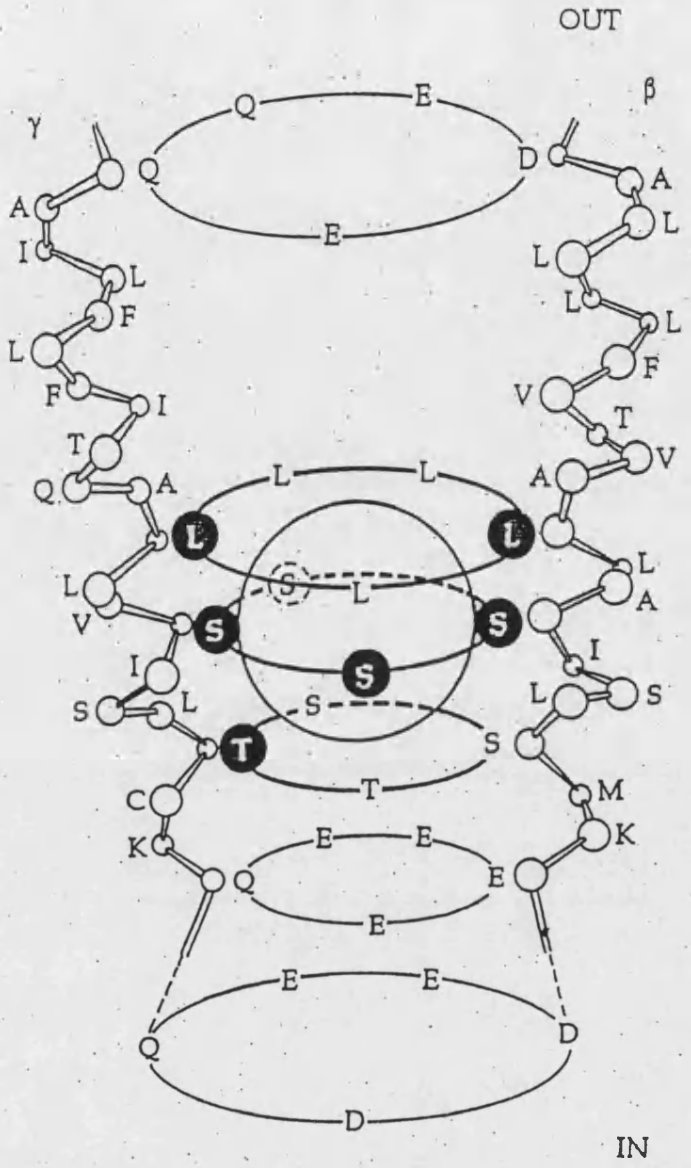

FIGURE 1.4. A model of the high affinity binding site of the open channel blocker, chlorpromazine. The sphere represents the space occupied by chlorpromazine. The M2 domains of the β and γ subunits are arranged as transmembrane α-helices, depicting the α-carbons of the indicated amino acids. The filled circles represent three rings of amino acids within the M2 domain of each nAChR subunit photolabelled by [^{3}H]-chlorpromazine Rings of negatively charged subunits are located at either end of the putative channel pore and have been implicated in ion transport following mutagenesis experiments. Taken from Revah *et al.*, 1990.

A ring of conserved leucine residues located near the centre of the lipid bilayer may be involved in the formation of the channel gate (Miyazawa *et al.*, 1999; Miyazawa *et al.*, 2003). Leu247 of the neuronal α7 subunit, is thought to be located close to the channel selectivity filter in a section of the ion channel that should demonstrate high conformational flexibility (Miyazawa *et al.*, 1999). Mutation of α7-Leu247 to polar serine or threonine residues dramatically alters the ion channel properties, creating a 200-fold increase in the sensitivity of the nAChR to ACh, a loss in desensitisation and changes in nAChR pharmacology, where competitive antagonists behave as agonists (Revah *et al.*, 1991; Bertrand *et al.*, 1992; Palma *et al.*, 1999a). The mutation converts the high affinity closed desensitised state into a state that conducts ions, implicating the leucine ring in the permeability of the ion channel when the nAChR is in a desensitised state (Revah *et al.*, 1991; Bertrand *et al.*, 1992).

Rings of negative charge at either side of M2 (at α-Glu259 and α-Glu280) may attract cations to the entrance of the channel, as mutation of the residues at the inner or outer mouth of M2 affects the ion selectivity of the channel pore (Imoto *et al.*, 1988; Galzi *et al.*, 1992). Mutation of the well conserved glutamate residue at the cytoplasmic end of M2 of the neuronal α7 subunit (E237A) reduces Ca^{2+} permeability by 1000-fold, but does not alter permeability to monovalent cations (Galzi *et al.*, 1992; Bertrand *et al.*, 1993). This suggests that the presence of a residue with negatively charged side chains is essential for the high calcium permeability of neuronal nAChRs and is critical for cation selectivity (Imoto *et al.*, 1988; Galzi *et al.*, 1992). Substitution of amino acids of the chick α7 subunit with corresponding residues from $GABA_A$ or glycine receptor subunits produced a conversion of ion selectivity from cationic to anionic (Galzi *et al.*, 1992; Corringer *et al.*, 1999). The α7-E237A mutation is necessary but not sufficient for the conversion of anion selectivity (requiring introduction of alanine or proline residues to the putative selectivity filter region), suggesting that the ring of negative charge at the cytoplasmic end of M2 may also provide a barrier to chloride ions (Corringer *et al.*, 2000).

1.2.5 The 3-Dimensional structure of the nAChR

The extremely high density and regular arrangement of nAChRs in the *Torpedo* electric organ allowed the structure of the electric organ nAChR to be analysed by electron microscopy following preservation of the structure by rapid freezing (see Toyoshima and Unwin, 1990; Unwin, 1993; Miyazawa *et al.*, 1999). The structure of the nAChR shown at a resolution of 17 Å (Toyoshima and Unwin, 1990; Unwin *et al.*, 2002) revealed a pseudo-5-fold symmetry of subunits seen as rods ~ 120 Å long and 20 Å wide, arranged around a narrow central pore that spans the membrane. The nAChR extends ~ 65 Å above the extracellular surface of the membrane, while the extension below the membrane into the interior of the cell is shorter (15 Å) and associated with an underlying density, attributed in part to interaction of the intracellular loop region of the nAChR with rapsyn, a 43 kDa protein involved in muscle-type nAChR clustering (Sealock, 1982; Moransard *et al.*, 2003) (see Section 1.5.4). The ACh-binding sites are located at ~ 30 Å above the surface of the cell membrane and the channel gate is thought to lie deep within the ion channel, 15 Å from the surface of the cytoplasmic membrane (Unwin, 1993; Miyazawa *et al.*, 1999; Tierney and Unwin, 2000). The predicted topology of the channel includes a wide opening (25 Å) in the extracellular domain, with the channel becoming gradually narrower to a point of constriction, becoming wider again at the intracellular domain (see Itier and Bertrand, 2001).

Recently, an ACh-binding protein (ACh-BP), released from glial cells of the snail *Lymnaea stagnalis* and involved in modulation of synaptic transmission through ACh binding, has been identified and its crystal structure resolved at 2.7 Å (Brejc *et al.*, 2001; Smit *et al.*, 2001). The ACh-BP forms homopentameric structures that closely resemble the N-terminal domain of nAChRs, containing many of the conserved residues involved in ligand binding (such as the vicinal cysteine residues) and able to bind nicotinic ligands including ACh, α-BTX, nicotine and epibatidine. The ACh-BP does not possess the transmembrane or intracellular domains observed in nAChRs, but has been used to gain

insights into the nAChR ligand binding domain (Brejc *et al.*, 2001). The ACh-BP crystal structure supports the biochemical analysis of the nAChR ligand binding site, revealing the sites within a cleft formed by a series of A - C loops from the face of one subunit and a series of β-strands contributing to loops E - F from the face of the adjacent subunit (Brejc *et al.*, 2001).

The most recent structural analysis of the *Torpedo* electric organ nAChR reveals the receptor structure at 4 Å (Miyazawa *et al.*, 2003) and suggests that the four transmembrane domains exist in the form of α-helices. The M2 helices of each of the five subunits form the lining of the pore, while the M1, M3 and M4 helices form an outer lipid-facing scaffold (Miyazawa *et al.*, 2003). The M2 α-helix contains a kink near the centre of the membrane at α-Pro265 that tilts the helix outwards, away from the pore, on either side. A kink in the vicinity of the conserved leucine residue (α-Leu251; Section 1.2.4), observed as a narrow strip of density in the structure of the closed-channel form of the nAChR, probably represents the channel gate (Unwin, 1993; Miyazawa *et al.*, 1999). At its narrowest point, at α-Leu251 and α-Val255 and over an 8 Å long hydrophobic stretch extending to α-Val259, the 6 - 7 Å diameter of the pore provides an energetic barrier to restrict the passage of monovalent ions (with an effective diameter of 8 Å) that cannot lose their first hydration shell without the presence of a polar surface (Miyazawa *et al.*, 2003).

The structure of each of the α subunits appears to be modified by its interaction with the neighbouring subunits and upon binding of ACh (Unwin *et al.*, 2002). Before ligand binding, the α subunits exist in a conformation that differs from the non-α subunits and this distorted configuration may result from subunit-subunit interactions. Upon ACh binding, the α subunits overcome the distortion and relax to switch configuration to that of the non-α subunits, so that the activated nAChR complex demonstrates a more symmetrical form (Unwin *et al.*, 2002). The conformational change involves a 15 - 16° clockwise rotation of the α subunit polypeptide chains on the inner surface of the

vestibule next to the central pore. The M2 pore-lining region and the M2 - M3 loop are both located close to the rotating polypeptide chains, so the switch in configuration could undermine the channel gate, pulling apart the weak interactions between the side chains of residues within M2, causing the pore to open (Unwin *et al.*, 2002; Miyazawa *et al.*, 2003).

1.3 The nAChR as an allosteric protein

There are four putative inter-convertible, functionally distinct conformational states in which nAChRs can exist (Lena and Changeux, 1993; Edelstein *et al.*, 1996). In the resting state (R), the ion channel is closed. In the activated state (A), the channel opens following ligand binding and demonstrates a low affinity for ACh (K_d of the *Torpedo* electric organ nAChR = 60 - 100 μM). During prolonged periods of agonist exposure, the nAChR is converted from the A state to a closed intermediate state of desensitisation (I), in which the affinity for ACh is higher than in the A state (K_d = 10 μM). A closed channel desensitised state (D) that exhibits a high affinity for ACh (K_d = 10 nM) and nicotinic ligands, leads to a progressive reduction in the number of nAChRs in the active state and a decline of the agonist-evoked current (Galzi and Changeux, 1995).

In an allosteric model of receptor function, the nAChR can change state spontaneously in the absence of ligand, though the probability of spontaneous channel activation is very low. Ligand binding to the ACh binding site or other allosteric sites modifies the equilibrium that exists between the different conformational states, probably by stabilising the state to which the ligand preferentially binds (Lena and Changeux, 1993; Edelstein *et al.*, 1996). Prolonged exposure to agonist causes nAChR desensitisation, a slow and reversible decline in the amplitude of the response that follows channel activation. Longer exposure to agonist permits slower rates of desensitisation, achieving longer lasting states of desensitisation (Dani, 2001). At the neuromuscular junction, ACh is cleared from the synaptic cleft in a few hundred microseconds by AChE or in a

few milliseconds by diffusion (Jones and Westbrook, 1996). Therefore, under normal physiological conditions, desensitisation may have little impact on cholinergic transmission. It may, however, become relevant in the brains of smokers, where tobacco smoking may cause levels of nicotine to build to a low steady concentration. In the brains of smokers, chronic exposure to nicotine creates a deficit in cholinergic receptor function following nAChR desensitisation that appears to be countered by an upregulation of receptor number (Olale *et al.*, 1997) (see Section 1.6.3).

1.4 Distribution and subunit composition of native neuronal nAChRs

Neuronal nAChRs are frequently classified into α-BTX-sensitive and α-BTX-insensitive sites. The nAChRs insensitive to α-BTX bind the nicotinic ligands, ACh, nicotine and cytisine with higher affinity and the majority of these sites appear to contain α4 and β2 subunits (Whiting *et al.*, 1987a; Zoli *et al.*, 1998). Heteromeric nAChRs containing α3 and β4 subunits appear to comprise the major α-BTX-insensitive nAChR subtype of the ganglia (Flores *et al.*, 1996). In the mammalian brain, high affinity [^{125}I]-α-BTX binding sites correspond to α7-containing nAChRs and transgenic mice with a homozygous null mutation for the α7 subunit do not contain [^{125}I]-α-BTX binding sites (Séguéla *et al.*, 1993; Orr-Urtreger *et al.*, 1997; Paterson and Nordberg, 2000). Receptors containing the α8 subunit are also sensitive to α-BTX, but have only been identified in the chicken (Britto *et al.*, 1992; Keyser *et al.*, 1993).

1.4.1 α-BTX-insensitive nAChR subtypes of the central nervous system

The major high affinity nAChR subtype in the central nervous system is thought to contain α4 and β2 subunits (Whiting *et al.*, 1987a; Flores *et al.*, 1992; Zoli *et al.*, 1998). High levels of mRNA corresponding to the α4 gene product are observed in the cortex and cerebellum, while β2 expression is fairly homogeneous in human brain (Paterson and Nordberg, 2000). A monoclonal antibody raised against the neuronal β2 subunit,

mAb270 was used to immunoprecipitate more than 90% of the high affinity [^{3}H]-nicotine binding sites from solubilised chick brain extracts (Whiting and Lindstrom, 1986; Nef *et al.*, 1988; Schoepfer *et al.*, 1988). Subunits of 79 kDa from rat brain and 75 kDa from chick brain, identified as α4, were also precipitated using mAb270 (Whiting *et al.*, 1987b; Whiting *et al.*, 1987c; Nef *et al.*, 1988).

The effects of genes corresponding to nAChR subunits have also been investigated using transgenic mice. Deletion of the gene encoding the β2 subunit leads to the complete loss of high affinity nicotinic-binding sites in the mouse brain (Picciotto *et al.*, 1995). Similarly, [^{3}H]-nicotine and [^{3}H]-epibatidine binding sites observed in the cortex or hippocampus of wild-type mice, are not detectable in mice lacking the α4 subunit ($\alpha4^{-/-}$) (Marubio and Changeux, 2000), providing further evidence for the role of α4 and β2 subunits in the major brain nAChR subtype. Minor populations of non-α4-containing nicotinic binding sites remain in brain regions such as the substantia nigra of $\alpha4^{-/-}$ mice and may correspond to α3- or α6-containing nAChRs (Marubio and Changeux, 2000).

In human thalamus, α3-containing nAChRs may correspond to the [^{3}H]-nicotine and [^{3}H]-cytisine binding observed (Paterson and Nordberg, 2000). Lower levels of α3 expression are observed in most cortical regions and the hippocampus (Paterson and Nordberg, 2000). Neuronal bungarotoxin (n-BTX) binds with high affinity to α3β2-type nAChRs (Luetje *et al.*, 1990; Cartier *et al.*, 1996) and [^{125}I]-n-BTX binding sites are observed in rat brain regions including the hypothalamus, ventral tegmental area (VTA) and substantia nigra. Distribution of the α2 subunit is fairly restricted in rat brain, with expression at high levels seen only in the interpenduncular nucleus of the brainstem (Wada *et al.*, 1989). The α5 subunit is most abundant in the human cortex, but has also been observed in post-mortem brain tissue of the medulla oblongata, pons, cerebellum and spinal cord (Paterson and Nordberg, 2000). Expression of α6 is observed in limited brain areas, such as the substantia nigra and VTA, frequently observed with β3 subunits (Goldner *et al.*, 1997; Le Novère *et al.*, 1999). The β3 subunit is also expressed in areas

of rat brain such as the reticular nucleus of thalamus (Deneris *et al.*, 1989), while β4 is expressed in most areas of rat cerebellum and striatum (Forsayeth and Kobrin, 1997). Overlapping expression patterns of α3 and β4 further suggests the co-assembly of these subunits (Flores *et al.*, 1996).

Immunoprecipitation with subunit-specific antibodies has been used to investigate the receptor subtypes present in the central nervous system. Such studies have, for example, suggested the presence of α2β2α5 nAChR complexes in chick optic lobe (Balestra *et al.*, 2000). Immunodepletion studies with extracts of chick brain indicate a major population of α4β2 nAChRs, with a smaller fraction of complexes also containing the α5 subunit (Conroy and Berg, 1998). Immunoprecipitation of brain extracts using antibodies generated against the cytoplasmic domains of the β3 and β4 subunits, demonstrate the co-assembly of both subunits with α4β2 in the cerebellum (Forsayeth and Kobrin, 1997). Therefore, a small proportion of α4β2β3β4 nAChRs appear to exist *in vivo* and this form of receptor complex is reminiscent of the muscle-type nAChR, in which the two α subunits interact with three different non-α subunits. In the central nervous system of the chick, β3 is expressed at the highest levels in the retina. Immunoprecipitation data suggest that β3 participates in two main populations of nAChR in this area, the first containing α6 and β4 subunits and the second, containing α2, α3, α4, β2 and β4 subunits (Vailati *et al.*, 2000). Loss of epibatidine binding from the striatum of $\beta3^{-/-}$ mice implicates the β3 subunit in striatal nAChRs, where it has been suggested to co-assemble into complexes also containing α6 and β2 subunits (Cordero-Erausquin *et al.*, 2000).

1.4.2 α-BTX-insensitive nAChR subtypes of the ganglia

Chick ciliary ganglia have been studied widely and RNase protection assays have shown that α3, α5, β2 and β4 (as well as α7, which forms α-BTX sensitive nAChRs) are expressed in these cholinergic neurones (Corriveau and Berg, 1993; Mandelzys *et al.*, 1994). Embryonic chick ciliary neurones show expression of at least four different

nAChR subtypes, containing: (i) α3, α5 and β4, (ii) α3, α5, β2 and β4, (iii) α7, (iv) a nAChR of unknown composition (Conroy *et al.*, 1992; Vernallis *et al.*, 1993; Conroy and Berg, 1995; Pugh *et al.*, 1995). Little, if any α4 is present, so the β2 in ciliary ganglia appears to co-assemble with α3, β4 and α5 subunits (Conroy and Berg, 1995). Neonatal rat sympathetic ganglia express α3, α5, (α7), β2 and β4, but not α2 or β3 (Corriveau and Berg, 1993; Zoli *et al.*, 1995), while α4 mRNA is seen in adult rats (Rust *et al.*, 1994).

1.4.3 α-BTX sensitive nAChRs in the brain and ganglia

Sites identified by [^{125}I]-α-BTX binding appear to closely parallel the expression of α7 mRNA in the rat brain (Clarke *et al.*, 1985; Séguéla *et al.*, 1993). Transgenic $\alpha7^{-/-}$ mice do not contain high affinity [^{125}I]-α-BTX binding sites, while the levels of [^{3}H]-nicotine binding sites remain unchanged in comparison to wild-type animals (Orr-Urtreger *et al.*, 1997). The levels of [^{125}I]-α-BTX binding sites are unaltered in the brains of $\alpha4^{-/-}$ or $\beta2^{-/-}$ mice in comparison to binding sites observed with wild-type animals (Zoli *et al.*, 1998; Marubio *et al.*, 1999).

In the human brain, α7 mRNA is detected at high levels in the hippocampus, brainstem, olfactory regions, amygdala and hypothalamus, with lower density in the cortex and cerebellum and only very low levels in the thalamus (Paterson and Nordberg, 2000). Expression of α7 mRNA is also observed widely within the peripheral ganglia (Rust *et al.*, 1994). In chick brain, three classes of α-BTX sensitive nAChRs are suggested, with the majority (approximately 70%) comprising α7 homomers and 20% composed of α7α8 heteromers (Gotti *et al.*, 1994). These proportions differ in chick retina, where the major nAChR subtype (50 - 70%) comprises α8 homomers, with 10 - 17% α7α8 heteromers and 14 - 27% α7 homomers (Keyser *et al.*, 1993; Gotti *et al.*, 1997).

1.4.4 The nAChR of the inner ear

Expression of the α9 and α10 subunits is largely restricted to the hair cells of the inner ear and neither subunit is observed in the central nervous system (Elgoyhen *et al.*, 1994; Hiel *et al.*, 1996; Elgoyhen *et al.*, 2001; Lustig *et al.*, 2001). Homomeric α9 and heteromeric α9α10 nAChRs, characterised upon expression in *Xenopus* oocytes, demonstrate a pharmacological profile unique among nAChRs that, consistent with their distinct localisation in cochlea hair cells, means that nAChRs containing α9 and α10 do not fall conveniently into the conventional classification of either muscle-type or neuronal nAChRs (Elgoyhen *et al.*, 1994; Rothlin *et al.*, 1999; Verbitsky *et al.*, 2000; Elgoyhen *et al.*, 2001). This unique profile (Sections 1.5.1 and 4.5) includes antagonism by α-BTX, strychnine and atropine and resembles that of the native cholinergic receptor of cochlea hair cells (Elgoyhen *et al.*, 1994; Guth and Norris, 1996; Rothlin *et al.*, 1999; Jagger *et al.*, 2000; Verbitsky *et al.*, 2000; Elgoyhen *et al.*, 2001).

1.5 Heterologous expression of nAChRs

In 1981, a decisive experiment demonstrated the expression and assembly of recombinant nAChRs of the *Torpedo* electric organ in *Xenopus* oocytes (Sumikawa *et al.*, 1981). When mRNA isolated from the *Torpedo* electric organ was injected into oocytes, the α, β, γ and δ subunits underwent correct post-translational modification events including glycosylation and removal of signal peptides from each subunit (Sumikawa *et al.*, 1981). Subsequent experiments revealed cell surface receptors that formed functional ion channels with properties resembling those of the native *Torpedo* electric organ nAChRs (Barnard *et al.*, 1982).

The *Xenopus* oocyte has been used widely as a heterologous expression system for the characterisation of both muscle-type and neuronal-type nAChRs. Injecting oocytes with known combinations of neuronal subunit cDNA or mRNA permits comparison with

native nAChRs, aiding the elucidation of nAChR composition. However, the usefulness of the oocyte as an expression system is limited for investigation of nAChRs by techniques such as radioligand binding, where heterologous expression in cultured mammalian cell lines may be more appropriate. In these cell lines, much larger quantities of protein can be generated and both transient and stable expression of nAChR protein can be accomplished. Mammalian cell lines may also provide an environment for nAChR expression that more closely resembles the native environment, compared to that provided by the *Xenopus* oocyte.

1.5.1 Characteristics of recombinant neuronal nAChRs

Analysis of pairwise combinations of neuronal subunits in heterologous expression systems has demonstrated differences in the pharmacological profiles of certain nAChR subtypes. A comprehensive study comparing the properties of recombinant α2β2, α2β4, α3β2, α3β4, α4β2 and α4β4 nAChR subtypes in *Xenopus* oocytes, suggested that the agonist profiles are affected by the nature of both the α and the β subunit, with the β subunit exerting the greatest influence (Parker *et al.*, 1998). For example, the affinity of each subtype for [^{3}H]-epibatidine differs, where the K_d values for α2β2, α2β4 and α4β2 nAChRs are 10.3±1.1 pM, 86.8±9.4 pM and 30.0±3.9 pM, respectively (Parker *et al.*, 1998).

Nicotine is a partial agonist of human α3β2 nAChRs and a full agonist of α3β4 nAChRs (Wang *et al.*, 1996; Wang *et al.*, 1998), while conotoxin MII specifically antagonises α3β2, but not α3β4 nAChRs (Cartier *et al.*, 1996; Wang *et al.*, 1996; Wang *et al.*, 1998). The α3β2 nAChRs also desensitise more rapidly than the α3β4 subtype and exposure to chronic nicotine induces efficient upregulation of α3β2, but not α3β4 nAChRs (Wang *et al.*, 1998). In *Xenopus* oocytes, the α5 subunit co-assembles efficiently with α3β2 and α3β4 nAChRs (Wang *et al.*, 1998), causing increases in the rates of desensitisation and the permeability to Ca^{2+} ions (Gerzanich *et al.*, 1998).

The α5 nAChR subunit also efficiently co-assembles with α4β2 in *Xenopus* oocytes causing an increase in the rate of desensitisation, a decreased sensitivity to ACh and a higher single channel conductance (Ramirez-Latorre *et al.*, 1996). Nicotinic receptors that contain α4 are distinguished by their high affinity for nicotine and their susceptibility to nicotine-induced upregulation and functional inactivation (Flores *et al.*, 1992; Peng *et al.*, 1994; Hsu *et al.*, 1996; Olale *et al.*, 1997).

Following pairwise expression of the α6 subunit with β subunits in *Xenopus* oocytes or mammalian cells, α6 assembles relatively inefficiently with β2 or β4 and not at all with β3 (Gerzanich *et al.*, 1997; Fucile *et al.*, 1998). However, α6-containing nAChRs appear to assemble much more efficiently with β2 or β4 when α3, α4 or α5 are also included (Fucile *et al.*, 1998; Kuryatov *et al.*, 2000).

Homomeric α7 and α8 ion channels expressed in *Xenopus* oocytes are highly permeable to calcium and undergo rapid desensitisation in the presence of agonist (Séguéla *et al.*, 1993; Gerzanich *et al.*, 1994). The M2 region of these two subunits show 100% sequence homology and agreeably, the ion permeabilities of the homomers are similar. However, pharmacological differences are observed, with α8 homomers generally appearing more sensitive to agonists and less sensitive to antagonists than the α7 nAChRs (Gerzanich *et al.*, 1994).

The ion channel properties of the α9 homomer are unaffected by the co-injection of any neuronal β subunit, but α9 appears to co-assemble with the α10 subunit (Elgoyhen *et al.*, 2001; Sgard *et al.*, 2002). Homomeric α9 and heteromeric α9α10 nAChRs expressed in *Xenopus* oocytes are activated by ACh and blocked reversibly by α-BTX, but also demonstrate a unique pharmacological profile that is neither classically nicotinic nor muscarinic (Elgoyhen *et al.*, 1994; Rothlin *et al.*, 1999; Verbitsky *et al.*, 2000; Elgoyhen *et al.*, 2001; Sgard *et al.*, 2002). 1,1-Dimethyl-4-phenlypiperazinium (DMPP) and the muscarinic agonist oxotremorine M, act as partial agonists, while nicotine inhibits ACh-

induced currents in *Xenopus* oocytes injected with α9 (Elgoyhen *et al.*, 1994; Elgoyhen *et al.*, 2001). The α9-containing nAChRs are also sensitive to the nicotinic antagonist, *d*-tubocurarine, the glycine receptor antagonist, strychnine, the $GABA_A$ receptor antagonist, bicuculline and the muscarinic receptor antagonist, atropine (Elgoyhen *et al.*, 1994; Rothlin *et al.*, 1999; Verbitsky *et al.*, 2000; Elgoyhen *et al.*, 2001). The nAChRs containing α9 desensitise rapidly and exhibit a very high permeability to calcium ions (Katz *et al.*, 2000; Elgoyhen *et al.*, 2001; Weisstaub *et al.*, 2002).

1.5.2 Comparison of native and recombinant nAChRs

Heterologous expression is a useful tool for the characterisation of nAChRs, but while the profiles of many recombinant nAChRs resemble those of native nAChRs, the profiles are not identical (Sivilotti *et al.*, 2000). Where variations in experimental technique do not account for the alternative profiles, these differences may reflect the influence of the cellular environment or heterogeneity of either the recombinant or native nAChRs. For example, when expressed in *Xenopus* oocytes, the *Torpedo* electric organ nAChR occurs only as pentameric nAChR units and not in the "dimeric" form cross-linked by a disulphide bond between the δ subunits observed with the native nAChR (Sumikawa *et al.*, 1981; DiPaola *et al.*, 1989).

The pharmacological profiles of the chick α7 and α8 homomeric ion channels expressed in *Xenopus* oocytes correlate well with the α-BTX sensitive nAChRs identified in chick optic lobe (Anand *et al.*, 1993a; Anand *et al.*, 1993b; Gotti *et al.*, 1994; Gotti *et al.*, 1997), but there are several differences observed in the ligand profile (Anand *et al.*, 1993b). For example, the recombinant α7 homomers demonstrate a 50-fold higher affinity for cytisine than the α7-containing nAChRs of embryonic chick brain (Anand *et al.*, 1993b). In addition, differences exist between the single channel conductance of α7 nAChRs in different expression systems, where two conductance states are observed in a mammalian cell line expressing α7 (19-23 pS and 32-45 pS) (Ragozzino *et al.*, 1997),

while only one conductance state is observed in *Xenopus* oocytes injected with α7 (45 pS) (Revah *et al.*, 1991; Bertrand *et al.*, 1992a). The rat adrenal medulla phaeochromocytoma PC12 cell line endogenously expresses α3, α4, α5, α7 and β4 subunits (Blumenthal *et al.*, 1997; Virginio *et al.*, 2002). The pharmacology of the α7-containing nAChR expressed in PC12 cells resembles that of recombinant α7 nAChRs expressed in the rat pituitary tumour-derived cell line, GH_4C_1 (which expresses only β4), with the same sensitivity for choline, MLA and dihydro-β-erythroidine (DHβE). However, using the open channel blocker, mecamylamine, a heterogeneous population of nAChRs was demonstrated in the PC12 cell line, while GH_4C_1 cells appeared to express only a single nAChR population (Virginio *et al.*, 2002).

Differences between native and recombinant nAChRs suggest that the α7 subunit may co-assemble with other nicotinic subunits *in vivo* (Anand *et al.*, 1993b; Yu and Role, 1998b; Yu and Role, 1998a; Palma *et al.*, 1999b; Crabtree *et al.*, 2000; Khiroug *et al.*, 2002; Virginio *et al.*, 2002). For example, α7 and β2 subunits were co-precipitated from transiently transfected kidney cells and functional α7β2 heteromers have been observed in *Xenopus* oocytes that demonstrate slower rates of desensitisation and differences in agonist sensitivity in comparison to α7 homomers (Khiroug *et al.*, 2002).

1.5.3 Influence of the host cell environment

The nature of the host cell environment is able to significantly affect the appropriate folding, assembly and cell surface expression of nAChRs and has been clearly demonstrated by observing expression of homomeric α7 and α8 nAChRs in mammalian cell lines (Blumenthal *et al.*, 1997; Cooper and Millar, 1997; Cooper and Millar, 1998; Sweileh *et al.*, 2000). While subunit protein can be detected in a variety of mammalian cell lines following transfection with α7 or α8 cDNA, correctly folded cell surface nAChRs are only detected in certain cell lines, such as human neuroblastoma SH-SY5Y cells. In contrast, misfolding in human embryonic kidney HEK293 cells, results in

subunit aggregation and retention in the endoplasmic reticulum (Cooper and Millar, 1997; Cooper and Millar, 1998). The effect of the host cell is also apparent between separate isolates of the same cell line (Blumenthal *et al.*, 1997). For example, three isolates of rat PC12 cells revealed differences in the ability to express functional α7 homomers, but were each able to express heteromeric ion channels (Blumenthal *et al.*, 1997). In addition, cells within the same cell line isolate can demonstrate differences in their ability to express cell surface nAChRs (Cooper and Millar, 1998).

Nicotinic receptors are synthesised in the endoplasmic reticulum, where a variety of post-translational processing events can occur, including glycosylation, formation of disulphide bonds, proteolytic cleavage and phosphorylation (Green and Millar, 1995). Post-translational modification can affect subunit folding and assembly. For example, disruption of cysteine residues involved in the formation of disulphide bonds reduces the efficiency of subunit folding (Green and Wanamaker, 1997).

Cell-specific folding is not a characteristic of the $5HT_{3A}$ receptor and the relatively inefficient folding and cell-surface expression of several nicotinic subunits can be enhanced through construction of subunit chimeras in which the C-terminal region of the nicotinic subunit is replaced with the corresponding region of the $5HT_{3A}$ subunit (Cooper and Millar, 1997; Cooper and Millar, 1998; Cooper *et al.*, 1999; Rakhilin *et al.*, 1999; Harkness and Millar, 2002). Chimeric subunits containing the N-terminal region of the α7 and α8 subunits, fused to the C-terminal domain of the $5HT_{3A}$ receptor subunit (Eiselé *et al.*, 1993; Cooper and Millar, 1998) readily form high levels of cell surface α-BTX binding sites in cell types which inefficiently fold wild-type subunits (Cooper and Millar, 1997; Cooper and Millar, 1998).

An enhancement of nAChR cell surface expression can also be achieved by incubation of transfected cells at lower temperature. Transfected HEK293 cells are generally cultured at 37°C, but incubation at 30°C has revealed a 5-fold upregulation of cell surface α4β2 nAChRs, while the total cellular protein levels remain unchanged (Cooper

et al., 1999). At lower temperatures, the rate of subunit turnover may be slowed, with a reduction in the rate of protein degradation. Such observations may also help to explain why heterologous expression of nAChRs has been most successful in *Xenopus* oocytes, in which proteins are expressed at 18°C, in comparison to mammalian cell lines incubated at 37°C.

1.5.4 Interaction of nAChRs with intracellular proteins

Identification of proteins that interact with nAChR subunits may provide a valuable insight into proteins or mechanisms involved in aspects of nAChR folding, assembly and cell surface expression as well as revealing aspects of signal transduction. For example, a 43-kDa protein, rapsyn, co-localises with muscle-type nAChRs and is involved in nAChR clustering at the postsynaptic membrane of the neuromuscular junction (Sealock, 1982; Froehner, 1991; Sanes and Lichtman, 2001; Moransard *et al.*, 2003). In muscle, it is suggested that pre-assembled rapsyn-nAChR complexes appear at the cell surface and are driven to clustering via a tyrosine kinase-dependent pathway, induced by agrin released from the motor nerve terminal (Sanes and Lichtman, 2001; Moransard *et al.*, 2003).

The intracellular loop region of the nAChR subunits, positioned between M3 and M4, contains potential sites for protein phosphorylation. Tyrosine kinase can phosphorylate the β, γ and δ subunits of the *Torpedo* electric organ nAChR (Huganir *et al.*, 1984) and cAMP-dependent kinase (PKA) phosphorylates the γ and δ subunits (Huganir and Greengard, 1983). Phosphorylation may influence nAChR desensitisation. For example, stimulation of protein kinase C (PKC), through addition of a phorbol ester to mouse or chick embryonic muscle cells, increases the rate of nAChR desensitisation and affects channel conductance upon application of agonist (Eusebi *et al.*, 1987). Application of forskolin, which activates adenylate cyclase and subsequently PKA, causes desensitisation of muscle nAChRs without affecting channel conductance and causes nAChR upregulation (Seamon *et al.*, 1981; Albuquerque *et al.*, 1986; Gopalakrishnan *et*

al., 1997). Therefore, receptor phosphorylation at separate sites with PKC and PKA has different effects on nAChR function.

Recently, the activity of recombinant α7 nAChRs has been enhanced through co-expression with the product of the RIC-3 gene (Halevi *et al.*, 2002; Halevi *et al.*, 2003). RIC-3 (resistant to inhibitors of cholinesterase) was identified during screening of genes required for nAChR activity in *Caenorhabditis elegans* and both *C. elegans* and human Ric-3 homologues have been cloned (Halevi *et al.*, 2002; Halevi *et al.*, 2003). The Ric-3 protein contains two putative transmembrane domains, with the N- and C-termini predicted to be intracellular, suggesting that Ric-3 is located on membranes. Ric-3 enhances the ACh-evoked whole cell currents in *Xenopus* oocytes expressing certain *C. elegans* nAChRs or expressing mammalian α7 nAChRs (Halevi *et al.*, 2002; Halevi *et al.*, 2003), though whether the effect of Ric-3 on nAChR activity is the result of a direct interaction between the proteins has not been demonstrated.

1.6 nAChR function in the central nervous system

Nicotine exerts a number of effects in the central nervous system, with administration of acute or chronic levels of nicotine in humans observed to enhance visual attention, perception and arousal (Jones *et al.*, 1999). Post-synaptic nAChRs involved in control of fast ACh-gated synaptic transmission (Section 1.6.1) are observed in the hippocampus and sensory cortex and are likely to be important in aspects of cognitive function (Levin and Simon, 1998; Jones *et al.*, 1999). Both the α7 and α4β2 nAChR subtypes have been implicated in memory and learning (Levin and Simon, 1998). The high Ca^{2+} permeability of nAChRs supports a role in regulation of early gene expression, providing a route for the entry of calcium at negative potentials at which NMDA receptors and voltage-gated calcium channels would be closed. The nAChR-mediated influx of Ca^{2+} can cause activation of second messenger cascades, which could play a role in a number of diverse functions including neuronal survival (Section 1.6.4) and neurotransmitter release (Section 1.6.3).

1.6.1 The role of postsynaptic nAChRs

The mediation of cholinergic transmission by postsynaptic nAChRs is well documented in autonomic ganglia and at the efferent synapse of the cochlea hair cells (Role and Berg, 1996). Nicotinic receptors expressed in outer hair cells of the cochlea are involved in modulating auditory nerve responses to acoustic stimulation and in protection from acoustic overstimulation (Sridhar *et al.*, 1997; Luebke and Foster, 2002; Maison *et al.*, 2002). In hair cells, α9-containing nAChRs function in association with calcium-activated potassium (K_{Ca}) channels, coupling entry of Ca^{2+} to the efflux of K^+. The resulting hyperpolarisation of outer hair cells causes a decrease in the amplification of basilar membrane motion, decreasing stimulation of the inner hair cells and resulting in suppression of the sound-evoked afferent discharge (Housley and Ashmore, 1991; Fuchs and Murrow, 1992; Maison *et al.*, 2002).

Identification of postsynaptic sites involved in cholinergic transmission in the brain has proved much more elusive than in the peripheral nervous system. Nicotinic receptors have been identified at postsynaptic sites on hippocampal interneurones and may include α7-containing nAChRs, as nicotine induced currents can be blocked by α-BTX and MLA (Hunt and Schmidt, 1978; Jones *et al.*, 1999). The minimal evidence for postsynaptic receptors suggests a role for nAChRs in aspects of brain function other than direct synaptic transmission (Role and Berg, 1996).

1.6.2 The role of presynaptic nAChRs

The primary roles for nAChRs in the central nervous system have been suggested to involve presynaptic functions, such as indirect mediation of synaptic transmission through subtle modulation of neurotransmitter release (Role and Berg, 1996; Wonnacott, 1997; Levin and Simon, 1998). For example, high affinity nicotine binding sites are observed on the terminals of dopamine neurones in the striatum (Wonnacott, 1997;

Wonnacott *et al.*, 2000). Cytisine is a partial agonist of these nAChRs in rat brain, suggesting the presence of an α4β2-containing nAChR subtype. However, antagonism of receptors with n-BTX in striatal preparations suggests a role for α3-containing nAChRs in presynaptic modulation of dopamine release (Wonnacott, 1997), so it is possible that a heterogeneous population of presynaptic nAChRs exists.

In addition to the heteroreceptors observed on nerve terminals involved in release of neurotransmitters such as dopamine, presynaptic receptors on cholinergic nerve terminals may serve as autoreceptors to modulate ACh-release via a feedback mechanism. Stimulation of autoreceptors following release of ACh from the nerve terminal could lead to the mobilisation of ACh from a reserve store to a readily releasable store, so the availability of neurotransmitter corresponds to the demand for its release (Wonnacott, 1997).

An alternative role for presynaptic nAChRs is in the modulation of other functional aspects at the nerve terminal. Nicotinic receptors are observed on growth cones, where they respond to ACh released by the growth cone and may participate in the regulation of neurite outgrowth (see Role and Berg, 1996; Wonnacott, 1997). When the extending neurite reaches a postsynaptic target, the subsequent increase in ACh release may signal an end to growth and the ensuing stabilisation and maturation of the synapse. Receptors containing α7 appear to be involved in this function, with their high Ca^{2+}-permeability playing a role via activation of Ca^{2+}-dependent signalling cascades (Lev *et al.*, 1995).

Tetrodotoxin (TTX) blocks voltage-gated sodium channels and, therefore, blocks the propagation of an action potential along the axon of a neurone. TTX can be used to distinguish between the modulation of neurotransmitter release by presynaptic nAChRs, which are insensitive to TTX treatment and transmitter release modulated by TTX-sensitive preterminal nAChRs. Facilitation of GABA release from CA1 interneurones of the hippocampus by ACh and choline is sensitive to TTX treatment and attributed to

nAChRs in preterminal locations (Alkondon *et al.*, 2000). The choline-induced increase in GABA-mediated postsynaptic current is blocked by MLA so may correspond to α7-containing nAChRs, while the block of the ACh-induced current by dihydro-β-erythroidine (DHβE), but not by MLA, is more suggestive of an α4β2 nAChR subtype.

1.6.3 Tobacco dependence

Tobacco smoking in humans and nicotine self-administration in animals appears to be associated with an increase in dopamine release that follows the action of nicotine upon mesencephalic dopaminergic neurones (see Lena and Changeux, 1998). Addictive drugs can exploit the intrinsic reward pathways of the nervous system that mediate the reinforcing effects of natural rewards such as food, by increasing dopamine-mediated activity (Jones *et al.*, 1999).

The mesolimbic dopaminergic system has its origins in the dopaminergic neurones of the ventral tegmental area (VTA) of the midbrain. The VTA projects to the nucleus accumbens (NAc), amygdala and limbic cortex. The VTA and its target NAc are thought to play a major role in reward and nicotine may induce an increase in dopamine transmission in the NAc (Raggenbass and Bertrand, 2002). The majority of neurones in the VTA possess β2-containing nAChRs and nicotine-induced dopamine release in the NAc does not occur in β2 knockout mice. In addition, $\beta2^{-/-}$ mice do not self-administer nicotine following priming with cocaine, suggesting that the β2 subunit is involved in nicotine addiction (Picciotto *et al.*, 1998).

Glutamatergic transmission from the prefrontal cortex provides excitatory control of VTA neurone activity and hence dopamine output in the reward pathway and may be under the modulatory influence of nicotine (see Mansvelder and McGehee, 2000). Block of α7-containing nAChRs in VTA neurones with MLA prevents nicotine-induced increases in dopamine release. Somatic nAChRs can directly excite VTA dopaminergic

neurones, but nAChR desensitisation means that this excitation is transient. However, activation of presynaptic α7-containing nAChRs present on glutamatergic terminals appears to promote long term potentiation (LTP) of the excitatory input from prefrontal cortex to the VTA, leading to more persistent elevations in dopamine release in the NAc that are independent of nAChR desensitisation (Mansvelder and McGehee, 2000). Stimulation of presynaptic nAChRs in the VTA promotes Ca^{2+} influx into the glutamatergic terminal, enhancing release of glutamate. The increase in glutamate release causes increased Ca^{2+} entry into postsynaptic dopaminergic neurones and subsequent induction of LTP and hence, long term excitation of areas of the brain involved in reward (Mansvelder and McGehee, 2000). A relatively short exposure to nicotine may cause long-lasting changes in the reward pathway of the brain, correlating to an early stage in nicotine addiction.

VTA neurones also receive innervation from GABAergic interneurones and from afferent projections from the NAc (see Mansvelder *et al.*, 2002). The afferent projections from the NAc possess nAChRs that demonstrate desensitisation characteristics distinct from the α7-containing nAChRs of the glutamatergic nerve terminals in the VTA and are thought to comprise α4β2 nAChRs. Therefore, the glutamatergic and GABAergic inputs would respond differently to a nicotine stimulus that may occur during tobacco smoking (Mansvelder *et al.*, 2002)

During chronic tobacco smoking, low concentrations of nicotine can cause an increase in nAChR number, demonstrated by an increase in the density of nicotinic ligand binding sites in the postmortem brain tissue of smokers (Benwell *et al.*, 1988) and in the brains of animals following chronic exposure to nicotine (Marks *et al.*, 1985; Schwartz and Kellar, 1985; Flores *et al.*, 1992; Marks *et al.*, 1992). These upregulated nAChRs accumulate in a deep state of desensitisation (Peng *et al.*, 1997; Fenster *et al.*, 1999) and the inappropriate changes in nAChR number could be important in mechanisms of nicotine addiction.

Not all nAChR subtypes are upregulated to the same extent and chronic nicotine exposure affects various nAChR subtypes differently (Olale *et al.*, 1997; Molinari *et al.*, 1998). The substantial desensitisation of α4β2 and α7 nAChRs contrasts to the effects of chronic nicotine on α3-subtypes and may reflect differences in the sensitivities of the nAChR subtypes for activation by nicotinic agonists (Hsu *et al.*, 1996; Olale *et al.*, 1997). In *Xenopus* oocytes, recombinant α7 nAChRs demonstrate the lowest sensitivity for acute activation by nicotine compared to α4β2- and α3-containing nAChRs, but show the highest sensitivity to inactivation by exposure to prolonged low concentrations of nicotine, probably reflecting the rapid desensitisation characteristic of α7 nAChRs. In a chronic smoker, blood plasma levels of nicotine of 100 - 500 nM (Lena and Changeux, 1998) would be sufficient to inactivate virtually all α4β2 nAChRs, ~ 90% of α7 nAChRs and 20% of α3-containing nAChRs (Olale *et al.*, 1997). This suggests that the behavioural effects, such as withdrawal and tolerance and the reward associated with tobacco smoking, depend on α7 and α4β2 nAChRs (Olale *et al.*, 1997).

1.6.4 Pathology

In addition to their involvement in complex brain function, nAChRs are implicated in the pathogenesis of several neurological disorders. A decrease in high affinity nicotine binding is a characteristic of several forms of neurodegenerative disease, including Alzheimer's disease, Parkinson's disease, Lewy-body disease and Downs syndrome (Picciotto and Zoli, 2002). While the brain areas showing a reduction in nicotine binding sites correlate to areas demonstrating neuronal loss, the disappearance of nAChRs appears to be more prominent than the loss of neurones, suggesting that the loss of nAChRs precedes neurodegeneration (Perry *et al.*, 1995).

Aged $\beta2^{-/-}$ mice do not express high affinity [^{3}H]-nicotine binding sites (Picciotto *et al.*, 1995) and show a loss of neurones in several brain regions in a manner resembling neurodegenerative disease (see Clementi *et al.*, 2000), suggesting that nAChRs provide

protection against neurodegenerative disorders during the ageing process (Picciotto and Zoli, 2002). This is consistent with epidemiological data that suggests chronic smoking can have neuroprotective effects and reduces the incidence of Parkinson's disease (Morens *et al.*, 1995). In addition, drug-induced neurotoxicity in cultured neurones can be alleviated through exposure to nicotine (Quik and Jeyarasasingam, 2000; Picciotto and Zoli, 2002). However, nicotine can be toxic to cells, particularly developing neurones, perhaps due to the inability of immature cells to cope with the increased calcium load (Picciotto and Zoli, 2002). The administration of nicotine may also influence whether the effect is protective or toxic, where extreme doses or continuous infusion of nicotine may prove toxic, while intermittent nicotine exposure, more likely to occur in the brains of smokers, may demonstrate a more protective effect (Picciotto and Zoli, 2002).

Patients with autosomal dominant frontal lobe epilepsy (ADNFLE) experience brief, clustered nocturnal motor seizures and are often misdiagnosed as suffering from sleep disorders. The clinical onset is usually in childhood and the disease often persists throughout adult life. Mutations have been identified in *CHRNA4*, the gene encoding the α4 nAChR subunit, which is expressed in all layers of the frontal cortex. Two missense mutations (S248F and S252L) in the M2 domain (involved in cation selectivity) of the α4 subunit were identified in families with ADNFLE. Functional studies have shown that the efficacy of the α4-S248F mutant channel is altered with respect to loss of Ca^{2+} permeability, increased desensitisation and reduced channel open-time and conductance (Weiland *et al.*, 1996). Two other mutations (V287L and V287M) have been found in *CHRNB2*, which encodes the nAChR β2 subunit. These mutations also affect the pore-forming M2 region, but in this case, the mutant nAChRs appear to be more sensitive to ACh and give larger responses with less desensitisation (Rodrigues-Pinguet *et al.*, 2003). The absence of seizures in $\alpha4^{-/-}$ and $\beta2^{-/-}$ mice also implicate the α4β2 subtype in the pathology of epilepsy (Picciotto *et al.*, 1998; Marubio *et al.*, 1999).

1.7 Aim of this study

This thesis describes experiments aimed at gaining a better understanding of nAChR assembly, subunit composition and pharmacology through heterologous expression of cloned nAChR subunits in mammalian cell lines. Heterologous expression is a valuable method to study neurotransmitter-gated ion channels, but expression of nAChRs in cultured cell lines has proved extremely challenging. Difficulties reported in the expression of recombinant α7 or α8 nAChRs in cultured cell lines (Puchacz *et al.*, 1994; Quik *et al.*, 1996; Cooper and Millar, 1997; Rangwala *et al.*, 1997; Cooper and Millar, 1998; Sweileh *et al.*, 2000) have led to the conclusion that appropriate subunit folding and assembly events are influenced strongly by the nature of the host cell type (Millar, 1999; Sivilotti *et al.*, 2000).

To overcome some of the challenges of recombinant nAChR expression in mammalian cells, the construction of a series of chimeric subunit cDNAs, containing the N-terminal domain of each rat nAChR subunit fused to the C-terminal domain of the $5HT_{3A}$ receptor subunit, will be examined. Previously constructed α7/$5HT_{3A}$ or α8/$5HT_{3A}$ chimeric receptors assemble efficiently in cells in which wild-type nAChRs misfold (Eiselé *et al.*, 1993; Cooper and Millar, 1998). Receptor assembly and subunit composition is investigated via expression of wild-type and chimeric subunits in mammalian cells and through detection of radioligand binding sites. The sub-cellular distribution of chimeric receptors is analysed through detection of epitope-tagged subunits in mammalian cells via enzyme-linked assays and by radioligand binding to intact cells. Pharmacological profiles for chimeric receptors are constructed by competition radioligand binding and compared to those of wild-type recombinant or native nAChRs to assess the validity of chimeras as models for nAChR characterisation.

Understanding the mechanisms that govern nAChR assembly and function should aid the elucidation of the mechanisms by which neurones achieve the accurate assembly of complex oligomeric nAChRs. Characterisation of nAChRs is pivotal to understanding their functional roles in the human brain and their potential as therapeutic targets for neurological disorders.

MATERIALS AND METHODS

CHAPTER 2

MATERIALS AND METHODS

All tissue culture media was obtained from Gibco BRL and all biochemicals were obtained from BDH unless otherwise specified.

2.1 PLASMID CONSTRUCTS AND SUBCLONING

2.1.1 Competent Cells

In general, plasmid constructs were transformed into chemocompetent XLI-Blue *Escherichia coli* (*E. coli*) cells (Stratagene). When subcloning required digestion with the *dam* methylation sensitive restriction enzyme, *BclI*, the *dcm-/dam- E. coli* strain, GM2163 was used (Dr. Ralf Schoepfer, University College London). When the construct being amplified was within the plasmid expression vector, pCDNA1neo, *E. coli* strain MC1061 was used, which contains a P3 episome. The P3 episome encodes the wild-type kanamycin resistance gene and amber mutations in the ampicillin and tetracycline resistance genes. Plasmid pCDNA1neo encodes the SupF suppressor transfer RNA (tRNA), which suppresses the amber mutations so that transformants can be selected with ampicillin and tetracycline.

Competent cells were generated according to the supplier's instructions. Cells from an agar stab were streaked onto SOB agar plates (20 g/L tryptone, 5 g/L yeast extract, 0.5 g/L NaCl, 2.5 mM KCl, 10 mM $MgCl_2$, 15 g/L agar) and grown at 37°C for ~ 17 h. A scraping of cells from the plate was used to inoculate 500 ml SOB media (20 g/L tryptone, 5 g/L yeast extract, 0.5 g/L NaCl, 2.5 mM KCl, 10 mM $MgCl_2$). The inoculated culture was grown at 37°C with shaking at 200 rpm until the optical density at 550 nm (OD_{550}) reached 0.5 - 0.55. Cells were pelleted by centrifugation at 2500 rpm (960 x *g*) for 15 min at 4°C in a Beckman J2-M1 centrifuge using a JA-14 rotor. The

cell pellet was resuspended in 40 ml ice-cold RF1 solution (100 mM RbCl, 50 mM $MnCl_2.4H_2O$, 30 mM potassium acetate, 10 mM $CaCl_2.2H_2O$, 15% (w/v) glycerol, pH adjusted to 5.8 with 1 M acetic acid, filter sterilised (0.22 μm)) and incubated on ice for 15 min. Cells were pelleted by centrifugation at 2500 rpm for 9 min and the cell pellet resuspended in 7 ml ice-cold RF2 solution (10 mM RbCl, 10 mM 3-*N*-morpholinopropanesulphonic acid (MOPS), 75 mM $CaCl_2.2H_2O$, 15% (w/v) glycerol, pH adjusted to 6.8 with 1 M NaOH, filter sterilised (0.22 μm)) and incubated on ice for 15 min. Aliquots of competent cells were snap frozen in a dry ice/ethanol bath and stored at -70°C.

2.1.2 Polymerase chain reaction (PCR)

Polymerase chain reaction (PCR) thermocycling was performed in a Peltier Thermal Cycler, PTC-225 (MJ Research). Typical reactions were performed in 20 μl volumes and contained 10 - 20 ng plasmid DNA, 250 μM dNTPs, 0.25 μM forward and reverse primers and 2.5 U *Pfu* polymerase (Stratagene) in 1X *Pfu* polymerase reaction buffer. *Pfu* polymerase was only used for the generation of PCR fragments for use in subcloning reactions. For standard PCR carried out as a diagnostic test, *Taq* polymerase (Stratagene) was used and reactions supplemented with 2.5 mM $MgCl_2$ in 1X *Taq* polymerase reaction buffer. *Pfu* polymerase possesses both 5'-3' DNA polymerase and 3'-5' exonuclease proof-reading activity, resulting in a 12-fold increase in DNA synthesis fidelity compared with *Taq* polymerase, which exhibits 5'-3' exonuclease activity.

Typical reactions for the generation of fragments for use in subcloning involved a 5 min denaturation step at 95°C, followed by thermocycling with denaturation at 95°C for 30 sec, annealing at 55°C for 30 sec and extension at 72°C for 90 sec, repeated for 30 cycles. A final extension step was carried out at 72°C for 5 min.

2.1.3 Restriction digestion of DNA

Typically, 2 - 3 μg plasmid DNA was subjected to digestion with 5 - 10 U restriction enzyme in a 20 - 30 μl reaction volume containing 1X reaction buffer compatible with the specific enzyme. Digests were incubated for 1 h at the incubation temperature required for optimal enzyme activity (usually 37°C, but some enzymes require incubation at 25°C or 55°C). For double digests in which the reaction buffers of the two enzymes were incompatible, digestion with the first enzyme was carried out in a 20 μl reaction volume for 1 h. The reaction mix was then diluted to 60 μl with milli-Q (MQ) water, the second reaction buffer added to a 1X final concentration and the digestion continued with the second enzyme for 1 h.

2.1.4 Dephosphorylation of DNA

When subcloning strategies involved digestion with a single enzyme, 5'-phosphate groups were removed from the digested DNA using calf intestinal alkaline phosphatase (CIAP; Promega) to prevent re-ligation of the plasmid vector. Typically, 2 - 3 μg digested plasmid DNA was incubated with 0.2 U CIAP for 30 min at 37°C. A further 0.2 U CIAP was added and the samples incubated again at 37°C for 30 min. For dephosphorylation of DNA with 5' recessed or blunt ends, DNA was incubated with CIAP at 37°C for 15 min, then at 56°C for 15 min to ensure accessibility of the recessed ends. A second aliquot of CIAP was added and the samples incubated at 37°C for a further 15 min, then at 56°C for 15 min.

2.1.5 Agarose gel electrophoresis and DNA purification

Agarose gel electrophoresis allows the visualisation and separation of digested plasmid DNA or PCR products according to molecular weight. Restriction enzyme digests or PCR products were separated by electrophoresis through 1% agarose gels (GibcoBRL)

and run against 1 µg *Hind*III digested Lambda (λ) DNA standard markers (Invitrogen) in order to estimate the relative size of the DNA bands. When the DNA fragments were required for further subcloning steps, low melting point agarose gels were used to allow subsequent purification. DNA bands were excised from the gel with a scalpel and transferred to microfuge tubes. DNA was extracted from the gel slices using the Wizard™ DNA clean-up system (Promega) according to the manufacturer's instructions. Briefly, the gel slices are dissolved in 1 ml Wizard™ DNA Clean-Up Resin and forced through a mini-column using a 2 ml syringe. DNA bound to the column is washed with 2 ml isopropanol and the excess isopropanol removed by centrifugation at 13000 rpm for 2 min in a bench-top microfuge. The DNA is eluted in 50 µl pre-warmed (65°C) MQ water, by centrifugation for 1 min at 13000 rpm. 5 µl purified DNA was run on a 1% agarose gel against *Hind*III digested λ DNA to assess the yield.

2.1.6 DNA Ligations

Ligation reactions typically contained a molar ratio of vector:insert of 1:3 in a reaction volume of 10 µl. Background levels of re-ligated vector were assessed through control reactions in which insert was substituted with MQ water. Reactions contained 1 mM ATP and 0.5 U T4 DNA ligase (Roche) and were incubated at 16°C overnight.

2.1.7 *E. coli* Transformations

2 µl ligation mixture or 1 - 20 ng plasmid DNA was added to 50 µl chemocompetent cells in a 5 ml polypropylene transformation tube (Falcon) pre-chilled on ice. The DNA and competent cells were mixed gently by swirling and incubated on ice for 30 min. The cells were subjected to heat-shock at 42°C for 90 sec and allowed to recover for 2 min on ice. 600 µl SOC medium (20 g/L tryptone, 5 g/L yeast extract, 0.5 g/L NaCl, 2.5 mM KCl, 10 mM $MgCl_2$, 20 mM glucose, sterilised by autoclaving at 10 lb./sq. in. for 15 min) was added to the cells and the tubes incubated at 37°C with shaking at 200 rpm for

1 h to allow expression of the plasmid's antibiotic resistance gene. 20 - 200 µl aliquots of transformation mixture were plated onto Luria-Bertani (LB)-agar plates (10 g/L tryptone, 5 g/L yeast extract, 10 g/L NaCl, pH 7.0 using NaOH, 15 g/L agar) containing inhibitory concentrations of an appropriate antibiotic (50 µg/ml ampicillin ± 10 µg/ml tetracycline) and grown at 37°C overnight (~ 17 h).

2.1.8 Screening colonies

Individual colonies were picked from the agar plates and screened for the presence of the correct DNA construct either by PCR or by extraction of DNA and subsequent restriction mapping. In a typical PCR of bacterial colonies, thermocycling steps followed a 5 min denaturation step to help lyse the bacterial cells and involved denaturation at 95°C for 30sec, annealing at 55°C for 30 sec, extension at 72°C for 60 sec, repeated for 30 cycles. A final extension step was carried out at 72°C for 5 min.

Where PCR was an inappropriate screening method, small scale, miniature preparations (mini-preps) of plasmid DNA were extracted via an alkaline lysis method (Sambrook *et al.*, 1989). 2 ml aliquots of LB medium (10 g/L tryptone, 5 g/L yeast extract, 10 g/L NaCl, pH 7.0 using NaOH) were inoculated with individual bacterial colonies and grown at 37°C with shaking at 225 rpm overnight. Bacterial cultures were pelleted by centrifugation at 13000 rpm for 1 min in a bench-top microfuge. Pellets were resuspended in 100 µl ice-cold Solution I (50 mM glucose, 25 mM Tris/Cl pH 8.0, 10 mM EDTA pH 8.0, autoclaved at 10 lb./ sq. in. for 15 min) and lysed with the addition of 200 µl Solution II (0.2 M NaOH, 1% SDS), mixing gently by inversion. 150 µl ice-cold Solution III (per 100 ml: 60 ml 5 M potassium acetate, 11.5 ml glacial acetic acid, 28.5 ml MQ water) was added and mixed to halt the lysis reaction and induce precipitation of chromosomal DNA. Samples were incubated on ice for 5 min and centrifuged at 13000 rpm, 5 min. The supernatant was phenol:chloroform (1:1, pH 8.0) extracted and ethanol precipitated, incubating in 2X volumes of 99% ethanol for 2 min at

room temperature. Samples were centrifuged for 5 min at 13000 rpm and the DNA pellets washed in 1 ml ice-cold 70% ethanol. Air-dried pellets were resuspended in 50 µl Tris-EDTA (TE) buffer, pH 8.0, containing 10 µg/ml RNase A (DNase-free, Sigma). Positive clones were identified by restriction mapping and subsequent agarose gel electrophoresis.

2.1.9 Large-scale preparation of plasmid DNA

Single *E. coli* colonies containing plasmid DNA were used to inoculate 250 ml LB medium cultures for large-scale plasmid DNA purification using Qiagen™ Plasmid Maxi Kit purification columns. Bacterial cultures were pelleted by centrifugation in a Beckman J2-M1 centrifuge for 10 min at 6000 rpm (6000 x *g*), 4°C using a JA-14 rotor. Pellets were resuspended in 10 ml ice-cold Buffer P1 (50 mM Tris-Cl pH 8.0, 10 mM EDTA, 100 µg/ml RNase A) and lysed with incubation in 10 ml Buffer P2 (200 mM NaOH, 1% (w/v) SDS) for 5 min at room temperature. Lysis was terminated and precipitation initiated by addition of 10 ml ice-cold Buffer P3 (3 M potassium acetate, pH 5.5), incubating on ice for 20 min. Samples were centrifuged at 13000 rpm (> 20000 x *g*) for 30 min at 4°C in a JA14 rotor. Sample supernatants were added to the Qiagen™ purification columns to extract the plasmid DNA following equilibration of the columns through addition of 10 ml Buffer QBT (750 mM NaCl, 50 mM MOPS pH 7.0, 15% (v/v) isopropanol). DNA bound to the columns was washed twice in 30 ml Buffer QC (1 M NaCl, 50 mM MOPS pH 7.0, 15% (v/v) isopropanol) and eluted in 15 ml Buffer QF (1.25 M NaCl, 50 mM Tris-Cl pH 8.5, 15% (v/v) isopropanol). Plasmid DNA was precipitated with 0.7 volumes (10.5 ml) isopropanol via centrifugation at 10500 rpm (≥ 15000 x *g*) for 30 min at 4°C in a JA17 rotor. DNA pellets were washed in ice-cold 70% ethanol and resuspended in 1 ml sterile MQ water. DNA purity and concentration was determined by measurement of absorbance at 260 nm (A_{260}) and 280 nm (A_{280}) in a BIO-RAD SmartSpec™ 3000 spectrophotometer. A_{260} = 1 represents approximately 50 µg/ml double stranded DNA. An A_{260}:A_{280} ratio of 1.6 - 2.0 indicates a pure DNA preparation.

Ratios significantly less than 1.6 indicate protein contamination and ratios greater than 2.0 indicate salt impurities. Maxi prep DNA of positive clones was analysed by restriction mapping and sequencing (Section 2.4).

2.1.10 Plasmid expression vectors

Expression Vector	Promoter	Inducible/ Constitutive	Poly-A Signal	Prokaryotic Selection	Eukaryotic Selection
pBSSK	LacZ	Constitutive		Ampicillin	-
pCDM6x1	CMV	Constitutive	SV40	*SupF (amp/tet)	-
pcDNA1neo	CMV	Constitutive	SV40	Kanamycin *SupF (amp/tet)	Neomycin (G418)
pcDNA3neo	CMV	Constitutive	Bgh	Kanamycin Ampicillin	Neomycin
pC1neo	CMV	Constitutive	SV40	Ampicillin	Neomycin
pRK5	CMV/SP6	Constitutive	SV40	Ampicillin	-
pZeoSV2(+)	SV40	Constitutive	SV40	Zeocin	Zeocin

Table 2.1. Summary of the plasmid expression vectors used in this study.
Abbreviations: amp, ampicillin; Bgh, bovine growth hormone; CMV, cytomegalovirus; poly-A, polyadenylation; SV40, Simian virus; tet, tetracycline
*SupF: Plasmid constructs expressing SupF transfer RNA require growth in a bacterial strain such as MC1061 that contains the P3 episome. The P3 episome contains amp and tet selectable markers, containing amber mutations and is corrected by the SupF transfer RNA.

2.1.11 Plasmid constructs

The rat α2, α3, α4, α5, α6, α7, β2, β3 and β4 subunit cDNAs were provided by Dr. Jim Patrick, Baylor College of Medicine, Houston. Dr. David Julius, University of California, provided the mouse $5HT_{3A}$ subunit cDNA (Maricq *et al.*, 1991) in the mammalian expression vector pCDM6x1. The $5HT_{3A}$ gene was excised from pCDM6x1 with the restriction enzyme *Xba*I and subcloned into the *Xba*I site of the mammalian expression vector pRK5.

The rat nAChR α9 and α10 subunit cDNAs (Elgoyhen *et al.*, 1994; Elgoyhen *et al.*, 2001) in the mammalian expression vector pC1neo, were provided by Dr. Jim Boulter, Los Angeles, CA and Dr. Belén Elgoyhen, Buenos Aires, Argentina, respectively. The α9 cDNA was excised from pC1neo with *Xba*I (5') and *Hind*III (3') and subcloned into the *Xba*I (5') / *Hind*III (3') sites of pRK5. The α10 sequence was excised from pC1neo with *Sma*I (5') and *Sal*I (3') and subcloned into the *Sma*I (5') / *Sal*I (3') sites of pRK5.

2.2 CONSTRUCTION OF CHIMERIC cDNA

Chimeric subunit cDNAs similar to $\alpha7^{(V201)}/5HT_{3A}$ described previously (Eiselé *et al.*, 1993; Cooper and Millar, 1998) were constructed containing the extracellular N-terminal domain of the nAChR subunits (α2, α3, α4, α5, α6, α9, α10, β2, β3 and β4), fused to the transmembrane and intracellular domain of the mouse $5HT_{3A}$ subunit in the mammalian expression vector, pRK5. The $\alpha3/5HT_{3A}$, $\alpha4/5HT_{3A}$, $\alpha5/5HT_{3A}$, $\beta2/5HT_{3A}$, $\beta3/5HT_{3A}$ and $\beta4/5HT_{3A}$ chimeras were constructed during an undergraduate research placement, prior to this PhD project, but details of their construction are included to allow direct comparison with the other chimeras. For specific details of the construction of the chimeras, see Section 3.2. For brevity, chimeras are referred to using the Greek letter, chi (χ).

Each nAChRs/$5HT_{3A}$ chimera was generated from an original $\alpha7^{(V201)}/5HT_{3A}$ chimera created by Dr. Sandra Cooper (this laboratory) in the pZeoSV expression vector (Cooper and Millar, 1997), subsequently subcloned into pRK5. In generating the pZeoSV-$\alpha7^{(V201)}/5HT_{3A}$ chimera, Dr. Cooper subcloned $\alpha7^{(V201)}/5HT_{3A}$ into pZeoSV(+) at *Hind*III (5') and *Bcl*I (3') sites, joining the $\alpha7$ and $5HT_{3A}$ subunit fragments at a *Bcl*I site at residue V201 of the $\alpha7$ sequence.

The $\alpha7^{(V201)}/5HT_{3A}$ sequence was excised from the pZeoSV(+) mammalian expression vector with *Eco*RI (5') and *Sca*I (3') and subcloned into the *Eco*RI (5') / *Sma*I (3') sites of the pRK5 expression vector to produce pRK5-$\alpha7^{(V201)}/5HT_{3A}$ ($\alpha7\chi$). The pRK5 plasmid was used to simplify the subcloning strategy as it does not contain a *Bcl*I site (T/GATCA). A unique *Bcl*I site was introduced to each nAChR cDNA at a position analogous to V201 in the $\alpha7$ sequence, just prior to M1, by silent mutagenesis using PCR. Details of the primers used are listed in Table 3.2. PCR thermocycling was performed as detailed in Section 2.1.2. PCR fragments were ethanol precipitated by the addition of 1/10th volume 3 M sodium acetate (pH 5.2) and 2 volumes 99% ethanol. Samples were chilled at -20°C for 1 h and centrifuged at 13000 rpm in a bench-top microfuge. DNA pellets were washed with 70% ethanol and resuspended in 50 µl MQ water.

Ethanol precipitated PCR products were digested with a suitable 5' restriction enzyme and *Bcl*I (3'). The $\alpha7$ portion of pRK5-$\alpha7^{(V201)}/5HT_{3A}$ was removed by restriction enzyme digest to produce a pRK5-/$5HT_{3A}$ cloning cassette. Gel purified nAChR fragments were cloned into the pRK5-/$5HT_{3A}$ cloning cassette to create the pRK5-nAChR/$5HT_{3A}$ subunit chimeras (Section 3.2). The fidelity of the chimeric constructs was verified by restriction mapping and sequencing.

2.3 CONSTRUCTION OF HA-EPITOPE TAGGED SUBUNITS

Epitope tags were introduced to the sequence of the α9, α10, α9χ and α10χ subunit cDNAs to allow detection of these subunits expressed in mammalian cells with an antibody raised to the epitope tag. A nine amino acid epitope tag (YPYDVPDYA) from human influenza haemagglutinin (HA) protein (Kolodziej and Young, 1991) was used in each case. HA epitope tags were introduced at one of three different positions to each subunit: into the N-terminal region following the putative signal peptide cleavage site, into the intracellular loop region, or at the extreme C-terminus. All constructs were verified by sequencing (Section 2.4) and immunoprecipitation (Section 2.8).

2.3.1 Introduction of the HA tag to the N-terminal region

The HA epitope tag was introduced into the sequence of each subunit or subunit chimera at a position following the putative cleavage site of the leader peptide, positioning the tag close to the extreme N-terminal end of the mature protein to create $\alpha9^{N\text{-}HA}$, $\alpha10^{N\text{-}HA}$, $\alpha9\chi^{N\text{-}HA}$ and $\alpha10\chi^{N\text{-}HA}$ in the pRK5 expression vector. The HA tag was inserted at a unique *Nhe*I site (G/CTAGC), created in the subunit sequence by site-directed mutagenesis (SDM). The HA tag was carefully designed and the position for the tag insertions selected to ensure that the reading frame of the subunit sequence would be maintained.

The QuikChange™ Site-Directed Mutagenesis Kit (Stratagene) was used to create point mutations in the cDNA sequence. Two primers were designed for each α9 and α10 subunit to create the desired mutations. The mutagenic primers anneal to the same sequence on opposite strands of the DNA and both have melting points (T_m) above 78°C.

$$T_m = \frac{81.5 + 0.41(\%GC) - 675}{\text{primer length in base pairs} - \%\text{mismatch}}$$

The mutation is in the middle of the primer, the primers have a GC content above 40%, were PAGE purified and terminate in a C or G residue.

SDM Primers for HA tags at the N-terminal:

OL559 *Nhe*I α9(+): 5' - GGA ATC AGA GCC GTA GAG CTA GCA AAT GGG AAA TAT GC - 3'

OL560 *Nhe*I α9(-): 5' - GC ATA TTT CCC ATT TGC TAG CTC TAC GGC TCT GAT TCC - 3'

OL561 *Nhe*I α10(+): 5' - GCT GAG GGG AGG CTA GCT CAC AAG CTG TTT CGT GAC - 3'

OL562 *Nhe*I α10(-): 5' - GTC ACG AAA CAG CTT GTG AGC TAG CCT CCC CTC AGC - 3'

*Nhe*I: G/CTAGC (+) = forward primer; (-) = reverse primer

Each 50 µl SDM PCR reaction contained 1X reaction buffer, 50 ng template DNA, 125 ng of each forward and reverse primers, 1 µl dNTP mix and 1 µl *PfuTurbo* DNA polymerase (2.5 U/µl; Stratagene). Reactions were heated to 95°C for 30 sec, then 12 thermocycling steps were performed that included denaturation at 95°C for 30 sec, annealing at 55°C for 1 min and extension at 68°C for 2 min/kb cDNA length (13.5 min for pRK5-α9 [6654 bp], pRK5-α9χ [6536 bp] and pRK5-α10χ [6482 bp] and 15.5 min for pC1neo-α10 [7644 bp]). PCR products were cooled on ice and digested with 1 µl *Dpn*I (10 U/µl) at 37°C for 1 h. 1 µl digested DNA was added to 50 µl XL1-Blue supercompetent cells in a pre-chilled Falcon 2059 polypropylene tube and incubated on ice for 30 min. Transformation was carried out via heat shock at 42°C for 45 sec, followed by incubation in 0.5 ml NZY$^+$ broth (10 g/L casein hydrolysate (NZ amine), 5 g/L yeast extract, 5 g/L NaCl, pH 7.5 with NaOH, 12.5 ml/L 1 M $MgCl_2$, 12.5 ml/L $MgSO_4$ and 10 ml/L 2M glucose) for 1 h at 37°C, with shaking at 225 rpm. 200 µl transformation mix was plated onto LB agar plates containing 50 µg/ml ampicillin, pre-treated with 20 µl 10% (w/v) X-Gal and 20 µl 100 mM isopropyl-1-thio-β-D-galactopyranoside (IPTG) and incubated at 37°C for 18 h. Colonies were screened for the presence of the mutation by digestion of mini-prep DNA (Section 2.1.8) with *Nhe*I at 37°C for 1 h. Maxi-prep DNA was prepared from positive clones, digested with *Nhe*I at 37°C for 1 h and gel purified.

Two oligonucleotides were generated that contained the sequence for the HA tag and complementary ends for subcloning into the *Nhe*I site:

OL563 HA *Nhe*I(+): 5' - CTAGCATACCCCTACGACGTGCCCGACTACGCC - 3'

OL564 HA *Nhe*I(-): 5' - CTAGGGCGTAGTCGGGACCGTCGTAGGGGTATG - 3'

n Bases complementary to overhang created by digestion with *Nhe*I

n LINKERS to maintain reading frame

n HA epitope tag

The OL563 and OL564 oligonucleotides were mixed at an equal molar ratio and annealed by heating to 80°C for 20 min in a hot block and cooling slowly to room temperature. The annealed primer duplex was subcloned into the subunit DNA digested with *Nhe*I to produce pRK5-$\alpha 9^{N\text{-}HA}$, pRK5-$\alpha 9\chi^{N\text{-}HA}$, pC1neo-$\alpha 10^{N\text{-}HA}$ and pRK5-$\alpha 10\chi^{N\text{-}HA}$ constructs. The $\alpha 10^{N\text{-}HA}$ construct was subsequently excised from pC1neo and subcloned into pRK5 using the *Sma*I (5') and *Sal*I (3') sites of both vector and insert, to produce pRK5-$\alpha 10^{N\text{-}HA}$.

2.3.2 Introduction of the HA tag to the intracellular loop region

The HA epitope tag was introduced into the sequence of each subunit or subunit chimera within the putative intracellular loop region, at positions avoiding potential phosphorylation motifs (for example, the S/TxK/R consensus motif for phosphorylation by PKC predicted using the PROSITE Database of Protein Families and Domains; http://ca.expasy.org/gci-bin/scanprosite). The HA tag was inserted at a unique *Nhe*I site, created by SDM (Section 2.3.1). The HA tag was carefully designed and the position for tag insertions selected to ensure that the reading frame of the subunit sequence would be maintained.

SDM Primers for HA tags in the intracellular loop:

OL593 α9 *Nhe*I i/c(+): 5' - C CAC AGC CAG GAG CTA GCA CAA GTC ACG AAG G - 3'

OL594 α9 *Nhe*I i/c(-): 5' - C CTT CGT GAC TTG TGC TAG CTC CTG GCT GTG G - 3'

OL595 $5HT_{3A}$ *Nhe*I(+): 5' - G GAT GAG ATG CGG GAG CTA GCA AGG GAC TGG C - 3'

OL596 $5HT_{3A}$ *Nhe*I(-): 5' - G CCA GTC CCT TGC TAG CTC CCG CAT CTC ATC C - 3'

OL602 α10 *Nhe*I(-): 5' - CTC CTG CTG GGA CAG CTA GCC AAA GGC CTG TG - 3'

OL603 α10 *Nhe*I(-): 5' - CA CAG GCC TTT GGC TAG CTG TCC CAG CAG GAG - 3'

*Nhe*I: G/CTAGC

The annealed primer pair containing the HA tag sequence (OL563/OL564 *Nhe*I HA; Section 2.3.1) was subcloned into the subunit DNA digested with *Nhe*I to produce pRK5-$\alpha 9^{I\text{-}HA}$, pRK5-$\alpha 9\chi^{I\text{-}HA}$, pC1neo-$\alpha 10^{I\text{-}HA}$ and pRK5-$\alpha 10\chi^{I\text{-}HA}$ constructs. The $\alpha 10^{I\text{-}HA}$ construct was subcloned into pRK5 using the *Sma*I (5') and *Sal*I (3') sites of both vector and insert, to produce pRK5-$\alpha 10^{I\text{-}HA}$.

2.3.3 Introduction of the HA tag to the extreme C-terminus

The HA epitope tag, followed by a stop codon, was introduced at the end of the coding sequence of each subunit cDNA by PCR to produce pRK5-$\alpha 9^{C\text{-}HA}$, pRK5-$\alpha 10^{C\text{-}HA}$, pRK5-$\alpha 9\chi^{C\text{-}HA}$ and pRK5-$\alpha 10\chi^{C\text{-}HA}$. The forward primer (+) contained a unique *Xba*I site, an ATG start codon and the sequence of the N-terminus of the α9 or α10 subunit. The reverse primer (-) contained a unique *Hind*III site, a stop codon, the HA epitope tag sequence and the DNA sequence for the C-terminus of the α9, α10 or $5HT_{3A}$ subunit. The *Xba*I and *Hind*III sites were introduced to allow subcloning of the purified PCR fragment into pRK5 (*Xba*I/*Hind*III).

PCR Primers for the introduction of C-terminal HA-epitope tags:

OL497 α9 *Xba*I(+): 5' - TGG TCT AGA ATG AAC CGG CCC CAT TCC TGC CTC TCC TTT - 3'

OL576 α9 HA(-): 5' - CGC AAG CTT TCA GGC GTA GTC GGG AAC GTC GTA GGG GTA ATC TGC TCT TGC TAT GAT - 3'

OL498 α10 *Xba*I(+): 5' - GGT TCT AGA ATG ACA AGG AGC CAC TAC CTG GAC GTC - 3'

OL571 α10 HA(-): 5' - CGC AAG CTT TCA GGC GTA GTC GGG AAC GTC GTA GGG GTA CAG GGC TTG CAC - 3'

OL495 $5HT_{3A}$ HA(-): 5' - CGC AAG CTT TCA GGC GTA GTC GGG AAC GTC GTA GGG GTA AGA ATG CCA AAT GGA - 3'

*Xba*I: T/CTAGA

*Hind*III: A/AGCTT

HA epitope tag

Start (ATG) or Stop (TGA) codon (where the Stop codon in the reverse sequence = TCA)

Thermocycling steps followed incubation at 95°C, 1 min and involved denaturation at 95°C for 30 sec, annealing at 70°C (5°C below the T_m of the primer pair) for 60 sec and extension at 72°C for 3 min, repeated for 30 cycles. A final extension step involved incubation at 72°C for 10 min.

2.4 SEQUENCING

Fluorescence-based cycle sequencing was carried out using the ABI Prism® BigDye® Terminator Cycle Sequencing Ready Reaction Kit (Applied Biosystems) according to the manufacturer's instructions. Briefly, template DNA (0.1 - 1.0 μg) and specific primer are mixed with 8 μl Terminator Ready Reaction Mix in 20 μl reaction volumes. Terminator Ready Reaction Mix contains BigDye® (dye-labelled ddNTP) terminators, FS. AmpliTaq® DNA polymerase, unlabelled dNTPs, $MgCl_2$ and buffer. FS. AmpliTaq® DNA polymerase is a variant of *Taq* DNA polymerase, with a point mutation in the active site that reduces discrimination for dideoxynucleotides (ddNTPs). Thermocycling

steps involve denaturation at 96°C for 30 sec, annealing at 50°C for 15 sec and extension at 60°C for 4 min, for 25 cycles. Reactions are ethanol/sodium acetate precipitated using 2 µl sodium acetate, pH 5.2 and 50 µl 99% ethanol per 20 µl reaction, incubated on ice for 10 min and centrifuged at 13000 rpm, 15 min in a microfuge. Pellets are washed in 250 µl 70% ethanol, air-dried and resuspended in 4 µl loading buffer (1 part 25 mM EDTA, pH 8.0 with blue dextran (50 mg/ml) to 5 parts deionised formamide). Fluorescent DNA fragments are resolved using an ABI Prism® 377 DNA Sequencer (Applied Biosystems) on a 4% polyacrylamide gel (19:1 acrylamide/bis-acrylamide solution; Amresco) containing 6 M urea and 1X TBE (National Diagnostics).

The pRK5 vector contains a SP6(+) priming site that was used to sequence the chimeric constructs in the forward direction. The following primers were also used to sequence the chimeric constructs (bp = base pair):

OL557 SP6(+):	5' - AT TTA GGT GAC ACT ATA G - 3' from start
OL606 α9 [400bp](+):	5' - C TCC ATC AGG ATT CCC AGC G - 3' from bp 400
OL608 α9 [750bp](+):	5' - C TCC GAG CCT TAC CCA GAT GTC - 3' from bp 750
OL597 α9 i/c loop(+):	5' - G GTG ATG AAT ATT CAC TTC TGT GGA GC - 3' from bp 1050
OL578 α9 M4(+):	5' - G GGC AGC GAG TGG AAG AAG GTC G - 3' from bp 1420
OL607 α10 [400bp](+):	5' - GG CGA CCA GAC ATC GTA CTT TAC - 3' from bp 400
OL432 α10 [660bp](+):	5' - G GAG AAC GTT GAA TGG CGG GTG - 3' from bp 660
OL598 α10 i/c loop(+):	5' - G CAC TAC TGT GGC CCT AAT GCA CAT CC - 3' from bp 1030
OL577 α10 M4(+):	5' - GTA ATG GAC CGC TTT TTC CTA GGC - 3' from bp 1330
OL428 $5HT_{3A}$(-):	5' - GG TAC CGG CCA CTG TAG GTC CTG - 3' from bp 1080
OL276 pRK5(-):	5' - AAG CTG CAA TAA ACA AGT TGG GC - 3'

2.5 CELL CULTURE AND TRANSFECTIONS

2.5.1 Cell lines

The human embryonic kidney cell line, tsA201, derived from the human embryonic kidney HEK293 cell line, was obtained from Dr. William Green, University of Chicago, IL. The rat pituitary-derived cell line, GH_4C_1, was obtained from the American Type Culture Collection. The conditionally immortal auditory hair cell lines, UB/OC-1 and UB/OC-2 (University of Bristol/Organ of Corti), derived from the H-2Kb-*ts*A58 transgenic mouse (Jat *et al.*, 1991; Holley *et al.*, 1997; Rivolta *et al.*, 1998) were obtained from Dr. Matthew Holley, University of Bristol, UK.

2.5.2 Cell culture

Human tsA201 cells were cultured in Dulbecco's modified Eagle's medium (DMEM) containing 2 mM L-Glutamax™ plus 10% heat-inactivated foetal calf serum (Sigma, Poole, UK), with penicillin (100 U/ml) and streptomycin (100 μg/ml) and were maintained in a humidified incubator containing 5% CO_2 at 37°C. GH_4C_1 cells were cultured in Nutrient Media F10 (HAMS) supplemented with 10% FCS, 5% horse serum, penicillin and streptomycin and maintained in a humidified incubator containing 5% CO_2 at 37°C. UB/OC-1 and UB/OC-2 were cultured in Modified Essential Medium (MEM) containing 10% FCS and 50 U/ml γ-interferon (Gibco BRL) in a humidified incubator containing 5% CO_2 at 33°C. Differentiation of UB/OC cells was induced by incubation of cells at 37°C for 14 days in MEM containing 10% FCS, but lacking γ-interferon.

2.5.3 Transient Transfection

Cells were trypsinised and re-plated 6 - 24 h before transfection to allow transfection at ~ 40% confluence. Cells were transiently transfected using the non-liposomal lipid formulation, Effectene™ Transfection Reagent (Qiagen, Crawley, UK) according to the manufacturer's instructions. Briefly, for transfection of each 10 cm culture dish (Corning) of cells, 0.6 μg total DNA is added to a microfuge tube and mixed with 120 μl Buffer EC. 4.8 μl Enhancer is added and incubated at room temperature for 5 min to condense the DNA (ratio of DNA to Enhancer is always 1 μg : 8 μl). 13 μl Effectene is added to the condensed DNA and incubated at room temperature for 10 min to produce condensed Effectene-DNA complexes. The Effectene-DNA complexes are mixed with 600 μl culture medium and added directly to the cells in 3 ml medium. Cells were transfected overnight, adding 6 ml fresh culture medium after approximately 17 h. When cells were transfected in 12-well plates (Corning) on 13 mm coverslips pre-coated with poly-D-lysine and collagen, 0.4 μg DNA, 80 μl Buffer EC, 3.2 μl Enhancer, 10 μl Effectene and 400 μl culture media were used and the final transfection mixture divided between 4 wells of cells in 0.5 ml medium, providing a final concentration of 0.1 μg total DNA per well. After overnight transfection, 1 ml fresh medium was added per well of the 12-well plate. Cells were assayed for expression approximately 40 - 48 h after transfection.

2.6 RADIOLIGAND BINDING

Reaction conditions for equilibrium radioligand binding, including the transfected cell line, the radioligand and the compounds used to determine non-specific binding all depended on the particular cDNA combinations being assayed. Typically, transiently transfected cells were washed in phosphate-buffered saline (PBS) and harvested by gentle scraping into 1 ml PBS. Cells were pelleted by centrifugation at 2000 rpm for 2 min and resuspended in 10 mM potassium phosphate buffer (per 100 ml of 1 M stock, pH 7.2: 71.7 ml 1 M K_2HPO_4, 28.3 ml 1 M KH_2PO_4) (for crude membrane preparations) or Hanks Buffered Saline Solution (HBSS; for intact cell suspensions) containing

protease inhibitors leupeptin (2 μg/ml) aprotinin (2 μg/ml) and pepstatin (1 μg/ml). Samples were kept on ice where possible. Cell preparations were typically incubated with radioligand for 150 min at 4°C in a total volume of 300 μl. Total and non-specific binding was determined in triplicate samples. The maximum number of radioligand binding sites detected can vary between experiments, due to variations in cell passage number or confluence, transfection efficiency or experimental technique. However, the binding affinities and patterns exhibited by cells expressing different subunit combinations were reproducible between experiments.

The protein concentration of cell membrane preparations was determined by a BioRad *DC* protein assay according to the manufacturer's instructions. Briefly, 20 μl cell suspension or bovine serum albumin (BSA) standard sample is added to a semi-microcuvette (Starstedt) and mixed with 100 μl Reagent A (alkaline copper tartrate solution). 800 μl Reagent B (a dilute Folin Reagent) is added, mixed and incubated at room temperature for 15 min. Colour development occurs after reduction of the Folin reagent by the copper-treated protein and provides a colorimetric assay. Protein concentration is determined by measurement of A_{750} and comparison against a standard curve constructed using BSA at concentrations of 0.1, 0.2, 0.4, 0.8, 1.2 and 1.5 mg/ml.

2.6.1 Tritiated radioligand binding

Samples were harvested using a Brandel Cell Harvester (Model M-36, Semaat, UK) in ice-cold 10 mM potassium phosphate buffer (for membrane preparations) or ice-cold PBS (for intact cells) onto GF/B glass fibre filters (Whatman) pre-soaked for 2 h in 0.5% (w/v) polyethylenimine (PEI). Filters were equilibrated for 24 h in 5 ml "Ready Safe" scintillation cocktail (Beckman) and counted for radioactivity in a scintillation counter.

For radioligand binding assays with tsA201 and UB/OC cells transiently transfected with combinations of chimeric and wild-type α9 and α10 subunit cDNAs (Chapter 4), cell membranes were incubated with 30 nM [^{3}H]-epibatidine (PerkinElmer Life Sciences, Boston; specific activity 56.2 Ci/mmol), 10 - 15 nM [^{3}H]-methylcarbamylcholine ([^{3}H]-

MCC; PerkinElmer Life Sciences; specific activity 80 Ci/mmol), 30 nM [^{3}H]-methyllycaconitine ([^{3}H]-MLA; Tocris Cookson Ltd, Avonmouth, UK; specific activity 26 Ci/mmol) or 50 nM [^{3}H]-strychnine (PerkinElmer Life Sciences; specific activity 23 Ci/mmol) for 2 h on ice. Non-specific binding was typically determined by addition of 1 mM nicotine and 1 mM carbamylcholine chloride (carbachol) . For [^{3}H]-MLA binding to tsA201 cells expressing chimeric α9 and α10 subunit cDNAs (α9χ and α10χ), non-specific binding typically yielded values of 200 cpm, representing ~ 5% of total binding.

For binding studies involving comparison of the expression of chimeric and wild-type α2 - α6 nAChR subunit cDNAs (Chapters 6 and 7), membrane preparations were incubated with saturating concentrations of [^{3}H]-epibatidine (15 nM). Non-specific binding was determined by the addition of 1 mM nicotine and 1 mM carbachol, giving typical values of 200 cpm and representing 1 - 5% of total binding.

During radioligand binding assays with the α7 or α7χ subunits (Chapters 4 and 6), cell membranes were incubated with 5 - 15 nM [^{3}H]-MLA for 2 h on ice. Non-specific binding was determined by the addition of 1 mM nicotine, 1 mM carbachol and 10 μM MLA and typically yielded values of 4000 cpm, representing 5% of total binding.

2.6.2 Saturation binding

Saturation binding studies were performed with membrane preparations of tsA201 cells transiently transfected with α7χ or α9χ and α10χ cDNAs. Increasing concentrations of [^{3}H]-MLA were used (0.01 - 50 nM). To obtain a sufficient block of the receptors to measure non-specific binding, 1 mM carbachol, 1 mM nicotine and 10 μM MLA were added. Care was taken to ensure that the number of nAChR binding sites used for binding studies was low enough to avoid significant (>10%) ligand depletion at low concentrations of radioligand. Preliminary experiments were conducted to ensure that incubation times were long enough to enable radioligand binding to reach equilibrium. Curves for equilibrium binding were fitted with the Hill equation by equally-weighted least-squares (CVFIT program, David Colquhoun, University College London). In all cases the calculated Hill coefficients (n_H) did not differ significantly from 1.

2.6.3 Competition binding

For competition binding assays with [^{3}H]-MLA, non-specific binding to cells transfected with the chimeric α9χ and α10χ cDNA was determined by addition of 10 mM nicotine, 10 mM carbachol and 100 μM *d*-tubocurarine. For cells transfected with α7χ cDNA, non-specific binding was determined in the presence of 3 μM MLA. Following estimation of K_d by saturation binding, [^{3}H]-MLA was used at a concentration approximating the K_d. Curves for equilibrium binding were fitted with the Hill equation by equally-weighted least-squares. In all cases the calculated Hill coefficients (n_H) did not differ significantly from 1. K_i values were derived from the competition curves using the equation: $K_i = IC_{50} / (1 + ([\text{radioligand}] / K_d))$

Competition binding for [^{3}H]-MLA binding sites to membrane preparations of transiently transfected tsA201 cells was tested using the following ligands:

	α9χα10χ	α7χ
Acetylcholine (ACh)	0.01 - 5000 μM	0.1 - 50000 μM
Atropine (Sigma)	0.01 - 5000 μM	0.5 - 30000 μM
Bicuculline (Sigma)	0.005 - 118 μM	0.005 - 118 μM
α-Bungarotoxin (α-BTX)	0.5 - 10000 nM	0.0001 - 30000 nM
Carbachol	0.1 - 50000 μM	0.01 - 50000 μM
1,1-Dimethyl-4-phenlypiperazinium (DMPP)	0.01 - 10000 μM	0.001 - 10000 μM
5-Hydroxytryptamine (5HT)	0.1 - 10000 μM	0.001 - 10000 μM
Methylcarbamylcholine (MCC)	0.1 - 5000 μM	0.01 - 10000 μM
Nicotine	0.5 - 5000 μM	0.01 - 5000 μM
Strychnine	0.01 - 5000 μM	0.01 - 5000 μM
d-Tubocurarine (*d*-TC)	0.5 - 50000 μM	0.0001 - 5000 μM

Table 2.2. Summary of the ligands used in competition binding studies with α7χ and α9χα10χ.

2.6.4 Estimation of surface [^{3}H]-MLA binding sites

Levels of radioligand binding sites on the surface of intact tsA201 cells transiently transfected with chimeric α9χ and/or α10χ subunit cDNAs were determined using [^{3}H]-MLA. Due to the concern that [^{3}H]-MLA may be able to cross the cell membrane (Davies *et al.*, 1999), a modified version of the tritiated radioligand binding method (Section 2.6.1) was used, in a protocol similar to that described by Whiteaker *et al.*, 1998. Transfected cells, grown in 10 cm plates, were gently resuspended in HBSS. Intact cells (typically 5 x 10^5 cells) were incubated in a total volume of 300 µl with 15 nM [^{3}H]-MLA in the presence of either (a) HBSS - to measure the total population of [^{3}H]-MLA binding sites, (b) 1 mM nicotine, 1 mM carbachol and 10 µM MLA - to measure non-specific binding or (c) 1 mM ACh - to block [^{3}H]-MLA binding sites on the cell surface. To determine the proportion of specific binding on the cell surface, binding assays with intact cells were performed in parallel with assays on cell membrane preparations (Section 2.6.1). Samples were harvested onto GF/B glass fibre filters in ice-cold PBS and assayed by scintillation counting.

2.6.5 Iodinated α-bungarotoxin ([^{125}I]-α-BTX) binding

Cell preparations were incubated with 1 - 5 nM [^{125}I]-α-BTX (specific activity 150 Ci/mmol; Amersham) in the presence of 2% BSA for 2 h on ice. Non-specific binding was determined by addition of 1 mM nicotine and 1 mM carbachol to triplicate samples. Samples were harvested using a Brandel Harvester (Model M-36, Semaat, UK) onto GF/A glass fibre filters (Whatman) pre-soaked in 0.5% PEI for 2 h with 4 washes in ice-cold PBS (intact cell suspensions) or 10 mM potassium phosphate buffer (membrane preparations). Bound [^{125}I]-α-BTX was determined by counting the filters in a Wallac 1261 gamma-counter.

2.7 ANTIBODIES

Antibody	Species Immunised	Isotype	Specificity	Source
mAbHA-7	Mouse	IgG	HA peptide†	Sigma
mAb α-HA Peroxidase	Mouse	IgG	HA peptide†	Sigma
Goat α-mouse IgG Peroxidase	Mouse	IgG (H+L)		Pierce
pAb5HT$_3$	Rabbit	IgG	Intracellular loop region of 5HT$_3$	Dr. R. McKernan‡
Goat α-rabbit IgG Peroxidase	Rabbit	IgG (H+L)		Pierce

Table 2.3. Summary of the antibodies used in this study.

† The nine amino acid synthetic peptide (YPYDVPDYA) corresponding to residues 98-106 of human influenza virus haemagglutinin (Kolodziej and Young, 1991)

‡ Merck Sharp and Dohme Research Laboratories, Harlow (Turton *et al.*, 1993).

2.8 METABOLIC LABELLING AND IMMUNOPRECIPITATION

Mammalian tsA201 cells were transiently transfected overnight (Section 2.5.3), washed twice and incubated for 20 min in L-methionine (Met) and L-cysteine (Cys) free media to starve cells of methionine. Cells were labelled with 250 μCi [^{35}S]-"Pro-mix" (Amersham), containing a mixture of [^{35}S]-Met and [^{35}S]-Cys, in 3 ml Met/Cys-free medium for 3 h at 37°C. Labelling was terminated by addition of 5 ml complete DMEM (containing 30 mg/ml Met and 48 mg/ml Cys and supplemented with 10% FCS) and chased for 2 h at 37°C. Cells were washed three times and harvested into 1 ml ice-cold PBS. Cells were pelleted in a benchtop centrifuge at 6000 rpm, 5 min at 4°C and resuspended in 400 μl ice-cold low salt lysis buffer (150 mM NaCl, 50 mM Tris/Cl pH 8.0, 5 mM EDTA, 1% Triton X-100) containing protease inhibitors (0.2 mM phenylmethylsulfonyl fluoride (PMSF), 2 mM *N*-ethylmaleimide (NEM) and 10 μg/ml each of pepstatin, leupeptin and apoprotinin).

Solubilised samples were pre-cleared by incubation with 40 µl Protein G-sepharose beads (Calbiochem) at 4°C overnight, rotating the tubes to ensure good mixing. Non-solubilised material and Protein G beads were pelleted by centrifugation at 13000 rpm, 30 min at 4°C in a benchtop centrifuge. The supernatant was transferred to a fresh tube and this cell lysate incubated with an appropriate antibody for 4 h, rotating at 4°C. The antibody-nAChR protein complex was immunoprecipitated by incubation with 20 µl Protein G beads for 3 h, rotating at 4°C. Beads carrying the antibody-nAChR complex were pelleted by centrifugation at 13000 rpm, 5 min and washed once in high salt lysis buffer (500 mM NaCl), once in medium salt lysis buffer (300 mM NaCl) and once in low salt lysis buffer (150 mM NaCl). Pellets were resuspended in 20 µl sodium dodecyl sulphate (SDS)-loading dye (50 mM Tris/Cl pH 6.8, 200 mM dithiothreitol (DTT), 2% SDS, 0.2% bromophenol blue, 10% glycerol) and separated on a SDS-polyacrylamide gel (Amresco) with a 5% stacking gel and a 7.5% resolving gel. The gel was fixed for 30 min in 30% methanol, 10% glacial acetic acid, then incubated for 30 min in Amplify solution (Amersham). The gel was dried and exposed to Kodak X-OMAT photographic film at -80°C with intensifying screens.

2.9 ENZYME-LINKED ASSAY

All antibodies used in enzyme-linked assays were diluted in HBSS supplemented with Ca^{2+} and Mg^{2+}, through addition of 25 µM $CaCl_2$ and $MgCl_2$ ($HBSS^{++}$) and containing 2% BSA and 5% FCS. Cells transfected with HA-tagged subunits were assayed using either mouse mAbHA-7 (1:1000 dilution of 3.1 mg/ml) and goat α-mouse IgG peroxidase conjugate (1:2000 dilution of 0.8 mg/ml) or a single mouse α-HA peroxidase conjugate (1:2000 dilution of 1.2 mg/ml).

Note: In assays using mouse α-HA peroxidase conjugate, incubation in secondary antibody (and the subsequent washing steps) was not required.

Cells were transiently transfected on 13 mm coverslips, pre-coated with poly-L-lysine and collagen. Cells were fixed in 3% paraformaldehyde (PFA) made up in PBS. Fixation in PFA can cause cell permeabilisation, so cells assayed for staining of cell surface nAChRs were fixed after labelling with primary antibody. During staining of permeabilised cells, cells required fixation prior to permeabilisation and were fixed prior to incubation in primary antibody Levels of staining were normalised to staining of permeabilised cells expressing $\alpha 9\chi^{N\text{-}HA}$ (Sections 2.3.1 and 5.3.2), which were included as a positive control in each set of transfections and were reproducible between experiments, generating A_{665} values approximating 2.

2.9.1 Staining of permeabilised cells

Cells were washed in $HBSS^{++}$ and fixed for 15 min. Cells were permeabilised in 0.1% Triton X-100 for 10 min and incubated in a blocking solution of $HBSS^{++}$ containing 2% BSA and 0.1% Triton X-100 for 10 min at room temperature. Cells were incubated with primary antibody for 1 h in a humidified chamber at room temperature, then washed 4 times in $HBSS^{++}$. Cells were incubated with horseradish peroxidase (HRP)-conjugated secondary antibody for 1 h in a humidified chamber and washed 4 times in $HBSS^{++}$. For quantification of labelled nAChR, coverslips were incubated with 3,3',5,5'-tetramethyl benzidine (TMB) liquid substrate for HRP (Sigma) for 30 min. The soluble blue reaction product formed was transferred to a cuvette and A_{655} measured.

2.9.2 Staining of surface receptors

Cells were washed in $HBSS^{++}$ and incubated in a blocking solution of $HBSS^{++}$ containing 2% BSA for 10 min at room temperature. Cells were incubated with primary antibody for 1 h in a humidified chamber at room temperature, washed 4 times in $HBSS^{++}$ and fixed for 15 min. Cells were washed 4 times in $HBSS^{++}$ and incubated with HRP-conjugated secondary antibody for 1 h in a humidified chamber. Cells were washed 4 times in $HBSS^{++}$, incubated with TMB liquid substrate for 30 min, the supernatant transferred to a cuvette and A_{655} measured.

RESULTS

CHAPTER 3

CONSTRUCTION OF CHIMERIC cDNA

3.1 Introduction

Heterologous expression of nicotinic subunits is a valuable tool for investigating aspects of nAChR assembly, but recombinant nAChRs have proved especially difficult to express efficiently in mammalian cell lines in comparison to other members of the ligand-gated ion channel superfamily. For example, expression of the homomeric α7 and α8 nAChRs is dependent upon the nature of the host cell environment (Cooper and Millar, 1997; Cooper and Millar, 1998; Sweileh *et al.*, 2000). Folding and assembly of the homomeric $5HT_{3A}$ receptor appears to be considerably less dependent upon the host cell type (e.g. Baker *et al.*, 2004). Chimeric subunits containing the N-terminal region of the α7 and α8 subunits, fused to the C-terminal domain of the $5HT_{3A}$ receptor subunit are readily expressed at the cell surface of cell types which inefficiently fold wild-type subunits (Eiselé *et al.*, 1993; Blumenthal *et al.*, 1997; Cooper and Millar, 1997; Rangwala *et al.*, 1997; Cooper and Millar, 1998). Construction of subunit chimeras allows investigation into the influence of different regions of an individual subunit upon aspects of receptor folding and assembly and also provides a model system by which nicotinic-type subunits can be expressed and investigated in mammalian cell lines.

3.2 Construction of nAChR/$5HT_{3A}$ subunit chimeras

Chimeric subunit cDNAs similar to the $\alpha7^{(V201)}/5HT_{3A}$ chimera described previously (Eiselé *et al.*, 1993; Cooper and Millar, 1997) were constructed containing the extracellular N-terminal domain of the rat nAChR subunits (α2, α3, α4, α5, α6, α9, α10, β2, β3 and β4), fused to the transmembrane and intracellular domain of the mouse $5HT_{3A}$ subunit in the mammalian expression vector, pRK5 (Figure 3.1; Table 3.1). The $\alpha3/5HT_{3A}$ (for brevity, referred to as α3χ), $\alpha4/5HT_{3A}$ (α4χ), $\alpha5/5HT_{3A}$ (α5χ), $\beta2/5HT_{3A}$

($\beta2\chi$), $\beta3/5HT_{3A}$ ($\beta3\chi$) and $\beta4/5HT_{3A}$ ($\beta4\chi$) chimeras were constructed during a six month undergraduate placement project prior to the start of this PhD project, but details of their construction are included to allow their direct comparison with the other chimeras.

An $\alpha7^{(V201)}/5HT_{3A}$ chimera was used to generate each of the other subunit chimeras. The original pZeoSV-$\alpha7^{(V201)}/5HT_{3A}$ chimera was constructed by Dr. Sandra Cooper (this laboratory) (Cooper and Millar, 1997). The $\alpha7^{(V201)}/5HT_{3A}$ construct cDNA was subcloned into pZeoSV(+) at *Hind*III (5') and *Bcl*I (3') restriction enzyme sites, fusing the $\alpha7$ and $5HT_{3A}$ subunit cDNA fragments at a *Bcl*I site at residue V201 of the $\alpha7$ sequence, located just prior to the first predicted transmembrane region, M1 (Cooper and Millar, 1997).

The $\alpha7^{(V201)}/5HT_{3A}$ chimera was excised from the pZeoSV(+) mammalian expression vector with *Eco*RI (5') and *Sca*I (3') and subcloned into the *Eco*RI (5') / *Sma*I (3') sites of the pRK5 expression vector to produce pRK5-$\alpha7^{(V201)}/5HT_{3A}$ ($\alpha7\chi$). Digestion with both *Sca*I (AGT/ACT) and *Sma*I (CCC/GGG) produces blunt ended fragments that are compatible for ligation, but ligation does not regenerate either the *Sca*I or *Sma*I site. The pRK5 vector was used to simplify the subcloning strategy as it does not contain a *Bcl*I site (T/GATCA). A unique *Bcl*I site was introduced to the cDNA of each nAChR subunit at a position just prior to M1, by silent mutagenesis using PCR (Section 2.1.2; Figure 3.1). The PCR primers used are listed in Table 3.2. The fidelity of the chimeric constructs was verified by restriction mapping and sequencing.

To construct each of the $\alpha2\chi$, $\alpha3\chi$, $\alpha4\chi$, $\alpha5\chi$, $\alpha6\chi$, $\alpha9\chi$, $\beta2\chi$ and $\beta4\chi$ subunit chimeras in pRK5, PCR was performed using a T7 forward primer and a novel reverse primer to introduce a *Bcl*I(-) site just prior to M1 (Table 3.2). The pRK5-$\alpha7^{(V201)}/5HT_{3A}$ ($\alpha7\chi$) construct was digested with *Eco*RI (5') and *Bcl*I (3') to excise the $\alpha7$ portion of the chimera and produce a pRK5-/$5HT_{3A}$ (*Eco*RI/*Bcl*I) cloning cassette. PCR-amplified

nAChR subunit N-terminal domains, purified by ethanol precipitation (Section 2.2), were digested with *Eco*RI (5') and *Bcl*I (3') and cloned into the pRK5-/5HT$_{3A}$ (*Eco*RI/*Bcl*I) cloning cassette to create the pRK5-α2$^{(F204)}$/5HT$_{3A}$, pRK5-α3$^{(F204)}$/5HT$_{3A}$, pRK5-α4$^{(F204)}$/5HT$_{3A}$, pRK5-α5$^{(F201)}$/5HT$_{3A}$, pRK5-α6$^{(F204)}$/5HT$_{3A}$, pRK5-α9$^{(L209)}$/5HT$_{3A}$, pRK5-β2$^{(F201)}$/5HT$_{3A}$ and pRK5-β4$^{(F201)}$/5HT$_{3A}$ subunit chimeras (Table 3.1).

To construct the β3χ chimera, the PCR products were digested with *Sac*I (5') and *Bcl*I (3') and cloned into the pRK5-/5HT$_{3A}$ (*Eco*RI/*Bcl*I) cloning cassette with the addition of an 8 base pair linker (AATTAGCT) to join the 3'-overhang (TTAA) and 5'-overhang (TCGA) created by digestion with *Eco*RI (G/AATTC) and *Sac*I (GAGCT/C), respectively, to generate pRK5-β3$^{(F202)}$/5HT$_{3A}$:

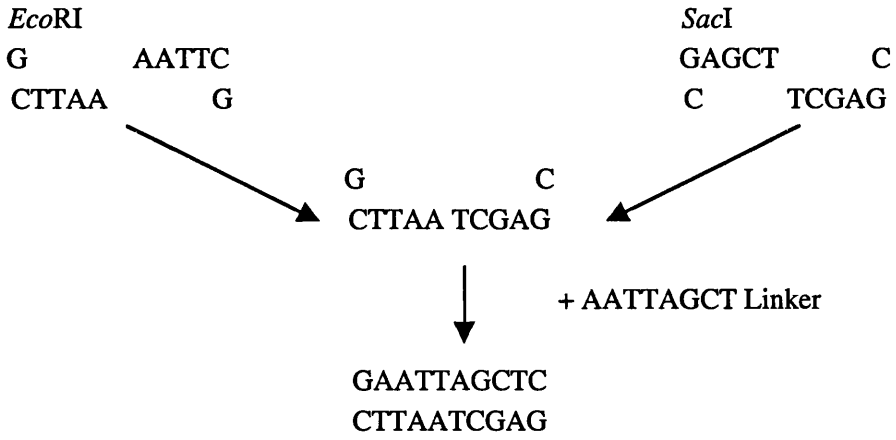

To construct the α10χ chimera, a unique *Xba*I site was introduced to the 5' end of the α10 cDNA and a unique *Bcl*I site was introduced just prior to M1 by PCR using novel forward (OL431 α10 *Xba*I) and reverse (OL404 α10 *Bcl*I) primers (Table 3.2). PCR products were digested with *Xba*I (5') and *Bcl*I (3'). The pRK5-α7$^{(V201)}$/5HT$_{3A}$ construct was digested with *Bcl*I (5') and *Sal*I(3') to excise the 5HT$_{3A}$ portion of the chimera. The α10 (*Xba*I/*Bcl*I) and 5HT$_{3A}$ (*Bcl*I/*Sal*I) fragments were subcloned into pRK5 (*Xba*I/*Sal*I) to create pRK5-α10$^{(L206)}$/5HT$_{3A}$.

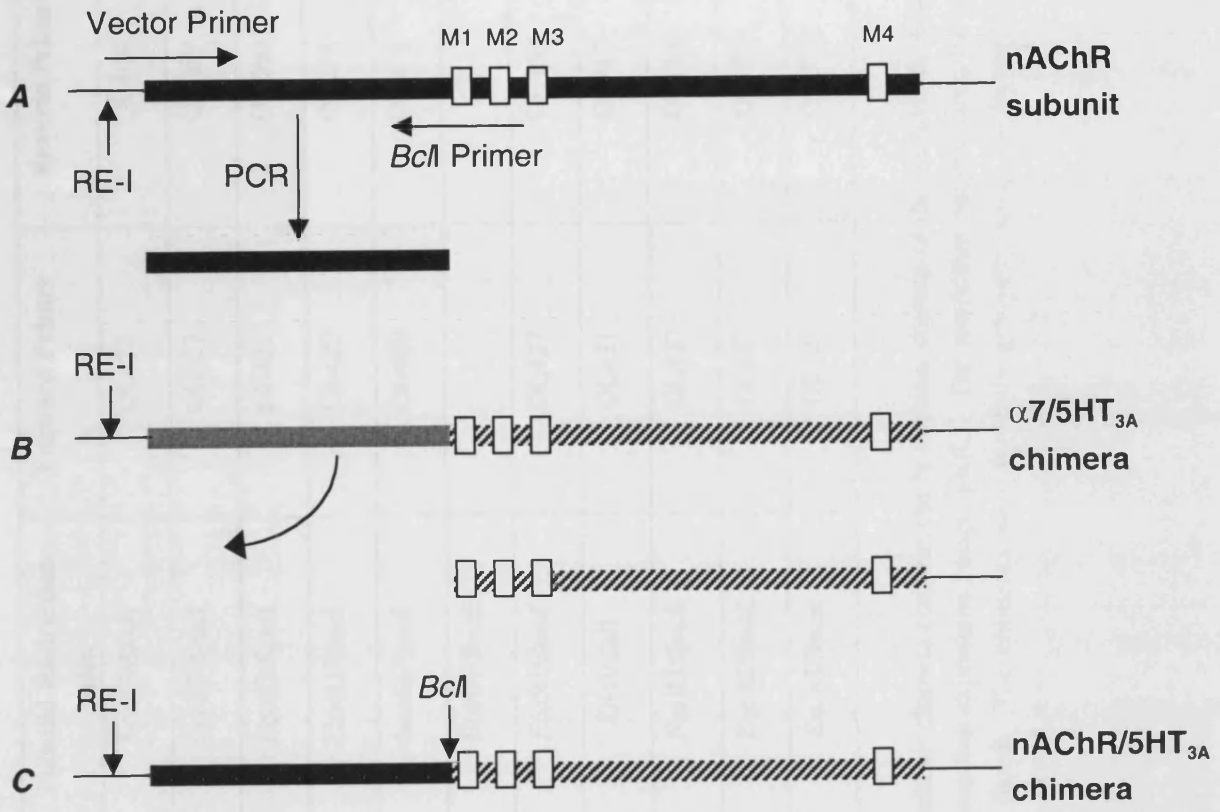

FIGURE 3.1. Construction of nAChR/$5HT_{3A}$ subunit chimeras. Each subunit chimera contains the N-terminal domain of an nAChR subunit (either α2, α3, α4, α5, α6, α9, α10, β2, β3 or β4) up to the first putative transmembrane region, M1, fused to the C-terminal region of the 5-hydroxytryptamine type 3 receptor ($5HT_{3A}$) subunit. Chimeric cDNAs were inserted into the mammalian expression vector, pRK5.

(*A*) The N-terminal region of the nAChR subunit up to M1 was generated by PCR using a forward primer specific to the RNA promoter 5' to the multiple cloning site of the mammalian expression vector, and a mutant reverse primer containing a *Bcl*I site. The PCR fragment was digested with restriction enzyme I (RE-I) (5') and *Bcl*I (3') and gel purified.

(*B*) pRK5-$\alpha7^{(V201)}/5HT_{3A}$ was digested with RE-I (5') and *Bcl*I (3') to excise the α7 portion of the chimera and produce a pRK5-/$5HT_{3A}$ (RE-I/*Bcl*I) cloning cassette.

(*C*) The nAChR (RE-I/*Bcl*I) PCR fragment was cloned into the pRK5-/$5HT_{3A}$ (RE-I/*Bcl*I) cloning cassette to create the pRK5-nAChR/$5HT_{3A}$ subunit chimera.

Plasmid-cDNA Construct	nAChR Subunit Restriction Sites	Subcloned From	Plasmid Restriction Sites	Forward Primer	Reverse Primer
pRK5-α2$^{(F204)}$/5HT$_{3A}$	*Eco*RI/*Bcl*I/*Sca*I	pcDNA1neo-α2	*Eco*RI/*Sma*I	OL427	OL404
pRK5-α3$^{(F204)}$/5HT$_{3A}$[a]	*Eco*RI/*Bcl*I/*Sca*I	pcDNA1neo-α3	*Eco*RI/*Sma*I	OL427	OL269
pRK5-α4$^{(F204)}$/5HT$_{3A}$[a]	*Eco*RI/*Bcl*I/*Sca*I	pcDNA1neo-α4	*Eco*RI/*Sma*I	OL427	OL260
pRK5-α5$^{(F201)}$/5HT$_{3A}$[a]	*Eco*RI/*Bcl*I/*Sca*I	pcDNA1neo-α5	*Eco*RI/*Sma*I	OL427	OL274
pRK5-α6$^{(F204)}$/5HT$_{3A}$	*Eco*RI/*Bcl*I/*Sca*I	pBSSK-α6	*Eco*RI/*Sma*I	OL400	OL401
pRK5-α7$^{(V201)}$/5HT$_{3A}$[a]	*Eco*RI/*Bcl*I/*Sca*I	pZeoSV2-α7$^{(V201)}$/5HT$_{3A}$[b]	*Eco*RI/*Sma*I	-	-
pRK5-α9$^{(L209)}$/5HT$_{3A}$	*Eco*RI/*Bcl*I/*Sca*I	pC1neo-α9	*Eco*RI/*Sma*I	OL427	OL469
pRK5-α10$^{(L206)}$/5HT$_{3A}$	*Xba*I/*Bcl*I/*Sal*I	pC1neo-α10	*Xba*I/*Sal*I	OL431	OL413
pRK5-β2$^{(F201)}$/5HT$_{3A}$[a]	*Eco*RI/*Bcl*I/*Sca*I	pcDNA1neo-β2	*Eco*RI/*Sma*I	OL427	OL261
pRK5-β3$^{(F202)}$/5HT$_{3A}$[a]	*Sac*I/*Bcl*I/*Sca*I	pcDNA1neo-β3	*Eco*RI/*Sma*I	OL427	OL273
pRK5-β4$^{(F201)}$/5HT$_{3A}$[a]	*Eco*RI/*Bcl*I/*Sca*I	pcDNA1neo-β4	*Eco*RI/*Sma*I	OL427	OL270

TABLE 3.1. Summary of the constructed rat/mouse nAChR/5HT$_{3A}$R chimeras. Each subunit chimera contains the N-terminal domain of the rat nAChR subunit up to M1, fused to the C-terminal region of the mouse 5HT$_{3A}$ receptor subunit, in the mammalian expression vector, pRK5. The restriction enzyme sites, the original rat nAChR subunit plasmid DNA and the PCR primers used in the subcloning are listed. The chimeras were typically generated using the original pRK5-α7$^{(V201)}$/5HT$_{3A}$ chimera[a], following excision of the α7 portion of this chimera to generate a pRK5-/5HT$_{3A}$ cloning cassette (Section 3.2).

[a] Constructed during a six month undergraduate placement.

[b] The pZeoSV2-α7$^{(V201)}$/5HT$_{3A}$ chimera was constructed by Dr. Sandra Cooper (Cooper and Millar, 1997).

Oligonucleotide	Details	Oligonucleotide sequence (5' - 3')
OL260	α4 *Bcl*I(-)	CG TCG GAT GAT CAC GGC ATA GGT G
OL261	β2 *Bcl*I(-)	CG ACG AAT GAT CAC GTC ATA GGT G
OL269	α3 *Bcl*I(-)	CAG GCG ACG GAT GAT CAC CGA GTA CGT GAT
OL270	β4 *Bcl*I(-)	GTT GCG CTT GAT GAT CAC GTC ATA GGT CAC
OL273	β3 *Bcl*I(-)	G CAG GCG TCT CAT GAT CAA AGA GTA GGT AAC
OL274	α5 *Bcl*I(-)	CAG CCG CTT AAT GAT CAA GGA GTA CGT GAT G
OL400	T7 pBS(+)	GTA ATA CGA CTC ACT ATA GGG CGA ATT GGG
OL401	α6 *Bcl*I(-)	GGG CAG CCT TCT GAT GAT CAC GGA GTA GGT
OL404	α2 *Bcl*I(-)	CAG CCG GCG GAT GAT CAC GTA GTA GGT
OL413	α10 *Bcl*I(-)	GCG GCG CAT GAT CAG AGT AAA G
OL427	T7(+)	TAA TAC GAC TCA CTA TAG GG
OL431	α10 *Xba*I(+)	CA TCG CTC TAG AAG ACT TGC GG
OL469	α9 *Bcl*I(-)	CCT CCT CTT GAT GAT CAC AGT GAA GGT

TABLE 3.2. The PCR primers used to generate the nAChR/$5HT_{3A}$ subunit chimeras.

(+) Forward primer

(-) Reverse primer

*Bcl*I T/GATCA

*Xba*I T/CTAGA

n Mutations introduced into the native nAChR subunit sequence to create the primer

3.3 Expression of chimeric subunit protein in tsA201 cells

To confirm that each subunit chimera could be expressed in mammalian cells, human embryonic kidney tsA201 cells transiently transfected with the chimeric subunit cDNAs were subjected to metabolic labelling and immunoprecipitation using an antiserum raised to the intracellular loop region of $5HT_{3A}$ ($pAb5HT_3$, Turton *et al.*, 1993) (Figure 3.2).

The molecular weights of mature unglycosylated nAChR subunits and their corresponding subunit chimeras were calculated from the protein amino acid sequences, using the Protein Information Resource at Georgetown University Medical Center, (http://pir.georgetown.edu/pirwww/search/comp_mw.shtml). Potential N-glycosylation sites were identified by searching the amino acid sequence of each subunit for NxS/T motifs (where x is any residue) (Tables 3.3 and 3.4).

Protein bands were detected for each nAChR/$5HT_{3A}$ subunit chimera following metabolic labelling and immunoprecipitation with $pAb5HT_3$ (Figure 3.2). The immunoreactive band detected for the $\beta3\chi$ chimera was faint in comparison to those detected for the other subunit chimeras in the exposure shown in Figure 3.2. However, additional immunoblotting experiments revealed the detection of a specific immunoreactive band for the $\beta3\chi$ subunit and this is highlighted in Figure 3.2.

The apparent molecular weights are indicated as molecular weight ranges in Table 3.4 to account for the detection of multiple protein bands for chimeras such as $\alpha9\chi$ and $\beta2\chi$ and for the error in measuring the migration distance of the broad immunospecific bands. Each chimeric subunit possesses more than one potential site for N-glycosylation (Table 3.4) and may explain the detection of multiple specific immunoreactive bands. The protein bands detected are of a size comparable to that expected from the predicted molecular weights (Table 3.4), suggesting full-length subunit protein is produced following the transient transfection of tsA201 cells with cDNA of chimeric constructs.

The molecular weight of each chimera is predicted to be 51 - 52 kDa (Table 3.4), with little variation in size between the chimeras. In Figure 3.2, slightly more variation in apparent molecular weight is observed, with the chimeric $\alpha 10\chi$ subunit migrating more rapidly on the SDS-polyacrylamide gel than the $\alpha 4\chi$ chimera, for example. The slight differences in the apparent molecular weight of the chimeric subunits, estimated according to their migration position on the SDS-polyacrylamide gel relative to protein molecular weight markers, may be a consequence of differences in glycosylation of the mature proteins. The $\alpha 4\chi$ chimera possesses 3 potential sites for N-glycosylation in its N-terminal domain, while the $\alpha 10\chi$ chimera contains only 2 potential N-glycosylation sites (Table 3.4). The comparison of predicted and apparent molecular weights shown for the wild-type nAChR subunits in Table 3.3 also demonstrates that some variation is observed between the expected size of mature proteins and the apparent size determined experimentally.

As full length protein was successfully produced for each of the nAChR/$5HT_{3A}$ subunit constructs, these chimeras were considered suitable for use in the investigation of nAChR expression in mammalian cell lines (Chapters 4 - 7).

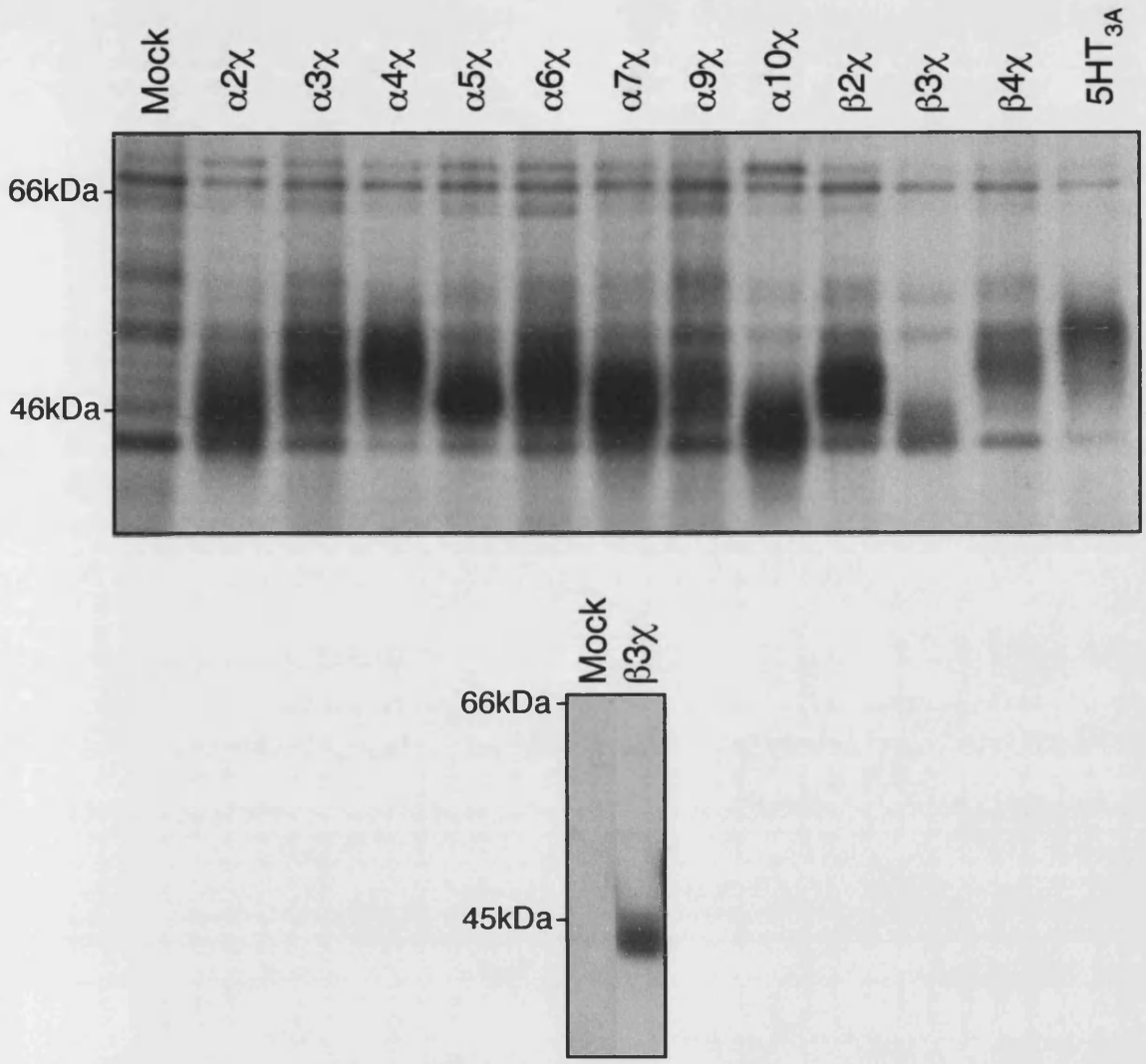

FIGURE 3.2. Heterologous expression of subunit chimeras determined by immunoprecipitation of metabolically labelled proteins from detergent-solubilised cells. Mammalian tsA201 cells were transfected with nAChR/$5HT_{3A}$ subunits constructed in the mammalian expression vector, pRK5. Cell lysates were immunoprecipitated with pAb$5HT_3$, a polyclonal antiserum raised to the intracellular loop region of the $5HT_{3A}$ subunit. The positions of molecular weight markers are indicated. Immunoreactive bands were detected corresponding to the each of the nAChR/$5HT_{3A}$ chimeric subunits. Due to the faint band produced for the β3χ subunit, an additional figure is included from a separate immunoblotting (rather than immunoprecipitation) experiment, using pAb$5HT_3$, to demonstrate the production of protein for this subunit upon expression in tsA201 cells.

Rat Subunit	Number of residues in the mature protein	Predicted molecular weight	Apparent molecular weight	Number of potential N-terminal N-glycosylation sites
α2	479	55	59[a]	2
α3	474	55	57[b]	2
α4	594	67	68[a]	3
α5	424	49	51 - 56[a,b]	2
α6	463	54	57[c]	2
α7	480	54	59[d]	3
α9	457	52	55[e] (human)	2
α10	423	47	55[e] (human)	2
β2	473	54	54 - 57[a,b]	2
β3	433	50	55[c]	2
β4	471	53	52[c]	4
$5HT_{3A}$	464	51	61[f]	3

TABLE 3.3. Molecular weights of the wild-type neuronal nAChR (rat) and $5HT_{3A}$ (mouse) receptor subunits. Molecular weights were predicted from the amino acid sequence of the mature subunit, using the Protein Information Resource (Georgetown University Medical Center website; http://pir.georgetown.edu/pirwww/search/comp_mw.shtml). Apparent molecular weights are data from previous studies ([a]Balestra *et al.*, 2000; [b]Wang *et al.*, 1996; [c]Vailati *et al.*, 1999; [d]Dominguez del Toro *et al.*, 1994; [e]Sgard *et al.*, 2002; [f]Mukerji *et al.*, 1996). Potential N-glycosylation sites within the N-terminal domain of each subunit were identified by searching the amino acid sequence of each subunit for NxS/T motifs (where x is any residue).

Subunit	Number of residues in the mature protein	Predicted molecular weight	Apparent molecular weight	Number of potential N-terminal N-glycosylation sites
$\alpha2^{F204}/5HT_{3A}$	451	52	45 - 48	2
$\alpha3^{F204}/5HT_{3A}$	451	52	46 - 50	2
$\alpha4^{F204}/5HT_{3A}$	451	52	48 - 50	3
$\alpha5^{F201}/5HT_{3A}$	448	51	47 - 49	2
$\alpha6^{F204}/5HT_{3A}$	451	52	48 - 50	2
$\alpha7^{V201}/5HT_{3A}$	449	52	47 - 49	3
$\alpha9^{L209}/5HT_{3A}$	456	52	47 - 49	2
$\alpha10^{L206}/5HT_{3A}$	453	51	45 - 46	2
$\beta2^{F201}/5HT_{3A}$	448	51	47 - 49	2
$\beta3^{F202}/5HT_{3A}$	449	51	45 - 46	2
$\beta4^{F201}/5HT_{3A}$	448	51	47 - 50	4
$5HT_{3A}$	464	51	52 - 53	3

TABLE 3.4. Molecular weights of the chimeric nAChR/$5HT_{3A}$ subunits. Predicted molecular weights were calculated from the amino acid sequence of the mature subunit protein, using the Protein Information Resource (Georgetown University Medical Centre website; http://pir.georgetown.edu/pirwww/search/comp_mw.shtml). Apparent molecular weights are data from this study, estimated following metabolic labelling and immunoprecipitation using the pAb$5HT_3$ antiserum, raised to the intracellular loop region of the $5HT_{3A}$ receptor subunit (Figure 3.2). Searching the amino acid sequence of each subunit for NxS/T motifs (where x is any residue) identified potential N-glycosylation sites.

CHAPTER 4

PHARMACOLOGICAL CHARACTERISATION OF nAChRs CONTAINING α9 AND α10 SUBUNITS

4.1 Introduction

Expression of the α9 and α10 subunits is largely restricted to the hair cells of the inner ear (Elgoyhen *et al.*, 1994; Hiel *et al.*, 1996; Elgoyhen *et al.*, 2001; Lustig *et al.*, 2001) and consequently, nAChRs containing α9 and α10 do not fall conveniently into the conventional classification of either muscle-type or neuronal nAChRs. Nicotinic receptors expressed in outer hair cells of the cochlea have been demonstrated to be responsible for modulating auditory nerve responses to acoustic stimulation and for protection from acoustic overstimulation (Sridhar *et al.*, 1997). A role for α9-containing nAChRs in auditory processing has been suggested by *in vivo* studies conducted with transgenic (Vetter *et al.*, 1999) and wild-type animals (Luebke and Foster, 2002).

When expressed alone in *Xenopus* oocytes, the α9 subunit, but not the α10 subunit, is capable of generating functional homomeric nAChRs (Elgoyhen *et al.*, 1994; Elgoyhen *et al.*, 2001; Sgard *et al.*, 2002). When α9 and α10 are co-expressed in oocytes, considerably larger whole-cell currents are observed, suggesting that these subunits may normally co-assemble to form heteromeric complexes (Elgoyhen *et al.*, 2001; Sgard *et al.*, 2002). Despite successful studies in oocytes, there have been no reports of the heterologous expression of α9- or α10-containing nAChRs, as either homomeric or heteromeric complexes, in other expression systems. Whilst much can be achieved by characterisation of oocyte-expressed nAChRs, some approaches to the pharmacological characterisation of α9α10 nAChRs, for example equilibrium binding studies, have been hindered by the lack of a suitable cultured cell-based expression system.

4.2 Heterologous expression of α9 and α10 subunits in tsA201 cells

To investigate the heterologous expression of α9-containing nAChRs in mammalian cell lines, rat α9 and α10 subunit cDNAs were introduced by transient transfection into cultured tsA201 cells. Membranes were isolated from cells co-transfected with α9 and α10 cDNAs and from cells transfected with α9 alone or α10 alone. Binding studies were performed with [^{3}H]-methyllycaconitine ([^{3}H]-MLA), a nicotinic receptor antagonist reported to bind with high apparent affinity to recombinant α9α10 nAChRs expressed in *Xenopus* oocytes (Verbitsky *et al.*, 2000). However, no evidence for specific high affinity [^{3}H]-MLA binding was obtained. Further binding studies were performed with a range of nicotinic radioligands including [^{125}I]-α-BTX, [^{3}H]-epibatidine and [^{3}H]-methylcarbamylcholine ([^{3}H]-MCC), none of which revealed specific high affinity binding. This observation is consistent with previous studies, which have failed to detect functional nAChRs in mammalian (HEK293) cells transfected with α9 and α10 cDNAs (Lustig *et al.*, 2001).

To confirm that α9 and α10 subunits were expressed in transfected cells, α9 and α10 cDNA constructs were tagged at their C-termini with the nine amino acid influenza haemagglutinin (HA) epitope tag (Kolodziej and Young, 1991) (see Sections 2.3.3 and 5.3). Cells transfected with the HA-tagged subunits (pRK5-α9$^{C\text{-}HA}$ and pRK5-α10$^{C\text{-}HA}$) were subjected to immunoblotting with mAbHA-7, which revealed immunoreactive protein bands of a size similar to that expected for full-length mature α9 and α10 subunits (see Sections 5.3.1 and 5.4 and Figure 5.4). The subunits were tagged at their extreme C-terminus, providing strong evidence that these correspond to full-length α9 and α10 subunits. However, some degradation of HA-tagged subunit protein may have occurred, suggested by "smearing" of the immunoreactive protein bands observed in Figure 5.4 may indicate that the HA-epitope tag disrupts protein stability (see Section 5.4). Since the α9 and α10 subunit polypeptides do appear to be expressed in transfected

cells, this suggests that the absence of a specific nicotinic radioligand binding is a consequence of inappropriate folding and/or assembly of the subunits.

4.3 Heterologous expression of α9 and α10 subunits in a cochlea hair cell line

Difficulties have been reported in the heterologous expression of other nAChR subunits (in particular the α7 and α8 subunits) in cultured mammalian cell lines (Puchacz *et al.*, 1994; Quik *et al.*, 1996; Cooper and Millar, 1997; Kassner and Berg, 1997; Rangwala *et al.*, 1997; Cooper and Millar, 1998; Sweileh *et al.*, 2000). This has led to the conclusion that appropriate subunit folding and assembly events are influenced strongly by the nature of the host cell type (Millar, 1999; Sivilotti *et al.*, 2000). While the α7 and α8 nAChRs appear to misfold in human embryonic kidney HEK293 cells, these nAChRs are expressed at the cell surface of cell lines including the human neuroblastoma SH-SY5Y cell line and rat phaeochromocytoma PC12 cells, both of which express an endogenous α7 subunit (Cooper and Millar, 1997; Cooper and Millar, 1998).

The α9 and α10 subunits are expressed in the hair cells of the inner ear (Elgoyhen *et al.*, 1994; Hiel *et al.*, 1996; Elgoyhen *et al.*, 2001; Lustig *et al.*, 2001). Conditionally immortal cochlea hair cell lines have been derived from the H-2Kb-*ts*A58 transgenic mouse ("Immortomouse"), which contains a conditionally expressed, temperature sensitive immortalising oncogene (a mutant of the tumour antigen, T-Ag, from the SV40 virus) (Jat *et al.*, 1991; Holley *et al.*, 1997; Rivolta *et al.*, 1998). The presence of the immortalising gene prevents terminal differentiation and perpetuates cell proliferation in cells maintained at 33°C in the presence of γ-interferon. The mouse cochlea-derived UB/OC-1 and UB/OC-2 (University of Bristol/Organ of Corti) cell lines express endogenous α9-containing nAChRs that demonstrate high calcium permeability and elicit ACh-induced inward currents that are blocked by nicotine and strychnine (Rivolta *et al.*, 1998; Jagger *et al.*, 1999).

The expression of α9-containing nAChRs was investigated in UB/OC cell lines to ascertain whether these cells permit the correct folding of a nicotinic binding site attributable to either endogenous nAChRs or to recombinant nAChRs following over-expression of α9 and/or α10 cDNAs. Membrane preparations of proliferating cultures of UB/OC-1 and UB/OC-2 cells (immortalised at slightly different stages of differentiation) (Rivolta *et al.*, 1998) were subjected to radioligand binding with [^{3}H]-MLA, [^{3}H]-strychnine and [^{3}H]-MCC to investigate the expression of endogenous nAChRs. However, no evidence for specific radioligand binding was observed in the untransfected cells. Similarly, cells transiently transfected with either α9, α10 or α9+α10 did not reveal any significant levels of specific radioligand binding (data not shown; n=4).

The conditionally immortal cochlea-derived UB/OC cell lines can be compelled to terminally differentiate when cultured at 37 - 39°C in the absence of γ-interferon (Jat *et al.*, 1991; Holley *et al.*, 1997). UB/OC-2 cells were incubated under permissive conditions for 6 - 14 days to allow differentiation of the cells, but cell membranes incubated with 15 nM [^{3}H]-MLA did not reveal any evidence for specific radioligand binding (data not shown; n=5).

4.4 Expression of α9/5HT$_{3A}$ and α10/5HT$_{3A}$ subunit chimeras in tsA201 cells

The relatively inefficient folding and cell-surface expression of several nAChR subunits (including α1, α4, α7, α8 and β2) can be enhanced by replacing the C-terminal region of nAChR subunits with the corresponding region of the 5HT$_{3A}$ subunit (Eiselé *et al.*, 1993; Blumenthal *et al.*, 1997; Rangwala *et al.*, 1997; Cooper and Millar, 1998; Cooper *et al.*, 1999; Harkness and Millar, 2002). Subunit chimeras were constructed in the pRK5 mammalian expression vector that contained the extracellular N-terminal domain of the rat α9 and α10 subunits respectively, fused to the transmembrane and intracellular domain of the mouse 5HT$_{3A}$ subunit (for brevity, these are referred to as α9χ and α10χ) (Table 3.1).

To examine whether these chimeras were able to generate functional receptors, as has been demonstrated for the $\alpha7/5HT_{3A}$ chimera (Eiselé *et al.*, 1993; Blumenthal *et al.*, 1997; Rangwala *et al.*, 1997; Cooper and Millar, 1998; Cooper *et al.*, 1999), the $\alpha9\chi$ and $\alpha10\chi$ cDNAs in pRK5 were injected into *Xenopus* oocytes. This work was carried out by Dr. Ruud Zwart in a collaboration with Dr. Emanuele Sher's group at Eli Lilly. Clear evidence for the expression of functional receptors was obtained by two-electrode voltage-clamp recordings, although responses were significantly smaller than have been observed with the $\alpha7/5HT_{3A}$ chimera (Eiselé *et al.*, 1993; Blumenthal *et al.*, 1997; Rangwala *et al.*, 1997). Small whole-cell responses to ACh were detected in oocytes injected with either $\alpha9\chi$ alone (13.6±7.7 nA; n=10) or with $\alpha10\chi$ alone (40.4±39.8 nA; n=24), demonstrating that both of these chimeras are able to form functional homomeric receptors (Figure 4.1). Responses detected in oocytes co-injected with the $\alpha9\chi$ and $\alpha10\chi$ cDNAs (12.5±3.9 nA; n=19) were not significantly larger than those recorded with either subunit alone. In all cases, responses to ACh were blocked completely and reversibly by a 2 min application of 1 μM α-BTX.

To examine whether problems encountered in the heterologous expression of α9 and α10 nAChRs in a mammalian cell line could be alleviated by expression of $nAChR/5HT_{3A}R$ chimeras, the $\alpha9\chi$ and $\alpha10\chi$ subunit cDNAs were introduced by transient transfection into tsA201 cells. Radioligand binding performed on membrane preparations derived from cells transfected with either the $\alpha9\chi$ chimera alone or the $\alpha10\chi$ chimera alone revealed specific binding with the nicotinic antagonist [^{3}H]-MLA at levels significantly above background (166±50 fmol/mg and 68±22 fmol/mg, respectively; Figure 4.2). However, when $\alpha9\chi$ and $\alpha10\chi$ were co-expressed, substantially higher levels of specific [^{3}H]-MLA binding were observed (802±160 fmol/mg; Figure 4.2). Levels of [^{3}H]-MLA binding detected in cells co-transfected with $\alpha9\chi$ and $\alpha10\chi$ were considerably higher than with $\alpha9\chi$ alone (4.3±0.3-fold, n=4) or with $\alpha10\chi$ alone (21.2±7.5-fold, n=6).

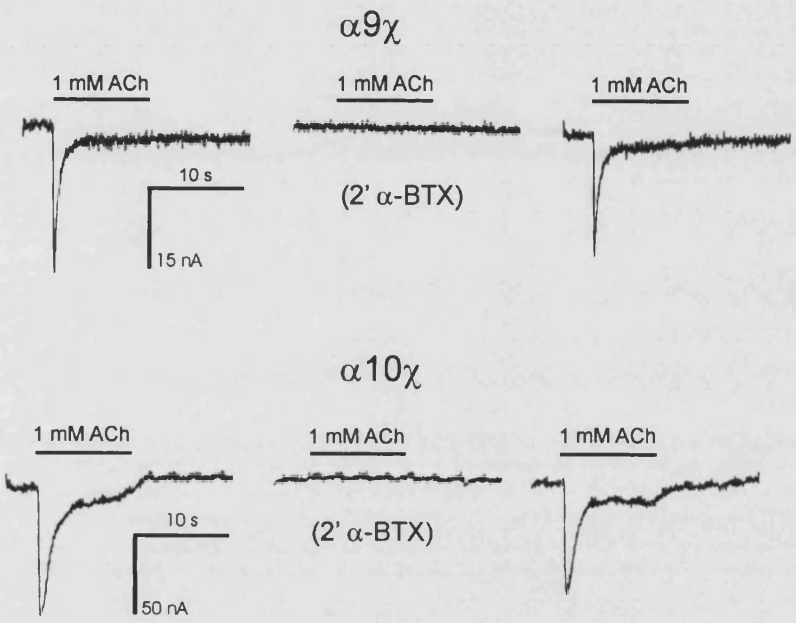

FIGURE 4.1. Functional responses in *Xenopus* oocytes injected with α9χ and α10χ subunit cDNAs. Application of 1 mM ACh to oocytes expressing α9χ or α10χ nAChRs induced small, transient inward currents that were completely abolished after 2 min pre-application of 1 μM α-BTX. The inhibitory effect of α-BTX on both chimeric nAChRs was almost completely reversed after 4-6 min of washout of the toxin. This work was carried out by Dr. Ruud Zwart, Eli Lilly, UK.

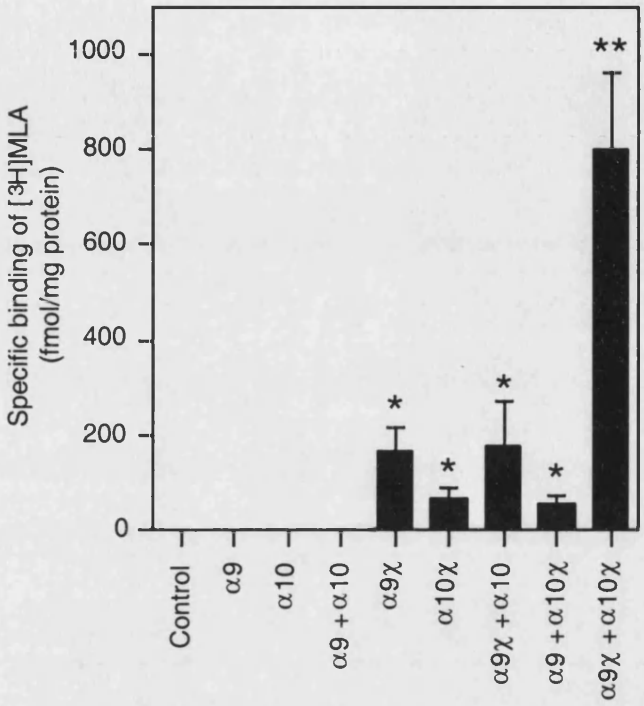

FIGURE 4.2. Specific [^{3}H]-MLA binding to cell membranes of tsA201 cells transiently transfected with wild-type (α9 and α10) and chimeric (α9χ and α10χ) subunits. Data are presented as means of 4 - 7 independent experiments performed in triplicate and show significant levels of radioligand binding in cells transfected with α9χ (166±50 fmol/mg protein), α10χ (68±22 fmol/mg protein) and α9χα10χ (802±160 fmol/mg protein). Significance determined by two-tailed Student's *t* test (*p<0.05; **p<0.01).

Proliferating cultures of UB/OC-1 and UB/OC-2 cells transiently transfected with the α9χ and α10χ subunit chimeras either alone or in combination did not reveal any significant levels of [^{3}H]-MLA binding (data not shown; n=3). The expression of the chimeric subunits in differentiating cultures of UB/OC cells has not been established (see Section 4.6).

4.5 Pharmacological characterisation of α9χα10χ nAChR complexes in tsA201 cells

Saturation radioligand binding performed on cells co-transfected with α9χ and α10χ revealed that [^{3}H]-MLA bound with high affinity (K_d = 7.5±1.2 nM, n=5; Figure 4.3). The data fit well to a single-site model during non-linear regression analysis (Figure 4.3). Scatchard analysis of the saturation binding data to membrane preparations of tsA201 cells expressing α9χα10χ did not suggest the presence of more than one class of high affinity binding site for [^{3}H]-MLA (Figure 4.3). The low levels of radioligand binding to α9χ and α10χ, when expressed alone, prevented an accurate determination of the affinity of [^{3}H]-MLA binding to homomeric α9χ and α10χ receptors.

Equilibrium competition binding studies were performed with a range of ligands to determine their affinity for α9χα10χ receptors (Figure 4.4; Table 4.1). The nicotinic antagonist α-BTX bound with high affinity (66±22 nM). Other nicotinic ligands bound with lower affinities, including *d*-tubocurarine (0.3±0.1 μM), 1,1-dimethyl-4-phenylpiperazinium (DMPP) (2.0±0.4 μM), ACh (2.7±2.5 μM), carbachol (10.4±2.2 μM), MCC (38.7±19.2 μM) and nicotine (42.9±6.2 μM). Specific competition binding was also observed with the glycine receptor convulsant strychnine, the GABA receptor antagonist, bicuculline and the muscarinic antagonist, atropine (66±7 nM, 0.6±0.3 μM and 9.9±1.3 μM, respectively). The rank order of K_i values is in good agreement with the relative potencies of these ligands identified from electrophysiological assays on both recombinant α9 and α9α10 nAChRs expressed in *Xenopus* oocytes and with native nAChRs expressed in hair cells (Housley and Ashmore, 1991; Fuchs and Murrow, 1992; Rothlin *et al.*, 1999; Verbitsky *et al.*, 2000) (Table 4.1).

A further series of radioligand binding studies were performed on tsA201 cells transfected with an $\alpha7^{(V201)}/5HT_{3A}$ subunit chimera ($\alpha7\chi$) (Eiselé *et al.*, 1993; Cooper and Millar, 1998) constructed in the pRK5 vector (Section 3.2). The rationale of these studies was to facilitate a comparison of $\alpha7\chi$ receptors with $\alpha9\chi\alpha10\chi$ receptors, but also to enable a comparison with radioligand binding data which has been reported previously with native $\alpha7$ nAChRs (Anand *et al.*, 1993b; Davies *et al.*, 1999). Thus, whereas radioligand binding data determined with $\alpha9\chi\alpha10\chi$ has been compared with EC_{50}/IC_{50} values for $\alpha9\alpha10$ nAChRs (Table 4.1), a direct comparison is possible between equilibrium radioligand binding data from $\alpha7\chi$ and $\alpha7$-containing nAChRs (Table 4.2). A similar pharmacological profile of recombinant $\alpha7\chi$ and native $\alpha7$ nAChRs would argue that $nAChR/5HT_{3A}$ subunit chimeras reflect the ligand binding properties of corresponding wild-type nAChRs.

Saturation radioligand binding experiments performed with tsA201 cells transfected with $\alpha7\chi$ revealed high affinity binding of [^{3}H]-MLA (1.2±0.2 nM; Figure 4.3). This is in close agreement with estimates of the affinity of [^{3}H]-MLA binding to rat brain $\alpha7$ nAChRs (1.9±0.3 nM) (Davies *et al.*, 1999). The linear nature of the Scatchard plot in Figure 4.3, along with the good fit of data to a single-site model in the non-linear regression analysis of the saturation binding data suggests the presence of a single class of radioligand binding site in membrane preparations of tsA201 cells transiently transfected with $\alpha7\chi$ (Figure 4.3). As illustrated in Table 4.2, competition binding studies performed on tsA201 cells transfected with $\alpha7\chi$ reveal a pharmacological profile with close similarity to that of the native $\alpha7$ nAChR (Anand *et al.*, 1993a; Davies *et al.*, 1999).

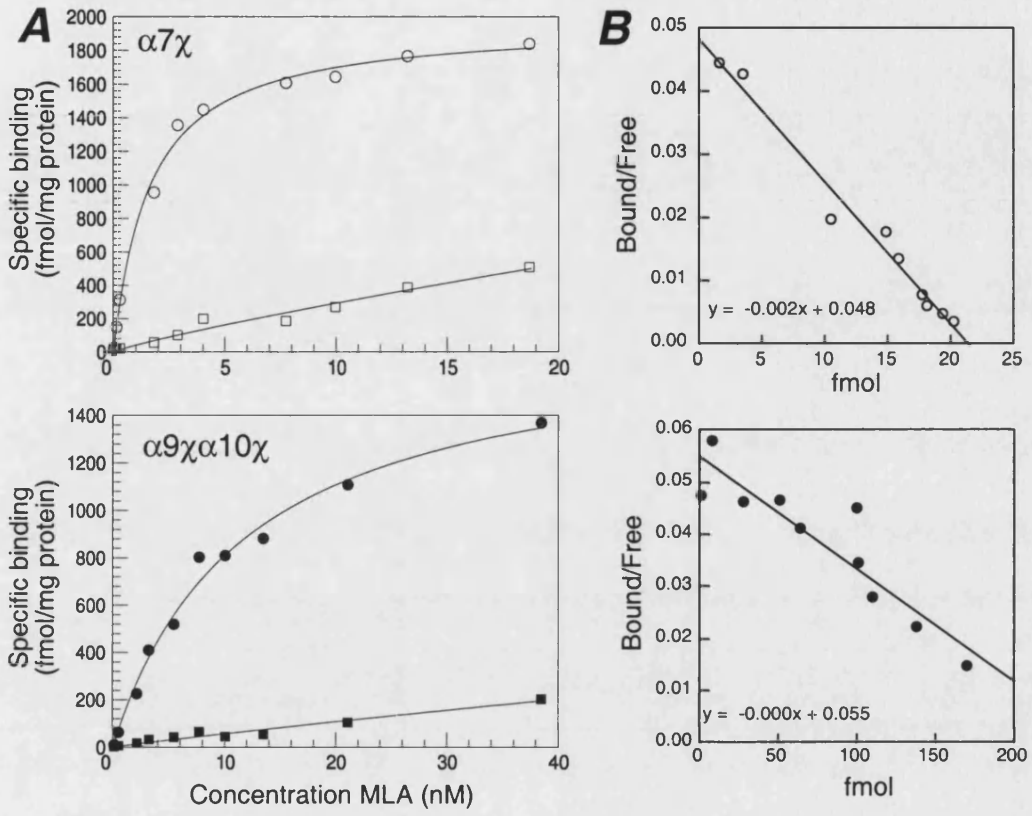

FIGURE 4.3. Specific binding of [^{3}H]-MLA to α7χ and α9χα10χ receptors expressed in tsA201 cells. (*A*) Equilibrium saturation radioligand binding was performed on membranes prepared from tsA201 cells transfected with α7χ (upper panel) or α9χ+α10χ (lower panel) subunit chimeras. Data represent specific binding (circles) and non-specific binding (squares). Data are from a single experiment performed in triplicate with K_d values of 11.8±4.0 nM (α9χα10χ) and 1.6±0.2 nM (α7χ), but are typical of 4 - 5 independent determinations, giving mean K_d values of 7.5±1.2 nM (α9χα10χ) and 1.2±0.2 nM (α7χ). (*B*) Scatchard Plots derived from the presented data that provide no evidence to suggest that the saturation radioligand binding to cells expressing α9χα10χ or α7χ represents more than one class of [^{3}H]-MLA binding site.

FIGURE 4.4. Pharmacological characterisation of α9χα10χ and α7χ receptors expressed in tsA201 cells. Equilibrium radioligand binding showing competition of [^{3}H]-MLA binding by α-BTX, ACh, atropine, bicuculline, carbachol, DMPP, *d*-tubocurarine (*d*-TC), MCC, nicotine and strychnine. Binding was performed on membranes prepared from tsA201 cells transfected with α9χ+α10χ (closed circles) or α7χ (open circles) subunit chimeras. Data points are means of triplicate samples. Each graph is from a single experiment but is typical of 3 - 4 individual experiments. Mean K_i values, derived from these and other competition radioligand binding studies, are presented in Tables 4.1 and 4.2.

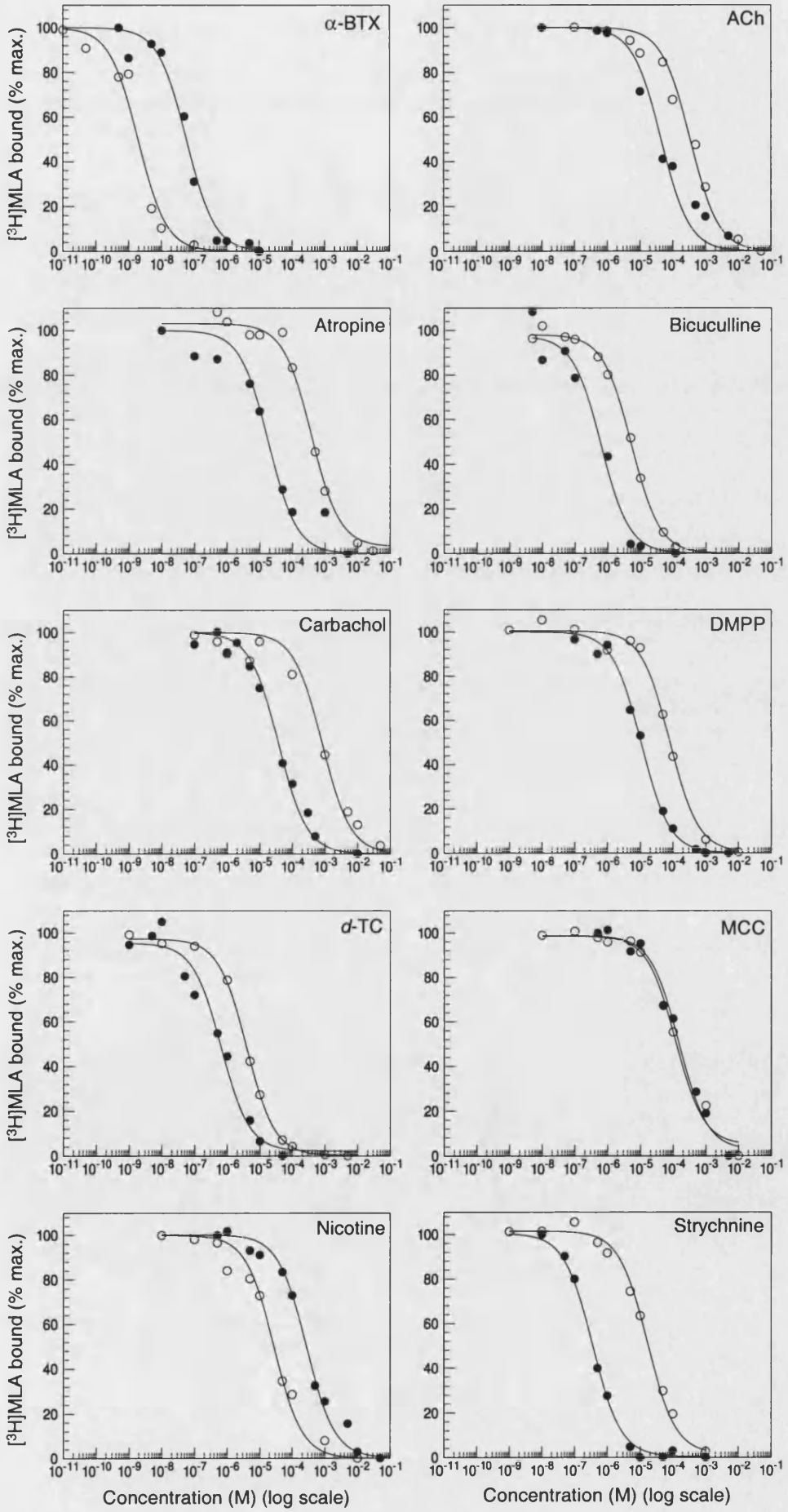
α-BTX
ACh
Atropine
Bicuculline
Carbachol
DMPP
d-TC
MCC
Nicotine
Strychnine
[3H]MLA bound (% max.)
Concentration (M) (log scale)

Ligand	α9χα10χ tsA201 cells (K_d/K_i)†	α9 oocyte (EC_{50}/IC_{50})‡	α9α10 oocyte (EC_{50}/IC_{50})§	α9α10* Hair cells (EC_{50}/IC_{50})¶
MLA	7.5±1.2 nM	1 nM	ND	ND
α-Bungarotoxin	66±22 nM	4 nM	nM range	nM range
Strychnine	66±7 nM	18 nM	20 nM	nM range
d-Tubocurarine	290±90 nM	300 nM	110 nM	nM range
Bicuculline	0.6±0.3 μM	0.8 μM	1 μM	~ 1 μM
DMPP	2.0±0.4 μM	ND	ND	ND
Acetylcholine	2.7±2.5 μM	11 μM	14 μM	7 μM
Atropine	9.9±1.3 μM	1 μM	1 μM	μM range
Carbachol	10.4±2.2 μM	64 μM	ND	87 μM
Methylcarbachol	38.7±19.2 μM	30 μM	ND	ND
Nicotine	42.9±6.2 μM	32 μM	4 μM	μM range
5HT	451±21 μM	251 μM	5.4 μM	7.5 μM

TABLE 4.1. Pharmacological properties of α9χα10χ nAChRs and comparison with native and recombinant receptors. Ligands are listed in order of decreasing affinity as determined by equilibrium radioligand binding with α9χα10χ receptors expressed in tsA201 cells. The rank order for these ligands is in good general agreement with estimates of agonist/antagonist potency derived from functional assays performed with either recombinant α9 or α9α10 nAChRs expressed in *Xenopus* oocytes or with native nAChRs expressed in hair cells. K_d values (for MLA) were determined by equilibrium saturation binding. K_i values (for all other ligands) were determined by competition binding performed with [^{3}H]-MLA. ND = data not determined.

* The subunit composition of native nAChRs expressed in hair cells is assumed to be α9α10.

† Data (this study) are means of 4-5 experiments each performed in triplicate.

‡ Data from Verbitsky *et al.*, 2000.

§ Data from Elgoyhen *et al.*, 2001.

¶ Data from several studies, as reviewed by Verbitsky *et al.*, 2000 and Elgoyhen *et al.*, 2001.

Ligand	α7χ tsA201 cells (K_d/K_i)†	α7* Native (brain) (K_d/K_i)
MLA	1.2±0.2 nM	1.9±0.3 nM ‡
α-Bungarotoxin	0.3±0.1 nM	1.8±0.5 nM ‡
Bicuculline	1.4±0.2 μM	ND
d-Tubocurarine	1.6±0.2 μM	ND
Strychnine	6.7±0.9 μM	5.4±0.5 μM §
Nicotine	28.8±8.7 μM	6.1±1.1 μM ‡
DMPP	28.9±5.3 μM	ND
Methylcarbachol	90±34 μM	10.6±0.6 μM ‡
Atropine	140±11 μM	198±10 μM §
Acetylcholine	129±39 μM	103±8.7 μM §
Carbachol	698±248 μM	580±205 μM §

TABLE 4.2. Pharmacological properties of α7χ nAChRs and comparison with native α7 receptors. Ligands are listed in order of decreasing affinity as determined by equilibrium radioligand binding with α7χ receptors expressed in tsA201 cells. The rank order for these ligands is in good general agreement with estimates of binding affinity determined with native α7 nAChRs expressed in rat or chick brain. K_d values (for MLA) were determined by equilibrium saturation binding. K_i values (for all other ligands) were determined by competition binding performed with [^{3}H]-MLA. ND = data not determined.

* The subunit composition of native α7-containing nAChRs is uncertain but data from rat brain (‡) are expected to correspond predominantly to homomeric α7 (Chen and Patrick, 1997; Drisdel and Green, 2000). Data from chick brain (§) are

expected to represent binding to a mixed population α7, α8 and α7α8 nAChRs (Keyser *et al.*, 1993).

† Data (this study) are means of three experiments each performed in triplicate.

‡ Data from Davies *et al.*, 1999, from rat brain α7 nAChR.

§ Data from Anand *et al.*, 1993b, from chick brain α7 nAChR.

4.6 Discussion

The expression of both functional homomeric α9 and heteromeric α9α10 nAChRs has been demonstrated upon expression of the α9 and α10 subunits in *Xenopus* oocytes (Elgoyhen *et al.*, 1994; Elgoyhen *et al.*, 2001). However, in the present study, no evidence for specific binding of nicotinic radioligands was detected in mammalian cells transfected with α9 and α10. The inability of the α9 and α10 subunits to assemble into nAChRs that bind radioligands such as [^{3}H]-MLA with high affinity when expressed in tsA201 cells, may suggest that subunit misfolding is a cell-specific event and is consistent with previous studies that have failed to detect the expression of α9-containing nAChRs in HEK293 cells (Lustig *et al.*, 2001).

The UB/OC-1 and UB/OC-2 cell lines express endogenous α9-containing nAChRs (Rivolta *et al.*, 1998; Jagger *et al.*, 2000), so it was somewhat surprising that these receptors could not be detected by radioligand binding of either proliferating or differentiating cultures of cells. Under differentiating conditions, expression of α9 mRNA is upregulated and a greater proportion of cells respond to ACh (Rivolta *et al.*, 1998; Jagger *et al.*, 1999). However, the absence of radioligand binding may be due to low levels of receptor expression even in differentiated cell cultures. Alternatively, the native α9-containing nAChRs of the UB/OC cell lines may not generate ligand binding sites of high enough affinity to be detected with either 30 nM [^{3}H]-MLA or 30 nM [^{3}H]-strychnine. Native α9-nAChRs in cochlea hair cells are antagonised by nanomolar concentrations of strychnine, but the affinity for MLA has not been determined (Verbitsky *et al.*, 2000). Specific [^{3}H]-MLA binding was not detected following over-expression of either wild-type α9 and α10 or chimeric α9χ and α10χ subunits in cultures of proliferating cells. The over-expression of these subunits in differentiating cultures of cells would require the generation of stable cell lines, as differentiation requires culture of cells under permissive conditions (37 - 39°C in the absence of γ-interferon) for approximately 14 days. Evidence for the expression of functional

endogenous nAChRs in these cell lines (Rivolta *et al.*, 1998; Jagger *et al.*, 1999) demonstrates the appropriate folding and assembly of nicotinic subunits in UB/OC cells, suggesting that the absence of radioligand binding, even upon over-expression of chimeric subunits, is a consequence of an alternative factor, such as a low transfection efficiency of these cells. The generation of stable cell lines would, therefore, be a major advantage to this study, allowing much greater expression of subunit protein.

The recent identification of α9 mRNA transcripts in SH-SY5Y cells (Valor *et al.*, 2003) implies that this cell line may provide an alternative system in which to study α9-containing nAChRs. It is interesting to note that in a study where constructs containing regions of the α9 promoter were expressed in SH-SY5Y cells, attempts to express these constructs in UB/OC-2 cells failed (Valor *et al.*, 2003). The expression of green-fluorescent protein under the control of a human cytomegalovirus (CMV) promoter in the UB/OC-2 cells revealed that the cells were efficiently transfected by calcium phosphate, but that the α9 constructs, under the control of SV40 promoters, were not expressed in these cells (Valor *et al.*, 2003). The reason that the activity of some promoters is restricted in this cell line is unknown, but may reflect the cell culture conditions. Expression of the α9 and α10 subunits in the present study was attempted using subunits in the pC1neo and/or pRK5 mammalian expression vectors, both under the control of a CMV promoter, suggesting that appropriate expression vectors were employed.

Several previous studies have reported inefficient folding and/or cell-surface expression of nAChR subunits when expressed heterologously in a variety of host cell types (Quik *et al.*, 1996; Cooper and Millar, 1997; Kassner and Berg, 1997; Rangwala *et al.*, 1997; Cooper and Millar, 1998; Sweileh *et al.*, 2000). A common feature of these studies is that inefficient folding and cell-surface expression of nAChRs can be attributed to sequences present within the C-terminal (transmembrane and intracellular) subunit domains (Eiselé *et al.*, 1993; Blumenthal *et al.*, 1997; Cooper and Millar, 1998; Cooper

et al., 1999; Harkness and Millar, 2002). High levels of functional cell-surface receptors have been detected in several cell lines after expression of α7χ or α8χ subunit chimeras, including host cell types in which few, if any, correctly folded nAChRs can be detected after expression of wild-type α7 or α8 (Eiselé *et al.*, 1993; Cooper and Millar, 1998).

While no evidence for specific binding of nicotinic radioligands was detected in mammalian cells transfected with α9 and α10, it was possible to detect specific high affinity [^{3}H]-MLA binding in a mammalian cell line transfected with chimeric α9χ and α10χ subunits. This permitted a detailed pharmacological characterisation of recombinant α9α10-type nAChRs by equilibrium radioligand binding for the first time. Successful heterologous expression of α9χ and α10χ subunit chimeras is consistent with previous studies with chimeras such as $\alpha7^{(V201)}/5HT_{3A}$ (Eiselé *et al.*, 1993; Cooper and Millar, 1998) and provides further evidence that inefficient folding of neuronal nAChR subunits into a conformation recognised by nicotinic radioligands can be attributed to their C-terminal region.

Whilst low levels of [^{3}H]-MLA binding were observed in cells transfected with either α9χ or α10χ alone, significantly higher levels of binding were detected in cells co-transfected with α9χ and α10χ, providing evidence of a requirement for heteromeric co-assembly for the efficient formation of a nicotinic binding site. This is consistent with co-expression studies of wild-type α9 and α10 in *Xenopus* oocytes, which report that responses in oocytes co-injected with α9 and α10 are ~100-fold larger than in oocytes injected only with α9 (Elgoyhen *et al.*, 2001; Sgard *et al.*, 2002). The present study also suggests that α9 and α10 N-terminal regions contain domains important for subunit co-assembly and agrees with several previous studies (performed with mutated and chimeric nAChR subunits), which have concluded that critical assembly domains are located at the N-terminus of nAChR subunits (Gu *et al.*, 1991; Yu and Hall, 1991; Sumikawa, 1992).

Non-linear regression and Scatchard analyses of the saturation binding data indicated the detection of a single class of high affinity radioligand binding sites (Figure 4.3), suggesting that α9χ or α10χ homomers (or α9χα10χ heteromers with differing stoichiometries) were either not generated or could not be differentiated from the high affinity [^{3}H]-MLA binding sites of the heteromeric α9χα10χ receptor via radioligand binding to membrane preparations of tsA201 cells transiently transfected with equal quantities of α9χ and α10χ cDNAs.

The presence of the entire N-terminal extracellular ligand-binding domain of the α9 and α10 subunits within the α9χ and α10χ chimeras would suggest that such chimeras might exhibit pharmacological properties which mimic those of native α9α10 nAChRs. Electrophysiological studies on recombinant α9-containing nAChRs expressed in *Xenopus* oocytes have revealed somewhat atypical pharmacological properties with modulation by a diverse collection of ligands including those known to bind with high affinity to muscarinic acetylcholine receptors, glycine receptors and GABA receptors (Rothlin *et al.*, 1999; Verbitsky *et al.*, 2000; Elgoyhen *et al.*, 2001). The pharmacological profile for the chimeric α9χα10χ receptor constructed in this study correlates well with data obtained from electrophysiological assays on both recombinant α9 and α9α10 nAChRs expressed in *Xenopus* oocytes and native nAChRs expressed in hair cells (Housley and Ashmore, 1991; Fuchs and Murrow, 1992; Rothlin *et al.*, 1999; Verbitsky *et al.*, 2000). The assumption that the α9χα10χ receptor can serve as a viable model for investigation of the α9α10 nAChR is supported by the comparison of equilibrium binding data obtained with the $\alpha7^{(V201)}/5HT_{3A}$ chimera to data obtained with native α7 nAChRs (Anand *et al.*, 1993a; Davies *et al.*, 1999).

Comparison of competition binding data conducted with α7χ and α9χα10χ (Figure 4.4) reveals that MLA, α-BTX and nicotine bind with higher affinity to α7χ than to α9χα10χ, whilst all other ligands tested bind with higher affinity to α9χα10χ than they do to α7χ (Tables 4.1 and 4.2). This is in agreement with previous studies, which have

reported that α9α10 nAChRs exhibit an atypical pharmacological profile (Rothlin *et al.*, 1999; Verbitsky *et al.*, 2000; Elgoyhen *et al.*, 2001), while α7 nAChRs demonstrate a more conventional nAChR profile (Anand *et al.*, 1993a; Davies *et al.*, 1999).

The finding that α9χ is able to generate a functional homomeric ion channel is consistent with the ability of both the α9 subunit and the $5HT_{3A}$ subunit to form homomeric ligand-gated ion channels (Maricq *et al.*, 1991; Elgoyhen *et al.*, 1994). This also demonstrates that replacement of the C-terminal region of the nAChR subunit with the $5HT_{3A}$ subunit sequence does not abolish the ability of the receptor to elicit functional responses and is consistent with previous studies of the α7χ chimera, for which a functional coupling between the α7 ligand binding domain and the channel domain of $5HT_{3A}$ has been demonstrated (Eiselé *et al.*, 1993).

Despite the inability of wild-type α10 to generate functional homomeric nAChRs when expressed in oocytes (Elgoyhen *et al.*, 2001), the chimeric α10χ subunit appears able to do so. This suggests that the wild-type α10 subunit contains an extracellular domain capable of forming a nicotinic ligand binding site (when folded into an appropriate conformation), despite the inability of wild-type α10 to form a functional homomeric ion channel. Interestingly, it has also been reported that a chimera containing the N-terminal region of the human α9 subunit fused to the C-terminal region of α10 (α9:α10) produces functional ion channels in oocytes (Sgard *et al.*, 2002). Thus, despite the inability of α10 to form functional homomeric nAChRs in heterologous expression systems, subunit chimeras containing either the N-terminus of α10 (with the C-terminus of $5HT_{3A}$) or the C-terminus of α10 (with the N-terminus of α9) are able to do so.

The observation that the functional responses detected in oocytes co-injected with the α9χ and α10χ cDNAs were not significantly larger than those obtained with either of the chimeric subunit alone is in contrast to co-expression studies of wild-type α9 and α10 in oocytes (Elgoyhen *et al.*, 2001; Sgard *et al.*, 2002). This discrepancy between chimeric

and wild-type subunits is surprising given the synergistic effect upon [^{3}H]-MLA binding, which is observed when the two chimeric subunits are co-expressed in mammalian cells. This may be a consequence of differences in the transmembrane pore-forming domains of the chimeric and wild-type subunits. In each of the homomeric or heteromeric receptors containing chimeric subunits, the residues of the 5HT3A subunit (see Section 1.2.4) provide the presumed transmembrane domain comprising the ion channel. If the coupling between agonist binding and channel opening domains in these chimeric subunits is relatively inefficient in both the homomeric and heteromeric complexes, this may explain why significantly larger whole-cell responses are not observed when α9χ and α10χ are co-expressed. Upon expression of the human α9:α10 chimera, containing the N-terminal domain of α9 fused to the C-terminal domain of α10 in *Xenopus* oocytes, large ACh-evoked whole cell responses were observed that were typically larger than the responses observed in cells expressing the wild-type α9 subunit alone (Sgard *et al.*, 2002). This reveals the influence of the C-terminal region of the α10 subunit on the ionic pore and gating properties of the recombinant nAChRs (Sgard *et al.*, 2002). In addition, functional characterisation of the α7/5HT$_{3A}$ chimera in *Xenopus* oocytes demonstrated that the ligand binding properties resembled α7, the ion channel properties resembled 5HT$_{3A}$, while the kinetics of current onset and desensitisation, (rapid for α7 and slow for 5HT$_{3A}$) were intermediate in the chimera, suggesting that the inter-conversion between the functional states of the receptors involve the structure of the complete receptor molecule (Eiselé *et al.*, 1993).

In summary, the construction and heterologous expression of α9χ and α10χ subunit chimeras has allowed, for the first time, an examination of the pharmacological properties of recombinant α9α10-type nAChRs in a mammalian cell line by radioligand binding. The equilibrium binding studies reported here, conducted with cells co-transfected with α9χ and α10χ, are in good general agreement with previous studies of wild-type α9α10 nAChRs conducted by electrophysiological techniques (Rothlin *et al.*,

1999; Verbitsky *et al.*, 2000). In particular, this study demonstrates specific high-affinity binding of the nicotinic antagonist MLA, together with evidence for an atypical pharmacological profile for α9α10 nAChRs.

These data have been accepted for publication in Molecular Pharmacology (Baker *et al.*, 2004).

4.7 Future directions

While the α9χ and α10χ subunits generate functional ion channels in response to ACh when expressed in *Xenopus* oocytes (Figure 4.1), the functional capabilities of the homomeric α9χ and α10χ or the heteromeric α9χα10χ complexes have yet to be determined in mammalian cells. The small size of the whole-cell responses observed in *Xenopus* oocytes (13.6±7.7 nA; n=10 for α9χ and 40.4±39.8 nA; n=24 for α10χ) may hinder the detection of functional responses in tsA201 cells.

While the radioligand binding data suggest the co-assembly of the α9χ and α10χ subunits, this has not been shown directly. Co-immunoprecipitation of subunits from transfected cells has not been attempted, as the two chimeric subunits migrate to similar positions when subjected to SDS-polyacrylamide gel electrophoresis (Figure 3.2) and would not be easily distinguished from each other using this technique. Sucrose gradient centrifugation could be used to assess whether the putative α9χα10χ nAChR demonstrates a sediment coefficient corresponding to a pentameric complex.

The radioligand binding studies did not permit the detection of α9-containing nAChRs in the UB/OC cell lines and a number of modifications could improve this investigation. The cells require approximately 14 days culture under permissive conditions to allow terminal differentiation, excluding the use of transient transfection to investigate the

over-expression of nicotinic subunits. The endogenous subunits may not be expressed at levels high enough to permit the detection of α9-containing nAChRs in the radioligand binding assay. Therefore, the production of stable cell lines expressing wild-type or chimeric subunits would enhance this study, by allowing the over-expression of nAChR subunits in differentiated cells. The use of techniques such as immunofluorescence with subunit-specific antibodies may also prove useful in investigating nAChR expression, particularly if the expression levels are low and preclude meaningful quantification via radioligand binding. The expression of other recombinant nAChRs, such as α4β2 or α7χ in the UB/OC cells may prove beneficial in the optimisation of transfection and radioligand binding assay conditions and in the comparison of the expression of different receptor subtypes in the cochlea-derived cell lines.

A recent study revealed that the α9 subunit is expressed in SH-SY5Y cells (Valor *et al.*, 2003), a cell line in which the homomeric α7 nAChR is expressed at the cell surface (Cooper and Millar, 1997). It would, therefore, be interesting to investigate the expression of α9-containing nAChRs in this cell line in comparison to nAChRs containing the α7 subunit.

CHAPTER 5

THE SUB-CELLULAR DISTRIBUTION OF α9χα10χ COMPLEXES

5.1 Introduction

Chapter 4 described evidence that chimeric α9χ and α10χ subunits can assemble into both homomeric and heteromeric complexes capable of binding [^{3}H]-MLA when expressed in tsA201 cells. The [^{3}H]-MLA binding assays were performed on membrane preparations of tsA201 cells transiently transfected with α9χ and α10χ subunits and measured the total levels of radioligand binding sites in the disrupted cells. The evidence for the formation of functional homomeric α9χ and α10χ receptors expressed in *Xenopus* oocytes, demonstrated by small whole cell responses to ACh, suggests that these chimeric receptors are expressed at the cell surface of oocytes (Figure 4.1). This chapter describes the experiments performed to investigate the sub-cellular distribution of complexes containing α9χ and α10χ chimeras expressed in tsA201 cells. Two approaches were used to assess whether the chimeric receptors were expressed at the cell surface: the construction of epitope-tagged subunits (Section 5.3) and radioligand binding assays on intact cells (Section 5.2).

5.2 Sub-cellular distribution investigated by radioligand binding

Radioligand binding performed on membrane preparations of tsA201 cells does not provide information regarding the sub-cellular distribution of the chimeric nAChRs. When using membrane impermeant radioligands such as [^{3}H]-MCC and [^{125}I]-α-BTX to characterise nAChRs, equilibrium radioligand binding assays can be performed on intact cells, enabling quantification of nAChR levels at the cell surface. MCC contains a charged quarternary ammonium atom, making it membrane impermeable (Whiteaker *et al.*, 1998), while the large size of the 8 kDa α-BTX peptide prevents permeation of the membrane. However, [^{3}H]-MLA is a potentially membrane permeant ligand (Davies *et*

al., 1999) and so cannot be used directly to look at the cell surface expression of α9χα10χ nAChRs in intact cells.

Non-radiolabelled, membrane impermeable ligands can be used to block cell surface receptors in an indirect approach to estimate the proportion of [^{3}H]-MLA binding sites at the cell surface(Section 2.6.4) (Whiteaker *et al.*, 1998; Fenster *et al.*, 1999). Specific binding to cell surface α9χα10χ receptors was determined by competition with 1 mM ACh, a membrane impermeant ligand (Whiteaker *et al.*, 1998; Fenster *et al.*, 1999). Competition binding to membrane preparations of tsA201 cells transiently transfected with α9χα10χ, established that a concentration of 1 mM ACh is sufficient to block α9χα10χ receptors (K_i ACh = 2.7±2.5 μM; Table 4.1). This concentration of ACh was found to block >95% of total [^{3}H]-MLA binding to cell membrane preparations. Application of ACh to intact cells should result in the block of only surface receptors (Whiteaker *et al.*, 1998; Fenster *et al.*, 1999). Total [^{3}H]-MLA binding was determined in the absence of unlabelled nicotinic ligands and non-specific binding was determined in the presence of 1 mM nicotine, 1 mM carbachol and 10 μM cold MLA to block both surface and internal [^{3}H]-MLA binding sites. Using these reaction conditions, specific binding to the total pool of receptors is calculated using the difference between "total" and "non-specific" radioligand binding. Specific binding to internal pools is the difference between binding in the presence of the ACh block and non-specific binding. Specific binding to cell surface receptors is calculated from the difference between total [^{3}H]-MLA binding and binding in the presence of ACh (Figure 5.1).

Assay of intact cells was performed in parallel with assay of disrupted cells, to compare the total levels of [^{3}H]-MLA binding and assess the degree of membrane permeation by the radioligand (Figure 5.2). The proportion of [^{3}H]-MLA binding sites on the cell surface are presented as a percentage of the total levels of radioligand binding detected in preparations of disrupted cells (Table 5.1).

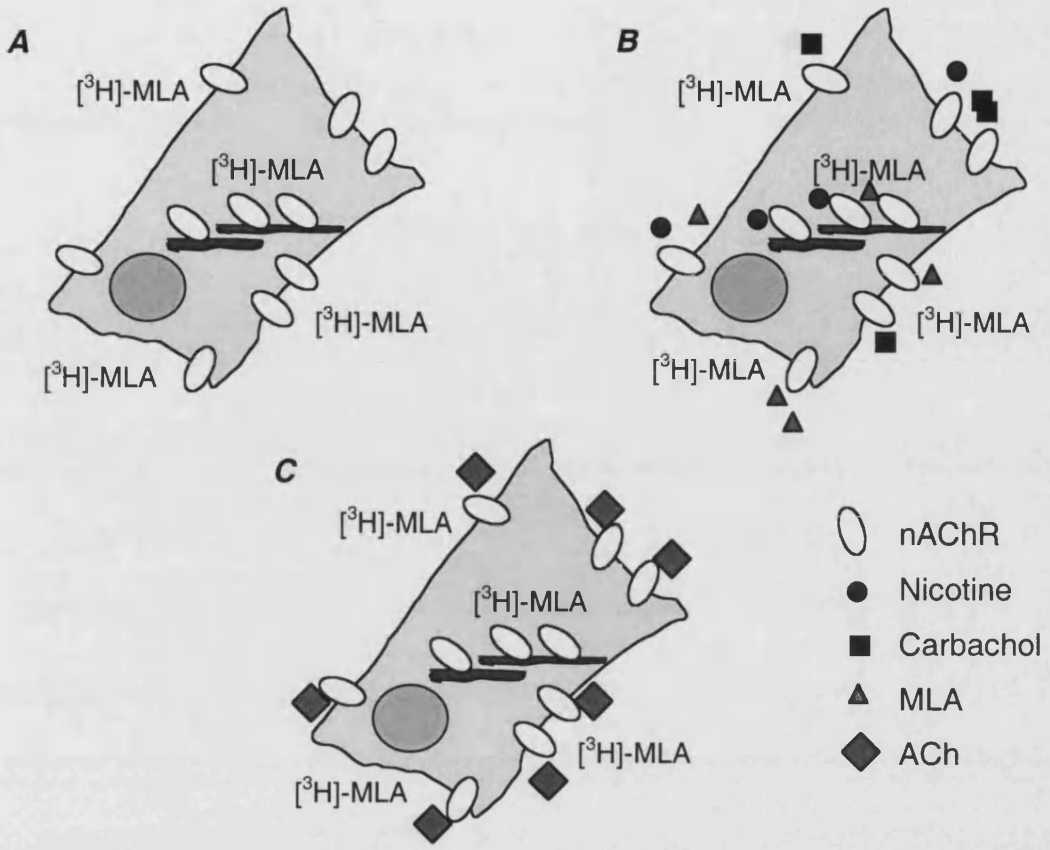

FIGURE 5.1. Binding protocol used to determine the proportion of nAChRs expressed at the cell surface with [^{3}H]-MLA. Equilibrium radioligand binding was performed on suspensions of intact cells transiently transfected with $\alpha 9\chi$ and $\alpha 10\chi$ chimeric subunits to estimate the proportion of receptors expressed at the cell surface. Binding was performed under three different reaction conditions in parallel, using the membrane permeant radioligand, [^{3}H]-MLA:

(*A*) Total Binding (**T**) in the presence of buffer to label surface and internal receptors

(*B*) Non-Specific Binding (**NS**) in the presence of 1 mM nicotine, 1 mM carbachol and 10 μM MLA to block surface and internal pools of receptors

(*C*) In the presence of 1 mM ACh to block binding to the cell surface receptors (**ACh**)

(*A*) - (*B*) = Total specific binding to the cell surface and the intracellular pools of receptor (**T** - **NS**)

(*A*) - (*C*) = Specific binding to cell surface receptors (**T** - **ACh**)

Specific [^{3}H]-MLA binding was detected to intact cells transiently transfected with α9χ+α10χ (25.7±6.0 fmol/10^6 cells, *n*=3) (Figure 5.2). Levels of non-specific [^{3}H]-MLA binding to intact cells, determined by competition with ACh, were very low (typically <3% total binding) and were not significantly different when binding was performed in competition with a combination of membrane-permeant and membrane-impermeant ligands (1 mM nicotine, 1 mM carbachol and 10 μM MLA), which would be expected to block binding of [^{3}H]-MLA to surface and internal sites. Comparison of binding with intact cells to binding studies performed in parallel with cell membrane preparations indicated that 83±16% (*n*=3) of total specific binding sites were located on the surface of tsA201 cells expressing α9χ+α10χ (Figure 5.2; Table 5.1).

As low levels of specific [^{3}H]-MLA binding were detected in membrane preparations of cells expressing either the α9χ or α10χ subunits alone, experiments were also performed on intact tsA201 cells transfected with these subunits in parallel with cells co-expressing both of the chimeras. Intact cells revealed 9.5±2.2 fmol/10^6 cells (*n*=3) of [^{3}H]-MLA binding to cells transfected with α9χ, with just 2.7±0.8 fmol/10^6 cells (*n*=3) of binding to cells expressing α10χ. However, higher levels of total specific [^{3}H]-MLA binding were detected with suspensions of intact cells transfected with α9χ alone, than in membrane preparations of the same cells (Figure 5.2). As both the intact cell suspensions and membrane preparations were derived from the same sample of transfected cells, this difference is not attributable to differences in transfection efficiency, but is related directly to the conditions used to disrupt the tsA201 cells. The loss of binding to membrane preparations of cells precluded the estimation of the proportion of [^{3}H]-MLA binding sites at the surface of cells expressing α9χ as a percentage of total binding in cell membrane preparations.

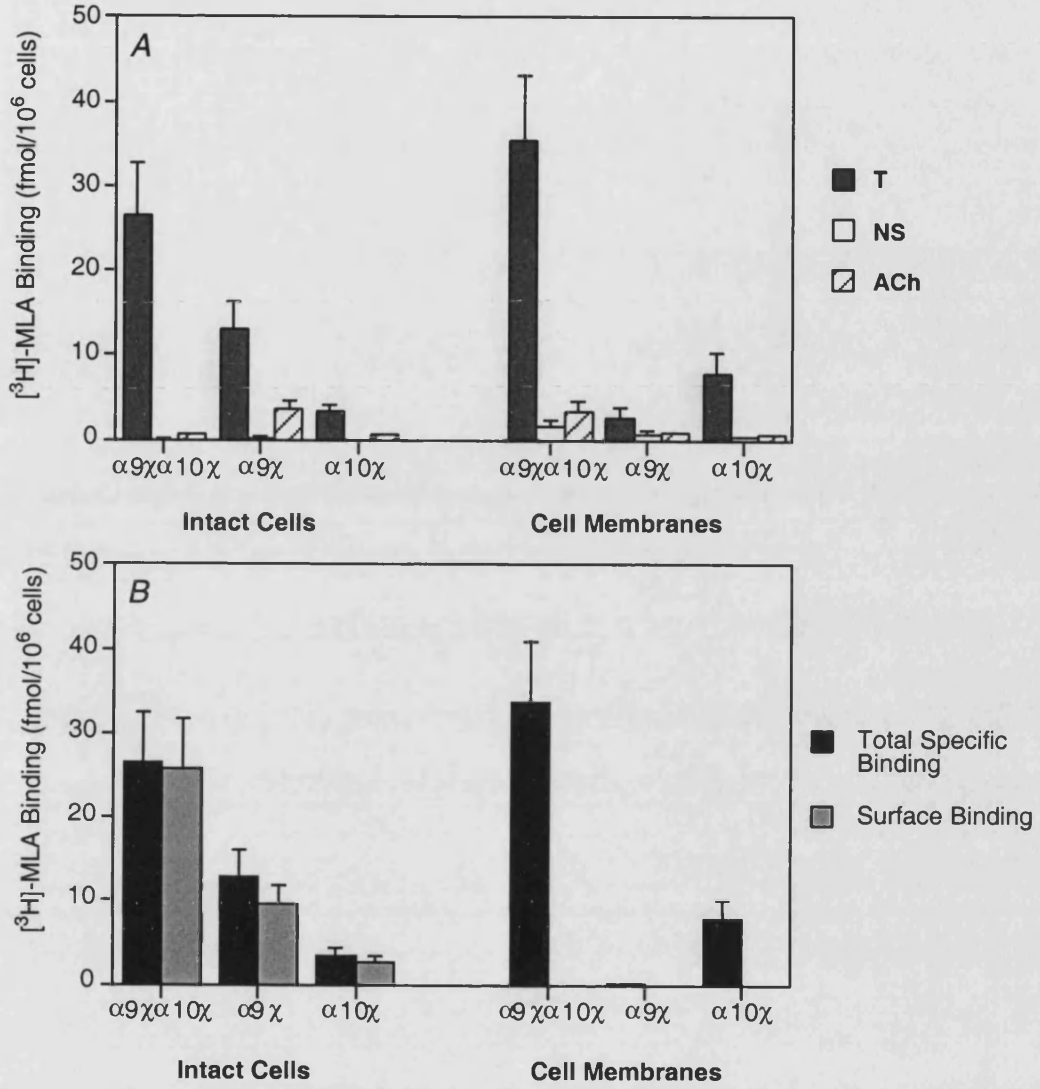

FIGURE 5.2. Cell surface expression of α9χα10χ receptors determined by [^{3}H]-MLA binding. Equilibrium radioligand binding was performed on intact or disrupted tsA201 cells transfected with α9χ and α10χ chimeras. Data are means (+ standard error) of 3 experiments performed in triplicate. (*A*) Binding was carried out under 3 reaction conditions using the membrane permeant radioligand, [^{3}H]-MLA: (1) Total Binding (**T**) in the presence of buffer to label surface and internal pools of receptor; (2) Non-Specific Binding (**NS**) in the presence of 1 mM nicotine, 1 mM carbachol + 10 μM MLA to block surface and internal pools; (3) In the presence of 1 mM ACh to block binding to surface receptors (**ACh**). (*B*) Total specific binding to surface and internal pools of receptor = **T** - **NS**; Specific binding to cell surface receptors = **T** - **ACh**. The proportion of α9χα10χ at the cell surface = (Specific binding to surface receptors / Total specific binding to cell membranes) = 83±16%.

	α9χα10χ Intact Cells	α9χα10χ Membranes	α9χ Intact Cells	α9χ Membranes	α10χ Intact Cells	α10χ Membranes
Total binding (**T**) (fmol/10^6 cells)	26.5±6.2	35.4±7.9	13.1±3.2	2.8±1.2	3.4±0.6	7.9±2.5
Non-Specific binding (**NS**) (fmol/10^6 cells)	-0.1±0.4	1.8±0.7	0.2±0.3	0.8±0.4	-0.2±0.2	0.3±0.2
Binding with ACh block (**ACh**) (fmol/10^6 cells)	0.8±0.2	3.4±1.3	3.6±1.0	1.0±0.1	0.6±0.2	0.6±0.1
Total specific binding (fmol/10^6 cells) [**T-NS**]	26.6±6.0	33.7±7.2	12.9±3.1	0.1±0.2	3.5±0.9	7.8±2.2
Surface binding (fmol/10^6 cells) [**T-ACh**]	25.7±6.0	N/A	9.5±2.2	N/A	2.7±0.8	N/A
Proportion of binding sites at cell surface (% of total specific binding in membranes)	83±16	N/A	ND (see Section 5.2)	N/A	35.2±1.5	N/A

TABLE 5.1. [^{3}H]-MLA binding to nAChR/5HT$_{3A}$R complexes at the cell surface. Equilibrium radioligand binding was carried out on suspensions of intact and disrupted cells transiently transfected with α9χ and α10χ chimeric subunits to estimate the proportion of receptors expressed at the cell surface. Binding was carried out using the membrane permeant radioligand, [^{3}H]-MLA in the presence of buffer (Total binding, **T**) or 1 mM nicotine, 1 mM carbachol and 10 μM MLA (Non-Specific binding, **NS**) or 1 mM ACh (to block cell surface receptors, **ACh**). Data are presented as means (± standard error) of 3 independent experiments performed in triplicate. N/A = not appropriate. ND = data not determined.

5.3 Sub-cellular distribution investigated with epitope-tagged subunits

The expression of nAChRs at the cell surface can be investigated using subunit-specific antibodies. For example, mAb299 specifically recognises an extracellular epitope of the α4 nAChR subunit and has been used to determine the relative proportions of α4 at the cell surface (Cooper *et al.*, 1999). However, suitable antibodies specific to the α9 and α10 subunits were not available. An alternative approach is to introduce recombinant epitope-tags into the sequence of a particular subunit that can be recognised by a monoclonal antibody (mAb). In this study, the nine amino acid epitope tag (YPYDVPDYA) from human influenza haemagglutinin (HA) protein was used and is recognised by mAbHA-7 (Kolodziej and Young, 1991) (Figure 5.3). The HA epitope tag was inserted into the sequence of each of the wild-type α9 and α10 and chimeric α9χ and α10χ subunits at one of three positions: (i) the N-terminus, following the putative cleavage site of the leader peptide ($^{N\text{-}HA}$), (ii) the extreme C-terminus ($^{C\text{-}HA}$), (iii) within the intracellular loop region ($^{I\text{-}HA}$).

5.3.1 Introduction of the HA tag to the extreme C-terminus

HA-epitope tags were introduced to the α9, α10, α9χ and α10χ subunits at their extreme C-termini by PCR to create $\alpha9^{C\text{-}HA}$, $\alpha10^{C\text{-}HA}$, $\alpha9\chi^{C\text{-}HA}$ and $\alpha10\chi^{C\text{-}HA}$ subunits in the expression vector, pRK5 (Section 2.3.3; Table 5.2). Mammalian tsA201 cells transiently transfected with C-terminally tagged subunits were subjected to immunoblotting with mAbHA-7 to demonstrate protein expression. This revealed immunoreactive protein of a size similar to that expected for full-length mature α9 and α10 subunits (Figure 5.4; Table 5.2). Detection of subunits tagged at their extreme C-termini provides strong evidence that these correspond to full-length subunit protein. However, the immunodetection revealed a smear of protein bands from ~50 kDa to below 46 kDa, which may indicate some protein degradation.

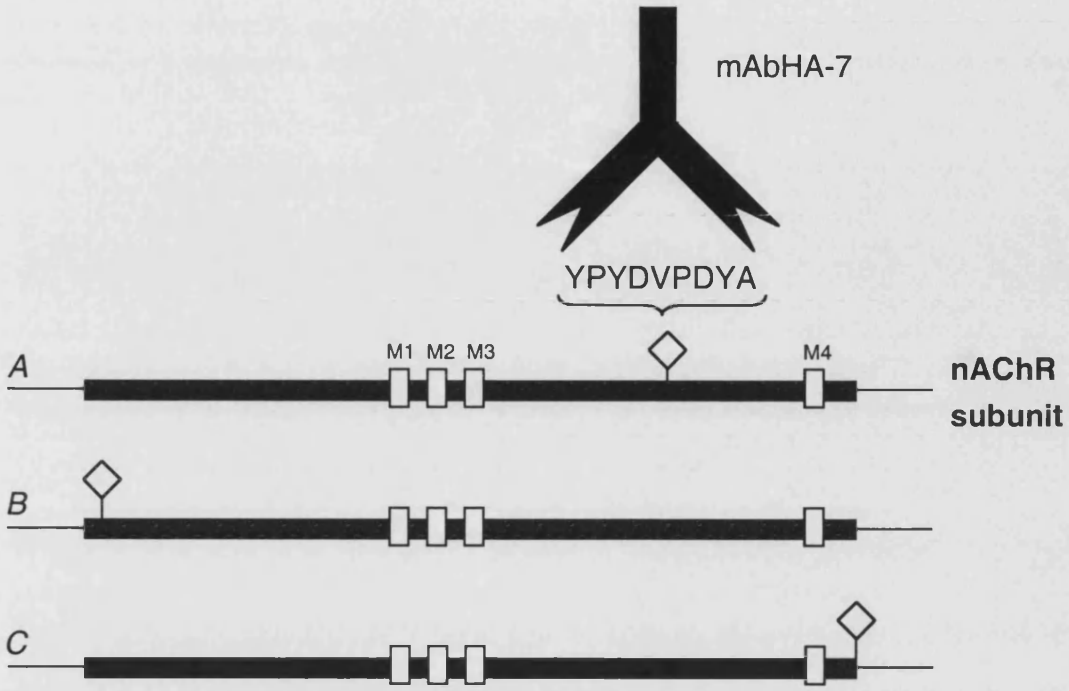

FIGURE 5.3. Rat nAChR-HA epitope tagged subunit constructs. A nine amino acid epitope tag (YPYDVPDYA) from human influenza haemagglutinin (HA) protein (Kolodziej and Young, 1991) was introduced into the cDNA sequence of the wild-type or chimeric α9 and α10 subunits. (*A*) HA epitope tags were introduced by site directed mutagenesis (SDM) into the intracellular loop region between putative transmembrane domains, M3 and M4, at a restriction enzyme *Nhe*I site ($^{I\text{-}HA}$). (*B*) HA epitope tags were introduced by SDM into the N-terminal domain at a restriction enzyme *Nhe*I site ($^{N\text{-}HA}$). (*C*) HA epitope tags were introduced to the extreme C-terminus by PCR ($^{C\text{-}HA}$). The HA epitope tag is recognised by the monoclonal antibody, mAbHA-7.

Subunit Tagged at the N-terminal			Subunit Tagged in the Intracellular Loop			Subunit Tagged at the C-terminal		
Construct	**Residue at which *Nhe*I site created**	**Apparent Mr**	**Construct**	**Residue at which *Nhe*I site created**	**Apparent Mr**	**Construct**	**Residue after which tag inserted**	**Apparent Mr**
pRK5-α9$^{N\text{-}HA}$	α9-T3	46	pRK5-α9$^{I\text{-}HA}$	α9-P345	45-48	pRK5-α9$^{C\text{-}HA}$	α9-D457	43-47
pRK5-α10$^{N\text{-}HA}$	α10-L5	46	pRK5-α10$^{I\text{-}HA}$	α10-L320	44-48	pRK5-α10$^{C\text{-}HA}$	α10-L423	40-46
pRK5-α9χ$^{N\text{-}HA}$	α9-T3	46-49	pRK5-α9χ$^{I\text{-}HA}$	$5HT_{3A}$-V425	46-50	pRK5-α9χ$^{C\text{-}HA}$	$5HT_{3A}$-S465	46-50
pRK5-α10χ$^{N\text{-}HA}$	α10-L5	44	pRK5-α10χ$^{I\text{-}HA}$	$5HT_{3A}$-V425	47-49	pRK5-α10χ$^{C\text{-}HA}$	$5HT_{3A}$-S465	45-49

TABLE 5.2. Summary of HA epitope-tagged α9, α10, α9χ and α10χ subunits. Each subunit contains the nine amino acid epitope tag (YPYDVPDYA) from human influenza haemagglutinin (HA) protein (Kolodziej and Young 1991). Epitope tags were introduced either at the N-terminal domain ($^{N\text{-}HA}$), within the intracellular domain ($^{I\text{-}HA}$) (at an *Nhe*I site created by SDM) or at the extreme C-terminus ($^{C\text{-}HA}$) (by PCR). Apparent molecular weights were estimated following metabolic labelling and immunoprecipitation using mAbHA-7 (Figure 5.4).

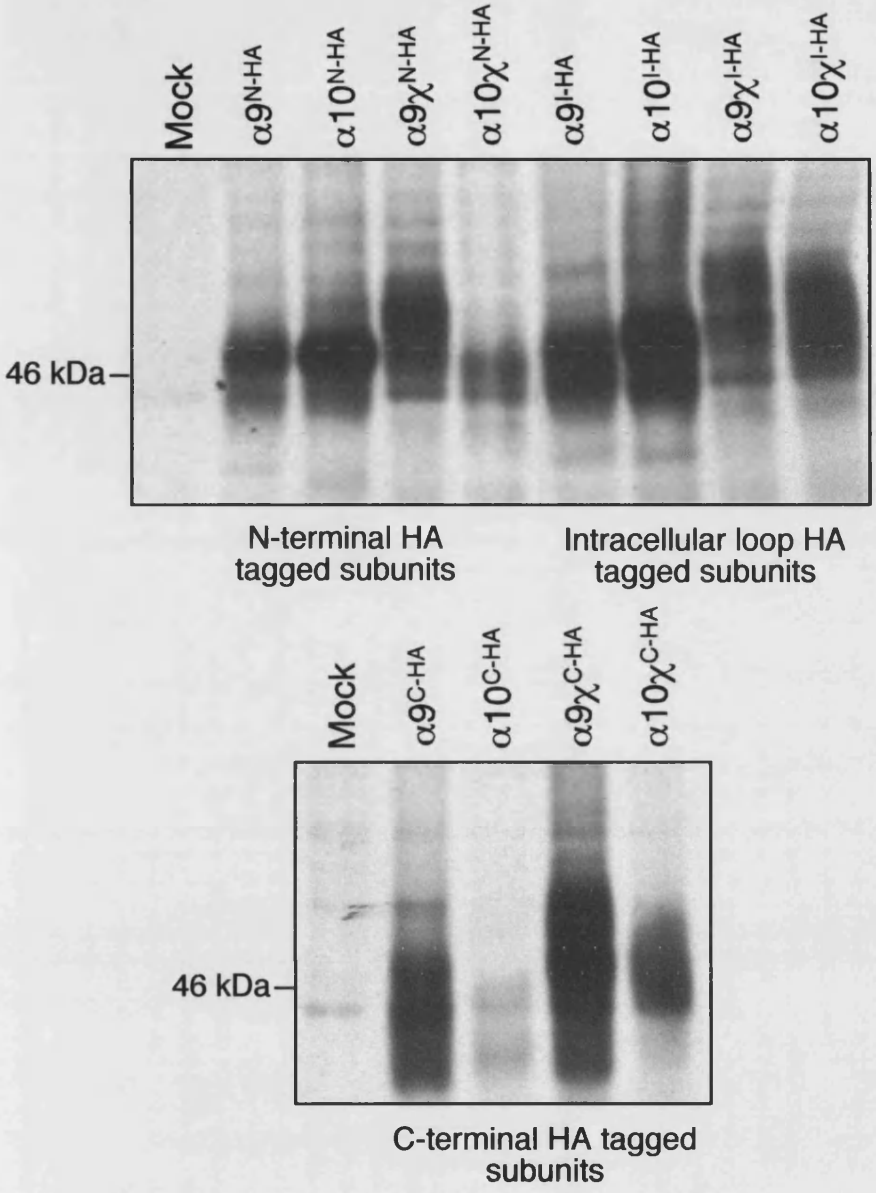

FIGURE 5.4. Heterologous expression of HA-tagged subunits determined by immunoprecipitation of metabolically labelled proteins from detergent-solubilised cells. Mammalian tsA201 cells were transfected with α9, α10, α9χ or α10χ subunits tagged with an HA epitope at their N-termini ($^{N\text{-}HA}$), in the intracellular loop region ($^{I\text{-}HA}$) or at their C-termini ($^{C\text{-}HA}$) and constructed in the mammalian expression vector, pRK5. Cell lysates were immunoprecipitated with a monoclonal mouse α-HA antibody, mAbHA-7. The positions of molecular weight markers are indicated. Immunoreactive bands were detected corresponding to the each of the HA epitope-tagged subunits.

To investigate the expression and distribution of the HA-tagged subunits, intact and permeabilised tsA201 cells transfected with combinations of wild-type and chimeric subunits were subjected to an enzyme-linked assay using horseradish peroxidase (HRP), as described previously (e.g. Cooper *et al.*, 1999). In the HRP-assay, subunit protein is detected through binding of a primary antibody to the specific subunit (in this case, mouse mAbHA-7, which specifically detects the HA epitope tag). The primary antibody is detected by a secondary antibody, conjugated to HRP (goat α-mouse IgG-conjugated HRP). Quantification of labelled nAChR is achieved via incubation with TMB liquid substrate for HRP, which forms a soluble blue reaction product, the absorbance of which is measured at 655 nm (Section 2.9). Expression of each of the pRK5-$\alpha 9^{C\text{-}HA}$, pRK5-$\alpha 10^{C\text{-}HA}$, pRK5-$\alpha 9\chi^{C\text{-}HA}$ and pRK5-$\alpha 10\chi^{C\text{-}HA}$ subunit proteins was detected in permeabilised cells, but no clear evidence was obtained for the expression of any subunit at the cell surface (Figure 5.5). Subunits were co-expressed in pairwise combinations of tagged and non-tagged subunits, but no evidence for cell surface expression was obtained (data not shown; n=3).

5.3.2 Introduction of the HA tag to the N-terminal region

The HA epitope tag was introduced into the sequence of each wild-type or chimeric subunit at a position following the putative cleavage site of the leader peptide, so that the tag would be positioned close to the extreme N-terminal end of the mature protein, to create $\alpha 9^{N\text{-}HA}$, $\alpha 10^{N\text{-}HA}$, $\alpha 9\chi^{N\text{-}HA}$ and $\alpha 10\chi^{N\text{-}HA}$ in the pRK5 expression vector. The HA tag was inserted at a unique *Nhe*I site (G/CTAGC), created in the subunit sequence by site-directed mutagenesis (SDM) (Section 2.3.1; Table 5.2). Immunoblotting of tsA201 cells transiently transfected with the subunits tagged at their N-termini using mAbHA-7, revealed specific protein bands for each subunit (Figure 5.4). The protein bands detected were of a size similar to that expected from the predicted molecular weights (Tables 3.3 and 3.4) and also migrated at a similar position to the subunits tagged at their extreme C-termini, suggesting the production of full-length subunit protein (Figure 5.4; Table 5.2).

Intact and permeabilised tsA201 cells transiently transfected with tagged subunits were subjected to HRP-assay. Specific protein expression was detected in permeabilised cells transfected with each of the $\alpha9^{N\text{-}HA}$, $\alpha10^{N\text{-}HA}$, $\alpha9\chi^{N\text{-}HA}$ and $\alpha10\chi^{N\text{-}HA}$ subunit cDNAs (Figure 5.5). Parallel assays carried out on intact cells revealed a significant level of mAbHA-7 binding at the surface of tsA201 cells transfected with $\alpha9\chi^{N\text{-}HA}$ alone (Figure 5.5). The assay indicated that a high proportion of the total $\alpha9\chi^{N\text{-}HA}$ protein was expressed at the cell surface (106.3±10.9%; n=12). Cell surface expression of the $\alpha9^{N\text{-}HA}$, $\alpha10^{N\text{-}HA}$ or $\alpha10\chi^{N\text{-}HA}$ subunits was not observed.

Combinations of tagged ($\alpha9^{N\text{-}HA}$, $\alpha10^{N\text{-}HA}$, $\alpha9\chi^{N\text{-}HA}$, $\alpha10\chi^{N\text{-}HA}$) and non-tagged ($\alpha9$, $\alpha10$, $\alpha9\chi$, $\alpha10\chi$) subunits were co-expressed in tsA201 cells. Intact and permeabilised cells were subjected to HRP-assay to investigate subunit co-assembly. Tagged $\alpha10^{N\text{-}HA}$ and $\alpha10\chi^{N\text{-}HA}$ subunits were co-expressed with non-tagged $\alpha9$ and $\alpha9\chi$ subunits, but no evidence was obtained for cell surface expression of $\alpha10^{N\text{-}HA}$ or $\alpha10\chi^{N\text{-}HA}$ subunits as either homomeric or heteromeric receptors (Figure 5.6). Tagged $\alpha9^{N\text{-}HA}$ and $\alpha9\chi^{N\text{-}HA}$ subunits were co-expressed with non-tagged $\alpha10$ and $\alpha10\chi$, but the $\alpha9^{N\text{-}HA}$ subunit was not detected at the cell surface either as a homomeric or heteromeric complex. However, significant levels of specific antibody binding were detected at the surface of cells transfected with $\alpha9\chi^{N\text{-}HA}$ (106.3±10.9% total protein; n=12) and $\alpha9\chi^{N\text{-}HA}$+$\alpha10$ (87±29%; n=3). A reduction in the levels of detectable cell surface receptors was observed with heteromeric $\alpha9\chi^{N\text{-}HA}$+$\alpha10\chi$ receptors in comparison to homomeric $\alpha9\chi^{N\text{-}HA}$ receptors (to 13±3%; n=3; Figure 5.6).

Membrane preparations of tsA201 cells transiently transfected with combinations of tagged $\alpha9\chi^{N\text{-}HA}$ and $\alpha10\chi^{N\text{-}HA}$ subunits and non-tagged $\alpha9\chi$ and $\alpha10\chi$ subunits were subjected to [^{3}H]-MLA binding to investigate whether the epitope tags affect the ligand binding site. In comparison to the levels of binding to non-tagged $\alpha9\chi\alpha10\chi$, the levels of [^{3}H]-MLA binding were reduced in cells expressing $\alpha9\chi^{N\text{-}HA}$+$\alpha10\chi^{N\text{-}HA}$, $\alpha9\chi^{N\text{-}}$

^{HA}+α10χ and α9χ+α10χ$^{N\text{-}HA}$, to 2±1%, 34±20% and 5±2% of binding to α9χα10χ, respectively (*n*=5) (Figure 5.7).

5.3.3 Introduction of the HA tag to the intracellular loop region

HA epitope tags were introduced to the intracellular loop region of each of the α9, α10, α9χ and α10χ subunits at a unique *Nhe*I site created by SDM to produce α9$^{I\text{-}HA}$, α10$^{I\text{-}HA}$, α9χ$^{I\text{-}HA}$ and α10χ$^{I\text{-}HA}$ in pRK5 (see Section 2.3.2; Table 5.2).

Epitope tags in the intracellular loop region should not disrupt the formation of the N-terminal ligand binding site directly, but would also not be recognised by antibodies applied at the extracellular surface (this is confirmed in Figure 5.5). It may be possible to ascertain the distribution of subunits containing epitope tags in the intracellular loop domain through confocal microscopy. However, when membrane preparations of tsA201 cells transfected with combinations of tagged (α9χ$^{I\text{-}HA}$ and α10χ$^{I\text{-}HA}$) and non-tagged (α9χ and α10χ) chimeric subunits were subjected to equilibrium radioligand binding using [^{3}H]-MLA, the levels of [^{3}H]-MLA binding were significantly reduced in cells expressing α9χ$^{I\text{-}HA}$+α10χ$^{I\text{-}HA}$ and α9χ+α10χ$^{I\text{-}HA}$, to 18±2% and 15±1% of binding to α9χ+α10χ, respectively (Figure 5.8).

Following metabolic labelling and immunoprecipitation with mAbHA-7 on tsA201 cells transiently transfected with the subunits tagged in the intracellular loop region, specific protein bands for each subunit were detected (Figure 5.4). The protein bands detected are of a size similar to that expected from the predicted molecular weights (Tables 3.3 and 3.4) and also correspond well to the protein bands detected for subunits tagged at their N- or C-termini (Figure 5.4), suggesting full-length subunit protein is produced following the transient transfection of tsA201 cells with cDNA of subunits tagged in the intracellular loop region. The effects of the subunit tags on [^{3}H]-MLA binding do not, therefore, appear to reflect a problem with protein production.

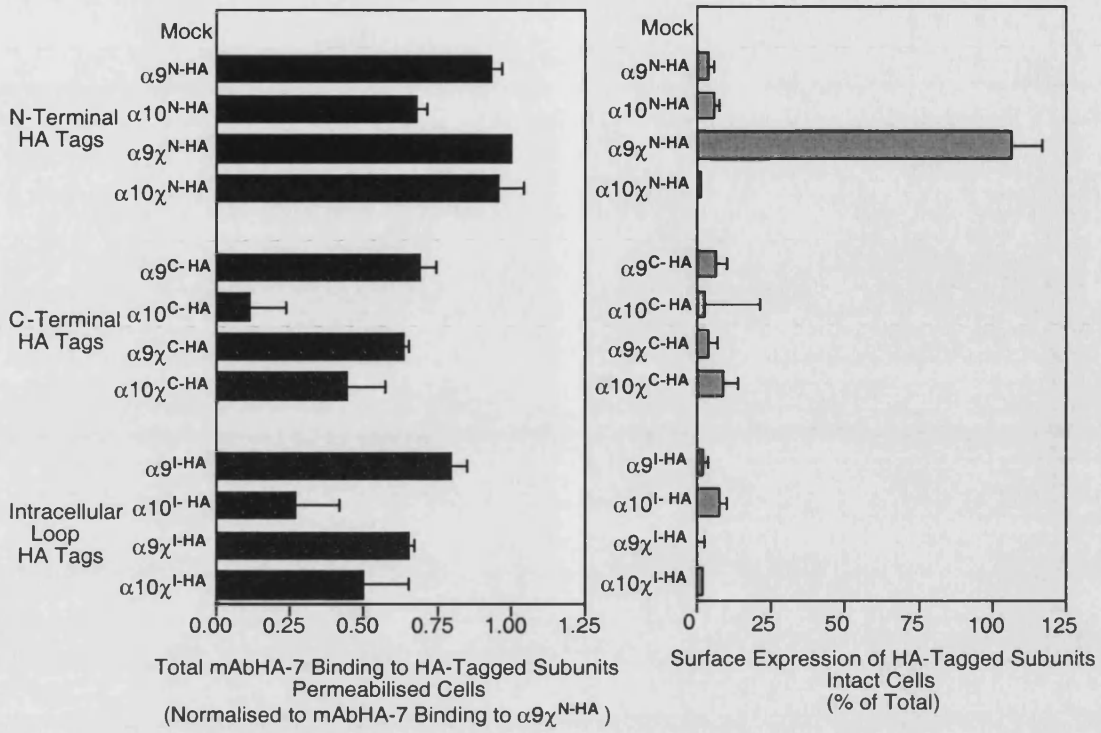

FIGURE 5.5. Expression of HA epitope tagged subunits in transfected cells. Mammalian tsA201 cells, grown on glass coverslips were transfected with α9, α10, α9χ and α10χ subunits tagged with the HA epitope at the N-terminal ($^{N\text{-}HA}$), C-terminal ($^{C\text{-}HA}$) or in the intracellular loop region between M3 and M4 ($^{I\text{-}HA}$). Transfected cells were labelled with a monoclonal mouse α-HA antibody, mAbHA-7. Levels of mAbHA-7 binding were determined in an enzyme-linked assay. Data are the means (+ standard error) of 3 independent experiments carried out in duplicate. (*A*) Detection of mAbHA-7 binding sites in permeabilised cells, normalised to mAbHA-7 binding to $\alpha9\chi^{N\text{-}HA}$. (*B*) The proportion of mAbHA-7 binding sites at the cell surface, determined from parallel experiments performed on permeabilised and intact cell monolayers. The background signal from untransfected cells has been subtracted. Specific cell surface mAbHA-7 binding was observed to cells transfected with $\alpha9\chi^{N\text{-}HA}$ (106±11% of binding to permeabilised cells expressing $\alpha9\chi^{N\text{-}HA}$).

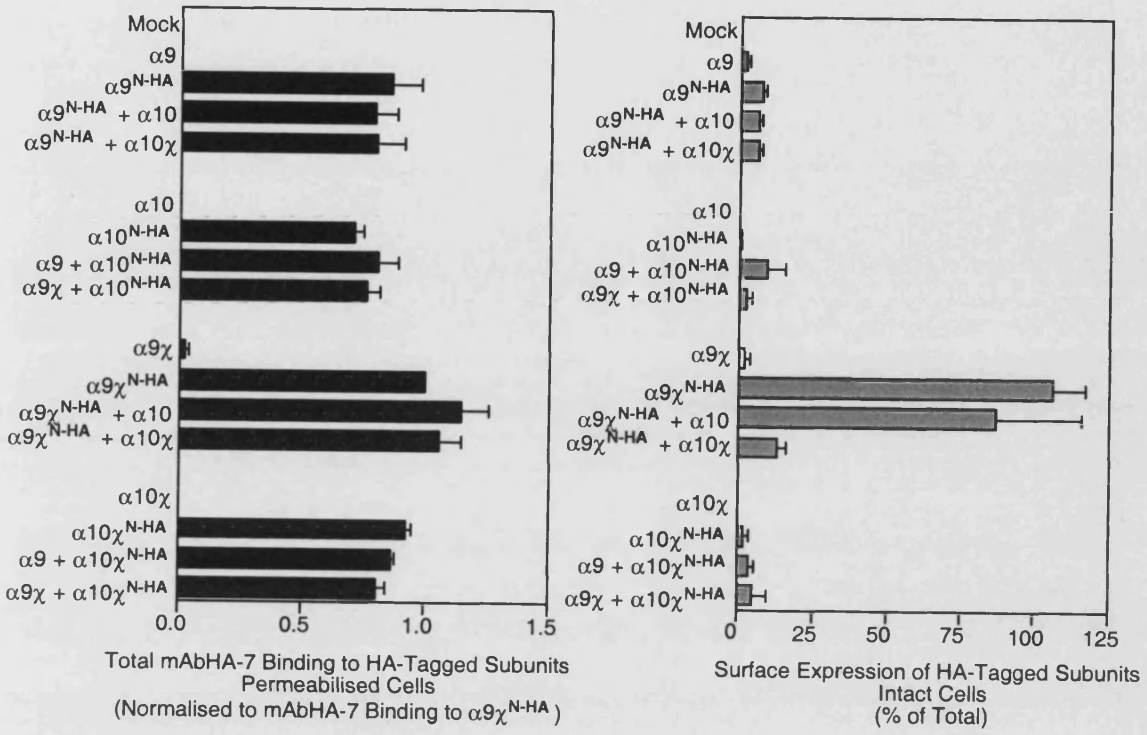

FIGURE 5.6. Expression of subunits containing an N-terminal HA epitope tag ($\alpha 9^{N\text{-}HA}$, $\alpha 10^{N\text{-}HA}$, $\alpha 9\chi^{N\text{-}HA}$, $\alpha 10\chi^{N\text{-}HA}$) in combination with non-tagged subunits (α9, α10, α9χ, α10χ). Transfected tsA201 cells were labelled with mAbHA-7 either after membrane permeabilisation or as intact cell monolayers. Levels of mAbHA-7 binding were determined in an enzyme-linked assay. Data are the means (+ standard error) of 3 independent experiments performed in duplicate. (*A*) Detection of mAbHA-7 binding sites in permeabilised cells, normalised to mAbHA-7 binding to $\alpha 9\chi^{N\text{-}HA}$. (*B*) The proportion of mAbHA-7 binding sites at the cell surface, determined from parallel experiments performed on permeabilised and intact cell monolayers. The background signal from untransfected cells has been subtracted. High levels of specific cell surface mAbHA-7 binding was observed upon expression of $\alpha 9\chi^{N\text{-}HA}$ alone or $\alpha 9\chi^{N\text{-}HA}$+α10. Binding to cells expressing $\alpha 9\chi^{N\text{-}HA}$+$\alpha 10\chi$ was reduced in comparison to binding to $\alpha 9\chi^{N\text{-}HA}$ alone (to 13±3% of binding to $\alpha 9\chi^{N\text{-}HA}$).

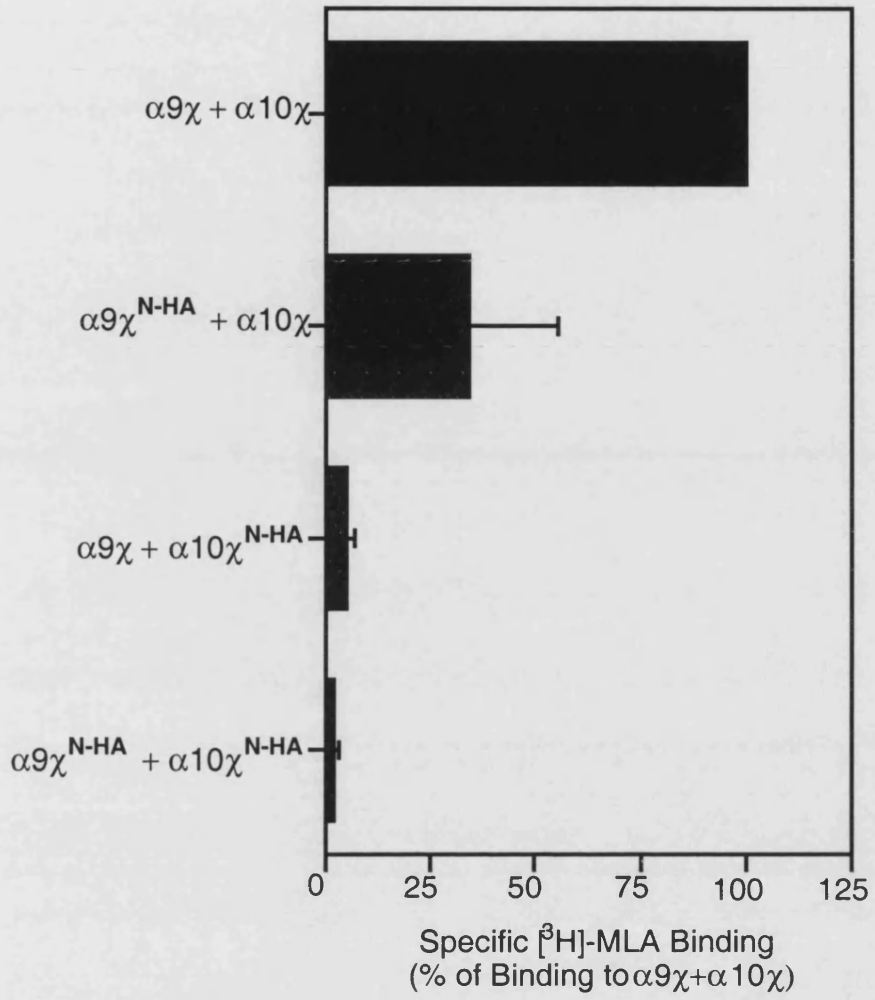

FIGURE 5.7. Specific [^{3}H]-MLA binding to cell membranes of tsA201 cells expressing chimeric subunits containing an N-terminal HA epitope tag ($\alpha9\chi^{N\text{-}HA}$ and $\alpha10\chi^{N\text{-}HA}$). Mammalian tsA201 cells were transiently transfected with combinations of tagged and non-tagged $\alpha9\chi$ and $\alpha10\chi$ chimeras. Data are means (+ standard error) of 4 - 5 independent experiments performed in triplicate and are presented as a percentage of the [^{3}H]-MLA binding to membrane preparations of cells expressing $\alpha9\chi$+$\alpha10\chi$. The levels of radioligand binding in cells transfected with $\alpha9\chi$+$\alpha10\chi$ are reduced when one or both of the chimeric subunits is substituted with a HA epitope-tagged subunit: $\alpha9\chi^{N\text{-}HA}$+$\alpha10\chi$ (34±20% of $\alpha9\chi$+$\alpha10\chi$ binding), $\alpha9\chi$+$\alpha10\chi^{N\text{-}HA}$ (5±2%) and $\alpha9\chi^{N\text{-}HA}$+$\alpha10\chi^{N\text{-}HA}$ (2±1%).

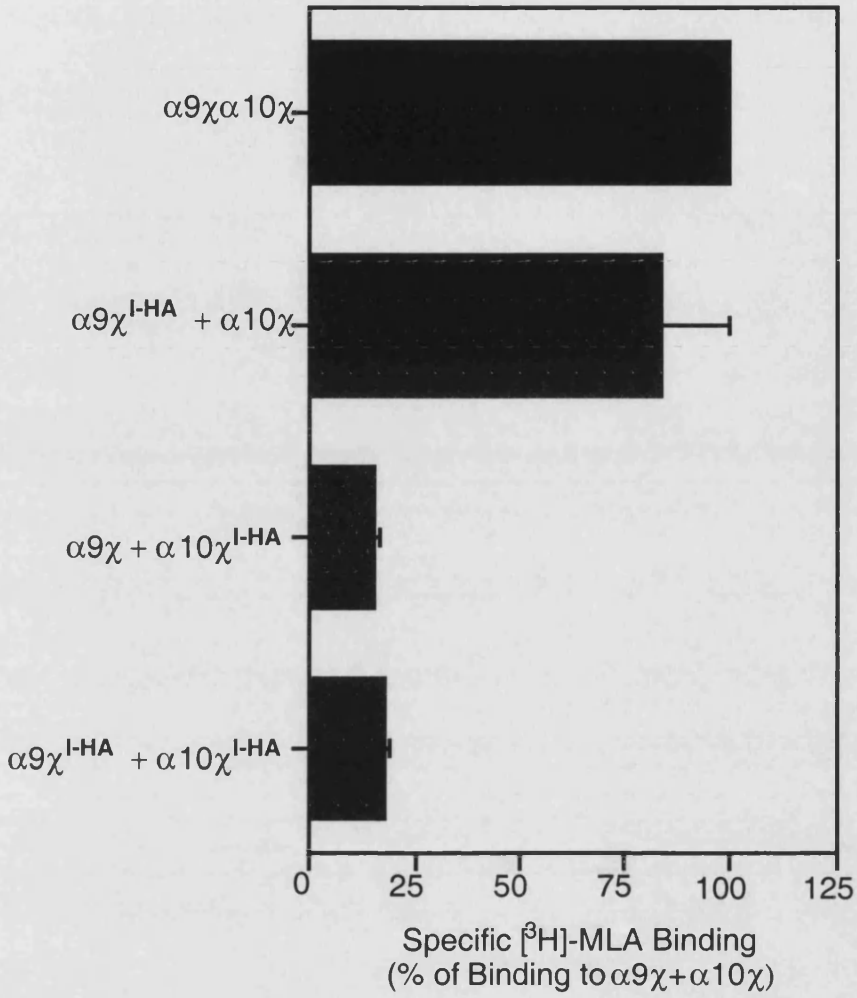

FIGURE 5.8. Specific [^{3}H]-MLA binding to cell membranes of tsA201 cells expressing chimeric subunits tagged in the intracellular loop region ($\alpha9\chi^{I\text{-}HA}$ and $\alpha10\chi^{I\text{-}HA}$). Mammalian tsA201 cells were transiently transfected with combinations of tagged and non-tagged $\alpha9\chi$ and $\alpha10\chi$ chimeras. Data are means (+ standard error) of 3 independent experiments performed in triplicate and are presented as a percentage of radioligand binding observed with the non-tagged $\alpha9\chi+\alpha10\chi$ complex. The levels of radioligand binding in cells transfected with $\alpha9\chi+\alpha10\chi$ are reduced when the chimeric $\alpha10\chi$ subunit is substituted with the HA epitope-tagged $\alpha10\chi^{I\text{-}HA}$ subunit: $\alpha9\chi+\alpha10\chi^{I\text{-}HA}$ (15±1% of $\alpha9\chi+\alpha10\chi$ binding) and $\alpha9\chi^{I\text{-}HA}+\alpha10\chi^{I\text{-}HA}$ (18±2% of $\alpha9\chi+\alpha10\chi$ binding).

5.4 Discussion

To determine the sub-cellular distribution of α9χα10χ complexes using the membrane permeable radioligand, [^{3}H]-MLA (Davies *et al.*, 1999), binding was performed on suspensions of intact tsA201 cells in the presence of the membrane impermeable competing ligand, ACh (Whiteaker *et al.*, 1998; Fenster *et al.*, 1999). Using this method, 83±16% (n=3) of total specific binding sites were located at the surface of cells expressing α9χ+α10χ. This is consistent with previous estimates of the proportion of nAChRs containing chimeric subunits at the cell surface. For example, 91.1±6.2% of α4χβ2 receptors and 44.3±8.7% of α4β2χ receptors are observed at the surface of tsA201 cells, as determined by radioligand binding with the membrane impermeable ligand, [^{3}H]-MCC (Harkness and Millar, 2002).

A surprising observation during these experiments was that higher levels of [^{3}H]-MLA binding were observed to intact cells transfected with α9χ alone than to membrane preparations of the same cells. The intact cell suspensions and the membrane preparations were derived from the same sample of transfected cells, so this difference appears to be directly attributable to the conditions under which the cells were disrupted, namely the assay buffer or the disruption of cells through centrifugation and resuspension. Cell membrane preparations were assayed in the presence of protease inhibitors (2 μg/ml leupeptin and aprotinin + 1 μg/ml pepstatin) to diminish protein degradation. As a substantial loss of α9χ [^{3}H]-MLA binding sites was observed following disruption of cells, it is also possible that a proportion of α9χα10χ [^{3}H]-MLA binding sites were lost under these reaction-specific conditions. If so, the proportion of cell surface α9χα10χ [^{3}H]-MLA binding sites, determined as ~83% of binding detected to membrane preparations, would be an overestimate of the cell surface receptor population. However, the total levels of [^{3}H]-MLA binding to α9χα10χ were comparable with both intact cells suspensions and membrane preparations (Figure 5.2). As [^{3}H]-MLA is a membrane permeable ligand (Davies *et al.*, 1999), the levels of

specific [^{3}H]-MLA binding to intact cells in the absence of competing ligands should represent populations of both surface and intracellular binding sites and should be comparable to the total levels of binding observed in cell membrane preparations. The levels of binding observed to intact cells expressing $\alpha9\chi$ alone were lower than the levels of binding to cells co-transfected with $\alpha9\chi$+$\alpha10\chi$, but it is possible that the estimate of binding sites for the $\alpha9\chi\alpha10\chi$ receptors included more than one receptor population ($\alpha9\chi$ and $\alpha9\chi\alpha10\chi$). The low levels of binding detected in membrane preparations of cells expressing $\alpha9\chi$ precluded the estimation of $\alpha9\chi$ nAChRs at the cell surface, but the specific binding to $\alpha9\chi$ complexes at the cell surface of intact cells is consistent with the high levels of antibody staining observed with the tagged $\alpha9\chi^{N\text{-}HA}$ chimera.

It is unclear at this stage why the levels of specific [^{3}H]-MLA binding to intact cells expressing $\alpha9\chi$ are reduced upon disruption of the cells, but does imply that the homomeric $\alpha9\chi$ complex is less stable than the heteromeric $\alpha9\chi\alpha10\chi$ complex under the reaction conditions specific to disrupted cells. Under these conditions, $\alpha9\chi$ may be more rapidly degraded or may be less able to fold into a conformation recognised by [^{3}H]-MLA. While the ability of $\alpha9\chi$ to form radioligand binding sites is compromised under the conditions used to disrupt the cells, co-expression with $\alpha10\chi$ appears to enhance the folding of the chimeric complex into a conformation capable of binding [^{3}H]-MLA. This provides further evidence for the interaction of these two subunits. It is apparent that some aspect of the stability or conformation of the $\alpha9\chi$-containing complex is affected by its interaction with $\alpha10\chi$ and this is consistent with previous studies with chimeric subunits. For example, when $\alpha4\chi$ or $\beta2\chi$ chimeras are expressed alone in tsA201 cells, high levels of each subunit are detected at the cell surface, although neither subunit produces high affinity [^{3}H]-epibatidine binding sites (Cooper *et al.*, 1999). The $\alpha4\chi$ and $\beta2\chi$ subunits assemble into complexes of the size predicted for pentameric nAChRs, but the homomeric subunit interactions are not resistant to detergent solubilisation during sucrose gradient centrifugation (Cooper *et al.*, 1999). In contrast, when the $\alpha4\chi$ or $\beta2\chi$ chimeras are expressed as heteromeric complexes (either with wild-type or chimeric

subunits), the subunit-subunit interactions are resistant to detergent solubilisation, suggesting a difference in the stability of the homomeric and heteromeric complexes (Cooper *et al.*, 1999). These results suggest that while α9χ (and α4χ) are able to assemble into complexes that bind radioligand, association with another subunit is required for the efficient formation of a stable high affinity radioligand binding site in mammalian cells.

Determination of the sub-cellular distribution of nAChRs with the membrane-permeable radioligand, [^{3}H]-MLA is an indirect method of ascertaining the proportion of cell surface receptors and is limited to the investigation of complexes that possess a high affinity ligand binding site. In the absence of subunit-specific antibodies, an HA epitope tag was inserted into each of the α9- and α10-type subunits to allow their detection when expressed in tsA201 cells. Enzyme-linked assays were performed on monolayers of intact and permeabilised tsA201 cells transiently transfected with the HA-tagged subunits. In these assays, the $\alpha9\chi^{N\text{-}HA}$ subunit was detected at the cell surface in high levels, while all other tagged subunits were only detected in permeabilised cells. Subunits tagged in the intracellular loop region would not be expected to be detected at the cell surface, as the epitope tag would be inaccessible to the mAbHA-7 antibody.

The α9χ chimera tagged at the extreme C-terminus ($\alpha9\chi^{C\text{-}HA}$) was not detected at the cell surface, while the $\alpha9\chi^{N\text{-}HA}$ chimera was detected in high levels. This may suggest that $\alpha9\chi^{C\text{-}HA}$ does not reach the cell surface and that the introduction of the epitope tag disrupts nAChR assembly or trafficking. The immunoreactive bands detected for subunits tagged at the C-terminal following metabolic labelling and immunoprecipitation (Figure 5.4) revealed a smear of protein bands, which may indicate some protein degradation. It is possible that addition of the HA tag at this position targets the subunits for degradation, preventing trafficking of the subunits to the cell surface. Alternatively, it is possible that this chimeric receptor is at the cell surface, but the epitope tag is not visible to mAbHA-7. The putative structure of nAChRs and $5HT_3$ receptors includes a

short hydrophobic extracellular carboxy terminal region (Figure 1.1) after which the epitope tag was inserted. However, it is possible that the C-terminus and/or the epitope tag remain embedded in the plasma membrane, which would obscure the tag from the antibody.

The significant reduction in the levels of detectable cell surface receptor observed upon co-expression of $\alpha9\chi^{N\text{-}HA}$+$\alpha10\chi$ (13±3%, n=3) in comparison to $\alpha9\chi^{N\text{-}HA}$ alone suggests that $\alpha9\chi^{N\text{-}HA}$ can co-assemble with the $\alpha10\chi$ subunit, as the addition of $\alpha10\chi$ affects the levels of $\alpha9\chi^{N\text{-}HA}$ detected at the cell surface. The heteromeric receptor complex formed through co-assembly of $\alpha9\chi^{N\text{-}HA}$ and $\alpha10\chi$ subunits may not be efficiently exported to the cell surface, as high levels of cell surface mAbHA-7 binding are not detected. However, this is in contrast to the levels of cell surface receptor estimated through radioligand binding (Section 5.2), which suggests that ~ 83% of detectable [^{3}H]-MLA binding sites are expressed at the surface of tsA201 cells transiently transfected with $\alpha9\chi$+$\alpha10\chi$. It is possible that during folding and assembly of the heteromeric receptor, the epitope tag is obscured from recognition by mAbHA-7, so that cell surface receptors are not detected. Alternatively, the reduced levels of cell surface expression may reflect the ability of the epitope tags to disrupt subunit oligomerisation and nAChR assembly.

Introduction of epitope tags to the N-terminal and intracellular loop regions of the $\alpha9\chi$ and $\alpha10\chi$ chimeras disrupted the formation of the ligand binding site of the $\alpha9\chi\alpha10\chi$ complex. Immunoprecipitation of each tagged subunit with mAbHA-7 revealed that the reduced levels of radioligand binding could not be attributed to a lack of subunit protein produced in the transfected cells (Figure 5.4). With the $\alpha9\chi^{N\text{-}HA}$ and $\alpha10\chi^{N\text{-}HA}$ chimeras, the epitope tag may interfere directly with crucial residues involved in ligand binding if the tags are not placed at the extreme N-terminus. Alternatively, introduction of the epitope tag may cause a conformational abnormality, with steric effects causing disruption to the ligand binding site. A study looking at the N-terminal region of the $\alpha7$ subunit demonstrated a contribution of the first 24 amino acids (G23 - N46) to

homomeric interactions in assembly of α7 nAChRs (Chio *et al.*, 2002). If the corresponding residues in the α9 or α10 subunits are involved in subunit co-assembly, then introduction of the epitope tags in this region might disrupt nAChR formation. The tagged subunits may, therefore, not assemble correctly and this may account for the lack of surface antibody binding observed with the $\alpha10\chi^{N\text{-}HA}$ chimera in particular. Therefore, the reduction in antibody staining observed at the surface of cells transfected with $\alpha9\chi^{N\text{-}HA}$+α10χ in comparison to $\alpha9\chi^{N\text{-}HA}$ alone does not necessarily represent the retention of non-tagged α9χα10χ within the cell. The tagged subunits may not be able to fold or assemble efficiently in the cell and, therefore, would not accurately represent the distribution of the non-tagged subunits.

Introduction of the HA epitope to the intracellular loop region of α10χ probably disrupts ligand binding indirectly, disrupting the appropriate folding or assembly of the subunits. The loop regions between M3 and M4 of nAChR subunits contain potential sites for interaction with intracellular proteins, such as protein kinases and molecular chaperones (see Section 1.5.4). The positions of the HA tags were selected to avoid putative phosphorylation motifs such as the S/TxK/R consensus motif for phosphorylation by PKC. However, the epitope tags might have disrupted binding sites of other proteins required for the appropriate assembly of the nAChRs.

It is somewhat surprising that the HA tags in the intracellular loop region affect α10χ, but not α9χ, as the two chimeric subunits are tagged at the same position within the intracellular loop region of their $5HT_{3A}$ C-terminal (Table 5.2). The α10-type subunit appears to be more sensitive to modification than the α9-type subunit. This suggests that both the N- and C-terminal domains of the subunits are involved in nAChR assembly and may reflect the order of subunit oligomerisation in the formation of pentameric nAChRs. The conformation of nAChR subunits is influenced by the interaction with other subunits (Green, 1999; Mitra *et al.*, 2001; Harkness and Millar, 2002). It is possible that when $\alpha9\chi^{I\text{-}HA}$ associates with other subunits, the resulting conformation of

the complex intermediate permits the association of additional subunits to form either homomeric or heteromeric pentamers. In contrast, the interaction of $\alpha 10\chi^{I\text{-}HA}$ with other subunits may produce a reaction intermediate with an inappropriate conformation that cannot complex efficiently with further subunits to generate a pentameric complex that binds radioligand. For a more detailed discussion of the assembly pathway of nAChRs, please refer to Section 7.3.

In summary, [^{3}H]-MLA binding to intact tsA201 cells in the presence of a membrane impermeable competing ligand suggested that 83±16% (n=3) of total specific $\alpha 9\chi$+$\alpha 10\chi$ binding sites were located at the cell surface, but the HA epitope tagged subunits have not proved ideal for the investigation of subunit distribution within the cell. The $\alpha 9\chi^{N\text{-}HA}$ subunit does appear to be expressed at the cell surface, consistent with the specific [^{3}H]-MLA binding to intact tsA201 cells expressing $\alpha 9\chi$. However, the N-terminal epitope tag disrupts the ligand binding site and may affect the conformation of the receptor, so it would be unwise to draw firm conclusions from the data obtained with this tagged subunit. Despite the obstacles encountered during these experiments, namely, the loss of [^{3}H]-MLA binding sites to membrane preparations of tsA201 cells expressing $\alpha 9\chi$ in comparison to intact cells and the disruption of radioligand binding caused by the HA epitope tags, it is apparent that the $\alpha 9\chi$ subunit behaves differently when expressed alone and when co-expressed with $\alpha 10\chi$, providing further evidence to suggest the co-assembly of the two chimeras.

5.5 Future directions

Due to the problems experienced using the HA epitope tags highlighted above, this particular project was not pursued further, but a number of modifications could be made if this project is to be continued at a later date. For example, a different epitope tag could be inserted, such as a FLAG (DYKDDDDK) or c-Myc (EQKLISEEDL) tag could be inserted at different locations, either within the N-terminal domain or the intracellular

loop region. Changing the position of the tag by a few residues may eliminate the disruption to subunit folding. This could also provide information as to critical residues or motifs present in the subunit sequence required for the appropriate folding, assembly or cell surface expression of nAChRs. Ideally, the sub-cellular distribution of the chimeric receptors would be addressed using subunit-specific antibodies, eliminating the need for the introduction of epitope tags to the subunits.

The difference between levels of [^{3}H]-MLA binding to $\alpha 9\chi$ in membrane preparations and intact cells is a surprising observation that requires additional experiments to explain this phenomenon. Sucrose gradient centrifugation could be used to ascertain whether the $\alpha 9\chi$, $\alpha 10\chi$ and $\alpha 9\chi\alpha 10\chi$ complexes are assembled as pentamers and whether the associated complexes are stable in the presence of detergent. Radioligand binding assays could be performed under different reaction conditions, using different buffers or additional protease inhibitors, to identify the source of the putative protein degradation.

CHAPTER 6

THE INFLUENCE OF SUBUNIT CHIMERAS UPON HETEROLOGOUS EXPRESSION OF α2-α7 CONTAINING nAChRs: PAIRWISE COMBINATIONS

6.1 Introduction

Characterisation of recombinant nAChRs generated by heterologous expression of defined subunit combinations can provide evidence for the likely subunit composition of pharmacologically distinct nAChR subtypes. However, while heteromeric nAChRs such as α4β2 and α3β4 form functional channels when expressed in *Xenopus* oocytes and in mammalian cell lines, folding is relatively inefficient, with low levels of nAChRs expressed at the surface of many mammalian cell types (Whiting *et al.*, 1991; Wong *et al.*, 1995; Buisson *et al.*, 1996; Lewis *et al.*, 1997; Ragozzino *et al.*, 1997). Expression of chimeric subunits can enhance the cell surface expression of α4β2 nAChRs, with a significant increase in binding of conformationally sensitive subunit specific antibodies or [^{3}H]-epibatidine apparent when α4 is substituted with a chimeric α4χ subunit and co-expressed with β2 (Cooper *et al.*, 1999; Harkness and Millar, 2002). This increase in antibody or radioligand binding is not due to an increase in the total levels of chimeric subunit protein in comparison to wild-type subunit and can, therefore, be attributed to more efficient folding and assembly of receptors (Cooper *et al.*, 1999).

Following the success of using α9χ and α10χ chimeras to investigate the pharmacological characteristics of α9-containing nAChRs (Section 4.5), an extensive investigation was performed using chimeric subunits constructed with the other known rat neuronal nAChR subunits. Chimeras were constructed analogous to the $\alpha7^{V201}/5HT_{3A}$ chimera (Eiselé *et al.*, 1993) using the N-terminal domain of the rat α2 - α6 and β2 - β4 subunits up to M1, fused to the C-terminal domain of the mouse $5HT_{3A}$ subunit (Chapter

3). Assembly of nAChRs containing α2 - α6 subunits was investigated via equilibrium radioligand binding with 3 - 10 nM [^{3}H]-epibatidine, which should represent a saturating concentration of radioligand. Epibatidine is a potent agonist of nAChRs isolated from the skin of the Amazonian poisonous frog, *Epidobates tricolor* that binds with high affinity to recombinant nAChRs containing α2, α3, α4 or α6 subunits expressed in *Xenopus* oocytes (Wang *et al.*, 1996; Parker *et al.*, 1998; Kuryatov *et al.*, 2000). Equilibrium binding with α7-containing nAChRs was performed with [^{3}H]-MLA (5 - 10 nM). Native α7-containing nAChRs of rat brain bind [^{3}H]-MLA with a K_i = 1.9 nM (Davies *et al.*, 1999) and the affinity of the recombinant α7χ receptor expressed in tsA201 cells for [^{3}H]-MLA is 1.2±0.2 nM (this study, Table 4.2).

6.2 nAChRs containing the α2 subunit

Wild-type α2 and chimeric α2χ subunits were expressed alone or in combination with either wild-type β2, β3 or β4 subunits, or chimeric β2χ, β3χ or β4χ subunits in tsA201 cells. Membrane preparations of transiently transfected cells were assayed for [^{3}H]-epibatidine binding and the results are presented in Tables 6.1 and 6.2 and Figure 6.1.

No evidence was obtained for the assembly of homomeric complexes capable of binding [^{3}H]-epibatidine when any of the wild-type α2, β2, β3 or β4 subunits or the chimeric β2χ, β3χ or β4χ subunits were expressed alone in tsA201 cells (Table 6.1). Low levels of specific [^{3}H]-epibatidine binding were, however, observed in cells expressing the α2χ chimera alone (26.5±7.5 fmol/mg protein; n=4). No evidence was obtained for the formation of specific high affinity [^{3}H]-epibatidine binding sites following co-expression of either α2 or α2χ with β3 or β3χ subunits.

Low levels of specific [^{3}H]-epibatidine binding were observed upon expression of the wild-type α2β2 nAChR in tsA201 cells (7.7±0.6 fmol/mg; n=3). The levels of radioligand binding to α2β2 increased upon substitution of one or both of the wild-type

subunits with a chimeric subunit (Table 6.2, Figure 6.1). Increases of 41±5-fold, 228±14-fold and 174±46-fold were observed in cells transfected with α2β2χ, α2χβ2 and α2χβ2χ combinations, respectively, in comparison to α2β2 (*n*=3). Low levels of [^{3}H]-epibatidine binding to the α2β4 nAChR (41±5 fmol/mg; *n*=3) increased by 3.1±0.1-fold, 9.7±0.6-fold and 20.7±1.2-fold upon expression of the α2β4χ, α2χβ4 and α2χβ4χ subunit combinations, respectively (*n*=3; Table 6.2, Figure 6.1).

Comparison of the two wild-type α2-containing nAChR subtypes revealed greater levels of [^{3}H]-epibatidine binding to α2β4 (41±5 fmol/mg) than α2β2 (7.7±0.6 fmol/mg). In addition, the influence of the chimeras on the α2β2 subtype was greater than on the α2β4 nAChR. For example, by replacing α2 with α2χ, a 228±14-fold increase was observed upon co-expression with β2, while co-expression of α2χ with β4 yielded only a 9.7±0.6-fold increase in [^{3}H]-epibatidine binding in comparison to α2β4 (Table 6.2). Replacing the α2 subunit with α2χ, produced a greater increase in radioligand binding in comparison to replacement of the β subunit with its corresponding chimeric subunit.

6.3 nAChRs containing the α3 subunit

Wild-type α3 and chimeric α3χ subunits were expressed alone or in combination with wild-type or chimeric β2 - β4 subunits in tsA201 cells. Cell membrane preparations were assayed for [^{3}H]-epibatidine binding and the results are presented in Figure 6.2 and Tables 6.1 and 6.2. Low levels of specific radioligand binding were observed in cells transfected with the α3χ chimera alone (67±28 fmol/mg protein; *n*=3; Table 6.1). No evidence was obtained for the assembly of homomeric α3 nAChRs or heteromeric nAChRs containing β3 or β3χ subunits detectable by [^{3}H]-epibatidine binding (*n*=3).

Low levels of specific radioligand binding were detected in cells transiently transfected with α3β2 (7.9±2.0 fmol/mg; *n*=3) and α3β4 (92.4±30.3 fmol/mg; *n*=3). Levels of [^{3}H]-epibatidine binding were enhanced upon replacement of one or both of the wild-type

subunits with a chimeric subunit (Figure 6.2). The levels of [^{3}H]-epibatidine binding to α3β2 nAChRs increased by 7.4±2.0-fold, 353±91-fold and 16±57-fold with the α3β2χ, α3χβ2 and α3χβ2χ combinations, respectively. In comparison to α3β4, levels of radioligand binding observed in cells expressing α3β4χ, α3χβ4 and α3χβ4χ increased by 3.6±0.6-fold, 11.6±2.7-fold and 8.1±1.3-fold, respectively (*n*=3; Table 6.2, Figure 6.2).

The levels of [^{3}H]-epibatidine binding were higher in cells expressing α3β4 than in cells expressing α3β2. Replacing the α3 subunit within the α3β2 or α3β4 nAChR subtypes with a subunit chimera produced a greater increase in radioligand binding than replacement of the wild-type β subunit. The effect of the subunit chimeras upon radioligand binding was greater for nAChRs containing β2 than those containing β4.

6.4 nAChRs containing the α4 subunit

Wild-type α4 and chimeric α4χ subunits were expressed alone or in combination with wild-type or chimeric β2 - β4 subunits in tsA201 cells and cell membrane preparations assayed for [^{3}H]-epibatidine binding. The results are presented in Table 6.2 and Figure 6.3. Low levels of specific [^{3}H]-epibatidine binding were observed in cells expressing the α4χ chimera alone (6.2±2.8 fmol/mg protein; *n*=3; Table 6.1). No evidence was obtained for the formation of homomeric α4 nAChRs or heteromeric nAChRs containing β3 or β3χ subunits (*n*=3).

Low levels of specific [^{3}H]-epibatidine binding were observed in cells transfected with α4+β2 (36±7 fmol/mg; *n*=3). In comparison to α4β2, increases of 14±3-fold, 49±7-fold and 60±17-fold were observed in cells expressing the α4β2χ, α4χβ2 and α4χβ2χ subtypes, respectively (Figure 6.3). The low levels of specific [^{3}H]-epibatidine binding in cells expressing the α4β4 nAChR (106±15 fmol/mg; *n*=3) increased by 3.3±0.5-fold, 6.2±0.7-fold and 16±57-fold with the α4β4χ, α4χβ4 and α4χβ4χ combinations, respectively (*n*=3; Table 6.2, Figure 6.3).

Comparison of wild-type α4β2 and α4β4 revealed higher levels of [^{3}H]-epibatidine binding to nAChRs containing β4 than those containing β2. Upon replacement of one wild-type subunit with a chimeric subunit, the increase observed in the levels of radioligand binding was greater for β2-containing subtypes than those containing β4.

6.5 nAChRs containing the α5 subunit

Wild-type α5 and chimeric α5χ subunits were expressed alone or in pairwise combination with wild-type or chimeric β2 - β4 subunits in tsA201 cells. Membrane preparations of cells were assayed for [^{3}H]-epibatidine binding. No evidence for [^{3}H]-epibatidine binding was obtained in preparations of cells transfected with any pairwise combination of subunits containing either wild-type α5 or chimeric α5χ (Tables 6.1 and 6.2; *n*=3).

6.6 nAChRs containing the α6 subunit

Results from the [^{3}H]-epibatidine binding with wild-type α6 and chimeric α6χ subunits expressed either alone or in combination with wild-type or chimeric neuronal β2 - β4 subunits in tsA201 cells are presented in Figure 6.4 and Tables 6.1 and 6.2. No evidence was obtained for the formation of a high affinity [^{3}H]-epibatidine binding site corresponding to homomeric α6 or α6χ nAChRs (Table 6.1). Specific [^{3}H]-epibatidine binding was not observed in cells in which the wild-type α6 subunit was expressed in any combination with wild-type or chimeric β subunits. However, high levels of specific radioligand binding were observed following pairwise expression of α6χβ2, α6χβ2χ, α6χβ4 or α6χβ4χ subunit combinations (Table 6.2, Figure 6.4). The levels of specific [^{3}H]-epibatidine binding observed with complexes containing α6χ were greater in cells expressing α6χβ2 than in those expressing α6χβ4. The α6χ chimera did not form a [^{3}H]-epibatidine binding site when co-expressed with wild-type β3 or chimeric β3χ subunits (Table 6.2).

6.7 nAChRs containing the α7 subunit

Assembly of putative heteromeric α7-containing nAChRs was investigated via [^{3}H]-MLA binding. Wild-type α7 and chimeric α7χ subunits were expressed alone or in pairwise combinations with wild-type β2, β3, β4 or chimeric β2χ, β3χ or β4χ subunits in tsA201 cells (Figure 6.5; Table 6.3). No evidence for specific [^{3}H]-MLA binding was observed in cells transfected with wild-type α7 either alone or in combination with any of the wild-type or chimeric β subunits (n=3). High levels of [^{3}H]-MLA binding were detected in cells transfected with each of the pairwise combinations of subunits that included the α7χ chimera. However, the levels of [^{3}H]-MLA binding detected to these pairwise combinations did not differ significantly from the levels of binding observed in cells expressing α7χ alone (Figure 6.5; Table 6.3).

The α7 and α7χ subunits were also co-expressed with α5 and α5χ subunits. Specific [^{3}H]-MLA binding was not observed in cells in which wild-type α7 was expressed with α5 or α5χ. High levels of specific [^{3}H]-MLA binding detected to membrane preparations of cells expressing α7χα5 and α7χα5χ subunit combinations did not differ significantly from levels of binding to α7χ alone (Figure 6.5; Table 6.3).

Expressed Subunit	Specific [^{3}H]-Epibatidine Binding (fmol/mg Protein)	n
α2	-	4
α3	-	5
α4	-	3
α5	-	3
α6	-	4
β2	-	6
β3	-	6
β4	-	5
α2χ	26.5±7.5	4
α3χ	67±28	5
α4χ	6.2±2.8	5
α5χ	-	3
α6χ	-	4
β2χ	-	6
β3χ	-	6
β4χ	-	6
Expressed Subunit	**Specific [^{3}H]-MLA Binding (fmol/mg Protein)**	***n***
α7	-	3
α7χ	4377±587	7

TABLE 6.1. Summary of radioligand binding to tsA201 cells expressing single nAChR subunits. Membrane preparations of tsA201 cells transiently transfected with wild-type or chimeric α2 - α6 and β2 - β4 subunits were subjected to [^{3}H]-epibatidine binding (5 - 15 nM), while specific radioligand binding to cell membranes expressing α7 and α7χ was determined using [^{3}H]-MLA (5 - 10 nM). Data are means (± standard error) of experiments performed in triplicate and are listed as fmol/mg protein.

Wild-type nAChR		α-Chimera			β-Chimera			Both Chimeras		
nAChR subtype	fmol/mg Protein	nAChR subtype	fmol/mg Protein	Fold Increase	nAChR subtype	fmol/mg Protein	Fold Increase	nAChR subtype	fmol/mg Protein	Fold Increase
α2β2	7.7±0.6	α2χβ2	1732±66	228±14	α2β2χ	305±29	41±5	α2χβ2χ	1276±320	174±46
α2β3	-	α2χβ3	-	-	α2β3χ	-	-	α2χβ3χ	-	-
α2β4	41±5	α2χβ4	387±41	9.7±0.6	α2β4χ	106±9	3.1±0.1	α2χβ4χ	843±133	20.7±1.2
α3β2	7.9±2.0	α3χβ2	2375±569	353±91	α3β2χ	48±10	7.4±2.0	α3χβ2χ	1467±367	216±57
α3β3	-	α3χβ3	-	-	α3β3χ	-	-	α3χβ3χ	-	-
α3β4	92±30	α3χβ4	866±91	11.6±2.7	α3β4χ	383±182	3.6±0.6	α3χβ4χ	637±83	8.1±1.3
α4β2	36±7	α4χβ2	1363±259	49±7	α4β2χ	369±57	14±3	α4χβ2χ	1453±75	60±17
α4β3	-	α4χβ3	-	-	α4β3χ	-	-	α4χβ3χ	-	-
α4β4	106±15	α4χβ4	389±61	3.9±0.7	α4β4χ	360±98	3.3±0.5	α4χβ4χ	632±68	6.2±0.7
α5β2	-	α5χβ2	-	-	α5β2χ	-	-	α5χβ2χ	-	-
α5β3	-	α5χβ3	-	-	α5β3χ	-	-	α5χβ3χ	-	-
α5β4	-	α5χβ4	-	-	α5β4χ	-	-	α5χβ4χ	-	-
α6β2	-	α6χβ2	3124±258	N/A	α6β2χ	-	N/A	α6χβ2χ	3189±257	N/A
α6β3	-	α6χβ3	-	-	α6β3χ	-	-	α6χβ3χ	-	-
α6β4	-	α6χβ4	862±74	N/A	α6β4χ	-	N/A	α6χβ4χ	915±104	N/A

TABLE 6.2. Summary of [^{3}H]-epibatidine binding to tsA201 cells expressing pairwise combinations of wild-type and chimeric subunits. Data are presented as means (± standard error) of 3 independent experiments performed in triplicate and are listed as fmol/mg of protein and as the fold increase in binding observed above the wild-type nAChR subtype upon replacement of wild-type subunits with the corresponding subunit chimeras. N/A = not appropriate.

nAChRs containing α2

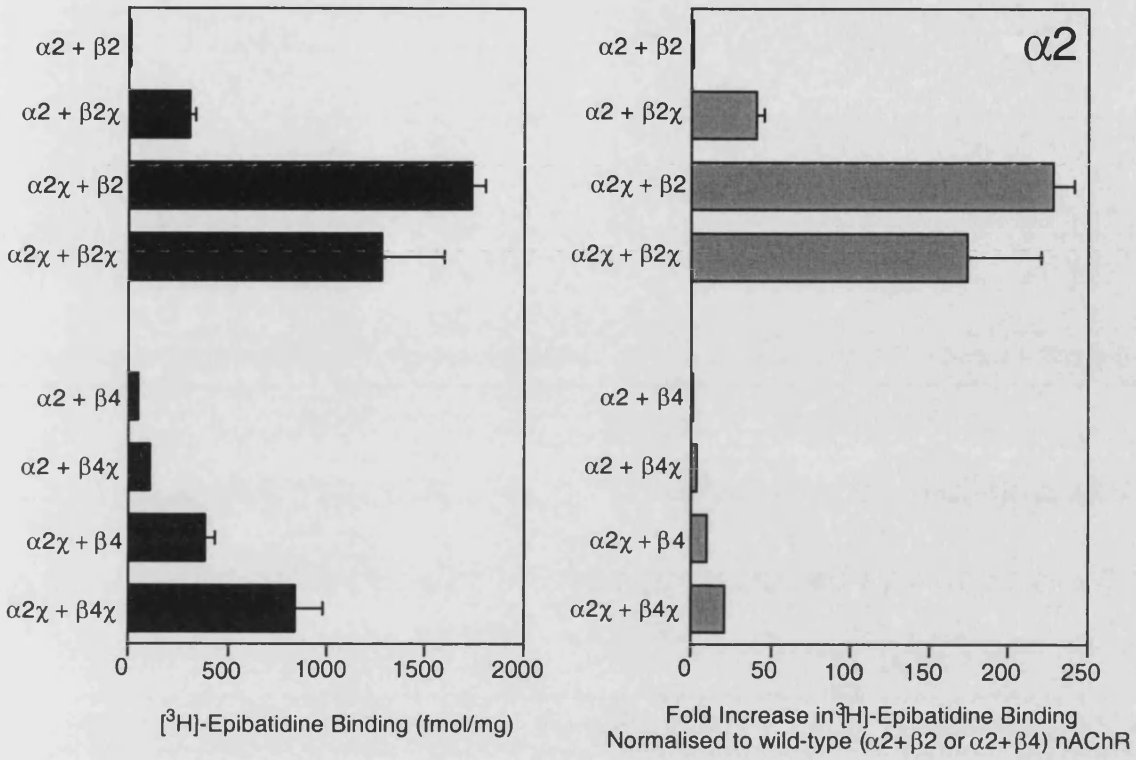

FIGURE 6.1. Specific [^{3}H]-epibatidine binding to α2-containing pairwise combinations of subunits. Mammalian tsA201 cells were transiently transfected with wild-type α2 and chimeric α2χ subunits in pairwise combinations with wild-type or chimeric β2 or β4 subunits. Data are presented as means of 3 independent experiments (+ standard error) performed in triplicate and reveal low levels of radioligand binding to membrane preparations when α2 is co-expressed with β2 or β4 subunits. Replacing wild-type α2, β2 or β4 subunits with the corresponding chimeric subunit enhances the levels of [^{3}H]-epibatidine binding. Absolute values for [^{3}H]-epibatidine binding (fmol/mg protein) and the relative fold increases above wild-type values observed upon expression of subunit chimeras are listed in Table 6.2.

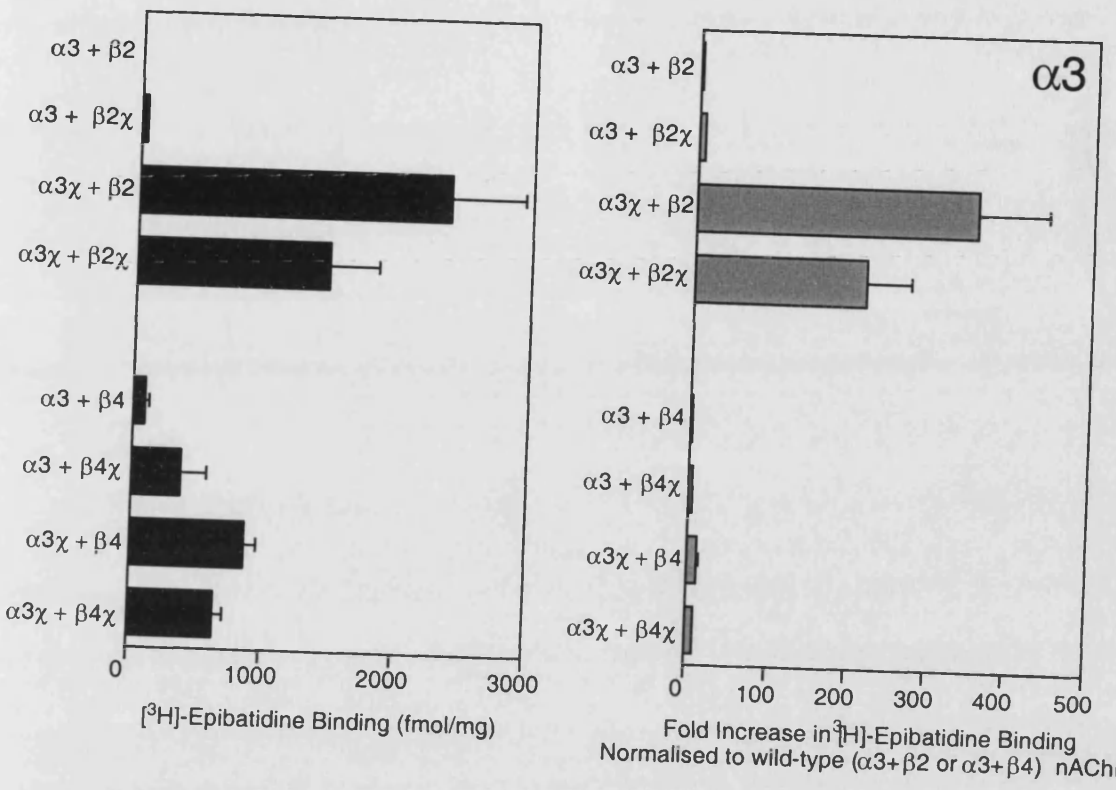

FIGURE 6.2. Specific [^{3}H]-epibatidine binding to α3-containing pairwise subunit combinations. Mammalian tsA201 cells were transiently transfected with wild-type α3 and chimeric α3χ subunits in pairwise combinations with wild-type β2 or β4 and chimeric β2χ or β4χ subunits. Data are presented as means of 3 independent experiments (+ standard error) performed in triplicate and reveal low levels of radioligand binding to membrane preparations when α3 is co-expressed with β2 or β4 subunits. Replacing wild-type α3, β2 or β4 subunits with the corresponding chimeric subunit enhances the levels of [^{3}H]-epibatidine binding. Absolute values for [^{3}H]-epibatidine binding (fmol/mg protein) and the relative fold increases above wild-type values observed upon expression of subunit chimeras are listed in Table 6.2.

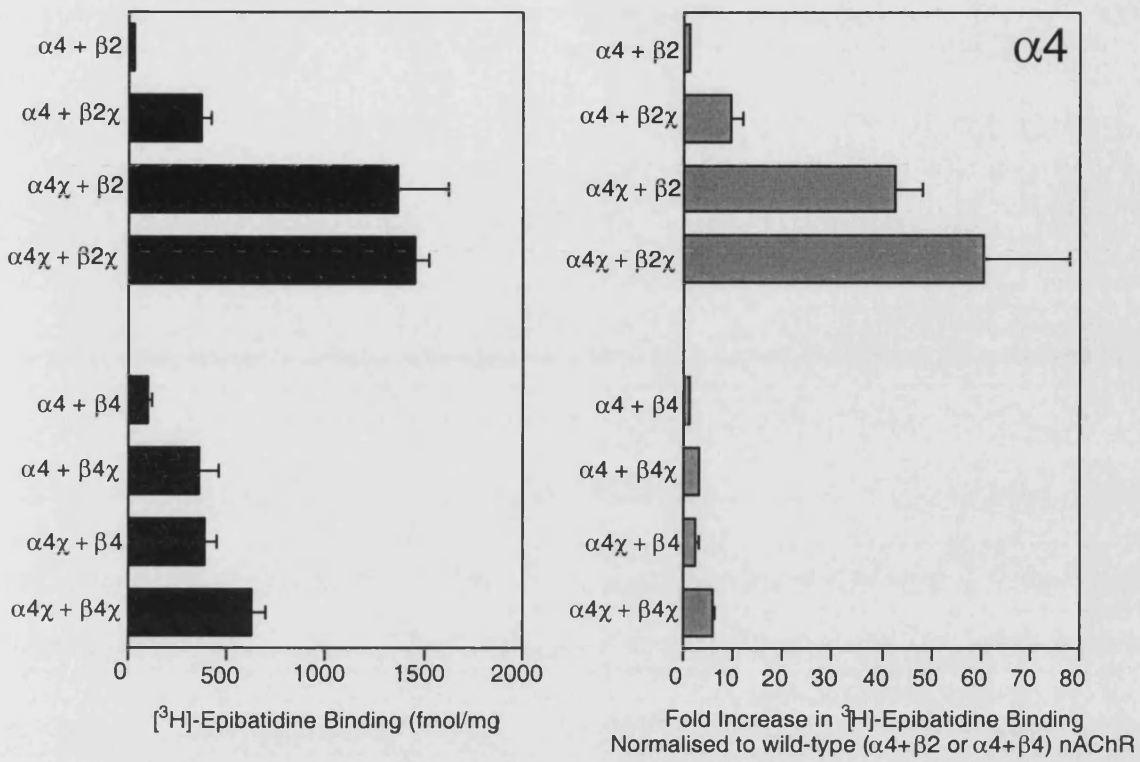

FIGURE 6.3. Specific [^{3}H]-epibatidine binding to α4-containing pairwise subunit combinations. Mammalian tsA201 cells were transiently transfected with wild-type α4 and chimeric α4χ subunits in combination with wild-type or chimeric β2 or β4 subunits. Data are presented as means of 3 independent experiments (+ standard error) performed in triplicate and reveal low levels of radioligand binding to membrane preparations when α4 is co-expressed with β2 or β4 subunits. Levels of [^{3}H]-epibatidine binding are enhanced by replacing wild-type α4, β2 or β4 subunits with the corresponding chimeric subunit. Absolute values for [^{3}H]-epibatidine binding (fmol/mg protein) and the relative fold increases above wild-type values observed upon expression of subunit chimeras are listed in Table 6.2.

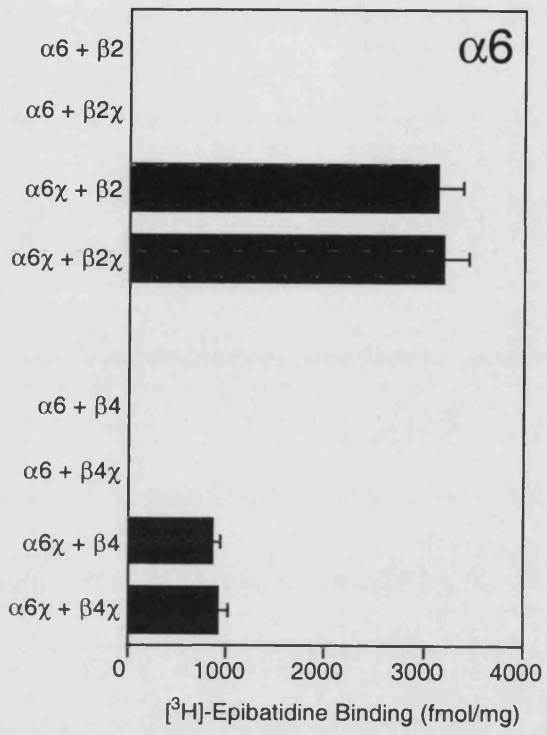

FIGURE 6.4. Specific [^{3}H]-epibatidine binding to α6-containing pairwise subunit combinations. Mammalian tsA201 cells were transiently transfected with wild-type α6 and chimeric α6χ subunits in combination with wild-type β2 or β4 and chimeric β2χ or β4χ subunits. Data are presented as means of 3 independent experiments (+ standard error) performed in triplicate. Significant levels of radioligand binding are only observed in cell membrane preparations when the wild-type α6 subunit is replaced with the α6χ chimera and co-expressed with wild-type or chimeric β2 or β4 subunits. Absolute [^{3}H]-epibatidine binding values (fmol/mg protein) are listed in Table 6.2.

Wild-type nAChR		α7χ chimera		β-type chimera		Both chimeras	
nAChR Subtype	**fmol/mg Protein**	**nAChR Subtype**	**fmol/mg Protein**	**nAChR Subtype**	**fmol/mg Protein**	**nAChR Subtype**	**fmol/mg Protein**
α7	-	α7χ	4377±587				
α7β2	-	α7χβ2	4068±717	α7β2χ	-	α7χβ2χ	4186±820
α7β3	-	α7χβ3	3712±750	α7β3χ	-	α7χβ3χ	4017±724
α7β4	-	α7χβ4	3840±728	α7β4χ	-	α7χβ4χ	4052±718
α7α5	-	α7χα5	5429±1216	α7α5χ	-	α7χα5χ	3872±539

TABLE 6.3. Summary of [^{3}H]-MLA binding to α7-containing nAChRs in tsA201 cells expressing combinations of wild-type and chimeric subunits. Data are presented as means (± standard error) of 3 independent experiments performed in triplicate. Expression of α5, β2, β3, β4, α5χ, β2χ, β3χ or β4χ subunits alone did not generate any significant levels of [^{3}H]-epibatidine binding (Tables 6.1 and 6.2). Specific radioligand binding is observed only when the chimeric α7χ subunit is included in the nAChR complex. Levels of binding detected with pair-wise combinations of α7χ-containing nAChRs do not differ significantly from the levels of binding observed with the α7χ alone.

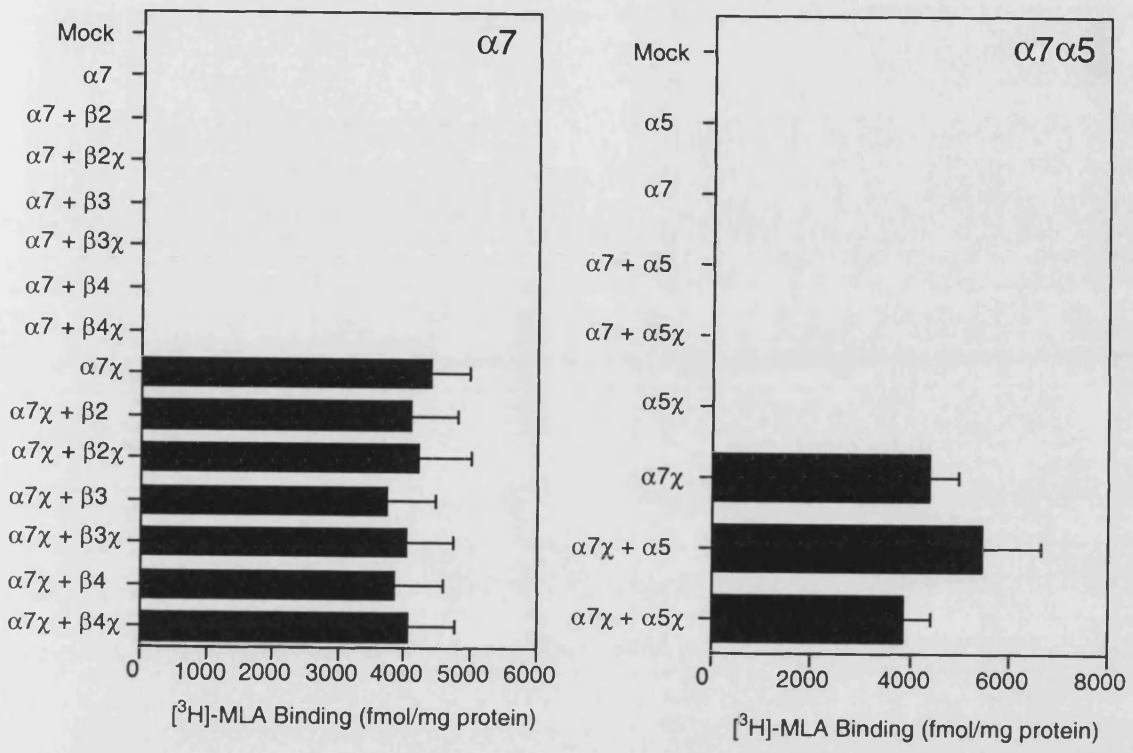

FIGURE 6.5. Specific [^{3}H]-MLA binding to α7-containing pairwise combinations of subunits. The α7 subunit was expressed with wild-type or chimeric β2, β3 or β4 subunits or expressed with wild-type or chimeric α5 in tsA201 cells. Specific [^{3}H]-MLA binding to cell membrane preparations is presented as means (+ standard error) of 3 independent experiments performed in triplicate. Significant levels of radioligand binding were only observed when the wild-type α7 subunit was replaced with the α7χ chimera. Levels of [^{3}H]-MLA binding detected with α7χ were not influenced by co-expression with any of the wild-type or chimeric α5, β2, β3 or β4 subunits. The host-cell dependent misfolding of the wild-type subunit was not alleviated upon co-expression with any of the wild-type or chimeric α5, β2, β3 or β4 subunits in tsA201 cells. Absolute values for [^{3}H]-MLA binding (fmol/mg protein) are listed in Table 6.3.

6.8 Discussion

6.8.1 The effects of chimeras on the α-BTX-insensitive nAChR subtypes

A large degree of variation is observed in the levels of [^{3}H]-epibatidine binding in cells expressing the different heteromeric nAChR subtype pairs (Table 6.2). There is an ~11-fold difference between the low levels of binding observed to cells expressing α2β2 nAChRs and the highest levels of binding to α4β4 nAChRs. The rank order of radioligand binding levels is α4β4 ≥ α3β4 > α2β4 ≥ α4β2 > α3β2 ≥ α2β2. No binding was observed upon expression of α6β2 or α6β4 subtypes. A clear difference between the nAChRs containing the β4 subunit and those containing β2 is apparent, with greater levels of radioligand binding observed with β4-containing nAChRs. This suggests that either the folding of the β4 subunit is more efficient than the β2 subunit, or that β4 assembles with the α subunits more efficiently than β2 does.

The nature of the α-type subunit also appears to influence nAChR expression, reflected by the differences in radioligand binding levels between subtypes in which the β subunit is constant and the α-type subunit varied. For example, levels of [^{3}H]-epibatidine binding to the α3β4 subtype (92±30 fmol/mg) were considerably higher than those observed with α2β4 (7.7±0.6 fmol/mg). This may reflect differences in the folding efficiency of the α-type subunit or in the efficiency of the co-assembly of the α and β subunits.

The effects of the different nAChR subunits on the efficiency of radioligand binding site formation are highlighted by the studies with chimeras. For each of the α2-, α3- and α4-containing nAChR subtypes, replacement of either one or both of the wild-type subunits with subunit chimeras increased the detectable levels of [^{3}H]-epibatidine binding. The extent of the observed increase is dependent on nAChR subtype and is influenced by the nature of both the α and the β subunit. For example, the low levels of [^{3}H]-epibatidine

binding observed to α2β2 increased by 228±14-fold upon replacement of α2 with the α2χ chimera. In comparison, replacing the wild-type α4 subunit with α4χ resulted in a 49±7-fold increase in radioligand binding. This difference may reflect the levels of radioligand binding observed with the wild-type nAChRs, which appear higher for the α4β2 nAChR subtype (41±5 fmol/mg) than the α2β2 subtype (7.7±0.6 fmol/mg). Therefore, assembly of wild-type α2β2 nAChRs appears to be less efficient than assembly of α4β2 nAChRs.

In the majority of cases, replacement of the wild-type α subunit with a subunit chimera caused a greater increase in the levels of radioligand binding than replacement of the β subunit with the corresponding chimeric subunit. Therefore, in comparison to the influence of the β subunit, the α subunit appears to exert the more dominant effect on the efficient formation of ligand binding sites. Previous studies have revealed a dominant-negative effect of the α4 subunit on nAChR assembly (Cooper *et al.*, 1999; Harkness and Millar, 2001; Harkness and Millar, 2002), with the high cell surface levels of β2χ reduced by 40% upon co-expression with α4 (Harkness and Millar, 2002). The critical influence of the α-type subunit is demonstrated particularly well by the α6-type nAChRs (Figure 6.4), where there is no evidence for high affinity [^{3}H]-epibatidine binding upon co-expression of wild-type α6 with any β-type subunits. However, when α6 is replaced with α6χ, radioligand binding is observed upon co-expression with each of the β2, β2χ, β4 or β4χ subunits. These results strongly implicate the use of chimeras as a valuable tool for investigation of α6-containing nAChRs in tsA201 cells. In a previous study, in which the C-terminal region of human α6 was replaced with the corresponding region of the α4 subunit, high levels of [^{3}H]-epibatidine binding were detected in HEK293 cells upon co-expression of the α6/α4 chimera with β2 or β4 subunits, while wild-type human α6β2 and α6β4 nAChRs were not detected by radioligand binding (Evans *et al.*, 2003). Therefore, the rat α6/5HT$_{3A}$ chimera (this study) and the human α6/α4 chimera (Kuryatov *et al.*, 2000; Evans *et al.*, 2003) both implicate the C-terminal region of nAChR subunits in receptor assembly.

With the α4β4 nAChR, the increases in the levels of radioligand binding observed in preparations of cells expressing the α4χβ4 and α4β4χ combinations were not significantly different (3.9±0.7-fold and 3.3±0.5-fold respectively; Figure 6.3) and may reflect the relative efficiency of α4β4 nAChR assembly in comparison to other nAChRs.

An interesting observation was the occurrence of specific [^{3}H]-epibatidine binding (albeit low levels) when the chimeric α2χ, α3χ and α4χ subunits were expressed alone in tsA201 cells. Homomeric α4χ complexes that bind [^{3}H]-epibatidine with low affinity have been noted previously (Cooper *et al.*, 1999). When expressed alone in tsA201 cells, the chimeric α4χ and β2χ subunits assemble into pentameric complexes that are expressed at the cell surface in high levels (Cooper *et al.*, 1999; Harkness and Millar, 2002). There have been no reports of the successful heterologous expression of homomeric α2 or α3 subunits, but small functional responses to high concentrations of ACh have been detected in *Xenopus* oocytes injected with rat α4 mRNA (Sargent, 1993). The formation of chimeric homomers suggests that the N-terminal domains of the α2, α3 and α4 subunits contain residues capable of forming a nicotinic ligand binding site when folded into an appropriate conformation. It is possible that the wild-type subunits rarely achieve this conformation without the presence of other nicotinic subunits. Also, as the levels of binding observed with the homomeric receptors are low, these complexes may fold inefficiently or demonstrate lower affinities for nicotinic ligands than heteromeric nAChR complexes, such as α3χβ4. It is clear that upon co-expression of β2 or β4 with the chimeric α subunits, the levels of [^{3}H]-epibatidine binding greatly increase, suggesting that while α2χ, α3χ and α4χ can fold to form a nicotinic ligand binding site, the presence of both the α and non-α subunit are required for the efficient formation of high affinity [^{3}H]-epibatidine binding site. This is consistent with evidence suggesting that the α subunits contain the primary determinants responsible for ligand binding, but that residues in the N-terminal domain of the non-α subunits contribute to the ligand binding sites (Section 1.2.3) (Kao and Karlin, 1986; Parker *et al.*, 1998; Brejc *et al.*, 2001).

6.8.2 The effects of chimeras on the α7-containing nAChRs

The α7 subunit is able to form functional homomeric ion channels when expressed alone in *Xenopus* oocytes (Couturier *et al.*, 1990a; Eiselé *et al.*, 1993; Séguéla *et al.*, 1993; Gerzanich *et al.*, 1994), but it has also been suggested that α7 may co-assemble with other subunits, such as β2 and α5, *in vivo* (Anand *et al.*, 1993b; Yu and Role, 1998b; Palma *et al.*, 1999b; Khiroug *et al.*, 2002; Virginio *et al.*, 2002). The α7χ chimera also forms functional homomeric ion channels when expressed in *Xenopus* oocytes and is able to overcome the host-cell specific misfolding observed with the α7 subunit (Eiselé *et al.*, 1993; Cooper and Millar, 1997; Sweileh *et al.*, 2000).

No evidence for the formation of heteromeric α7-containing nAChRs was obtained via [^{3}H]-MLA binding performed on cells transfected with α7 or α7χ in combination with wild-type or chimeric α5 or neuronal β subunits. Misfolding of the wild-type α7 subunit in tsA201 cells was not alleviated by co-expression with any of the wild-type α5, β2, β3 or β4 subunits or the chimeric α5χ, β2χ, β3χ or β4χ subunits. Therefore, while the host cell-dependent misfolding of α7 can be alleviated through replacement of the C-terminal domain of α7 with that of the $5HT_{3A}$ subunit (Cooper and Millar, 1997; Cooper and Millar, 1998), the misfolding of α7-containing nAChRs in tsA201 cells is not due to the inefficient folding of a partnering α5 or neuronal β subunit.

In addition, co-expression of wild-type or chimeric α5 or β subunits with the α7χ chimera did not affect the levels of [^{3}H]-MLA binding observed to homomeric α7χ complexes (Figure 6.5; Table 6.3). While this does not provide any evidence for subunit co-assembly, it does not preclude the possibility, as co-assembly may not affect the ligand binding properties of the receptor complex. However, homomeric α7 nAChRs possess five ligand binding interfaces (Palma *et al.*, 1996), so the addition of a subunit that does not form a ligand binding interface might be expected to influence the ligand binding properties. Assembly of the α7χ homomer may be the preferred stoichiometry

in tsA201 cells, such that the effect of the putative heteromeric nAChR population on the observed levels of [^{3}H]-MLA is not detectable. Studies with wild-type α7 could be attempted in cell lines in which α7 folds more efficiently, such as the rat pituitary GH_4C_1 cells (Sweileh *et al.*, 2000), to assess the possible co-assembly of α7 with chimeric subunits.

6.8.3 Summary and conclusions

The rationale for using chimeric subunits was to enhance the inefficient folding and assembly of nAChRs in mammalian cells and this has been successfully achieved within this study. Expression of chimeric subunits in combination with wild-type or other chimeric subunits enhanced the expression of nAChRs containing each of the α2, α3, α4 and α6 subunits and implicates the C-terminal domain of nicotinic subunits in aspects of nAChR assembly. Expression of the homomeric α7 nAChR is also enhanced through construction of a chimeric subunit and has been shown in previous studies (Eiselé *et al.*, 1993; Cooper and Millar, 1997).

The extent to which chimeras increase radioligand binding is influenced by both the α and β subunit. For wild-type nAChRs containing α2, α3 or α4 subunits, expression levels are greater in cells in which the expressed nAChRs contain β4 rather than β2 subunits. Upon replacement of the β subunit with the corresponding chimera, the observed increase in radioligand binding is greater for β2-containing nAChRs than nAChRs containing β4, suggesting that β2 folds or assembles with the α subunits less efficiently than the β4 subunit is able to. The role of the α subunit is illustrated by differences in binding observed when the β subunit is constant and the co-expressed α subunit is varied, where the enhancing effect of chimeras is greater for α2-containing nAChRs than those containing α4.

The patterns of subunit co-assembly following pairwise co-expression of wild-type and chimeric subunits in tsA201 cells are highly consistent with previous data (for example, see Papke *et al.*, 1989; Wang *et al.*, 1996; Stauderman *et al.*, 1998; Kuryatov *et al.*, 2000; Millar, 2003). Specifically, the α2, α3, α4 and α6 subunits are able to co-assemble with β2 and β4 subunits. No evidence for specific radioligand binding was observed upon co-expression of any α-type subunit in combination with β3 or upon co-expression of any β-type subunit with α5. This is consistent with the suggestion that α5 and β3 subunits do not contribute directly to the ligand binding site, but demonstrate a more structural role within the pentameric complex (Sargent, 1993; Ramirez-Latorre *et al.*, 1996; Wang *et al.*, 1996; Kuryatov *et al.*, 2000). Replacement of wild-type subunits with nAChR/$5HT_{3A}$ subunit chimeras did not influence the ability of the α5 or β3 nAChR subunits to assemble with other subunits to form a ligand binding interface, though whether the subunits are able to associate to form complexes that do not possess a ligand binding site is not apparent from this particular study. Previous studies have suggested that α5 can associate with β2 when expressed in *Xenopus* oocytes, forming non-functional aggregates that do not bind [^{3}H]-epibatidine (Wang *et al.*, 1996).

In addition to providing further direct evidence for the co-assembly of subunits such as α2 and β4, the use of chimeras has been used effectively to enhance nAChR expression in a heterologous expression system. This is particularly apparent for nAChRs containing α6, where wild-type α6 subunits do not generate detectable [^{3}H]-epibatidine binding sites when expressed with neuronal β subunits in tsA201 cells (Section 6.6). The use of chimeras also provides information regarding the regions of individual subunits that are responsible for aspects of receptor folding and assembly, implicating the C-terminal region of the subunits in efficient nAChR assembly (see also Cooper and Millar, 1997; Cooper and Millar, 1998; Cooper *et al.*, 1999; Baker *et al.*, 2004). Comparison of different nAChR subtypes implies that the nature of the N-terminal domain contributes to nAChR assembly and that formation of the ligand binding site is influenced by both the α- and β-type subunits. As the patterns of subunit co-assembly

suggested by this study appear to confirm previous suggestions of subunit co-assembly, they are equally validated by these accounts, providing strong evidence to suggest that nAChR/$5HT_{3A}$ subunit chimeras can serve as viable models for the characterisation of nAChRs in mammalian cell lines.

6.9 Future directions

It would be particularly interesting to investigate the functional capabilities of nAChRs containing chimeric subunits in comparison to wild-type nAChRs. This would also help to ascertain whether the different nAChR subtypes form pentameric complexes. Expression in *Xenopus* oocytes suggests that the $\alpha 9\chi$ and $\alpha 10\chi$ chimeras are able to form functional homomeric ion channels (Section 4.4), though the functional capabilities of these chimeras in mammalian cell lines are as yet unknown. The $\alpha 7\chi$ chimera is able to form functional homomeric ion channels when expressed in both *Xenopus* oocytes (Eiselé *et al.*, 1993) and mammalian cells (Rakhilin *et al.*, 1999).

The subunit chimeras suggest that the C-terminal region of nAChR subunits contribute to nAChR folding and assembly. Additional chimeras could be constructed containing different proportions of nAChR/$5HT_{3A}$ receptor subunits in order to ascertain whether specific sequences within the nAChR subunit govern receptor expression.

The radioligand binding assays performed on membrane preparations of cells do not establish the sub-cellular distribution of the assembled nAChRs. Previous studies suggest that nAChRs containing chimeric subunits are expressed at the cell surface of tsA201 cells at high levels (Cooper and Millar, 1997; Cooper and Millar, 1998; Cooper *et al.*, 1999; Harkness and Millar, 2002) (this study, Section 5.2). Cell surface expression of the nAChRs could be estimated via radioligand binding to intact cells or with quantitative HRP-assays using subunit-specific antibodies (e.g. Cooper *et al.*, 1999; Harkness and Millar, 2002).

CHAPTER 7

THE INFLUENCE OF SUBUNIT CHIMERAS UPON nAChR SUBTYPES CONTAINING THREE DIFFERENT SUBUNITS: TRIPLET COMBINATIONS CONTAINING α5

7.1 Introduction

In Chapter 6, the influence of subunit chimeras upon the heterologous expression of pairwise combinations of nAChR subunits in tsA201 cells was described. There is, however, also evidence for the assembly of nAChRs containing more than two different nAChR subunit types in both native and heterologous expression systems (see Millar, 2003). The aim of the work described in this chapter was to examine whether evidence for co-assembly of the α5 or α5χ subunits could be obtained from their co-expression with a range of nAChR subunit combinations. Since α5 and α5χ are unable to form binding sites when expressed in pairwise combinations with any other subunit (Section 6.5, Sargent, 1993), changes in the levels of binding upon expression of α5 as a third subunit in a triplet combination would provide evidence for subunit co-assembly.

7.2 Triplet combinations of nAChR subunits including α5

Wild-type α5 and chimeric α5χ subunits were co-expressed with a variety of heteromeric nAChR subtypes containing wild-type or chimeric α2, α3, α4 or α6 subunits in combination with wild-type or chimeric β2 or β4 subunits in tsA201 cells. Cell membrane preparations were assayed for [^{3}H]-epibatidine binding and the results are presented in comparison to data obtained with pairwise combinations of subunits discussed in Sections 6.2 - 6.6.

Pairwise combinations of wild-type or chimeric α subunits expressed with α5 or α5χ were performed as control reactions. No evidence for specific [^{3}H]-epibatidine binding was observed upon co-expression of α5 or α5χ with any other wild-type or chimeric α subunit.

7.2.1 The α2- and α2χ-containing nAChRs

The α5 and α5χ subunits were co-expressed with nAChRs containing pairwise combinations of wild-type or chimeric α2 and β2 or β4 subunits in tsA201 cells. The results are presented in Table 7.1 and Figures 7.1 and 7.2.

The levels of [^{3}H]-epibatidine binding detected in membrane preparations of cells expressing nAChR subtypes containing wild-type α2 (Figure 7.1) or chimeric α2χ (Figure 7.2) were not affected by the addition of the wild-type α5 subunit.

The levels of [^{3}H]-epibatidine binding to the α2β2 nAChR subtype increased significantly upon addition of the chimeric α5χ subunit (540±100% of binding in the absence of α5χ; $p<0.05$; Table 7.1, Figure 7.1). In contrast, upon co-expression of α5χ with the α2β2χ, α2χβ2 and α2χβ2χ subtypes, the levels of [^{3}H]-epibatidine binding were significantly reduced to 13±3%, 85±3% and 70±20% of binding in the absence of α5χ, respectively (Table 7.1). Addition of α5χ to α2β4 and α2β4χ caused a complete elimination of [^{3}H]-epibatidine binding (Figure 7.1), while co-expression of α5χ with α2χβ4 and α2χβ4χ substantially reduced binding to 44±2% and 33±4% of binding in the absence of α5χ, respectively ($p<0.001$; Figure 7.2).

7.2.2 The α3- and α3χ-containing nAChRs

The results obtained following expression of α5 or α5χ with nAChRs containing the α3 and α3χ subunits in combination with wild-type or chimeric β2 or β4 subunits are presented in Table 7.2 and Figures 7.3 and 7.4.

Addition of the wild-type α5 subunit did not significantly affect the levels of [^{3}H]-epibatidine binding to tsA201 cells expressing any of the α3- or α3χ-containing nAChR subtypes. The levels of specific [^{3}H]-epibatidine binding observed to tsA201 cells transiently transfected with nAChRs containing wild-type α3 (α3β2, α3β2χ, α3β4 or α3β4χ), were not affected by co-expression with α5χ (Figure 7.3). However, addition of α5χ to nAChR complexes containing the chimeric α3χ subunit (α3χβ2, α3χβ2χ, α3χβ4 and α3χβ4χ) resulted in significant reductions in the levels of radioligand binding (to 60±10%, 40±10%, 60±4% and 50±3% of binding in the absence of α5χ, respectively; Figure 7.4; Table 7.2).

7.2.3 The α4- and α4χ-containing nAChRs

The results obtained following co-expression of α5 or α5χ with nAChRs containing α4 or α4χ subunits in combination with wild-type or chimeric β2 or β4 subunits are presented in Table 7.3 and Figures 7.5 and 7.6. Co-expression of wild-type α5 with the α4β2 nAChR subtype resulted in a small, but significant increase in [^{3}H]-epibatidine binding (160±20% of binding in the absence of α5). The levels of [^{3}H]-epibatidine binding to the α4β2χ, α4χβ2 or α4χβ2χ nAChR subtypes were not significantly affected by co-expression with the α5 subunit (n=3; Table 7.3). Addition of α5 did not affect the levels of binding to the α4β4 and α4β4χ nAChR subtypes (Figure 7.3), while small, but significant increases in radioligand binding to the α4χβ4 and α4χβ4χ nAChRs were observed upon co-expression with the α5 subunit (140±3% and 130±2% of binding in the absence of α5, respectively; p<0.05; Table 7.3, Figure 7.4).

Upon co-expression with the chimeric α5χ subunit, a small, but significant increase in [^{3}H]-epibatidine binding to the α4β2 nAChR was observed (260±40% of binding in the absence of α5χ; p<0.05; Figure 7.3, Table 7.3). The levels of binding to the α4β2χ nAChR subtype were significantly reduced upon addition of α5χ (to 20±1% of binding in the absence of α5χ; p<0.001), but addition of α5χ did not influence the levels of binding to the α4χβ2 or α4χβ2χ nAChR subtypes (Table 7.3). Upon co-expression with α5χ, [^{3}H]-epibatidine binding to the α4β4 and α4β4χ subtypes was completely abolished (Figure 7.3), binding to α4χβ4 was unaffected by α5χ (Figure 7.4) and binding to the α4χβ4χ nAChR was reduced (to 60±2% of binding in the absence of α5χ; p<0.001; Table 7.3).

7.2.4 The α6- and α6χ-containing nAChRs

The results obtained following expression of α5 or α5χ with nAChRs containing α6 or α6χ subunits in combination with wild-type or chimeric β2 or β4 subunits in tsA201 cells are presented in Table 7.4 and Figure 7.7. No evidence for specific [^{3}H]-epibatidine binding was observed to membrane preparations of tsA201 cells expressing any nAChR subtype that contained the wild-type α6 subunit.

Specific [^{3}H]-epibatidine binding was detected in cells in which α6χ was included in the subunit combination (Figure 7.7). Upon co-expression with the wild-type α5 subunit, the levels of radioligand binding observed to cells expressing the α6χβ2, α6χβ2χ and α6χβ4χ subtypes were significantly reduced to 77±3, 69±6 and 81±3% of binding in the absence of α5, respectively (Table 7.4). Co-expression of α5 with the α6χβ4 subtype did not significantly affect the levels of [^{3}H]-epibatidine binding. Addition of α5χ to the α6χβ2χ and α6χβ4χ complexes reduced ligand binding to 59±6% and 52±4% of binding in the absence of α5χ, respectively, while the reductions observed with the α6χβ2 and α6χβ4 subtypes were not statistically significant (n=3).

nAChR Subtype	[^{3}H]-Epibatidine Binding: fmol/mg Protein	+α5		+α5χ	
		fmol/mg Protein	% of Total	fmol/mg Protein	% of Total
α2	-	-	-	-	-
β2	-	-	-	-	-
β4	-	-	-	-	-
α2β2	7.7±0.6	17±5	240±80	41±7	540±100*
α2β2χ	305±29	345±26	120±20	39±4.4	13±0.3***
α2β4	40±5	56±11	140±10	1.9±2.1	4±5***
α2β4χ	106±9	203±43	110±30	2.7±4.4	1±4***
α2χ	26±8	3.8±3.7	-	0±0.5	-
β2χ	-	-	-	-	-
β4χ	-	-	-	-	-
α2χβ2	1732±66	1819±94	110±2	1471±28	85±3*
α2χβ2χ	1276±320	2054±404	190±40	742±21	70±20*
α2χβ4	387±41	438±60	110±10	171±20	44±2***
α2χβ4χ	843±133	986±103	120±10	260±16	33±4***

TABLE 7.1. Summary of [^{3}H]-epibatidine binding to the α2- and α2χ-containing triplet subunit combinations. Mammalian tsA201 cells were transiently transfected with triplet combinations of wild-type and chimeric subunits. Data are means (± standard error) of 3 independent experiments performed in triplicate and are listed as fmol/mg of protein and as the effect of co-expression of α5 or α5χ upon binding to each nAChR subtype (% of Total). Significance determined by a two-tailed Student's *t*-test (*p<0.05; ***p<0.001).

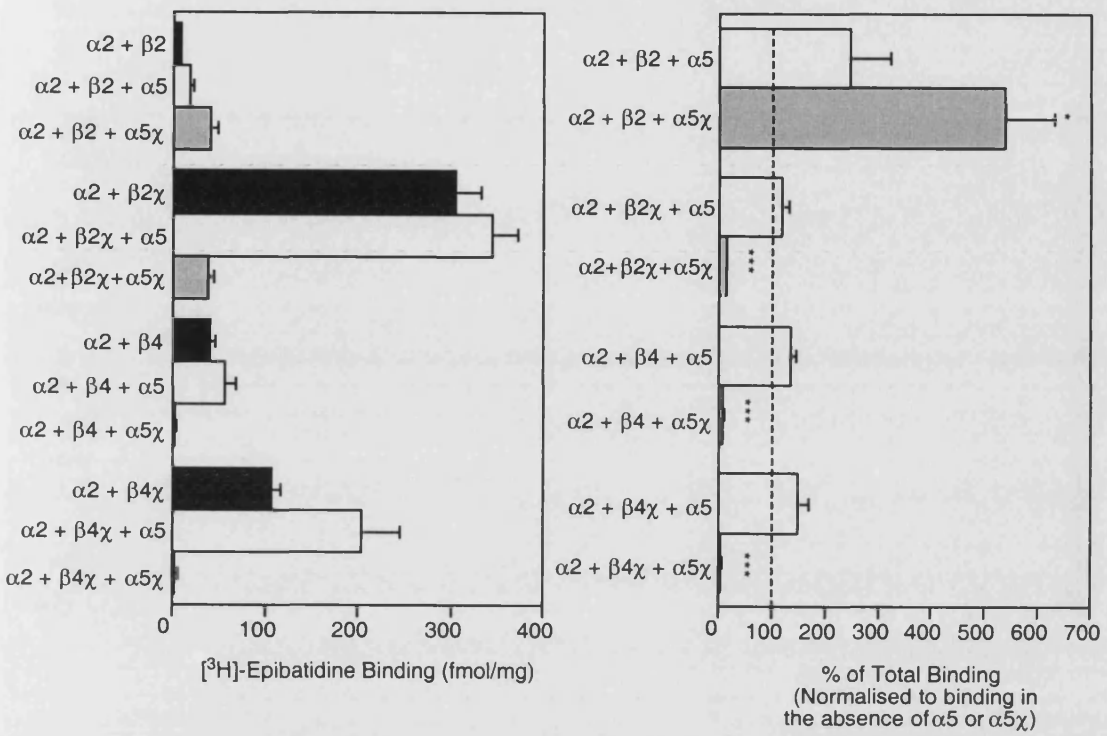

FIGURE 7.1. Specific [^{3}H]-epibatidine binding to α2-containing triplet subunit combinations. Cell membranes were prepared from tsA201 cells transiently transfected with the wild-type α2 subunit in combination with wild-type α5 and β2 or β4 subunits or their corresponding chimeric subunits (α5χ and β2χ or β4χ). Data are means (+ standard error) of 3 independent experiments performed in triplicate and are presented in comparison to selected data obtained with pairwise combinations of subunits shown in Figure 6.1. Absolute values for [^{3}H]-epibatidine binding (fmol/mg protein) and the effect of co-expression of α5 or α5χ upon binding to each nAChR subtype (% of Total Binding) are listed in Table 7.1. Pairwise combinations of wild-type α2 with wild-type α5 or chimeric α5χ did not yield significant levels of [^{3}H]-epibatidine binding. Significance determined by a two-tailed Student's *t* test (*p<0.05; ***p<0.001).

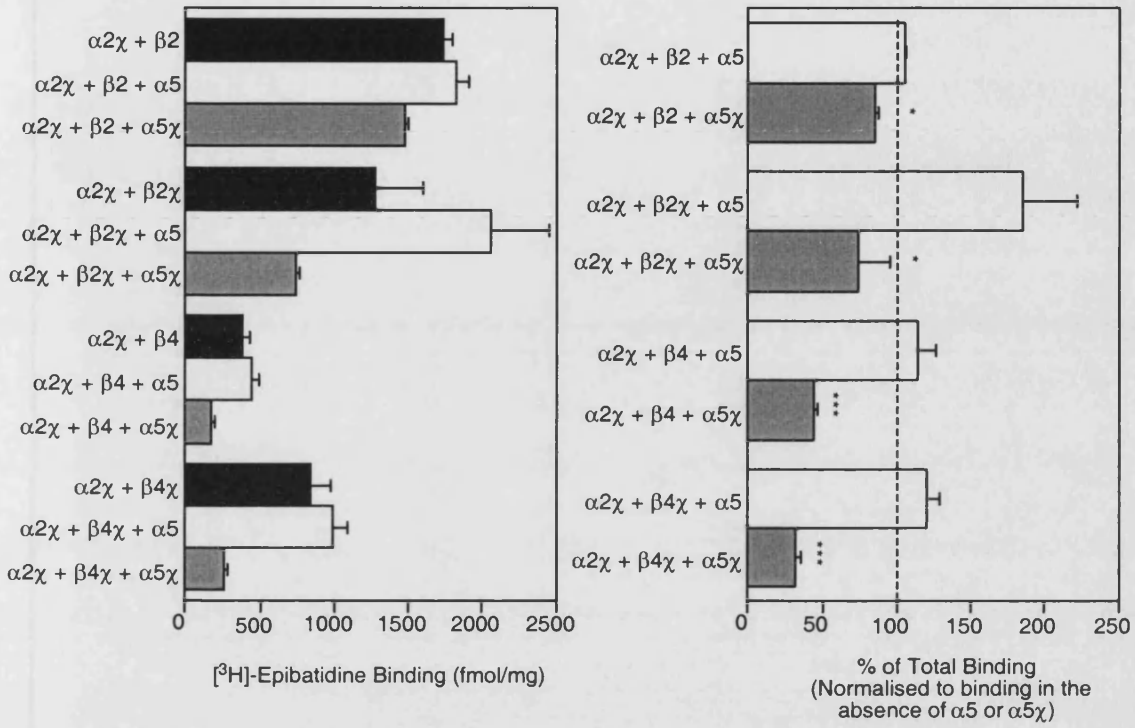

FIGURE 7.2. Specific [^{3}H]-epibatidine binding to α2χ-containing triplet subunit combinations. Cell membranes were prepared from tsA201 cells transiently transfected with the chimeric α2χ subunit in combination with wild-type α5 and β2 or β4 subunits or their corresponding chimeric subunits (α5χ or β2χ or β4χ). Data are means of 3 independent experiments (+ standard error) performed in triplicate and are presented in comparison to selected data obtained with pairwise combinations of subunits shown in Figure 6.1. Absolute values for [^{3}H]-epibatidine binding (fmol/mg protein) and the effect of co-expression of α5 or α5χ upon binding to each nAChR subtype (% of Total Binding) are listed in Table 7.1. Pairwise combinations of chimeric α2χ with wild-type α5 or chimeric α5χ did not yield significant levels of high affinity [^{3}H]-epibatidine binding. Significance determined by a two-tailed Student's *t* test (*p<0.05; ***p<0.001).

nAChR Subtype	[^{3}H]-Epibatidine Binding: fmol/mg Protein	+α5		+α5χ	
		fmol/mg Protein	% of Total	fmol/mg Protein	% of Total
α3	-	-	-	-	-
β2	-	-	-	-	-
β4	-	-	-	-	-
α3β2	7.9±2.0	11.5±1.2	190±50	13.4±1.3	220±70
α3β2χ	48±10	57±18	120±30	40±8	90±10
α3β4	92±30	154±50	170±30	88±16	110±20
α3β4χ	383±182	603±69	260±80	270±49	110±30
α3χ	67±28	61±28	-	5.2±2.0	-
β2χ	-	-	-	-	-
β4χ	-	-	-	-	-
α3χβ2	2375±569	2086±234	90±20	1144±43	60±10*
α3χβ2χ	1467±367	1691±470	110±10	564±116	40±10**
α3χβ4	866±91	860±186	100±10	473±38	60±4***
α3χβ4χ	637±83	641±67	100±10	304±24	50±3***

TABLE 7.2. Summary of [^{3}H]-epibatidine binding to the α3- and α3χ-containing triplet subunit combinations. Mammalian tsA201 cells were transiently transfected with triplet combinations of wild-type and chimeric subunits. Data are means (± standard error) of 3 independent experiments performed in triplicate and are listed as fmol/mg of protein and as the effect of co-expression of α5 or α5χ upon binding to each nAChR subtype (% of Total). Significance determined by a two-tailed Student's *t*-test (*p<0.05; **p<0.01; ***p<0.001).

α3-containing nAChRs

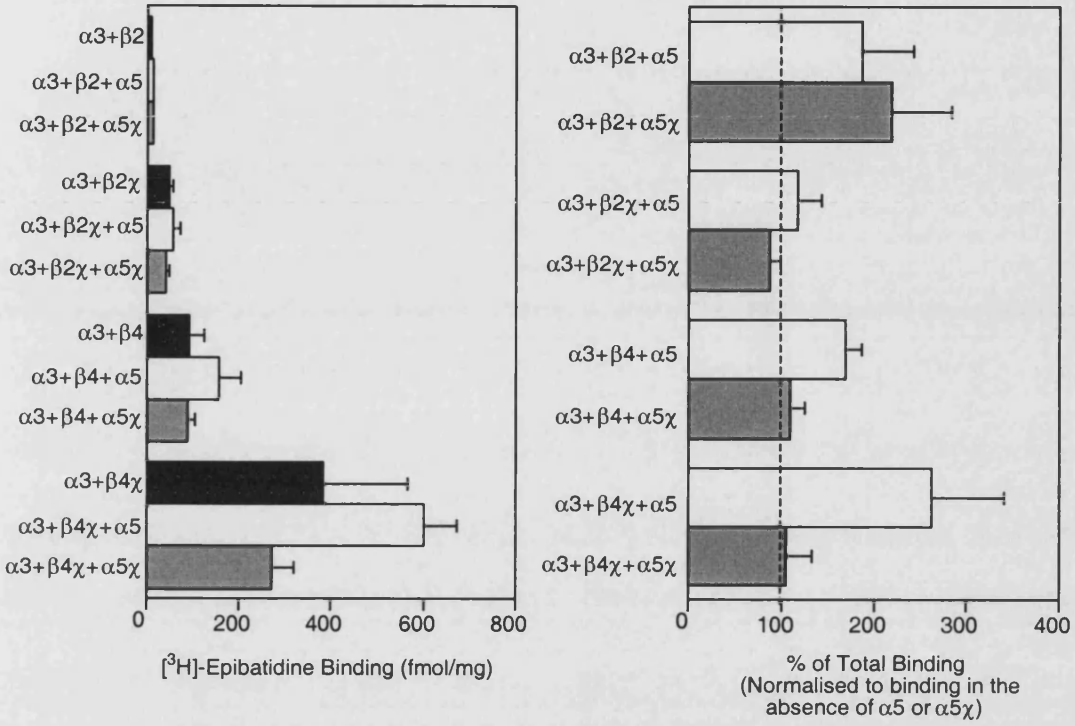

FIGURE 7.3. Specific [^{3}H]-epibatidine binding to α3-containing triplet subunit combinations. Cell membranes were prepared from tsA201 cells transiently transfected with the wild-type α3 subunit in combination with wild-type α5 and β2 or β4 subunits or their corresponding chimeric subunits (α5χ and β2χ or β4χ). Data are means (+ standard error) of 3 independent experiments performed in triplicate and are presented in comparison to selected data obtained with pairwise combinations of subunits shown in Figure 6.2. Absolute values for [^{3}H]-epibatidine binding (fmol/mg protein) and the effect of co-expression of α5 or α5χ upon binding to each nAChR subtype (% of Total Binding) are listed in Table 7.2. Pairwise combinations of wild-type α3 with wild-type α5 or chimeric α5χ did not yield significant levels of [^{3}H]-epibatidine binding. Significance determined by a two-tailed Student's *t* test.

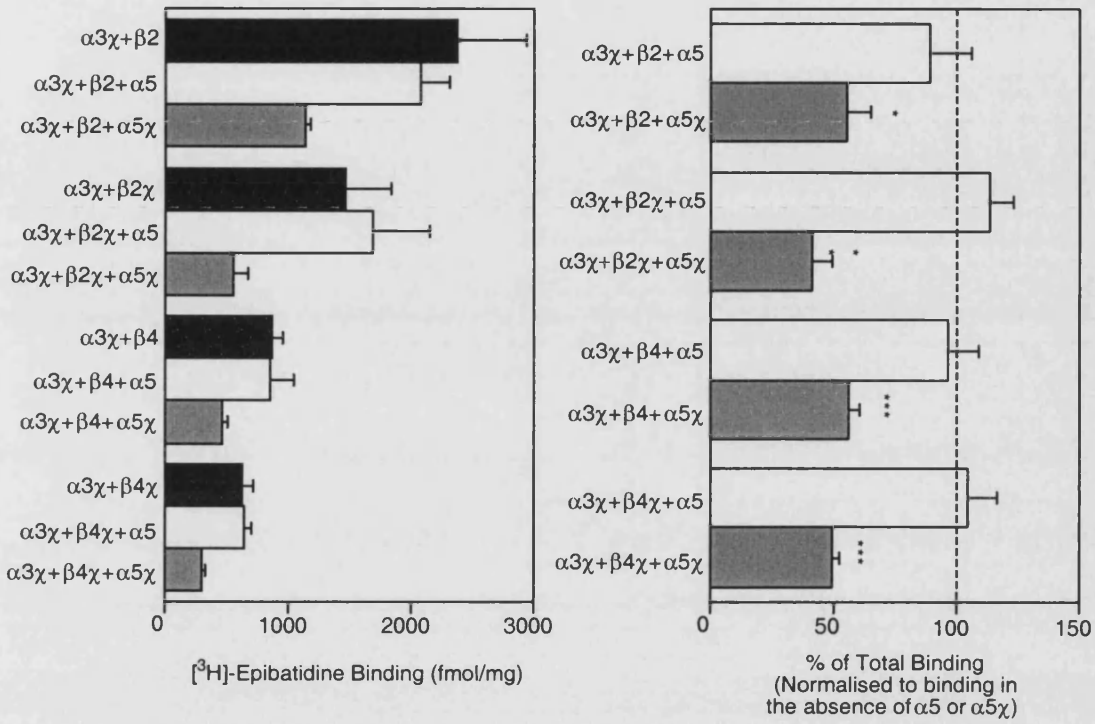

FIGURE 7.4. Specific [^{3}H]-epibatidine binding to α3χ-containing triplet subunit combinations. Cell membranes were prepared from tsA201 cells transiently transfected with the chimeric α3χ subunit in combination with wild-type α5 and β2 or β4 subunits or their corresponding chimeric subunits (α5χ and β2χ or β4χ). Data are means (+ standard error) of 3 independent experiments performed in triplicate and are presented in comparison to selected data obtained with pairwise combinations of subunits shown in Figure 6.2. Absolute values for [^{3}H]-epibatidine binding (fmol/mg protein) and the effect of co-expression of α5 or α5χ upon binding to each nAChR subtype (% of Total Binding) are listed in Table 7.2. Pairwise combinations of chimeric α3χ with wild-type α5 or chimeric α5χ did not yield significant levels of high affinity [^{3}H]-epibatidine binding. Significance determined by a two-tailed Student's *t* test (*p<0.05; ***p<0.001).

nAChR Subtype	[^{3}H]-Epibatidine Binding: fmol/mg Protein	+α5		+α5χ	
		fmol/mg Protein	% of Total	fmol/mg Protein	% of Total
α4	-	-	-	-	-
β2	-	-	-	-	-
β4	-	-	-	-	-
α4β2	36±7	57±12	160±20*	101±32	260±40*
α4β2χ	369±57	494±98	130±10	69±9	20±1***
α4β4	106±15	111±14	110±2	1.3±0.02	2±1***
α4β4χ	360±98	340±19	90±2	3.0±0.5	0.9±0.2***
α4χ	6.2±2.8	15±11	-	2.6±3.2	-
β2χ	-	-	-	-	-
β4χ	-	-	-	-	-
α4χβ2	1363±259	1890±179	150±30	1511±157	120±10
α4χβ2χ	1453±75	1840±99	130±10	1233±161	80±10
α4χβ4	389±61	533±71	140±3***	341±3.8	90±10
α4χβ4χ	632±68	815±98	130±2***	301±127	60±2***

TABLE 7.3. Summary of [^{3}H]-epibatidine binding to the α4- and α4χ-containing triplet subunit combinations. Mammalian tsA201 cells were transiently transfected with triplet combinations of wild-type and chimeric subunits. Data are means (± standard error) of 3 independent experiments performed in triplicate and are listed as fmol/mg of protein and as the effect of co-expression of α5 or α5χ upon binding to each nAChR subtype (% of Total). Significance determined by a two-tailed Student's *t*-test (*p<0.05; ***p<0.001).

α4-containing nAChRs

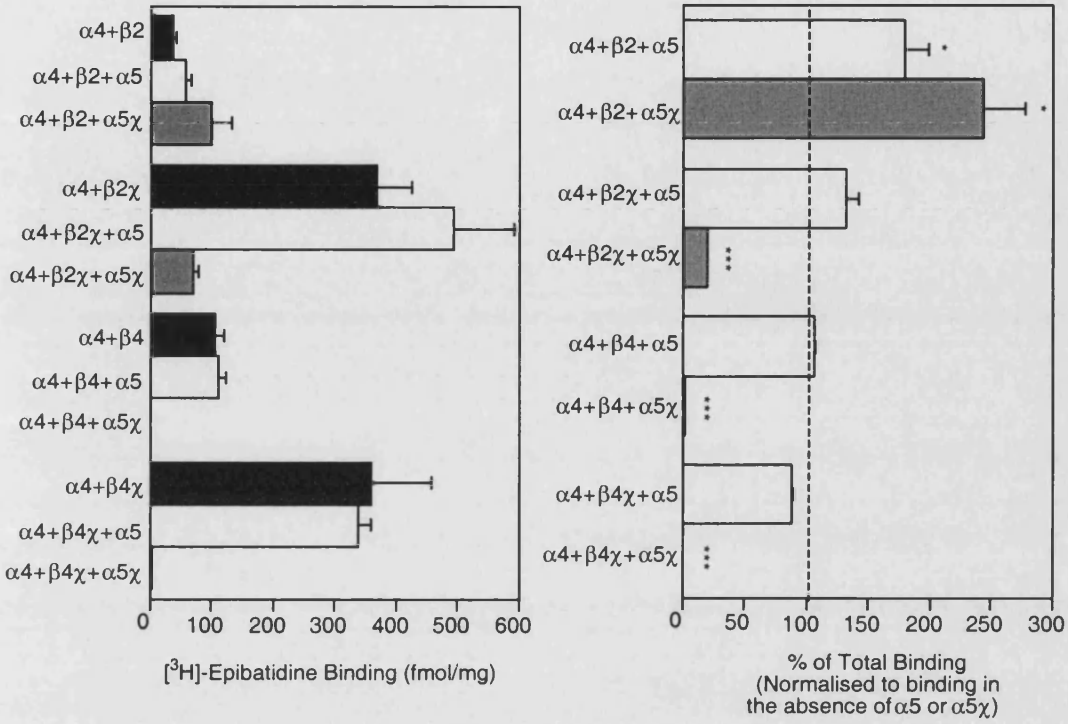

FIGURE 7.5. Specific [^{3}H]-epibatidine binding to α4-containing triplet subunit combinations. Cell membranes were prepared from tsA201 cells transiently transfected with the wild-type α4 subunit in combination with wild-type α5 and β2 or β4 subunits or their corresponding chimeric subunits (α5χ and β2χ or β4χ). Data are means (+ standard error) of 3 independent experiments performed in triplicate and are presented in comparison to selected data obtained with pairwise combinations of subunits shown in Figure 6.3. Absolute values for [^{3}H]-epibatidine binding (fmol/mg protein) and the effect of co-expression of α5 or α5χ upon binding to each nAChR subtype (% of Total Binding) are listed in Table 7.3. Pairwise combinations of wild-type α4 with wild-type α5 or chimeric α5χ did not yield significant levels of [^{3}H]-epibatidine binding. Significance determined by a two-tailed Student's *t* test (*p<0.05; ***p<0.001).

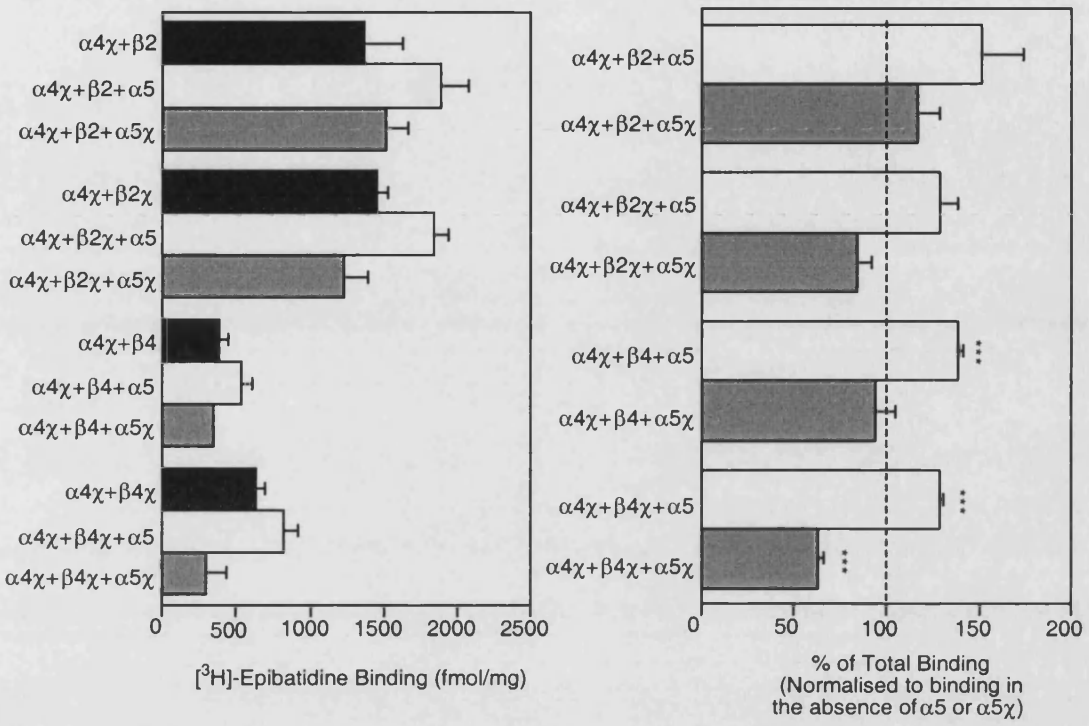

FIGURE 7.6. Specific [^{3}H]-epibatidine binding to α4χ-containing triplet subunit combinations. Cell membranes were prepared from tsA201 cells transiently transfected with the chimeric α4χ subunit in combination with wild-type α5 and β2 or β4 subunits or their corresponding chimeric subunits (α5χ and β2χ or β4χ). Data are means (+ standard error) of 3 independent experiments performed in triplicate and are presented in comparison to selected data obtained with pairwise combinations of subunits shown in Figure 6.3. Absolute values for [^{3}H]-epibatidine binding (fmol/mg protein) and the effect of co-expression of α5 or α5χ upon binding to each nAChR subtype (% of Total Binding) are listed in Table 7.3. Pairwise combinations of chimeric α4χ with wild-type α5 or chimeric α5χ did not yield significant levels of high affinity [^{3}H]-epibatidine binding. Significance determined by a two-tailed Student's *t* test (***p<0.001).

nAChR Subtype	[^{3}H]-Epibatidine Binding: fmol/mg Protein	+α5		+α5χ	
		fmol/mg Protein	% of Total	fmol/mg Protein	% of Total
α6	-	-	-	-	-
β2	-	-	-	-	-
β4	-	-	-	-	-
α6β2	-	-	-	-	-
α6β2χ	-	-	-	-	-
α6β4	-	-	-	-	-
α6β4χ	-	-	-	-	-
α6χ	-	-	-	-	-
β2χ	-	-	-	-	-
β4χ	-	-	-	-	-
α6χβ2	3124±258	2392±183	77±3**	2009±387	65±13
α6χβ2χ	3189±257	2211±322	69±6*	1906±287	59±6**
α6χβ4	862±74	645±52	80±10	538±46	65±9
α6χβ4χ	915±104	773±81	81±3*	464±47	52±4***

TABLE 7.4. Summary of [^{3}H]-epibatidine binding to the α6- and α6χ-containing triplet subunit combinations. Mammalian tsA201 cells were transiently transfected with triplet combinations of wild-type and chimeric subunits. Data are means (± standard error) of 3 independent experiments performed in triplicate and are listed as fmol/mg of protein and as the effect of co-expression of α5 or α5χ upon binding to each nAChR subtype (% of Total). Significance determined by a two-tailed Student's *t*-test (*p<0.05; **p<0.01; ***p<0.001).

α6χ-containing nAChRs

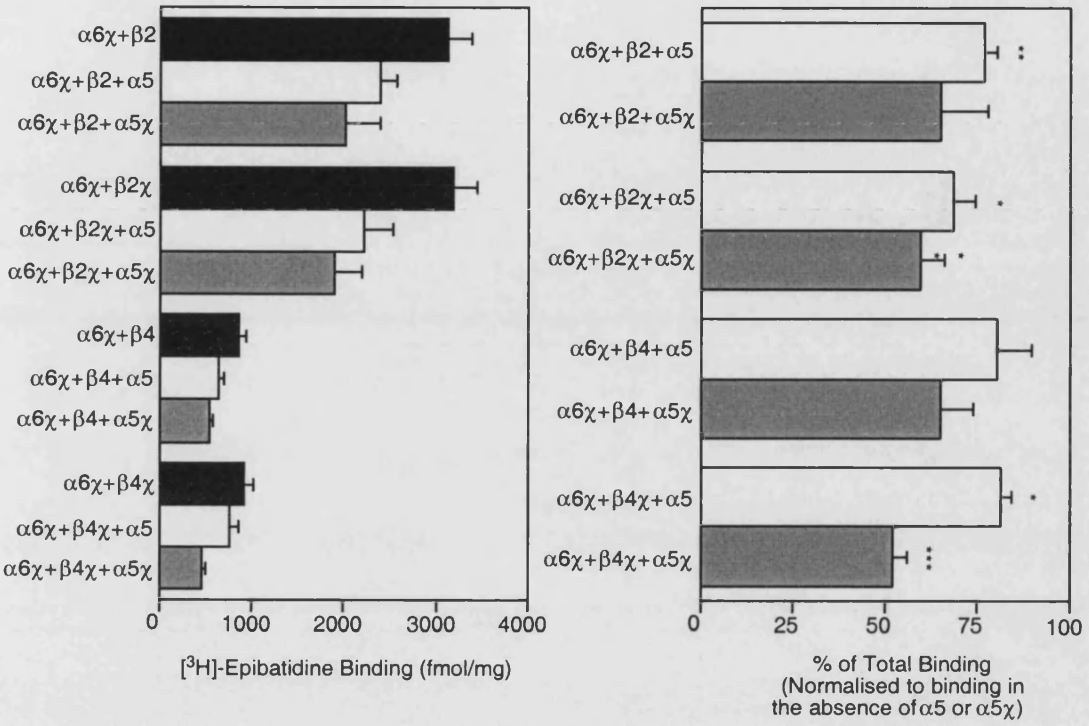

FIGURE 7.7. Specific [^{3}H]-epibatidine binding to α6χ-containing triplet subunit combinations. Cell membranes were prepared from tsA201 cells transiently transfected with the chimeric α6χ subunit in combination with wild-type α5 and β2 or β4 subunits or their corresponding chimeric subunits (α5χ and β2χ or β4χ). Data are means (+ standard error) of 3 independent experiments performed in triplicate and are presented in comparison to selected data obtained with pairwise combinations of subunits shown in Figure 6.4. Pairwise combinations of chimeric α6χ with wild-type α5 or chimeric α5χ did not yield significant levels of high affinity [^{3}H]-epibatidine binding. Absolute values for [^{3}H]-epibatidine binding (fmol/mg protein) and the effect of co-expression of α5 or α5χ upon binding to each nAChR subtype (% of Total Binding) are listed in Table 7.4. Significance determined by a two-tailed Student's *t* test (*p<0.05; **p<0.01; ***p<0.001).

7.3 Discussion

7.3.1 The influence of the α5 and α5χ subunits

Figure 7.8 illustrates the effects of α5 (or α5χ) on the levels of [^{3}H]-epibatidine binding to α2β2, α2β4, α3β2, α3β4, α4β2 and α4β4 wild-type nAChR subtypes. Expression of the α6β2 and α6β4 subtypes in tsA201 cells did not lead to the formation of detectable radioligand binding sites (Sections 6.6 and 7.2.4) and this lack of binding was not alleviated through co-expression with the α5 subunit. The absence of radioligand binding observed upon expression of rat α6 with β2 or β4 in mammalian cell lines (Section 6.6) does not, therefore, reflect a requirement for the α5 subunit. An alternative or additional nAChR subunit or a different cell-specific factor, such as a molecular chaperone may be required. Additional studies have suggested that the β3 subunit does not alleviate the inefficient folding of α6β4 nAChRs in tsA201 cells, as co-expression of α6β4β3 or α6β4β3χ subunit combinations did not generate high affinity [^{3}H]-epibatidine binding sites (data not shown; n=3).

Upon addition of the wild-type α5 subunit, the levels of binding to the α4β2 nAChR increased slightly (160±20% of binding in the absence of α5; Table 7.3), suggesting that α5 is able to co-assemble with the α4β2 nAChR in tsA201 cells. In a previous study, in which wild-type chick α4, β2 and α5 subunits were co-expressed in HEK293 cells, the levels of [^{3}H]-epibatidine binding to α4β2 nAChRs were not significantly altered upon addition of the α5 subunit, though co-assembly of α5 with α4β2 nAChRs was demonstrated by immunoprecipitation (Conroy and Berg, 1998). In the present study, the increase in [^{3}H]-epibatidine binding observed upon co-expression of α5 with rat α4β2 nAChRs in tsA201 cells was very small (Figure 7.5) and suggests that cellular factors other than the α5 subunit influence the inefficient folding of the recombinant α4β2 nAChR in tsA201 cells. The difference between the results of this and previous studies may also reflect host-cell or species differences.

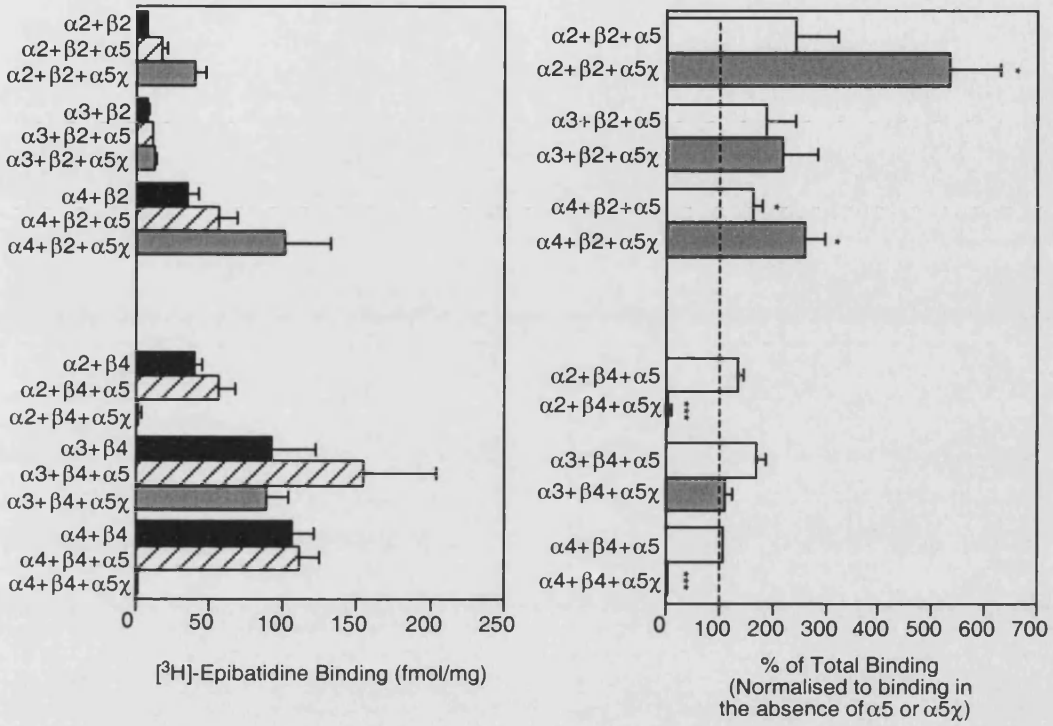

FIGURE 7.8. Specific [^{3}H]-epibatidine binding to wild-type nAChR subtypes and the effect of α5 and α5χ. Data are means (+ standard error) of 3 independent experiments performed in triplicate and are taken from Figures 7.1, 7.3 and 7.5 to compare the effects of adding α5 or α5χ to each of the wild-type nAChR combinations. Absolute values for [^{3}H]-epibatidine binding (fmol/mg protein) and the effect of co-expression of α5 or α5χ upon binding to each nAChR subtype (% of Total Binding) are listed in Tables 7.1 - 7.3. Significance determined by paired Student's *t* test (*p<0.05; ***p<0.001).

The levels of radioligand binding to each of the other wild-type nAChR subtypes expressed in tsA201 cells were not significantly affected by co-expression with the wild-type α5 subunit (Figure 7.8). Previous studies have demonstrated the co-assembly of α5 with each of the α2β2, α3β2, α3β4, α4β2 and α6β2 nAChR subtypes (see Millar, 2003). The α5 subunit may occupy a position within the nAChR pentamer analogous to that of the β1 subunit within the muscle-type nAChR complex (Figure 1.2). In this position, the α5 subunit may not contribute directly to the ligand binding interfaces, but would contribute to the lining of the ion channel (Wang *et al.*, 1996; Conroy and Berg, 1998; Gerzanich *et al.*, 1998). For example, co-expression of α5 with α3β2 or α3β4 nAChRs in *Xenopus* oocytes does not affect [^{3}H]-epibatidine binding affinity, but does increase the rate of nAChR desensitisation (Wang *et al.*, 1996). It is possible that incorporation of the α5 subunit into the pentameric complex of nAChR subtypes, such as α3β4, in tsA201 cells does not affect the ligand binding properties of the nAChR and is, therefore, not detected by [^{3}H]-epibatidine binding.

Chimeric subunits were used to investigate whether incorporation of α5 into nAChR complexes could alter the efficiency of nAChR expression, as demonstrated previously with other combinations of chimeric subunits (Chapters 4 and 6, Cooper *et al.*, 1999; Harkness and Millar, 2002; Baker *et al.*, 2004). Increases in the levels of radioligand binding to α2β2 and α4β2 nAChRs were observed upon co-expression with α5χ (540±100% and 260±40% of binding in the absence of α5χ, respectively; $p<0.05$). These data suggest that α5χ is able to co-assemble with these nAChR subtypes and enhance the formation of [^{3}H]-epibatidine binding sites when expressed in tsA201 cells. This is consistent with previous studies that have suggested the formation of α2β2α5 and α4β2α5 nAChRs in chick brain (Conroy and Berg, 1998; Balestra *et al.*, 2000). The levels of radioligand binding detected to the α3β2 and α3β4 nAChR subtypes were not significantly altered by co-expression with α5χ. While this does not provide any evidence for the co-assembly of an α5-type subunit with the α3β2 or α3β4 nAChRs, it does not eliminate the possibility that the chimeric α5χ subunit is incorporated into the

nAChR complex at a position that does not affect the formation of the ligand binding site. The results do suggest that the inefficient folding of these particular wild-type nAChR subtypes in tsA201 cells is not due to the absence of the α5 subunit.

An interesting observation was that the levels of binding observed to α2β4 and α4β4 were completely abolished upon expression with α5χ (Figure 7.8). There have been no reports to suggest the formation of α2β4α5 or α4β4α5 complexes (Millar, 2003), but the α2β4 and α4β4 subtypes were significantly influenced by the addition of α5χ. Abolition of radioligand binding upon co-expression of α5χ with α2β4 or α4β4 nAChRs suggests that α5χ associates with at least one of the α-type or β4 subunits. However, the subunit-subunit interactions that occur are not beneficial with respect to the formation of ligand binding sites. Specific [^{3}H]-epibatidine binding was not observed upon pairwise co-expression of α5 or α5χ with α2, α4 or β4, though whether these subunit combinations can form protein aggregates that do not bind radioligand has not been determined. Immunoprecipitation and sucrose gradient studies have demonstrated the assembly of α5β2 aggregates in *Xenopus* oocytes that do not possess ligand binding capabilities (Wang *et al.*, 1996). In contrast, α5 does not form complexes with α3 in *Xenopus* oocytes that are stable in Triton X-100 (Wang *et al.*, 1996).

The abolition of radioligand binding to the α2β4 and α4β4 nAChR subtypes upon co-expression with α5χ is in contrast to the influence of this chimera on the levels of binding to the α2β2 and α4β2 subtypes, which increased upon addition of α5χ. Therefore, the interaction of the α5χ subunit with the different nAChR subtypes is influenced by the nature of the β subunit. However, α5χ did not affect the levels of radioligand binding to the α3β2 or α3β4 nAChRs, suggesting that the nature of the α-type subunit also influences nAChR assembly.

Significant reductions in the levels of [^{3}H]-epibatidine binding to a number of the nAChR subtypes containing other chimeric subunits were observed upon co-expression

with α5χ. For example, the levels of binding to α2χβ4, α4β2χ and α6χβ2χ and to each of the nAChR subtypes containing α3χ, decreased upon co-expression with α5χ. Therefore, α5χ displaces a proportion of the ligand-binding interfaces of each of these chimeric receptor subtypes. It is possible that α5χ interacts with other chimeric subunits in a promiscuous manner, allowing interactions to occur that would not be observed between wild-type subunits. For example, it has been suggested that the α5 subunit does not associate with the wild-type α3 subunit until α3 has associated with β2 (Wang *et al.*, 1996). If this association is prevented by the nature of the C-terminal domain, the restrictive interactions may be eliminated in the subunit chimeras, as the $5HT_{3A}$ subunit is able to assemble into functional homomeric complexes (Maricq *et al.*, 1991; Eiselé *et al.*, 1993). However, it does not appear that subunit chimeras assemble without regard for the N-terminal domain, as co-expression with α5χ did not reduce the levels of radioligand binding observed to every nAChR subtype that contained another chimeric subunit. For example, the levels of [^{3}H]-epibatidine binding observed in cells expressing α3β4χ and α4χβ4 combinations were unaffected by co-expression with α5χ. In addition, the levels of [^{3}H]-MLA binding to membrane preparations of cells expressing homomeric α7χ complexes were unaffected by the addition of α5χ (Section 6.7). Also, the negative effect of α5χ on the formation of the ligand binding site was not restricted to nAChRs containing another chimeric subunit, as radioligand binding to the wild-type α2β4 and α4β4 nAChRs was abolished upon co-expression with α5χ (Figure 7.8) and binding to α6χβ2, α6χβ2χ and α6χβ4χ was reduced upon co-expression with wild-type α5 (Figure 7.7).

The chimeric α5χ subunit exerted different effects on different nAChR subtypes. For example, co-expression of α5χ with α2χβ4 and α2χβ4χ substantially reduced binding (to 44±2% and 33±4% of binding in the absence of α5χ, respectively; $p<0.001$), while the addition of α5χ to α2β4 and α2β4χ abolished [^{3}H]-epibatidine binding completely ($p<0.001$; Table 7.1). The associations that occur between chimeric α2χ and the β4-type subunits thus appear to differ to the interactions between wild-type α2 and the β4-type

subunits. The association between α2 and β4 also differs to the association between α2 and β2. Therefore, the nature of both the N- and C-terminal domains of each of the α and β subunits appear to influence subunit association and nAChR assembly. This is consistent with previous studies, where the effects of mutated and chimeric nAChR subunits have been used to identify critical assembly domains located at the N-terminus of nAChR subunits (Gu *et al.*, 1991; Yu and Hall, 1991; Sumikawa, 1992) and have also implicated the C-terminal region in cell-specific folding and subunit oligomerisation (Cooper and Millar, 1997; Cooper and Millar, 1998; Eertmoed and Green, 1999).

Co-expression of human α6 and β2 subunits in *Xenopus* oocytes generates high levels of specific [^{3}H]-epibatidine binding that are reduced upon addition of human α5 (Kuryatov *et al.*, 2000). This is consistent with the reduction in binding to the α6χβ2 and α6χβ2χ complexes observed upon co-transfection with α5 observed in this study (Table 7.4). When expressed in *Xenopus* oocytes, the human α6 and β2 subunits do not assemble into functional pentameric arrays, but form large ligand-binding aggregates (Kuryatov *et al.*, 2000). The α5 subunit is able to disrupt the formation of α6β2 aggregates, leading to the production of a proportion of functional α6β2α5 nAChRs (Kuryatov *et al.*, 2000). In addition, the aggregation of α5 and β2 subunits has been demonstrated in *Xenopus* oocytes (Wang *et al.*, 1996). Therefore, the addition of α5 to the α6χβ2 and α6χβ2χ complexes may reduce the formation of potential ligand binding aggregates and/or increase the formation of α5β2 aggregates, creating a reduction in the detectable levels of ligand binding. It would be interesting to examine the functional capabilities of the α6χβ2 and α6χβ2χ complexes, to establish whether disruption of the α6χβ2 binding interfaces by α5 results in a detrimental or beneficial effect with respect to the formation of viable pentameric receptor complexes. While it is not clear which interactions are taking place, it is apparent that the α5 subunit is able to disrupt the ligand binding interfaces formed between α6χ and the β-type subunits.

7.3.2 Models of nAChR assembly and the influence of α5χ on pathways of subunit oligomerisation

Two models have been proposed for subunit oligomerisation and assembly pathways of muscle-type nAChRs and are illustrated in Figure 7.9 (see Green and Millar, 1995; Green, 1999). In these models, the ordered pathways of nAChR assembly indicate the importance of each individual subunit-subunit interaction and suggest that subunit conformation is affected by interaction with other subunits, where only certain conformations are permissive for nAChR assembly.

The pathways of nAChR assembly were proposed following experiments in which the α-BTX binding capabilities of nAChR complex intermediates were monitored (Green and Millar, 1995). Upon heterologous expression and immunoprecipitation of incomplete recombinant nAChRs, the simplest combinations of [^{125}I]-α-BTX-labelled subunits that could be co-precipitated were α-γ and α-δ heterodimers (Figure 7.9A). Co-expression of α and β subunits did not allow precipitation of [^{125}I]-α-BTX with anti-β antibodies. The first model of nAChR assembly (the Heterodimer Model; Figure 7.9A), suggests that the mature α subunit (α_{TX}), which possesses α-BTX-binding ability, associates with γ or δ to form α-γ and α-δ heterodimers. The two heterodimers oligomerise with each other and with the β subunit to form the pentameric $\alpha_2\beta\gamma\delta$ nAChRs (Blount and Merlie, 1989; Green and Millar, 1995; Green, 1999).

In the second model (Sequential Model; Figure 7.9B), suggested following the stable expression of all four nAChR subunits in mammalian cells cultured at low temperature (Green and Claudio, 1993), α-β-γ trimers form rapidly. These trimers may be preceded by α-β, α-γ and β-γ heterodimers, but these species were not isolated in these experiments (Green, 1999). Pulse-chased labelling with [^{35}S]-methionine demonstrated the subsequent assembly of α-β-γ-δ tetramers, before the addition of the second α subunit to form the final $\alpha_2\beta\gamma\delta$ pentamers (Green and Claudio, 1993; Green, 1999).

Therefore, while α-δ heterodimers (Heterodimer Model) may be able to assemble when expressed in the absence of other subunits in heterologous systems, this may not represent the natural pathway of assembly *in vivo* (Green and Wanamaker, 1998; Green, 1999).

The nAChR subunits are synthesised and undergo folding transitions and post-translational modifications within the endoplasmic reticulum (Green and Millar, 1995; Green, 1999; Keller and Taylor, 1999). Initial subunit associations may occur prior to the completion of subunit folding, due to the rapidity of some subunit associations (Green and Millar, 1995). The subunit N-terminal domains probably mediate these initial subunit-subunit interactions, where the N-terminal domains of partially-translated subunits interact with other completed subunits (Green and Millar, 1995; Keller and Taylor, 1999). The initial interactions appear to lack specificity and may occur to protect critical subunit domains from the cellular environment or to prevent misfolding of these domains (Eertmoed and Green, 1999). This would suggest that the initial interactions that occur between α5χ and the other nAChR or nAChR/$5HT_{3A}$R subunits are governed by the N-terminal domains and may not be affected by the presence of the C-terminal $5HT_{3A}$ sequences within the chimeras.

In the Sequential Model of nAChR assembly, folding and receptor maturation is a continuous process, with folding events occurring after each step of subunit oligomerisation to allow the association of the next subunit (Green, 1999). Subunit conformation is modified upon association with a partnering subunit for both muscle-type and neuronal nAChRs, where the proportion of nAChR subunits recognised by subunit-specific antibodies is altered upon co-expression with other subunits (Mitra *et al.*, 2001; Harkness and Millar, 2002). Evidence to implicate subunit C-terminal domains in subunit oligomerisation has also been provided by chimeras containing regions of *Torpedo* electric organ γ and δ subunits (Eertmoed and Green, 1999). Chimeras containing the N-terminal domain of the δ subunit up to M1, fused to the C-

terminal domain of the γ subunit (δ221γ) are able to substitute for the δ subunit, but not for the γ subunit when expressed with the other *Torpedo* electric organ nAChR subunits in tsA201 cells. However, the corresponding γ215δ chimera does not substitute for either the γ or δ subunits and blocks the formation of all intracellular α-BTX binding sites. The γ215δ chimera associates with either α or β subunits, but not with both, blocking nAChR assembly prior to the appearance of α-β-γ trimers (see Sequential Model, Figure 7.9B) (Eertmoed and Green, 1999).

If the N-terminal domains of each neuronal nAChR subunit interact non-specifically, this suggests that both the α5 and α5χ subunits are able to associate with each of the other wild-type or chimeric nAChR subunits upon co-expression in mammalian cells. In this case, it is the interactions between the C-terminal domains of each subunit that govern whether the association is productive. A conformational change may occur to strengthen the association between productive pairs that permits the association of a third subunit in the formation of trimers (Eertmoed and Green, 1999). Three possible situations can be considered, whereby the initial subunit-subunit association is:

1) Stable (or stabilised through additional conformational change) and leads to the formation of a pentameric nAChR complex.
2) Stable, but inappropriate for pentamer formation and either progresses no further along the assembly pathway or leads to the formation of protein aggregates.
3) Not stable and either dissociates or is degraded (Eertmoed and Green, 1999; Green, 1999).

The γ215δ chimera (Eertmoed and Green, 1999) exerts a dominant-negative effect upon nAChR assembly, where the associations within intermediate complexes are strengthened, but formation of the complete nAChR pentamer is prevented. A similar mechanism may explain the abolition of binding observed upon co-expression of α5χ with the α2β4 and α4β4 nAChR subtypes. In this scheme, α5χ would be able to interact with either the α-type subunit or the β4 subunit, but the resulting associations would not

permit the formation of trimers. Alternatively, α5χ may associate with α-β heterodimers or other intermediate complexes along the assembly pathway, but the principle would be the same, whereby assembly intermediates that contain α2β4α5χ or α4β4α5χ subunit combinations are not viable to progress along the assembly pathway. In contrast, where the levels of radioligand binding to nAChRs subtypes are unaffected by the addition of α5χ (such as α3β4), the conformation of complex intermediates would presumably either exclude the assembly of α5χ, or be permissive for the oligomerisation of additional subunits. The small increases in radioligand binding observed upon co-expression of α5χ with α2β2 and α4β2 suggests that the complex intermediates are permissive for the formation of pentameric nAChRs that contain α5χ.

It is not clear from the binding experiments alone at which point along the assembly pathway α5χ is able to associate with other subunits and, in certain cases, block the assembly pathway. However, it is tempting to attribute this association to an early stage, such as the formation of heterodimers, analogous to that of the γ215δ chimera (Eertmoed and Green, 1999), or at the formation of subunit trimers, due to the complete block of binding observed upon co-expression of α5χ with the α2β4 and α4β4 nAChR subtypes. This suggests that the interactions between α5χ and the other subunits occur at a stage early enough in the pathway to reduce the pool of viable α-β interactions and prevent the formation of any ligand-binding pentamers. If the α5χ subunit was the last subunit be integrated into the pentameric complex, then a mixed population of pentameric nAChRs might be expected (±α5χ), with a proportion of α2β4 or α4β4 nAChRs that are able to bind radioligand. In addition, the α5 subunit has been suggested to assume a position in the pentameric complex analogous to that of the β1 subunit of the muscle-type nAChR. If the pathways of the muscle-type and neuronal nAChRs are comparable, this would suggest that α5 associates with an α and a β subunit at the trimer (or possibly heterodimer stage) of the assembly pathway (Figure 7.9B).

The differences in the effects of α5χ may also highlight differences in the efficiency of particular subunit-subunit interactions. For example, in order for α5χ to completely block the formation of ligand binding interfaces when expressed with α2 and β4, the formation of α5χ-containing intermediate complexes must occur more efficiently than intermediates containing only α2 and β4 subunits, otherwise a mixed population of nAChRs would be expected to appear that includes α2β4 pentamers, which would generate ligand binding sites (these are not observed).

The studies with nAChR subunits expressed in pairwise combinations (Chapter 6) suggest that β4 associates more efficiently with α3χ than with α3. However, the levels of radioligand binding to α3χβ4 are reduced (though not abolished) upon co-expression with α5χ (while α3β4 is unaffected by α5χ and α3χβ4 is unaffected by α5). It is possible that, for example, α5χ-β4 associations occur efficiently, but are not permissive for the formation of viable ligand binding sites when the other α-type subunit is α3χ. Therefore, upon co-expression of α3χ, β4 and α5χ, the two different chimeras may compete for association with β4, where α3χ-β4 associations are permissive for the formation of α3χβ4 pentamers, while α5χ-β4 associations do not permit the formation of nAChRs with equivalent ligand binding properties. This would result in a mixed population of subunit complexes with different ligand binding capabilities, reducing the observed levels of [^{3}H]-epibatidine binding.

In the Sequential Model of nAChR assembly, the γ subunit mediates subunit oligomerisation (Green and Wanamaker, 1998). During assembly, the δ subunit and the second α subunit associate between different subunit pairs, but both subunits interact with the same γ interface (Figure 7.10). The β subunit also associates with this interface in the formation of trimers. The interface of the γ subunit appears to change specificity to permit the incorporation of different subunits into the assembly complex (Green and Wanamaker, 1998). If the assembly pathways of the muscle-type and neuronal nAChRs are analogous, then subunit oligomerisation would be mediated by the neuronal β

subunit. The β subunit would interact with the α subunit and with α5 (or another β subunit) in the formation of a trimer. A conformational change would then occur that permits association of another β subunit, followed by a second α subunit. Mediation of trimer formation via the β subunit is consistent with a study of α3β2α5 nAChRs in *Xenopus* oocytes, in which β2 associated with α5, but formed non-ligand binding aggregates in the absence of α3, while α3 and α5 did not form a stable association in the absence of β2 (Wang *et al.*, 1996). In the present study, the role of the β subunit is highlighted upon co-expression of wild-type nAChRs with α5χ, where α5χ prevented the formation of ligand binding pentamers when expressed with α2β4 or α4β4, while ligand binding to the α2β2 or α4β2 nAChR subtypes increased upon addition of α5χ. The α subunit also appears to influence nAChR assembly, as the levels of ligand binding with α3β4 nAChRs were unaffected by the addition of α5χ. This is compatible with the presented model, in which subunit oligomerisation is determined by the conformation of each assembly intermediate, where subunit conformation is modified following the addition of each subunit (Green and Millar, 1995; Green and Wanamaker, 1998; Eertmoed and Green, 1999; Green, 1999; Mitra *et al.*, 2001; Harkness and Millar, 2002) and may provide a mechanism for the selective assembly of specific nAChR subtypes.

7.3.3 Summary and conclusions

Wild-type nAChR subunits and nAChR/$5HT_{3A}$ subunit chimeras were expressed in triplet combinations to investigate the potential co-assembly of α5 with different nAChR subtypes. In previous studies, the α5 subunit has been observed to participate in the formation of nAChRs containing more than one α-type subunit, including α3β2α5 and α4β2α5 nAChRs (Wang *et al.*, 1996; Conroy and Berg, 1998). However, the α3β2α5 and α4β2α5 nAChR subtypes could not be distinguished from α3β2 or α4β2 nAChRs through the use of radioligand binding and co-assembly was demonstrated through other techniques, such as immunoprecipitation (Wang *et al.*, 1996; Conroy and Berg, 1998).

Therefore, the aim of this study was to investigate whether the ability of the chimeric subunits to alter the levels of nAChRs able to generate ligand binding sites (Chapter 6) would be extended to α5χ. If the levels of radioligand binding detected in cells transfected with pairwise combinations of wild-type subunits (e.g. α3β2) increased following addition of α5χ, this would indicate the co-assembly of these nAChRs with an α5-type subunit and provide further evidence for the ability of subunit chimeras to enhance the efficiency of nAChR expression.

Upon co-expression of α5χ with α2β2 and α4β2 nAChR subtypes, significant increases in radioligand binding were observed (540±100% and 260±40% of binding in the absence of α5χ, respectively), suggesting that these nAChR subtypes are able to co-assemble with an α5-type subunit to form complexes capable of binding [^{3}H]-epibatidine when expressed in tsA201 cells. However, α5χ was also observed to disrupt the ligand binding interfaces formed between certain subunits, such as α4β4 and α3χβ2, where the levels of radioligand binding to these nAChR subtypes decreased upon co-expression with α5χ. Therefore, α5χ appears able to associate with other nAChR or nAChR/5HT$_{3A}$ subunits, but for the majority of nAChR subtypes tested, this interaction is not beneficial with respect to the formation of a high affinity nicotinic binding site. Replacing the C-terminal region of α5 with the corresponding region of 5HT$_{3A}$ appears to alter the ability of the α5-type subunit to interact efficiently with other nicotinic or chimeric subunits and this is consistent with the studies with the other chimeras (Chapters 4 and 6, Cooper *et al.*, 1999; Harkness and Millar, 2002; Baker *et al.*, 2004). These studies have provided an insight into nAChR assembly, where the differences in the ligand binding profiles of each nAChR subtype support previous evidence to suggest that both the N- and C-terminal regions of each of the α and β nAChR subunits are involved in aspects of subunit oligomerisation (Green and Millar, 1995; Eertmoed and Green, 1999; Keller and Taylor, 1999).

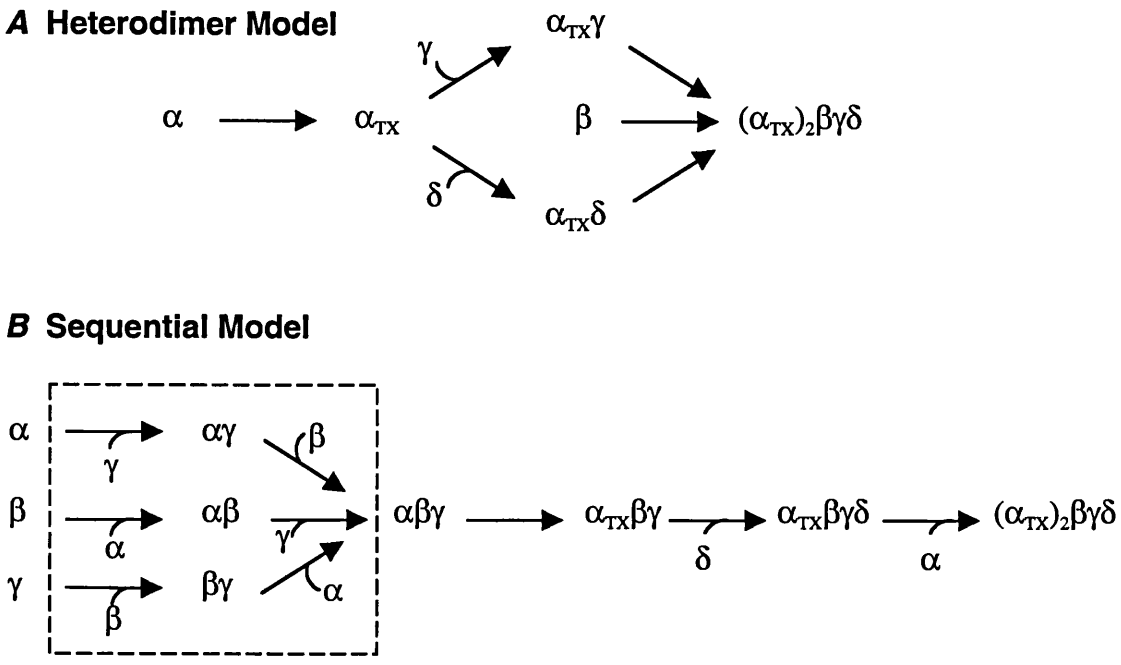

FIGURE 7.9. Models of the assembly of the muscle-type nAChR. Two models suggested for the pathway of nAChR subunit oligomerisation in the assembly of pentameric nAChRs. (*A*) The mature α subunit (α_{TX}) associates with γ or δ subunits to form αγ and αδ heterodimers. The heterodimers oligomerise with the β subunit and with each other to form $\alpha_2\beta\gamma\delta$ pentamers. (*B*) Rapidly formed αβγ trimers (possibly preceded by αβ, αγ and βγ dimers) associate with δ to form αβγδ tetramers. Addition of the second α subunit completes the formation of the $\alpha_2\beta\gamma\delta$ pentamers. "α_{TX}" represents the mature α subunit as determined by the ability of the subunit to bind α-BTX. Adapted from Green and Millar, 1995.

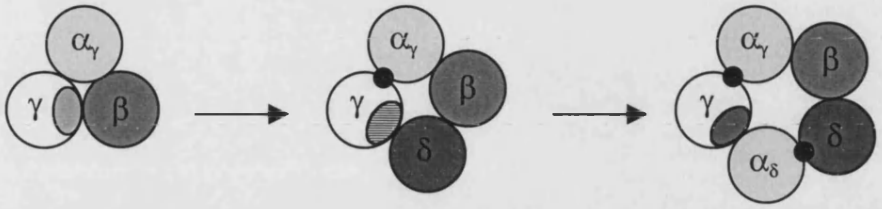

FIGURE 7.10. Subunit oligomerisation of the muscle-type nAChR. Folding events following subunit oligomerisation result in a change in subunit specificity at the site at which the α_δ and γ subunits associate in the final pentamer, such that the interface of the γ subunit mediates subunit oligomerisation and nAChR assembly. Adapted from Green and Wanamaker, 1998.

7.4 Future directions

Sucrose gradient centrifugation and immunoprecipitation techniques may reveal which subunit combinations associate as pentameric complexes or protein aggregates. The nAChR/$5HT_{3A}$ subunit chimeras may prove useful in these studies, as the interactions between chimeras and other subunits appear more stable than the associations between wild-type subunits. This would be particularly relevant to the studies with the α5χ chimera, where assessing the possible associations between different subunits may help to elucidate the nature of the intermediate complexes proposed to form along the nAChR assembly pathway.

It would be interesting to perform a similar set of binding assays to those described with the α5 and α5χ subunits, using the β3 and β3χ subunits to assess whether the dominant negative effect exerted by α5χ on subunit combinations such as α4β4, with respect to the formation of viable ligand binding interfaces, is unique to this particular subunit.

Further pharmacological characterisation of selected subunit combinations could be performed in order to compare the pharmacological profiles of these receptors to native nAChRs. For example, the profiles for α2β2α5 and α2β2α5χ could be compared to that of the α2β2α5 nAChR immunodepleted from chick optic lobe (Balestra *et al.*, 2000).

As mentioned in Section 6.9, the functional capabilities of nAChRs containing chimeric subunits and the sub-cellular distribution of the assembled nAChRs remain to be determined.

DISCUSSION

CHAPTER 8

DISCUSSION

8.1 Molecular and cell biological characterisation of nAChRs

Nicotinic receptors are involved in a variety of functional processes including synaptic transmission and modulation of neurotransmitter release. In addition, nAChRs have been implicated in several neurological disorders and in the mediation of nicotine addiction (Section 1.6). The muscle-type nAChR has been widely studied and characterisation of this receptor has provided a model for the study of other members of the ligand-gated ion channel superfamily (Devillers-Thiéry *et al.*, 1993). Thus, a detailed knowledge of neuronal nAChRs is not only important in understanding the functional roles of nAChRs and their potential as therapeutic targets, but to gaining insight into the function of other ion channel receptors in the nervous system.

In this study, aspects of nAChR structure, assembly and expression were analysed through heterologous expression of cloned nAChR subunits in mammalian cell lines. Heterologous expression systems allow the assembly of recombinant nAChRs from defined subunit combinations to be investigated and compared with native nAChRs. Expression of nAChRs outside the native cellular environment has demonstrated the influence of the host-cell environment on nAChR assembly (Millar, 1999; Sivilotti *et al.*, 2000) and provides a platform to identify specific cellular factors involved in nAChR folding, assembly and cell surface expression. However, achieving efficient expression of neuronal nAChRs in mammalian cell lines has proved difficult and this study was intended to investigate molecular and cell biological techniques to overcome some of the challenges of heterologous expression of recombinant nAChRs. Specifically, manipulation of nAChR subunit DNA was used to analyse aspects of nAChR assembly, pharmacology and sub-cellular distribution.

8.2 Construction of chimeric subunits enhances the expression of a variety of nAChR subtypes

Previous studies have revealed that the relatively inefficient folding and cell-surface expression of several nAChRs can be enhanced by replacing the C-terminal region of some nAChR subunits with the corresponding region of the $5HT_{3A}$ receptor subunit (Eiselé *et al.*, 1993; Blumenthal *et al.*, 1997; Rangwala *et al.*, 1997; Cooper and Millar, 1998; Cooper *et al.*, 1999; Harkness and Millar, 2002). In this study, subunit chimeras analogous to the previously described $\alpha7^{V201}/5HT_{3A}$ chimera (Eiselé *et al.*, 1993; Cooper and Millar, 1997), were constructed and comprised a series of chimeras containing the N-terminal domain of each of the known rat neuronal nAChR subunits (Table 3.1).

Each subunit chimera was expressed in mammalian cells, either alone or in combination with wild-type or other chimeric subunits in order to obtain a profile of nAChR expression in mammalian cells. This extensive study was by no means exhaustive, but has provided an insight into the assembly and expression of several nAChR subtypes and generated evidence to support current models of the structure-function relationship of nAChR subunit domains. The use of subunit chimeras has also provided a model system for the characterisation of nAChR subtypes that are not otherwise expressed efficiently in mammalian cells.

The construction of subunit chimeras has been used previously to enhance the expression of α7, α8 and α4β2 nAChRs (Eiselé *et al.*, 1993; Blumenthal *et al.*, 1997; Rangwala *et al.*, 1997; Cooper and Millar, 1998; Cooper *et al.*, 1999; Harkness and Millar, 2002). In this study, replacement of each of the rat α2, α3, α4, α6, α7, α9, α10, β2 and β4 nAChR subunits with the corresponding chimera, increased the detectable levels of nAChRs expressed in tsA201 cells, demonstrated by radioligand binding (Chapters 4 and 6). In addition, the levels of [^{3}H]-epibatidine binding to the α2β2 and α4β2 nAChR subtypes were increased slightly upon co-expression with a chimeric α5χ subunit,

suggesting that appropriate folding of an α5-type subunit can influence the efficient expression of heteromeric nAChRs in tsA201 cells (Chapter 7). Whether subunit chimeras also enhance the folding of the β3 subunit was not apparent from the radioligand binding studies, as the β3 subunit does not form ligand binding interfaces when expressed in pairwise combinations with other nAChR subunits in heterologous expression systems (Chapter 6, Sargent, 1993), but it seems likely, given that the C-terminal region of each of the other known nAChR subunits can be implicated in the inefficient folding of nAChRs in mammalian cell lines.

Each of the α2β2, α2β4, α3β2, α3β4, α4β2 and α4β4 nAChR subtypes demonstrate low levels of [^{3}H]-epibatidine binding when expressed transiently in tsA201 cells (Chapter 6). Increases as great as 350-times basal levels of binding were achieved upon replacement of a wild-type subunit with its corresponding chimera (α3χβ2). Replacement of either the α or the β type subunit with the corresponding chimeric subunit influenced the levels of radioligand binding, suggesting that inefficient folding of each nAChR subunit restricts nAChR assembly. Perhaps the most striking effects exerted by the chimeras are observed with nAChRs containing the α6 or α9 and α10 subunits. As observed with the homomeric α7 nAChR (Cooper and Millar, 1997), wild-type rat α6-containing nAChRs and α9α10 nAChRs fail to assemble into complexes able to bind radioligand when expressed heterologously in tsA201 cells (Sections 6.6 and 4.2). Therefore, construction of nAChR/5HT$_{3A}$R subunit chimeras has permitted expression of rat α9α10-type and α6-containing nAChRs in a mammalian cell line. With the α9χα10χ complex, this allowed a detailed characterisation of the ligand binding properties of an α9-type nAChR in tsA201 cells that not only provided evidence to support the unique pharmacological profile of native α9-containing nAChRs (Housley and Ashmore, 1991; Fuchs and Murrow, 1992; Verbitsky *et al.*, 2000), but also demonstrated the use of chimeras as a viable model for the characterisation of wild-type nAChRs (Baker *et al.*, 2004).

The comparable pharmacological profiles of wild-type and chimeric α9-containing nAChRs suggests that the ligand binding domain is largely unaffected by the construction of subunit chimeras, consistent with the structural model that attributes ligand binding to the large extracellular N-terminal of the nAChR (see Figure 1.1). The chimeric nAChRs also appear to be expressed at the cell surface in high levels (Section 5.2, Cooper and Millar, 1998; Cooper *et al.*, 1999; Harkness and Millar, 2002; Baker *et al.*, 2004) and are able to form functional channels (Section 4.4, Eiselé *et al.*, 1993; Rakhilin *et al.*, 1999), suggesting that the modification to the C-terminal region of the nAChR subunits does not disrupt the ability of the subunits to form viable pentameric complexes. However, while the chimeras may retain functional capabilities and the ligand binding properties may not be altered, the ion channel properties and the coupling of agonist binding at the N-terminal region to the opening of the ion channel in the C-terminal domain (Unwin *et al.*, 2002; Miyazawa *et al.*, 2003) may be expected to differ between wild-type and chimeric nAChRs.

8.3 The α subunit exerts a dominant-negative effect on nAChR expression in tsA201 cells

Replacement of either α or β nAChR subunits with their corresponding subunit chimeras within heteromeric nAChR complexes enhances the levels of radioligand binding. In the case of the α2-, α3-, α4- and α6-containing nAChRs, the α subunit appears to exert the dominant effect on restricting the efficient expression of nAChRs in tsA201 cells (Chapter 6). With nAChR subtypes such as α2β2 and α3β4, replacement of the α subunit with an α chimera results in a greater increase in radioligand binding levels than replacement of the β subunit with a β chimera. This effect is most prominent with the α6 subunit, which fails to form detectable ligand binding complexes when co-expressed with wild-type or chimeric β subunits in tsA201 cells. In contrast, high levels of binding are observed upon co-expression of the α6χ chimera with β2 or β4 subunits.

The efficient folding of both the α9 and α10 subunits appears necessary for the formation of heteromeric complexes (Chapter 4), suggesting that each α subunit exhibits a strong influence with respect to nAChR expression in mammalian cells. While α9χ homomers and α9χα10χ heteromers appear to assemble in transfected tsA201 cells, the levels of nicotinic radioligand binding observed in cells co-transfected with chimeric α9χ and wild-type α10 (or α9+α10χ) do not differ from the levels of binding observed with the α9χ (or α10χ) homomer. This is in contrast to other heteromeric nAChRs, such as the α4β2 nAChR, where each of the α4χβ2, α4β2χ and α4χβ2χ subtypes form complexes that demonstrate higher levels of radioligand binding than the wild-type α4β2 nAChR when expressed in tsA201 cells, with the α4 subunit exerting the dominant effect on receptor assembly (this study, Cooper *et al.*, 1999; Harkness and Millar, 2002). The C-terminal region of both the wild-type α9 and α10 subunits appears to critically restrict the efficient formation of a high affinity radioligand binding site in transfected tsA201 cells, suggesting that the appropriate folding of each of the α-type subunits is essential for assembly of heteromeric α9α10 nAChRs.

Previous studies have demonstrated the dominant nature of the α4 subunit, with respect to the efficient expression of nAChRs capable of binding radioligand at the surface of tsA201 cells (Cooper *et al.*, 1999; Harkness and Millar, 2001; Harkness and Millar, 2002). The present study suggests that the dominant-negative feature of the α4 subunit in nAChR assembly can be extended to each of the other neuronal nAChR α subunits that participate in formation of the ligand binding site. The α5 subunit is not included, as this unique α-classified subunit does not appear to form ligand binding interfaces with other subunits in pairwise combinations (Chapters 6 and 7, Boulter *et al.*, 1990; Couturier *et al.*, 1990b; Sargent, 1993; Ramirez-Latorre *et al.*, 1996; Wang *et al.*, 1996; Conroy and Berg, 1998; Gerzanich *et al.*, 1998).

Each of the α2χ, α3χ, α4χ, α9χ and α10χ chimeras appear able to form homomeric complexes, demonstrated by the low levels of radioligand binding observed in tsA201 cells transiently transfected with each subunit chimera alone (Section 4.4 and Chapter 6). The α5χ, β2χ, β3χ and β4χ chimeras do not form homomeric complexes able to bind radioligand, but the β2χ chimera has been shown previously to assemble into pentameric homomers that are expressed at the surface of tsA201 cells in high levels (Cooper *et al.*, 1999; Harkness and Millar, 2002). The low levels of binding observed with the α2χ, α3χ, α4χ, α9χ and α10χ homomers are greatly enhanced when these subunits participate in the formation of heteromeric nAChRs, supporting the suggestion that while the binding interface of the α subunit provides components that are sufficient for radioligand binding, the complementary components of the adjacent β subunit (or α10χ subunit in the case of α9χα10χ) are also required for the formation of a high affinity nicotinic ligand binding site (Kao and Karlin, 1986; Galzi *et al.*, 1990; Czajkowski *et al.*, 1993; Fu and Sine, 1994; Corringer *et al.*, 1995; Martin *et al.*, 1996; Prince and Sine, 1996; Brejc *et al.*, 2001).

The nature of the particular α subunit is also able to influence the efficiency of nAChR expression, where nAChRs containing the α4 subunit demonstrate higher basal levels of [^{3}H]-epibatidine binding in tsA201 cells than α2-containing nAChRs do, irrespective of the nature of the β subunit. In addition, the enhancing effect of introducing subunit chimeras is greater for the α2-containing nAChRs than those containing α4. Therefore, the α4 subunit appears to fold or assemble with the β subunit more efficiently than the α2 subunit is able to.

8.4 nAChRs containing the β4 subunit assemble more efficiently than β2-containing nAChRs

The studies with chimeric subunits suggest that the α subunits fold less efficiently than the β2 or β4 subunits (Section 8.3). In addition, the radioligand binding experiments performed in this study with combinations of wild-type and chimeric subunits, suggest that the β2 subunit folds and assembles with α subunits less efficiently than the β4 subunit does. The levels of [^{3}H]-epibatidine binding are consistently higher in cells expressing pairwise combinations of nAChRs containing the β4 subunit than those containing β2 (Chapter 6), despite the fact that β2-containing nAChRs demonstrate higher affinities for [^{3}H]-epibatidine than nAChRs containing β4 (Parker *et al.*, 1998). Also, greater increases in the levels of radioligand binding are detected upon replacement of the β2 subunit with β2χ, than upon replacement of β4 with β4χ, when co-expressed with any of the α2, α3 or α4 subunits.

The physiological significance of this observation is not clear, especially as β2 is the most widely expressed subunit in the nervous system, with fairly homogeneous distribution in human brain (Paterson and Nordberg, 2000). The differences in subunit folding efficiency may reflect the nature of the host cell environment, where the assembly of β2-containing nAChRs may employ subtype-specific chaperone proteins. There is evidence demonstrating the subtype-specific action of intracellular proteins that influence nAChR expression. For example, the Ric-3 protein is suggested to be involved in nAChR folding and assembly in the endoplasmic reticulum and while Ric-3 enhances the ACh-evoked whole cell currents in *Xenopus* oocytes expressing recombinant α7 nAChRs, co-expression of human Ric-3 with recombinant α4β2 or α3β4 appears to inhibit nAChR activity (Halevi *et al.*, 2002; Halevi *et al.*, 2003).

The studies in which α5χ was co-expressed with different nAChR subtypes (Chapter 7), revealed differences in the interaction of α5χ with the β2 and β4 subunits. While the levels of radioligand binding observed with α2β2 and α4β2 nAChRs increased upon addition of α5χ (to 540±100% and 260±40% of binding in the absence of α5χ, respectively), binding to the α2β4 and α4β4 nAChR subtypes was completely abolished upon co-expression with α5χ. While the precise nature of the subunit interactions that occur upon expression of these subunit combinations has not been established, this may suggest that the α5 subunit assembles more efficiently with β2 than with β4 to form viable nAChRs that contain α5 within the pentameric structure. Subtypes of nAChR that contain both the β2 and β4 subunits have been demonstrated in the nervous system, such as α3α5β2β4 nAChRs in embryonic chick ciliary neurones (Conroy and Berg, 1995) and a α4β2β3β4 subtype in rat cerebellum (Forsayeth and Kobrin, 1997). These subtypes, containing four different nAChR subunits, are reminiscent of the muscle-type nAChR. The more efficient folding of β4 may indicate that the β4 subunit mediates the assembly of pentameric nAChRs in these subtypes, assuming the role of the muscle-type γ subunit, while β2 assumes the role of the δ subunit and complexes with α4-β3-β4 trimers during nAChR assembly, for example (see Figure 7.10).

8.5 The subunit N-terminal domains influence nAChR assembly

Comparing the ligand binding profiles of different nAChR subtypes demonstrates the importance of the N-terminal domain of nicotinic subunits in subunit oligomerisation. This is apparent when comparing the profiles of nAChRs in which each of the subunits contains the C-terminal region of $5HT_{3A}$. In complexes such as α3χβ2χ, α3χβ4χ and α3χβ4χα5χ, the C-terminal domain of every subunit within the complex (which may be a mixed population with α3χβ4χα5χ) is identical. Therefore, any differences in the ligand binding profiles of these subunits implicate the N-terminal domains in nAChR expression. The β2χ-containing subtypes demonstrate consistently higher levels of binding than nAChRs containing β4χ, irrespective of the nature of the α-type chimera

(Chapter 6). In addition, as mentioned in Section 8.3, subunits such as $\alpha 2\chi$ are able to form homomeric ligand-binding complexes, but high affinity ligand binding sites are only detected upon co-expression of the homomers with a β-type subunit, providing evidence of a requirement for heteromeric co-assembly of subunit N-terminal domains for the efficient formation of a nicotinic binding site.

It has been suggested that the N-terminal domains of nAChR subunits mediate the initial interactions that occur between subunits during translational events, where the N-terminal domains of partially-translated subunits are able to interact with the N-terminal domains of other completed subunits (Green and Millar, 1995; Keller and Taylor, 1999). In addition, previous studies have identified specific residues in the N-terminal domain that direct the order of subunit assembly and the arrangement of the subunits in the pentameric nAChR structure (Gu *et al.*, 1991; Sumikawa, 1992; Sugiyama *et al.*, 1996; Keller and Taylor, 1999).

8.6 The subunit C-terminal domains influence nAChR assembly

A common feature of the studies with chimeric subunits is that inefficient folding and cell-surface expression of nAChRs can be attributed to sequences present within the C-terminal (transmembrane and intracellular) subunit domains (this study, Eiselé *et al.*, 1993; Blumenthal *et al.*, 1997; Rangwala *et al.*, 1997; Cooper and Millar, 1998; Cooper *et al.*, 1999; Harkness and Millar, 2002; Baker *et al.*, 2004). The high expression levels of nAChR/$5HT_{3A}$R subunit chimeras and the homomeric $5HT_{3A}$ receptor in mammalian cell lines suggest that the assembly of $5HT_{3A}$ receptors is more efficient than that of the nAChRs. The nAChR and $5HT_{3A}$ receptor subunits may interact with different intracellular proteins, where the over-expression of nAChR subunits in mammalian cells may require co-expression with specific cellular factors to chaperone subunit folding and oligomerisation.

While the N-terminal domains of nAChR subunits appear to mediate the initial interactions between subunits, the nature of the C-terminal domain (or the subunit structure as a whole) may govern which subunit associations are productive and proceed along the assembly pathway (Eertmoed and Green, 1999). This has been demonstrated in previous studies employing chimeras (Eertmoed and Green, 1999) and in this study using α5χ, where α5χ prevents the formation of ligand binding sites upon expression with the α2β4 and α4β4 nAChRs. As the α5χ chimera can disrupt ligand binding interfaces of α2β4 nAChRs, while radioligand binding is unaffected by addition of the wild-type α5 subunit, this suggests that the introduction of the C-terminal region of the $5HT_{3A}$ subunit to α5 permits stable subunit interactions that would not otherwise occur with wild-type subunits. This demonstrates the importance of the C-terminal domain of nicotinic subunits in subunit oligomerisation events.

8.7 Summary and Conclusions

The aim of this project was to overcome some of the challenges of heterologous expression of recombinant nAChRs in order to gain a better understanding of the structural and functional properties of neurotransmitter-gated ion channels. Through manipulation of nAChR subunit DNA in the construction of subunit chimeras, the expression of nAChRs containing each of the rat α2, α3, α4, α6, α9, α10, β2 and β4 subunits was enhanced, as demonstrated by radioligand binding studies performed on transfected tsA201 cells. These results attribute the inefficient folding of nicotinic subunits into conformations that are recognised by nicotinic radioligands, to the subunit C-terminal domain. These observations are particularly significant for the α9, α10 and α6 subunits, as the construction of nAChR/$5HT_{3A}$ subunit chimeras has allowed the successful expression of rat α9/α10- and α6-containing nAChRs in a mammalian cell line that is not observed with wild-type subunits. The detailed pharmacological characterisation of α9χα10χ receptors suggest that the chimeric receptors retain the ligand binding properties of the wild-type nAChRs, are expressed at the cell surface in

high levels and can form functional ion channels and can, therefore, provide viable models for the study of wild-type nAChRs.

Comparison of the ligand binding profiles of nAChRs with different subunit compositions revealed the influence of both the α and β subunit on the efficient formation of nAChRs with ligand binding capabilities, demonstrating the requirement of appropriate interactions between subunit N-terminal domains in the formation of high affinity ligand binding interfaces. These conclusions correlate well with previous models of nAChR assembly and suggest that the entire structure of the nicotinic subunit is involved in the ability of these proteins to fold, assemble and access the cell surface in the specific internal environment of the mammalian host cells.

Elucidation of the mechanisms by which nAChRs assemble appropriately is critical to understanding the functional roles of these complex oligomeric proteins *in vivo*. The large number of different nicotinic subunits means that the potential for nAChR subtypes, each with different subunit composition and stoichiometry is immense. Defining pathways of subunit oligomerisation and characterisation of the various nAChR subtypes in heterologous systems can aid the definition of native nAChRs, of which their apparent roles in neurological disorders and nicotine addiction has made nAChRs attractive as potential therapeutic targets.

REFERENCES

REFERENCES

Albuquerque EX, Deshpande SS, Aracava Y, Alkondon M and Daly JW. (1986). A possible involvement of cyclic AMP in the expression of desensitization of the nicotinic acetylcholine receptor. A study with forskolin and its analogs. *FEBS Letts.* **199**, 113-120.

Alkondon M, Braga MFM, Pereira EFR, Maelicke A and Albuquerque EX. (2000). α7 Nicotinic acetylcholine receptors and modulation of gabaergic synaptic transmission in the hippocampus. *Eur. J. Pharmacol.* **393**, 59-67.

Anand R, Conroy WG, Schoepfer R, Whiting P and Lindstrom J. (1991). Neuronal nicotinic acetylcholine receptors expressed in *Xenopus* oocytes have a pentameric quaternary structure. *J. Biol. Chem.* **266**, 11192-11198.

Anand R, Peng X, Ballesta JJ and Lindstrom J. (1993a). Pharmacological characterization of α-bungarotoxin-sensitive acetylcholine receptors immunoisolated from chick retina: contrasting properties of α7 and α8 subunit-containing subtypes. *Mol. Pharmacol.* **44**, 1046-1050.

Anand R, Peng X and Lindstrom J. (1993b). Homomeric and native α7 acetylcholine receptors exhibit remarkably similar but non-identical pharmacological properties, suggesting that the native receptor is a heteromeric protein complex. *FEBS Letts.* **327**, 241-246.

Baker ER, Zwart R, Sher E and Millar NS. (2004). Pharmacological properties of α9α10 nicotinic acetylcholine receptors revealed by heterologous expression of subunit chimeras. *Mol. Pharmacol.*, In press.

Balestra B, Vailati S, Moretti M, Hanke W, Clementi F and Gotti C. (2000). Chick optic lobe contains a developmentally regulated α2α5β2 nicotinic receptor subtype. *Mol. Pharmacol.* **58**, 300-311.

Ballivet M, Nef P, Couturier S, Rungger D, Bader CR, Bertrand D and Cooper E. (1988). Electrophysiology of a chick neuronal nicotinic acetylcholine receptor expressed in *Xenopus* oocytes after cDNA injection. *Neuron.* **1**, 847-852.

Barnard EA, Miledi R and Sumikawa K. (1982). Translation of exogenous messenger RNA coding for nicotinic acetylcholine receptors produces functional receptors in *Xenopus* oocytes. *Proc. R. Soc. Lond. B.* **215**, 241-246.

Benwell MEM, Balfour DJK and Anderson JM. (1988). Evidence that tobacco smoking increases the density of (-)-[^{3}H]nicotine binding sites in human brain. *J. Neurochem.* **50**, 1243-1247.

Bertrand D, Bertrand S and Ballivet M. (1992a). Pharmacological properties of the homomeric alpha 7 receptor. *Neurosci. Lett.* **146**, 87-90.

Bertrand D, Devillers-Thiéry A, Revah F, Galzi J-L, Hussy N, Mulle C, Bertrand S, Ballivet M and Changeux J-P. (1992b). Unconventional pharmacology of a neuronal nicotinic receptor mutated in the channel domain. *Proc. Natl. Acad. Sci. USA.* **89**, 1261-1265.

Bertrand D, Galzi JL, Devillers-Thiéry A, Bertrand S and Changeux JP. (1993). Mutations at two distinct sites within the channel domain M2 alter calcium permeability of neuronal alpha 7 nicotinic receptor. *Proc. Natl. Acad. Sci. USA.* **90**, 6971-6975.

Blount P and Merlie JP. (1988). Native folding of an acetylcholine receptor alpha subunit expressed in the absence of other receptor subunits. *J. Biol. Chem.* **263**, 1072-1080.

Blount P and Merlie JP. (1989). Molecular basis of the two nonequivalent ligand binding sites of the muscle nicotinic acetylcholine receptor. *Neuron.* **3**, 349-357.

Blumenthal EM, Conroy WG, Romano SJ, Kassner PD and Berg DK. (1997). Detection of functional nicotinic receptors blocked by α-bungarotoxin on PC12 cells and dependence of their expression on post-translational events. *J. Neurosci.* **17**, 6094-6104.

Boorman JPB, Groot-Kormelink PJ and Sivilotti LG. (2000). Stoichiometry of human recombinant neuronal nicotinic receptors containing the β3 subunit expressed in *Xenopus* oocytes. *J. Physiol.* **529**, 565-577.

Boulter J, Connolly J, Deneris E, Goldman D, Heinemann S and Patrick J. (1987). Functional expression of two neuronal nicotinic acetylcholine receptors from cDNA clones identifies a gene family. *Proc. Natl. Acad. Sci. USA.* **84**, 7763-7767.

Boulter J, Evans K, Goldman D, Martin G, Treco D, Heinemann S and Patrick J. (1986). Isolation of a cDNA clone coding for a possible neural nicotinic acetylcholine receptor α-subunit. *Nature.* **319**, 368-374.

Boulter J, O'Shea-Greenfield A, Duvoisin RM, Connolly JG, Wada E, Jensen A, Gardner PD, Ballivet M, Deneris ES, McKinnon D, Heinemann S and Patrick J. (1990). α3, α5, and β4: three members of the rat neuronal nicotinic acetylcholine receptor-related gene family form a gene cluster. *J. Biol. Chem.* **265**, 4472-4482.

Brejc K, van Dijk WJ, Klaassen RV, Schuurmans M, van der Oost J, Smit AB and Sixma TK. (2001). Crystal structure of an ACh-binding protein reveals the ligand-binding domain of nicotinic receptors. *Nature.* **411**, 269-276.

Brisson A and Unwin PNT. (1985). Quaternary structure of the acetylcholine receptor. *Nature.* **315**, 474-477.

Britto LR, Hamassaki-Britto DE, Ferro ES, Keyser KT, Karten HJ and Lindstrom JM. (1992). Neurons of the chick brain and retina expressing both alpha-bungarotoxin-sensitive and

alpha-bungarotoxin-insensitive nicotinic acetylcholine receptors: an immunohistochemical analysis. *Brain Res.* **590**, 193-200.

Buisson B, Gopalakrishnan M, Arneric SP, Sullivan JP and Bertrand D. (1996). Human α4β2 neuronal nicotinic acetylcholine receptor in HEK 293 cells: a patch-clamp study. *J. Neurosci.* **16**, 7880-7891.

Carbonetto ST, Fambrough DM and Muller KJ. (1978). Nonequivalence of α-bungarotoxin receptors and acetylcholine receptors in chick sympathetic neurons. *Proc. Natl. Acad. Sci. USA.* **75**, 1016-1020.

Cartier GE, Yoshikami D, Gray WR, Luo S, Olivera BM and McIntosh JM. (1996). A new α-conotoxin which targets α3β2 nicotinic acetylcholine receptors. *J. Biol. Chem.* **271**, 7522-7528.

Changeux J-P, Bertrand D, Corringer P-J, Dehaene S, Edelstein S, Lena C, Le Novére N, Marubio L, Picciotto M and Zoli M. (1998). Brain nicotinic receptors: structure and regulation, role in learning and reinforcement. *Brain Res. Rev.* **26**, 198-216.

Changeux J-P, Kasai M and Lee C-Y. (1970). Use of a snake venom toxin to characterise the cholinergic receptor protein. *Proc. Natl. Acad. Sci.* **67**, 1241-1247.

Chen D and Patrick JW. (1997). The α-bungarotoxin-binding nicotinic acetylcholine receptor from rat brain contains only the α7 subunit. *J. Biol. Chem.* **272**, 24024-24029.

Chiara DC, Middleton RE and Cohen JB. (1998). Identification of tryptophan 55 as the primary site of [^{3}H]nicotine photoincorporation in the γ-subunit of the *Torpedo* nicotinic acetylcholine receptor. *FEBS Letts.* **423**, 223-226.

Chio CL, Alberts GL, Bin Im W, Slightom JL and Gill GS. (2002). Discovery of a protein sequence in the N-terminal region of the human neuronal nicotinic acetylcholine receptor involved in homomeric interactions. *Neurosci. Lett.* **334**, 49-52.

Clarke PBS, Schwartz RD, Paul SM, Pert CB and Pert A. (1985). Nicotinic binding in rat brain: autoradiographic comparison of [^{3}H]acetylcholine, [^{3}H]nicotine, and [^{125}I]-α-bungarotoxin. *J. Neurosci.* **5**, 1307-1315.

Claudio T, Ballivet M, Patrick J and Heinemann S. (1983). Nucleotide and deduced amino acid sequences of *Torpedo californica* acetylcholine receptor γ subunit. *Proc. Natl. Acad. Sci. USA.* **80**, 1111-1115.

Clementi F, Fornasari D and Gotti C. (2000). Neuronal nicotinic receptors: important new players in brain function. *Eur. J. Pharmacol.* **393**, 3-10.

Conroy WG and Berg DK. (1995). Neurons can maintain multiple classes of nicotinic acetylcholine receptors distinguished by different subunit compositions. *J. Biol. Chem.* **270**, 4424-4431.

Conroy WG and Berg DK. (1998). Nicotinic receptor subtypes in the developing chick brain: appearance of a species containing the α4, β2 and α5 gene products. *Mol. Pharmacol.* **53**, 392-401.

Conroy WG, Vernallis AB and Berg DK. (1992). The α5 gene product assembles with multiple acetylcholine receptor subunits to form distinctive receptor subtypes in brain. *Neuron.* **9**, 679-691.

Cooper E, Couturier S and Ballivet M. (1991). Pentameric structure and subunit stoichiometry of a neuronal nicotinic acetylcholine receptor. *Nature.* **350**, 235-238.

Cooper ST, Harkness PC, Baker ER and Millar NS. (1999). Upregulation of cell-surface α4β2 neuronal nicotinic receptors by lower temperature and expression of chimeric subunits. *J. Biol. Chem.* **274**, 27145-27152.

Cooper ST and Millar NS. (1997). Host cell-specific folding and assembly of the neuronal nicotinic acetylcholine receptor α7 subunit. *J. Neurochem.* **68**, 2140-2151.

Cooper ST and Millar NS. (1998). Host cell-specific folding of the neuronal nicotinic receptor α8 subunit. *J. Neurochem.* **70**, 2585-2593.

Cordero-Erausquin M, Marubio LM, Klink R and Changeux J-P. (2000). Nicotinic receptor function: new perspectives from knockout mice. *Trends Pharmacol. Sci.* **21**, 211-217.

Corringer P-J, Bertrand S, Galzi J-L, Devillers-Thiéry A, Changeux J-P and Bertrand D. (1999). Mutational analysis of the charge selectivity filter of the α7 nicotinic acetylcholine receptor. *Neuron.* **22**, 831-843.

Corringer P-J, Galzi J-L, Eiselé J-L, Bertrand S, Changeux J-P and Bertrand D. (1995). Identification of a new component of the agonist binding site of the nicotinic α7 homooligomeric receptor. *J. Biol. Chem.* **270**, 11749-11752.

Corringer P-J, Le Novére N and Changeux J-P. (2000). Nicotinic receptors at the amino acid level. *Ann. Rev. Pharmacol. Toxicol.* **40**, 431-438.

Corriveau RA and Berg DK. (1993). Coexpression of multiple acetylcholine receptor genes in neurons: quantification of transcripts during development. *J. Neurosci.* **13**, 2662-2671.

Couturier S, Bertrand D, Matter JM, Hernandez MC, Bertrand S, Millar N, Valera S, Barkas T and Ballivet M. (1990a). A neuronal nicotinic acetylcholine receptor subunit (α7) is developmentally regulated and forms a homo-oligomeric channel blocked by α-BTX. *Neuron.* **5**, 847-856.

Couturier S, Erkman L, Valera S, Rungger D, Bertrand S, Boulter J, Ballivet M and Bertrand D. (1990b). α5, α3, and non-α3. Three clustered avian genes encoding neuronal nicotinic acetylcholine receptor-related subunits. *J. Biol. Chem.* **265**, 17560-17567.

Crabtree GW, Chen J, Ramirez-Latorre JA, Davis TI and Role LW. (2000). α7-containing heteromeric neuronal nicotinic acetylcholine receptors expressed in *Xenopus* oocytes. *Soc. Neurosci. Abstr.* **26**, 1633.

Czajkowski C, Kaufmann C and Karlin A. (1993). Negatively charged amino acid residues in the nicotinic receptor delta subunit that contribute to the binding of acetylcholine. *Proc. Natl. Acad. Sci. USA.* **90**, 6285-6289.

Dani JA. (2001). Overview of nicotinic receptors and their roles in the central nervous system. *Biol. Psychiatry.* **49**, 166-174.

Davies ARL, Hardick DJ, Blagbrough IS, Potter BVL, Wolstenholme AJ and Wonnacott S. (1999). Characterisation of the binding of [^{3}H]methyllycaconitine: a new radioligand for α7-type neuronal nicotinic acetylcholine receptors. *Neuropharmacol.* **38**, 679-690.

Deneris ES, Boulter J, Swanson LW, Patrick J and Heinemann S. (1989). β3: a new member of nicotinic acetylcholine receptor gene family is expressed in brain. *J. Biol. Chem.* **264**, 6268-6272.

Deneris ES, Connolly J, Boulter J, Wada E, Wada K, Swanson LW, Patrick J and Heinemann S. (1988). Primary structure and expression of β2: a novel subunit of neuronal nicotinic acetylcholine receptors. *Neuron.* **1**, 45-54.

Devillers-Thiéry A, Galzi JL, Eiselé J-L, Bertrand S, Bertrand D and Changeux J-P. (1993). Functional architecture of the nicotinic acetylcholine receptor: A prototype of ligand-gated ion channels. *J. Membrane Biol.* **136**, 97-112.

DiPaola M, Czajkowski C and Karlin A. (1989). The sidedness of the COOH terminus of the acetylcholine receptor δ subunit. *J. Biol. Chem.* **264**, 15457-15463.

Dominguez Del Toro E, Juiz JM, Peng X, Lindstrom J and Criado M. (1994). Immunocytochemical localization of the α7 subunit of the nicotinic acetylcholine receptor in the rat central nervous system. *J. Comp. Neurol.* **349**, 325-342.

Dougherty DA and Stauffer DA. (1990). Acetylcholine binding by a synthetic receptor: Implications for biological recognition. *Science.* **250**, 1558-1560.

Drisdel RC and Green WN. (2000). Neuronal α-bungarotoxin receptors are α7 subunit homomers. *J. Neurosci.* **20**, 133-139.

Duvoisin RM, Deneris ES, Patrick J and Heinemann S. (1989). The functional diversity of the neuronal nicotinic acetylcholine receptors is increased by a novel subunit: β4. *Neuron.* **3**, 487-496.

Edelstein SJ, Schaad O, Henry E, Bertrand D and Changeux J-P. (1996). A kinetic mechanism for nicotinic acetylcholine receptors based on multiple allosteric transitions. *Biol. Cybern.* **75**, 361-379.

Eertmoed AL and Green WN. (1999). Nicotinic receptor assembly requires multiple regions throughout the γ subunit. *J. Neurosci.* **19**, 6298-6308.

Eiselé J-L, Bertrand S, Galzi J-L, Devillers-Thiéry A, Changeux J-P and Bertrand D. (1993). Chimaeric nicotinic-serotonergic receptor combines distinct ligand binding and channel specificities. *Nature.* **366**, 479-483.

Elgoyhen AB, Johnson DS, Boulter J, Vetter DE and Heinemann S. (1994). α9: an acetylcholine receptor with novel pharmacological properties expressed in rat cochlear hair cells. *Cell.* **18**, 705-715.

Elgoyhen AB, Vetter DE, Katz E, Rothlin CV, Heinemann SF and Boulter J. (2001). α10: a determinant of nicotinic cholinergic receptor function in mammalian vestibular and cochlear mechanosensory hair cells. *Proc. Natl. Acad. Sci. USA.* **98**, 3501-3506.

Eusebi F, Grassi F, Nervi C, Caporale C, Adamo S, Zani BM and Molinaro M. (1987). Acetylcholine may regulate its own nicotinic receptor-channel through the C-kinase system. *Proc. R. Soc. Lond. B. Biol. Sci.* **230**, 355-365.

Evans NM, Bose S, Benedetti G, Zwart R, Pearson KH, McPhie GI, Craig PJ, Benton JP, Volsen SG, Sher E and Broad LM. (2003). Expression and functional characterisation of a human chimeric nicotinic receptor with α6β4 properties. *Eur. J. Pharmacol.* **466**, 31-39.

Fenster CP, Whitworth TL, Sheffield EB, Quick MW and Lester RAJ. (1999). Upregulation of surface α4β2 nicotinic receptors is initiated by receptor desensitization after chronic exposure to nicotine. *J. Neurosci.* **19**, 4804-4814.

Flores CM, DeCamp RM, Kilo S, Rogers SW and Hargreaves KM. (1996). Neuronal nicotinic receptor expression in sensory neurons of the rat trigeminal ganglion: Demonstration of α3β4, a novel subtype in the mammalian nervous system. *J. Neurosci.* **16**, 7892-7901.

Flores CM, Rogers SW, Pabreza LA, Wolfe BB and Kellar KJ. (1992). A subtype of nicotinic cholinergic receptor in rat brain is composed of α4 and β2 subunits and is up-regulated by chronic nicotine treatment. *Mol. Pharmacol.* **41**, 31-37.

Forsayeth JR and Kobrin E. (1997). Formation of oligomers containing the β3 and β4 subunits of the rat nicotinic receptor. *J. Neurosci.* **17**, 1531-1538.

Froehner SC. (1991). The submembrane machinery for nicotinic acetylcholine receptor clustering. *J. Cell Biol.* **114**, 1-7.

Fu D-X and Sine SM. (1994). Competitive antagonists bridge the α–γ subunit interface of the acetylcholine receptor through quaternary ammonium-aromatic interactions. *J. Biol. Chem.* **269**, 26152-26157.

Fuchs PA and Murrow BW. (1992). A novel cholinergic receptor mediates inhibition of chick cochlear hair cells. *Proc. R. Soc. Lond. B.* **248**, 35-40.

Fucile S, Matter J-M, Erkman L, Ragozzino D, Barabino B, Grassi F, Alemà S, Ballivet M and Eusebi F. (1998). The neuronal α6 subunit forms functional heteromeric acetylcholine receptors in human transfected cells. *Eur. J. Neurosci.* **10**, 172-178.

Galzi J-L, Bertrand D, Devillers-Thiéry A, Revah F, Bertrand S and Changeux J-P. (1991a). Functional significance of aromatic amino acids from three peptide loops of the alpha 7 neuronal nicotinic receptor site investigated by site-directed mutagenesis. *FEBS Letts.* **294**, 198-202.

Galzi J-L and Changeux J-P. (1995). Neuronal nicotinic receptors: Molecular organization and regulations. *Neuropharmacol.* **34**, 563-582.

Galzi J-L, Devillers-Thiéry A, Hussy N, Bertrand S, Changeux J-P and Bertrand D. (1992). Mutations in the channel domain of a neuronal nicotinic receptor convert ion selectivity from cationic to anionic. *Nature.* **359**, 500-505.

Galzi J-L, Revah F, Black D, Goeldner M, Hirth C and Changeux J-P. (1990). Identification of a novel amino acid alpha-tyrosine 93 within the cholinergic ligands-binding sites of the acetylcholine receptor by photoaffinity labeling. Additional evidence for a three-loop model of the cholinergic ligands-binding sites. *J. Biol. Chem.* **265**, 10430-10437.

Galzi J-L, Revah F, Bouet F, Menez A, Goeldner M, Hirth C and Changeux J-P. (1991b). Allosteric transitions of the acetylcholine receptor probed at the amino acid level with a photolabile cholinergic ligand. *Proc. Natl. Acad. Sci. USA.* **88**, 5051-5055.

Gerzanich V, Anand R and Lindstrom J. (1994). Homomers of α8 and α7 subunits of nicotinic receptors exhibit similar channels but contrasting binding site properties. *Mol. Pharmacol.* **45**, 212-220.

Gerzanich V, Kuryatov A, Anand R and Lindstrom J. (1997). "Orphan" α6 nicotinic AChR subunit can form a functional heteromeric acetylcholine receptor. *Mol. Pharmacol.* **51**, 320-327.

Gerzanich V, Wang F, Kuryatov A and Lindstrom J. (1998). α5 subunit alters desensitization, pharmacology, Ca^{++} permeability and Ca^{++} modulation of human neuronal α3 nicotinic receptors. *J. Pharmacol. Exp. Ther.* **286**, 311-320.

Giraudat J, Dennis M, Heidmann T, Chang JY and Changeux J-P. (1986). Structure of the high-affinity binding site for noncompetitive blockers of the acetylcholine receptor: serine-262 of the δ subunit is labeled by [^{3}H]-chlorpromazine. *Proc. Natl. Acad. Sci. USA.* **83**, 2719-2723.

Goldman D, Deneris E, Luyten W, Kochhar A, Patrick J and Heinemann S. (1987). Members of a nicotinic acetylcholine receptor gene family are expressed in different regions of the mammalian central nervous system. *Cell.* **48**, 965-973.

Goldner FM, Dineley KT and Patrick JW. (1997). Immunohistochemical localization of the nicotinic acetylcholine receptor subunit α6 to dopaminergic neurons in the substantia nigra and ventral tegmental area. *NeuroReport.* **8**, 2739-2742.

Gopalakrishnan M, Molinari EJ and Sullivan JP. (1997). Regulation of human α4β2 neuronal nicotinic acetylcholine receptors by cholinergic channel ligands and second messenger pathways. *Mol. Pharmacol.* **52**, 524-534.

Gotti C, Hanke W, Maury K, Moretti M, Ballivet M, Clementi F and Bertrand D. (1994). Pharmacology and biophysical properties of α7 and α7-α8 α-bungarotoxin receptor subtypes immunopurified from the chick optic lobe. *Eur. J. Neurosci.* **6**, 1281-1291.

Gotti C, Moretti M, Maggi R, Longhi R, Hanke W, Klinke N and Clementi F. (1997). α7 and α8 nicotinic receptor subtypes immunoprecipitated from chick retina have different immunological, pharmacological and functional properties. *Eur. J. Neurosci.* **9**, 1201-1211.

Green L, Sytkowski A, Vogel A and Nirenberg M. (1973). α-Bungarotoxin used as a probe for acetylcholine receptors of cultured neurons. *Nature.* **243**, 163-166.

Green WN. (1999). Ion channel assembly: creating structures that function. *J. Gen Physiol.* **113**, 163-169.

Green WN and Claudio T. (1993). Acetylcholine receptor assembly: subunit folding and oligomerization occur sequentially. *Cell.* **74**, 57-69.

Green WN and Millar NS. (1995). Ion-channel assembly. *Trends Neurosci.* **18**, 280-287.

Green WN and Wanamaker CP. (1997). The role of the cystine loop in acetylcholine receptor assembly. *J. Biol. Chem.* **272**, 20945-20953.

Green WN and Wanamaker CP. (1998). Formation of the nicotinic acetylcholine receptor binding site. *J. Neurosci.* **18**, 5555-5564.

Gu Y, Camacho P, Gardner P and Hall ZW. (1991). Identification of two amino acid residues in the epsilon subunit that promote mammalian muscle acetylcholine receptor assembly in COS cells. *Neuron.* **6**, 879-887.

Guth PS and Norris CH. (1996). The hair cell acetylcholine receptors: a synthesis. *Hearing Res.* **98**, 1-8.

Halevi S, McKay J, Palfreyman M, Yassin L, Eshel M, Jorgensen EM and Treinin M. (2002). The *C. elegans ric-3* gene is required for maturation of nicotinic acetylcholine receptors. *EMBO J.* **21**, 1012-1020.

Halevi S, Yassin L, Eshel M, Sala F, Sala S, Criado M and Treinin M. (2003). Conservation within the RIC-3 gene family: effectors of mammalian nicotinic acetylcholine receptor expression. *J. Biol. Chem.* **278**, 3411-3417.

Hamilton SL, McLaughlin M and Karlin A. (1979). Formation of disulphide linked oligomers of acetylcholine receptor in membrane from *Torpedo* electric tissue. *Biochemistry.* **18**, 155-163.

Harkness PC and Millar NS. (2001). Inefficient cell-surface expression of hybrid complexes formed by the co-assembly of neuronal nicotinic acetylcholine receptor and serotonin receptor subunits. *Neuropharmacol.* **41**, 79-87.

Harkness PC and Millar NS. (2002). Changes in conformation and sub-cellular distribution of α4β2 nicotinic acetylcholine receptors revealed by chronic nicotine treatment and expression of subunit chimeras. *J. Neurosci.* **22**, 10172-10181.

Hiel H, Elgoyhen AB, Drescher DG and Morley BJ. (1996). Expression of nicotinic acetylcholine receptor mRNA in the adult rat peripheral vestibular system. *Brain Res.* **738**, 347-352.

Holley MC, Nishida Y and Grix N. (1997). Conditional immortalization of hair cells from the inner ear. *Int. J. Dev. Neurosci.* **15**, 541-552.

Housley GD and Ashmore JF. (1991). Direct measurement of the action of acetylcholine on isolated outer hair cells of the guinea pig cochlea. *Proc. R. Soc. Lond. B.* **244**, 161-167.

Hsu YN, Amin J, Weiss DS and Wecker L. (1996). Sustained nicotine exposure differentially affects α3β2 and α4β2 neuronal nicotinic receptors expressed in *Xenopus* oocytes. *J. Neurochem.* **66**, 667-675.

Hucho F, Layer P, Kiefer HR and Bandini G. (1976). Photoaffinity labeling and quaternary structure of the acetylcholine receptor from *Torpedo californica. Proc. Natl. Acad. Sci. USA.* **73**, 2624-2628.

Hucho F, Oberthur W and Lottspeich F. (1986). The ion channel of the nicotinic acetylcholine receptor is formed by the homologous helices MII of the receptor subunits. *FEBS.* **205**, 137-142.

Huganir RI and Greengard P. (1983). cAMP-dependent protein kinase phosphorylates the nicotinic acetylcholine receptor. *Proc. Natl. Acad. Sci. USA.* **80**, 1130-1134.

Huganir RL and Greengard P. (1990). Regulation of neurotransmitter receptor desensitization by protein phosphorylation. *Neuron.* **5**, 555-567.

Huganir RL, Miles K and Greengard P. (1984). Phosphorylation of the nicotinic acetylcholine receptor by an endogenous tyrosine-specific kinase. *Proc. Natl. Acad. Sci. USA.* **81**, 6968-6972.

Hunt S and Schmidt J. (1978). Some observations on the binding patterns of αbungarotoxin in the central nervous system of the rat. *Brain Res.* **157**, 213-232.

Imoto K, Busch C, Sakmann B, Mishina M, Konno T, Nakai J, Bujo H, Mori Y, Fukuda K and Numa S. (1988). Rings of negatively charged amino acids determine the acetylcholine receptor channel conductance. *Nature.* **335**, 645-648.

Itier V and Bertrand D. (2001). Neuronal nicotinic receptors: from protein structure to function. *FEBS Letts.* **504**, 118-125.

Jagger DJ, Griesinger CB, Rivolta MN, Holley MC and Ashmore JF. (2000). Calcium signalling mediated by the α9 acetylcholine receptor in a cochlear cell line from the Immortomouse. *J. Physiol.* **527**, 49-54.

Jagger DJ, Holley MC and Ashmore JF. (1999). Ionic currents expressed in a cell line derived from the organ of Corti of the Immortomouse. *Eur. J. Physiol.* **438**, 8-14.

Jat PS, Noble MD, Ataliotis P, Tanaka Y, Yannoutsos N, Larsen L and Kioussis D. (1991). Direct derivation of conditionally immortal cell lines from an *H-2K^b*-tsA58 transgenic mouse. *Proc. Natl. Acad. Sci. USA.* **88**, 5096-5100.

Jones MV and Westbrook GI. (1996). The impact of receptor desensitization on fast synaptic transmission. *Trends Neurosci.* **19**, 96-101.

Jones S, Sudweeks S and Yakel JL. (1999). Nicotinic receptors in the brain: correlating physiology with function. *Trends Neurosci.* **22**, 555-561.

Kao PN, Dwork AJ, Kaldany RRJ, Silver M, Wideman J, Stein J and Karlin A. (1984). Identification of the alpha-subunit half cysteine specifically labeled by an affinity reagent for acetylcholine receptor binding site. *J. Biol. Chem.* **259**, 11662-11665.

Kao PN and Karlin A. (1986). Acetylcholine receptor binding site contains a disulfide cross-link between adjacent half-cystinyl residues. *J. Biol. Chem.* **261**, 8085-8088.

Karlin A, Holtzman E, Yodh N, Lobel P, Wall J and Hainfeld J. (1983). The arrangement of the subunits of the acetylcholine receptor of *Torpedo californica*. *J. Biol. Chem.* **258**, 6678-6681.

Kassner PD and Berg DK. (1997). Differences in the fate of neuronal acetylcholine receptor protein expressed in neurons and stably transfected cells. *J. Neurobiol.* **33**, 968-982.

Katz E, Verbitsky M, Rothlin CV, Vetter DE, Heinemann SF and Elgoyhen AB. (2000). High calcium permeability and calcium block of the α9 nicotinic acetylcholine receptor. *Hearing Res.* **141**, 117-128.

Keller ST and Taylor P. (1999). Determinants responsible for assembly of the nicotinic acetylcholine receptor. *J. Gen. Physiol.* **113**, 171-176.

Keyser KT, Britto LR, Schoepfer R, Whiting P, Cooper J, Conroy W, Brozozowska-Prechtl A, Karten HJ and Lindstrom J. (1993). Three subtypes of α-bungarotoxin-sensitive nicotinic acetylcholine receptors are expressed in chick retina. *J. Neurosci.* **13**, 442-454.

Khiroug SS, Harkness PC, Lamb PW, Sudweeks SN, Khiroug L, Millar NS and Yakel JL. (2002). Rat nicotinic receptor α7 and β2 subunits co-assemble to form functional heteromeric nicotinic receptor channels. *J. Physiol.* **540**, 425-434.

Kolodziej PA and Young RA. (1991). Epitope tagging and protein surveillance. *Methods Enzymol.* **194**, 508-519.

Kurosaki T, Fukuda K, Konno T, Mori Y, Tanaka K, Mishina M and Numa S. (1987). Functional properties of nicotinic acetylcholine receptor subunits expressed in various combinations. *FEBS Lett.* **214**, 253-258.

Kuryatov A, Olale F, Cooper J, Choi C and Lindstrom J. (2000). Human α6 AChR subtypes: subunit composition, assembly, and pharmacological responses. *Neuropharmacol.* **39**, 2570-2590.

Lamar E, Miller K and Patrick J. (1990). Amplification of genomic sequences identifies a new gene, α6, in the nicotinic acetylcholine receptor gene family. *Soc. Neurosci. Abstr.* **16**, 681.

LaPolla RJ, Mayne KM and Davidson N. (1984). Isolation and characterisation of a cDNA clone for the complete coding region of the δ subunit of the mouse acetylcholine receptor. *Proc. Natl. Acad. Sci. USA.* **81**, 7970-7974.

Le Novère N, Zoli M, Lena C, Picciotto MR, Merlo-Pich E and Changeux J-P. (1999). Involvement of α6 nicotinic receptor subunit in nicotine-elicited locomotion, demonstrated by *in vivo* antisense oligonucleotide infusion. *NeuroReport.* **10**, 2497-2501.

Lee CY and Chang CC. (1966). Modes of action of purified toxins from elapid venoms on neuromuscular transmission. *Mem. Inst. Butantan. Sao Paulo.* **33**, 555-572.

Lena C and Changeux J-P. (1993). Allosteric modulations of the nicotinic acetylcholine receptor. *Trends Neurosci.* **16**, 181-186.

Lena C and Changeux J-P. (1998). Allosteric nicotinic receptors, human pathologies. *J. Physiol.* **92**, 63-74.

Lev S, Moreno H, Martinexz R, Canoli P, Peles E, Musacchio JM, Plowman GD, Rudy B and Schlessinger J. (1995). Protein tyrosine kinase PYK2 involved in Ca^{2+}-induced regulation of ion channels and MAP kinase functions. *Nature.* **376**, 737-745.

Levin ED and Simon BB. (1998). Nicotinic acetylcholine involvement in cognitive function in animals. *Psychopharmacol.* **138**, 217-230.

Lewis TM, Harkness PC, Sivilotti LG, Colquhoun D and Millar NS. (1997). The ion channel properties of a rat recombinant neuronal nicotinic receptor are dependent on the host cell type. *J. Physiol.* **505**, 299-306.

Luebke AE and Foster PK. (2002). Variation in inter-animal susceptibility to noise damage is associated with α9 acetylcholine receptor subunit expression levels. *J. Neurosci.* **22**, 4241-4247.

Luetje CW, Wada K, Rogers S, Abramson SN, Tsuji K, Heinemann S and Patrick J. (1990). Neurotoxins distinguish between different neuronal nicotinic acetylcholine receptor subunit combinations. *J. Neurochem.* **55**, 632-640.

Lukas RJ, Changeux J-P, Le Novère N, Albuquerque EX, Balfour DJK, Berg DK, Bertrand D, Chiappinelli AA, Clarke PBS, Collins AC, Dani JA, Grady SR, Kellar KJ, Lindstrom JM, Marks MJ, Quik M, Taylor PW and Wonnacott S. (1999). International union of pharmacology. XX. current status of the nomenclature for nicotinic acetylcholine receptors and their subunits. *Pharmacol. Rev.* **51**, 397-401.

Lustig LR, Peng H, Hiel H, Yamamoto T and Fuchs PA. (2001). Molecular cloning and mapping of the human nicotinic acetylcholine receptor α10 (CHRNA10). *Genomics.* **73**, 272-283.

Maison SF, Luebke AE, Liberman MC and Zuo J. (2002). Efferent protection from acoustic injury is mediated via α9 nicotinic acetylcholine receptors on outer hair cells. *J. Neurosci.* **22**, 10838-10846.

Mandelzys A, Pié B, Deneris ES and Cooper E. (1994). The developmental increase in ACh current densities on rat sympathetic neurons correlates with changes in nicotinic ACh receptor α-subunit gene expression and occurs independent of innervation. *J. Neurosci.* **14**, 2357-2364.

Mansvelder HD, Keath JR and McGehee DS. (2002). Synaptic mechanisms underlie nicotine-induced excitability of brain reward areas. *Neuron.* **33**, 905-919.

Mansvelder HD and McGehee DS. (2000). Long-term potentiation of excitatory inputs to brain reward areas by nicotine. *Neuron.* **27**, 349-357.

Maricq AV, Peterson AS, Brake AJ, Myers RM and Julius D. (1991). Primary structure and functional expression of the $5HT_3$ receptor, a serotonin-gated ion channel. *Science.* **254**, 432-437.

Marks MJ, Pauly JR, Gross SD, Deneris ES, Hermans-Borgmeyer I, Heinemann SF and Collins AC. (1992). Nicotine binding and nicotine receptor subunit RNA after chronic nicotine treatment. *J. Neurosci.* **12**, 2765-2784.

Marks MJ, Stitzel JA and Collins AC. (1985). Time course study of the effects of chronic nicotine infusion on drug response and brain function. *J. Pharmacol. Exp. Ther.* **235**, 619-628.

Martin M, Czajkowski C and Karlin A. (1996). The contribution of aspartyl residues in the acetylcholine receptor γ and δ subunits to the binding of agonists and competitive antagonists. *J. Biol. Chem.* **271**, 13497-13503.

Marubio LM, Arroyo-Jimenez M, M. C-E, Lena C, Le Novére N, Kerchove d'Exaerde A, Huchet M, Damaj MI and Changeux J-P. (1999). Reduced antinociception in mice lacking neuronal nicotinic receptor subunits. *Nature.* **398**, 805-810.

Marubio LM and Changeux J-P. (2000). Nicotinic acetylcholine receptor knockout mice as animal models for studying receptor function. *Eur. J. Pharmacol.* **393**, 113-121.

McGehee DS and Role LW. (1995). Physiological diversity of nicotinic acetylcholine receptors expressed by vertebrate neurons. *Annu. Rev. Physiol.* **57**, 521-546.

Miledi R, Molinoff P and Potter LT. (1971). Isolation of the cholinergic receptor protein of the *Torpedo* electric tissue. *Nature.* **229**, 554-557.

Millar NS. (1999). Heterologous expression of mammalian and insect neuronal nicotinic acetylcholine receptors in cultured cell lines. *Biochem. Soc. Trans.* **27**, 944-950.

Millar NS. (2003). Assembly and subunit diversity of nicotinic acetylcholine receptors. *Biochem. Soc. Trans.* **31**, 869-874.

Mishina M, Takai T, Imoto K, Noda M, Takahashi T, Numa S, Methfessel C and Sakman B. (1986). Molecular distinction between fetal and adult forms of muscle acetylcholine receptor. *Nature.* **313**, 364-369.

Mitra M, Wanamaker CP and Green WN. (2001). Rearrangement of nicotinic receptor α subunits during formation of the ligand binding sites. *J. Neurosci.* **21**, 3000-3008.

Miyazawa A, Fujiyoshi Y, Stowell M and Unwin N. (1999). Nicotinic acetylcholine receptor at 4.6 Å resolution: transverse tunnels in the channel wall. *J. Mol. Biol.* **288**, 765-786.

Miyazawa A, Fujiyoshi Y and Unwin N. (2003). Structure and gating mechanism of the acetylcholine receptor pore. *Nature.* **423**, 949-955.

Molinari EJ, Delbono O, Messi ML, Renganathan M, Arneric SP, Sullivan JP and Gopalakrishnan M. (1998). Up-regulation of human α7 nicotinic receptors by chronic treatment with activator and antagonist ligands. *Eur. J. Pharmacol.* **347**, 131-139.

Moransard M, Borges LS, Willmann R, Marangi PA, Brenner HR, Ferns MJ and Fuhrer C. (2003). Agrin regulates rapsyn interaction with surface acetylcholine receptors, and this underlies cytoskeletal anchoring and clustering. *J. Biol. Chem.* **278**, 7350-7359.

Morens DM, Grandinetti A, Reed D, White LR and Ross GW. (1995). Cigarette smoking and protection from Parkinson's disease: false association of etiologic clue? *Neurology.* **45**, 1041-1051.

Mukerji J, Haghighi A and Séguéla P. (1996). Immunological characterization and transmembrane topology of 5-hydroxytryptamine$_3$ receptors by functional epitope tagging. *J. Neurochem.* **66**, 1027-1032.

Nef P, Mauron A, Stalder R, Alliod C and Ballivet M. (1984). Structure, linkage, and sequence of the two genes encoding the δ and γ subunits of the nicotinic acetylcholine receptor. *Proc. Natl. Acad. Sci. USA.* **81**, 7975-7979.

Nef P, Oneyser C, Alliod C, Couturier S and Ballivet M. (1988). Genes expressed in the brain define three distinct neuronal nicotinic acetylcholine receptors. *EMBO J.* **7**, 595-601.

Nelson ME, Kuryatov A, Choi CH, Zhou Y and Lindstrom J. (2003). Alternate stoichiometries of α4β2 nicotinic acetylcholine receptors. *Mol. Pharmacol.* **63**, 332-341.

Neubig RR and Cohen JB. (1979). Equilibrium binding of [^{3}H]tubocurarine and [^{3}H]acetylcholine by *Torpedo* postsynaptic membranes: stoichiometry and ligand interactions. *Biochemistry.* **18**, 5464-5475.

Noda M, Furutani Y, Takahashi H, Toyosata M, Tanabe T, Shimizu S, Kikyotani S, Kayano T, Hirose T, Inayama S, Miyata T and Numa S. (1983a). Cloning and sequence analysis of calf cDNA and human genomic DNA encoding α-subunit precursor of muscle acetylcholine receptor. *Nature.* **305**, 818-823.

Noda M, Takahashi H, Tanabe T, Toyosato M, Furutani Y, Hirose T, Asai M, Inayama S, Miyata T and Numa S. (1982). Primary structure of α-subunit precursor of *Torpedo californica* acetylcholine receptor deduced from cDNA sequence. *Nature.* **299**, 793-797.

Noda M, Takahashi H, Tanabe T, Toyosato M, Kikyotani S, Furutana Y, Hirose T, Takashima H, Inayama S, Miyata T and Numa S. (1983b). Structural homology of *Torpedo californica* acetylcholine receptor subunits. *Nature.* **302**, 528-532.

Noda M, Takahashi H, Tanabe T, Toyosato M, Kikyotani S, Hirose T, Asai M, Takashima H, Inayama S, Miyata T and Numa S. (1983c). Primary structures of β- and δ-subunit precursors of *Torpedo californica* acetylcholine receptor deduced from cDNA sequences. *Nature.* **301**, 251-255.

Nomoto H, Takahashi N, Nagaki Y, Endo S, Arata Y and Hayashi K. (1986). Carbohydrate structures of acetylcholine receptor from *Torpedo californica* and distribution of oligosaccharides among the subunits. *Eur. J. Biochem.* **157**, 133-142.

Olale F, Gerzanich V, Kuryatov A, Wang F and Lindstrom J. (1997). Chronic nicotine exposure differentially affects the function of human α3, α4, and α7 neuronal nicotinic receptor subtypes. *J. Pharmacol. Exp. Ther.* **283**, 675-683.

Orr-Urtreger A, Goldner FM, Saeki M, Lorenzo I, Goldberg L, De Biasi M, Dani JA, Patrick JW and Beaudet AL. (1997). Mice deficient in the α7 neuronal nicotinic acetylcholine receptor lack α-bungarotoxin binding sites and hippocampal fast nicotinic currents. *J. Neurosci.* **17**, 9165-9171.

Palma E, Bertrand S, Binzoni T and Bertrand D. (1996). Neuronal nicotinic α7 receptor expressed in *Xenopus* oocytes presents five putative binding sites for methyllycaconitine. *J. Physiol.* **491**, 151-161.

Palma E, Fucile S, Barabino B, Miledi R and Eusebi F. (1999a). Strychnine activates neuronal α7 nicotinic receptors after mutations in the leucine ring and transmitter binding site domains. *Proc. Natl. Acad. Sci.* **96**, 13421-13426.

Palma E, Maggi L, Barabino B, Eusebi F and Ballivet M. (1999b). Nicotinic acetylcholine receptors assembled from the α7 and β3 subunits. *J. Biol. Chem.* **274**, 18335-18340.

Papke RL, Boulter J, Patrick J and Heinemann S. (1989). Single-channel currents of rat neuronal nicotinic acetylcholine receptors expressed in *Xenopus* oocytes. *Neuron.* **3**, 589-596.

Parker MJ, Beck A and Luetje CW. (1998). Neuronal nicotinic receptor β2 and β4 subunits confer large differences in agonist binding affinity. *Mol. Pharmacol.* **54**, 1132-1139.

Parker MJ, Harvey SC and Luetje CW. (2001). Determinants of agonist binding affinity on neuronal nicotinic receptor β subunits. *J. Pharmacol. Exp. Ther.* **299**, 385-391.

Paterson D and Nordberg A. (2000). Neuronal nicotinic receptors in the human brain. *Prog. Neurobiol.* **61**, 75-111.

Patrick J and Stallcup WB. (1977). Immunological distinction between acetylcholine receptor and the α-bungarotoxin component on sympathetic neurons. *Proc. Natl. Acad. Sci. USA.* **74**, 4689-4692.

Pederson SE and Cohen JB. (1990). *d*-Tubocurarine binding sites are located at α-γ and α-δ subunit interfaces of the nicotinic acetylcholine receptor. *Proc. Natl. Acad. Sci. USA.* **87**, 2785-2789.

Peng X, Gerzanich V, Anand R, Wang F and Lindstrom J. (1997). Chronic nicotine treatment up-regulates α3 and α7 acetylcholine receptor subtypes expressed by the human neuroblastoma cell line SH-SY5Y. *Mol. Pharmacol.* **51**, 776-784.

Peng X, Gerzanich V, Anand R, Whiting PJ and Lindstrom J. (1994). Nicotine-induced increase in neuronal nicotinic receptors results from a decrease in the rate of receptor turnover. *Mol. Pharmacol.* **46**, 523-530.

Perry EK, Morris CM, Court JA, Cheng A, Fairbairn AF, McKeith JG, Irving D, Brown A and Perry RH. (1995). Alteration in nicotinic binding sites in Parkinson's disease, Lewy Body Dementia and Alzheimer's disease: Possible index of early neuropathology. *Neuroscience.* **64**, 385-395.

Picciotto MR and Zoli M. (2002). Nicotinic receptors in aging and dementia. *J. Neurobiol.* **53**, 641-655.

Picciotto MR, Zoli M, Lena C, Bessis A, Lallemand Y, Le Novére N, Vincent P, Merlo Pich E, Brulet P and Changeux J-P. (1995). Abnormal avoidance learning in mice lacking functional high-affinity nicotine receptor in the brain. *Nature.* **374**, 65-67.

Picciotto MR, Zoli M, Rimondini R, Lena C, Marubio LM, Merlo Pich E, Fuxe K and Changeux J-P. (1998). Acetylcholine receptors containing the β2 subunit are involved in the reinforcing properties of nicotine. *Nature.* **391**, 173-177.

Prince RJ and Sine SM. (1996). Molecular dissection of subunit interfaces in the acetylcholine receptor. *J. Biol. Chem.* **271**, 25770-25777.

Puchacz E, Buisson B, Bertrand D and Lukas RL. (1994). Functional expression of nicotinic acetylcholine receptors containing rat α7 subunits in human SH-SY5Y neuroblastoma cells. *FEBS Letts.* **354**, 155-159.

Pugh PC, Corriveay RA, Conroy WG and Berg DK. (1995). Novel subpopulation of neuronal acetylcholine receptors among those binding α-bungarotoxin. *Mol. Pharmacol.* **47**, 717-725.

Quik M, Choremis J, Komourian J, Lukas RJ and Puchacz E. (1996). Similarity between rat brain nicotinic α-bungarotoxin receptors and stably expressed α-bungarotoxin binding sites. *J. Neurochem.* **67**, 145-154.

Quik M and Jeyarasasingam G. (2000). Nicotinic receptors and Parkinson's disease. *Eur. J. Pharmacol.* **393**, 223-230.

Raggenbass M and Bertrand D. (2002). Nicotinic receptors in circuit excitability and epilepsy. *J. Neurobiol.* **53**, 580-589.

Ragozzino D, Fucile S, Giovannelli A, Grassi F, Mileo AM, Ballivet M, Alema S and Eusebi F. (1997). Functional properties of neuronal nicotinic acetylcholine receptor channels expressed in transfected human cells. *Eur. J. Neurosci.* **9**, 480-488.

Rakhilin S, Drisdel RC, Sagher D, McGehee DS, Vallejo Y and Green W, N. (1999). α-bungarotoxin receptors contain α7 subunits in two different disulfide-bonded conformations. *J. Cell Biol.* **146**, 203-217.

Ramirez-Latorre J, Yu CR, Qu F, Perin F, Karlin A and Role L. (1996). Functional contributions of α5 subunit to neuronal acetylcholine receptor channels. *Nature.* **380**, 347-351.

Rangwala F, Drisdel RC, Rakhilin S, Ko E, Atluri P, Harkins AB, Fox AP, Salman SB and Green WN. (1997). Neuronal α-bungarotoxin receptors differ structurally from other nicotinic acetylcholine receptors. *J. Neurosci.* **17**, 8201-8212.

Revah F, Bertrand D, Galzi J-L, Devillers-Thiéry A, Mulle C, Hussy N, Bertrand S, Ballivet M and Changeux J-P. (1991). Mutations in the channel domain alter desensitization of a neuronal nicotinic receptor. *Nature.* **353**, 846-849.

Revah F, Galzi J-L, Giraudat J, Haumont PY, Lederer F and Changeux J-P. (1990). The noncompetitive blocker [^{3}H]chlorpromazine labels three amino acids of the acetylcholine receptor γ subunit: implications for the α-helical organization of regions MII and for the structure of the ion channel. *Proc. Natl. Acad. Sci. USA.* **87**, 4675-4679.

Reynolds JA and Karlin A. (1978). Molecular weight in detergent solution of acetylcholine receptor from *Torpedo californica. Biochemistry.* **17**, 2035-2038.

Rivolta MN, Grix N, Lawlor P, Ashmore JF, Jagger DJ and Holley MC. (1998). Auditory hair cell precursors immortalized from the mammalian inner ear. *Proc. R. Soc. Lond. B.* **265**, 1595-1603.

Rodrigues-Pinguet N, Jia L, Li M, Figl A, Klaassen A, Truong A, Lester H and Cohen BN. (2003). Five ADNFLE mutations reduce the Ca^{2+} dependence of the mammalian α4β2 acetylcholine response. *J. Physiol.* **550**, 11-26.

Role LW and Berg DK. (1996). Nicotinic receptors in the development and modulation of CNS synapses. *Neuron.* **16**, 1077-1085.

Rothlin CV, Katz E, Verbitsky M and Elgoyhen AB. (1999). The α9 nicotinic acetylcholine receptor shares pharmacological properties with type A γ-aminobutyric acid, glycine, and type 3 serotonin receptors. *Mol. Pharmacol.* **55**, 248-254.

Rust G, Burgunder J-M, Lauterburg TE and Cachelin AB. (1994). Expression of neuronal nicotinic acetylcholine receptor subunit genes in the rat autonomic nervous system. *Eur. J. Neurosci.* **6**, 478-485.

Sambrook J, Fritsh EF and Maniatis T. (1989). Molecular Cloning: A Laboratory Manual. *Cold Spring Harbor Laboratory Press*, Plainview, NY.

Sanes JR and Lichtman JW. (2001). Induction, assembly, maturation and maintenance of a postsynaptic apparatus. *Nature Rev. Neurosci.* **2**, 791-805.

Sargent PB. (1993). The diversity of neuronal nicotinic acetylcholine receptors. *Annu. Rev. Neurosci.* **16**, 403-443.

Schoepfer R, Conroy WG, Whiting P, Gore M and Lindstrom J. (1990). Brain α-bungarotoxin binding protein cDNAs and mAbs reveal subtypes of this branch of the ligand-gated ion channel gene superfamily. *Neuron.* **5**, 35-48.

Schoepfer R, Whiting P, Esch F, Blacher R, Shimasaki S and Lindstrom J. (1988). cDNA clones coding for the structural subunit of a chicken brain nicotinic acetylcholine receptor. *Neuron.* **1**, 241-248.

Schwartz RD and Kellar KJ. (1985). In vivo regulation of [^{3}H]acetylcholine recognition sites in brain by nicotinic cholinergic drugs. *J. Neurochem.* **45**, 427-433.

Sealock R. (1982). Visualization at the mouse neuromuscular junction of a submembrane structure in common with *Torpedo* postsynaptic membranes. *J. Neurosci.* **2**, 918-923.

Seamon KB, Padgett W and Daly JW. (1981). Forskolin: Unique deterpine activator of adenylate cyclase in membranes and in intact cells. *Proc. Natl. Acad. Sci. USA.* **78**, 3363-3367.

Séguéla P, Wadiche J, Dineley-Miller K, Dani JA and Patrick JW. (1993). Molecular cloning, functional properties, and distribution of rat brain α7: a nicotinic cation channel highly permeable to calcium. *J. Neurosci.* **13**, 596-604.

Sgard F, Charpantier E, Bertrand S, Walker N, Caput D, Graham D, Bertrand D and Besnard F. (2002). A novel human nicotinic receptor subunit, α10, that confers functionality to the α9-subunit. *Mol. Pharmacol.* **61**, 150-159.

Sine SM. (1993). Molecular dissection of subunit interfaces in the acetylcholine receptor: Identification of residues that determine curare selectivity. *Proc. Natl. Acad. Sci. USA.* **90**, 9436-9440.

Sivilotti LG, Colquhoun D and Millar NS. (2000). Comparison of native and recombinant neuronal nicotinic receptors: problems of measurement and expression. *In Handbook of Exp. Pharmacol.* **144**, Neuronal Nicotinic Receptors. Clementi F, Fornasari D and Gotti C, editors. Springer, Berlin. 379-416.

Smit AB, Syed NI, Schaap D, van Minnen J, J. K, Kits KS, Lodder H, van der Schors RC, van Elk R, Sorgedrager B, Brejc K, Sixma T and Geraerts WPM. (2001). A glial-derived acetylcholine-binding protein that modulates synaptic transmission. *Nature.* **411**, 261-268.

Sridhar TS, Brown MC and Sewell WF. (1997). Unique postsynaptic signalling at the hair cell efferent synapse permits calcium to evoke changes on two time scales. *J. Neurosci.* **17**, 428-437.

Stauderman KA, Mahaffy LS, Akong M, Velicelebi G, Chavez-Noriega L, Crona JH, Johnson EC, Elliot KJ, Gillespie A, Reid RT, Adams P, Harpold MM and Corey-Naeve J. (1998). Characterization of human recombinant neuronal nicotinic acetylcholine receptor subunit combinations α2β4, α3β4 and α4β4 stably expressed in HEK293 cells. *J. Pharmacol. Exp. Ther.* **284**, 777-789.

Stroud RM, McCarthy MP and Shuster M. (1990). Nicotinic acetylcholine receptor superfamily of ligand-gated ion channels. *Biochemistry.* **29**, 11009-11023.

Sugiyama N, Boyd AE and Taylor P. (1996). Anionic residue in the α-subunit of the nicotinic acetylcholine receptor contributing to subunit assembly and ligand binding. *J. Biol. Chem.* **271**, 26575-26581.

Sumikawa K. (1992). Sequences on the N-terminus of ACh receptor subunits regulate their assembly. *Brain Res. Mol. Brain Res.* **13**, 349-353.

Sumikawa K, Houghton M, Emtage JS, Richards BM and Barnard EA. (1981). Active multi-subunit ACh receptor assembly by translation of heterologous mRNA in *Xenopus* oocytes. *Nature.* **292**, 862-864.

Sweileh W, Wenberg K, Xu J, Forsayeth J, Hardy S and Loring RH. (2000). Multistep expression and assembly of neuronal nicotinic receptors is both host-cell- and receptor-subtype-dependent. *Mol. Brain Res.* **75**, 293-302.

Takai T, Noda M, Mishina M, Shimizu S, Furutani Y, Kayano T, Ikeda T, Kubo T, Takahashi H, Takahashi T, Kuno M and Numa S. (1985). Cloning, sequencing and expression of cDNA for a novel subunit of acetylcholine receptor from calf muscle. *Nature.* **315**, 761-764.

Tanabe T, Noda M, Furutani Y, Takai T, Takahashi H, Tanaka K, Hirose T, Inayama S and Numa S. (1984). Primary structure of the β subunit precursor of calf muscle acetylcholine receptor deduced from cDNA sequence. *Eur. J. Biochem.* **144**, 11-17.

Taylor P, Malany S, Molles BE, Osaka H and Tsigelny I. (2000). Subunit interface selective toxins as probes of nicotinic acetylcholine receptor structure. *Eur. J. Physiol.* **440**, R115-R117.

Tierney ML and Unwin N. (2000). Electron microscopic evidence for the assembly of soluble pentameric extracellular domains of the nicotinic acetylcholine receptor. *J. Mol. Biol.* **303**, 185-196.

Toyoshima C and Unwin N. (1990). Three-dimensional structure of the acetylcholine receptor by cryoelectron microscopy and helical image reconstruction. *J. Cell Biol.* **111**, 2623-2635.

Turton S, Gillard NP, Stephenson FA and McKernan RM. (1993). Antibodies against the 5-HT_3-A receptor identify a 54 kDa protein affinity-purified from NCB20 cells. *Mol. Neuropharmacol.* **3**, 167-171.

Unwin N. (1993). Nicotinic acetylcholine receptor at 9 Å resolution. *J. Mol. Biol.* **229**, 1101-1124.

Unwin N, Miyazawa A, Li J and Fujiyoshi Y. (2002). Activation of the nicotinic acetylcholine receptor involves a switch in conformation of the α subunits. *J. Mol. Biol.* **319**, 1165-1176.

Vailati S, Hanke W, Bejan A, Barabino B, Longhi R, Balestra B, Moretti M, Clementi F and Gotti C. (1999). Functional α6-containing nicotinic receptors are present in chick retina. *Mol. Pharmacol.* **56**, 11-19.

Vailati S, Moretti M, Balestra B, McIntosh M, Clementi F and Gotti C. (2000). β3 subunit is present in different nicotinic receptor subtypes in chick retina. *Eur. J. Pharmacol.* **393**, 23-30.

Valor LM, Castillo M, Ortiz JA and Criado M. (2003). Transcriptional regulation by activation and repression elements located at the 5'-noncoding region of the human α9 nicotinic receptor subunit gene. *J. Biol. Chem.* **278**, 37249-37255.

Verbitsky M, Rothlin CV, Katz E and Elgoyhen AB. (2000). Mixed nicotinic-muscarinic properties of the α9 nicotinic cholinergic receptor. *Neuropharmacol.* **39**, 2515-2524.

Vernallis AB, Conroy WG and Berg DK. (1993). Neurons assemble acetylcholine receptors with as many as three kinds of subunits while maintaining subunit segregation among receptor subtypes. *Neuron.* **10**, 451-464.

Vetter DE, Liberman MC, Mann J, Barhanin J, Boulter J, Brown MC, Saffiote-Kolman J, Heinemann SF and Elgoyhen AB. (1999). Role of α9 nicotinic ACh receptor subunits in the development and function of cochlear efferent innervation. *Neuron.* **23**, 93-103.

Virginio C, Giacometti A, Aldegheri L, Rimland JM and Terstappen GC. (2002). Pharmacological properties of rat α7 nicotinic receptors expressed in native and recombinant cell systems. *Eur. J. Pharmacol.* **445**, 153-161.

Wada E, Wada K, Boulter J, Deneris E, Heinemann S, Patrick J and Swanson LW. (1989). Distribution of alpha 2, alpha 3, alpha 4, and beta 2 neuronal nicotinic receptor subunit

mRNAs in the central nervous system: a hybridization histochemical study in the rat. *J. Comp. Neurol.* **284**, 314-335.

Wada K, Ballivet M, Boulter J, Connolly J, Wada E, Deneris ES, Swanson LW, Heinemann S and Patrick J. (1988). Functional expression of a new pharmacological subtype of brain nicotinic acetylcholine receptor. *Science*. **240**, 330-334.

Wang F, Gerzanich V, Wells GB, Anand R, Peng X, Keyser K and Lindstrom J. (1996). Assembly of human neuronal nicotinic receptor α5 subunit with α3, β2, and β4 subunits. *J. Biol. Chem.* **271**, 17656-17665.

Wang F, Nelson ME, Kuryatov A, Olale F, Cooper J, Keyser K and Lindstrom J. (1998). Chronic nicotine treatment up-regulates human α3β2 but not α3β4 acetylcholine receptors stably transfected in human embryonic kidney cells. *J. Biol. Chem.* **273**, 28721-28732.

Weiland S, Witzemann V, Villarroel A, Propping P and Steinlein OK. (1996). An amino acid exchange in the second transmembrane segment of a neuronal nicotinic receptor causes partial epilepsy by altering its desensitization kinetics. *FEBS Letts.* **398**, 91-96.

Weisstaub N, Vetter D, Elgoyhen AB and Katz E. (2002). The α9α10 nicotinic acetylcholine receptor is permeable to and is modulated by divalent cations. *Hearing Res.* **3906**, 1-14.

Whiteaker P, Sharples CGV and Wonnacott S. (1998). Agonist-induced up-regulation of α4β2 nicotinic acetylcholine receptors in M10 cells: pharmacological and spatial definition. *Mol. Pharmacol.* **53**, 950-962.

Whiting P, Esch F, Shimasaki S and Lindstrom J. (1987a). Neuronal nicotinic acetylcholine receptor beta-subunit is coded for by the cDNA clone alpha 4. *FEBS Letts.* **219**, 459-463.

Whiting P, Schoepfer R, Lindstrom J and Priestley T. (1991). Structural and pharmacological characterization of the major brain nicotinic acetylcholine receptor subtype stably expressed in mouse fibroblasts. *Mol. Pharmacol.* **40**, 463-472.

Whiting PJ and Lindstrom JM. (1986). Purification and characterization of a nicotinic acetylcholine receptor from chick brain. *Biochemistry*. **25**, 2082-2093.

Whiting PJ, Liu R, Morley BJ and Lindstrom JM. (1987b). Structurally different neuronal nicotinic acetylcholine receptor subtypes purified and characterized using monoclonal antibodies. *J. Neurosci.* **7**, 4005-4016.

Whiting PJ, Schoepfer R, Swanson LW, Simmons DM and Lindstrom JM. (1987c). Functional acetylcholine receptor in PC12 cells reacts with a monoclonal antibody to brain nicotinic receptors. *Nature*. **327**, 515-518.

Wong ET, Holstad SG, Mennerick SJ, Hong SE, Zorumski CF and Isenberg KE. (1995). Pharmacological and physiological properties of a putative ganglionic nicotinic receptor α3β4, expressed in transfected eucaryotic cells. *Mol. Brain Res.* **28**, 101-109.

Wonnacott S. (1997). Presynaptic nicotinic ACh receptors. *Trends Neurosci.* **20**, 92-98.

Wonnacott S, Kaiser S, Mogg A, Soliakov L and Jones AW. (2000). Presynaptic nicotinic receptors modulating dopamine release in the rat striatum. *Eur. J. Pharmacol.* **393**, 51-58.

Yu CR and Role LW. (1998a). Functional contribution of the α5 subunit to neuronal nicotinic channels expressed by chick sympathetic ganglion neurones. *J. Physiol.* **509**, 667-681.

Yu CR and Role LW. (1998b). Functional contribution of the α7 subunit to multiple subtypes of nicotinic receptors in embryonic chick sympathetic neurones. *J. Physiol.* **509**, 651-665.

Yu XM and Hall ZW. (1991). Extracellular domains mediating epsilon subunit interactions of muscle acetylcholine receptor. *Nature.* **352**, 64-67.

Zoli M, Le Novére N, Hill JA and Changeux J-P. (1995). Developmental regulation of nicotinic ACh receptor subunit mRNAs in the rat central and peripheral nervous systems. *J. Neurosci.* **15**, 1912-1939.

Zoli M, Lena C, Picciotto MR and Changeux J-P. (1998). Identification of four classes of brain nicotinic receptors using β2 mutant mice. *J. Neurosci.* **18**, 4461-4472.

Zwart R and Vijverberg HPM. (1998). Four pharmacologically distinct subtypes of α4β2 nicotinic acetylcholine receptor expressed in *Xenopus laevis* oocytes. *Mol. Pharmacol.* **54**, 1124-1131.